The background of the entire page is a soft, teal-colored watercolor wash. The color is not uniform, with lighter, almost white areas where the paint was more diluted and darker, more saturated teal areas where it was more concentrated. The texture is organic and painterly, with visible brushstrokes and blending.

# Translational research of combined anticancer therapies targeting the MAPK pathway

Sanne Huijberts



**Translational research of combined anticancer  
therapies targeting the MAPK pathway**

Sanne. C. F. A. Huijberts

**Printing of this thesis was financially supported by**

- Utrecht Institute of Pharmaceutical Sciences (UIPS)
- Oncology Graduate School Amsterdam

**Lay out**

Sanne C.F.A. Huijberts

**Printed by**

Ridderprint

© Sanne C.F.A. Huijberts, 2020

ISBN: 978-94-6375-980-9

The research described in this thesis was conducted at the Department of Pharmacology, the Division of Molecular Pathology of the Netherlands Cancer Institute and the Clinical Research unit of the Antoni van Leeuwenhoek hospital.

# **Translational research of combined anticancer therapies targeting the MAPK pathway**

Translationeel onderzoek van gecombineerde behandelingen gericht op de MAPK signaaltransductie route

(met een samenvatting in het Nederlands)

PROEFSCHRIFT

ter verkrijging van de graad van doctor aan de Universiteit Utrecht  
op gezag van de rector magnificus, prof. dr. H.R.B.M. Kummeling,  
ingevolge het besluit van het college voor promoties  
in het openbaar te verdedigen op

woensdag 14 oktober 2020 des ochtends te 11.00 uur

door

SANNE CORNELIA FRANCINA ADRIANA HUIJBERTS

geboren op 1 november 1988  
te Sint Michielsgestel

**Promotoren:** Prof. dr. J.H. Beijnen  
Prof. dr. R. Bernards

**Copromotoren:** Dr. N. Steeghs  
Dr. F. L. Opdam



# Contents

	<b>Preface</b>	9
<b>Chapter 1</b>	<b>General introduction</b>	13
<b>Chapter 2</b>	<b>Sequential treatment for resistant <i>BRAFV600E</i> mutant melanoma</b>	
Chapter 2.1	An acquired vulnerability of drug-resistant melanoma with therapeutic potential. <i>Cell. 2018 May;173(6):1413-1425</i>	21
Chapter 2.2	Vorinostat in patients with resistant <i>BRAFV600E</i> mutated advanced melanoma: a proof of concept study. <i>Future Oncology. 2020 Apr;16(11):619-629</i>	61
Chapter 2.3	A proof of concept study of sequential treatment with the histone deacetylase inhibitor vorinostat plus BRAF and/or MEK inhibitors in patients with resistant <i>BRAFV600E</i> mutated advanced melanoma. <i>Interim analysis</i>	79
<b>Chapter 3</b>	<b>Double or triple targeted combinations for the treatment of <i>BRAFV600E</i> mutant colorectal cancer</b>	
Chapter 3.1	Binimetinib, encorafenib, and cetuximab triplet therapy for patients with <i>BRAFV600E</i> -mutant metastatic colorectal cancer: Safety lead-in results from the phase III BEACON colorectal cancer study. <i>Journal of Clinical Oncology. 2019 Jun;37(17):1460-1469</i>	93
Chapter 3.2	Encorafenib, binimetinib and cetuximab combined therapy for patients with <i>BRAFV600E</i> mutant metastatic colorectal cancer. <i>Future Oncology. 2020 Feb;16(6):161-173</i>	121
Chapter 3.3	Mutational profiles causing resistance in patients with <i>BRAFV600E</i> mutant colorectal cancer treated with cetuximab and encorafenib +/- binimetinib or alpelisib. <i>Submitted for publication</i>	143



<b>Chapter 4</b>	<b>Combining pan-HER and MEK inhibitors for <i>KRAS</i> mutant solid tumors</b>	
Chapter 4.1	Phase I study of the pan-HER inhibitor dacomitinib plus the MEK1/2 inhibitor PD-0325901 in patients with <i>KRAS</i> -mutation-positive colorectal, non-small cell lung and pancreatic cancer. <i>British Journal of Cancer. 2020 Apr;122(8):1166-1174</i>	171
Chapter 4.2	Phase I study of lapatinib and trametinib in patients with <i>KRAS</i> -mutant colorectal, non-small cell lung, and pancreatic cancer. <i>Cancer Chemotherapy and Pharmacology. 2020 May;85(5):917-930</i>	193
Chapter 4.3	Phase I study of afatinib plus selumetinib in patients with <i>KRAS</i> mutated colorectal, non-small cell lung and pancreatic cancer. <i>Submitted for publication</i>	217
<b>Chapter 5</b>	<b>Conclusions and perspectives</b>	239
<b>APPENDIX</b>	Summary Nederlandse samenvatting List of publications Affiliations Dankwoord Curriculum Vitae	248



## Preface

Malignancies are the second leading cause of death worldwide and about 1 in 6 deaths are cancer-related, which makes cancer one of the greatest problems for public health.(1) While malignancies had initially been treated with only surgery or radiotherapy, the first anticancer drug was discovered in 1942 during the Second World War. The alkylating chemotherapeutic agent, nitrogen mustard, was the start of a new treatment modality.(2)

For decades, the focus of drug development in oncology was on cytotoxic agents directed to DNA and DNA synthesis and interfering with cell replication and survival in especially fast-dividing cells. Tumor histology was the basis for selecting a chemotherapeutic regimen until the human genome was unraveled in 2001.(3) After this discovery it became clear that cancer should not only be classified histologically, but also at the genetic level. Histologically similar tumors showed different genetic patterns. Onco- and tumor suppressor genes were revealed and molecular biological research gathered insights into the interplay of cellular signal transduction pathways, which regulate cell growth.(4, 5) Moreover, Hanahan *et al.* increased the understanding of tumor biology by mapping the eight hallmarks of tumor development, including self-sufficiency in growth signals, insensitivity to anti-growth signals, evading apoptosis, limitless replicative potential, sustained angiogenesis, tissue invasion and metastasis, reprogramming of energy metabolism and evading immune destruction. Genomic instability is the basis of these hallmarks and leads to the widespread genetic diversity of cancers.(6, 7) These insights have led to the development of immunotherapies and targeted agents against genetic aberrations and proteins that drive tumor initiation and progression.(5, 6) A large proportion of these proteins are kinases, for which a long list of inhibitory agents is currently available.

Several inhibitors are targeting kinases of the mitogen-activated protein kinase (MAPK) pathway, which plays a major role in cancer development and progression in a broad spectrum of human cancers.(8) Two commonly mutated genes of the MAPK pathway include the v-RAF murine sarcoma viral oncogene homolog B (*BRAF*) gene and the Kirsten rat sarcoma viral oncogene homolog (*KRAS*) gene. Activating mutations in the *KRAS* or *BRAF* gene result in persistent activation of the MAPK pathway and high rates of cancer cell proliferation.

Researchers started with the investigation of single agents to inhibit *BRAF* or *KRAS* mutations. For the first-in-class *BRAF* inhibitor vemurafenib, favorable responses were observed in *BRAF*<sup>V600E</sup> mutated melanoma. Unfortunately, vemurafenib monotherapy was not beneficial in all patients with melanoma nor in other tumor types with a *BRAF*<sup>V600E</sup> mutation. On top of that, the initially responsive tumors develop resistance to *BRAF* inhibition in six to eight months.(9) Furthermore, targeting the *KRAS* protein directly is even more difficult. Two or more kinase inhibitors can be combined to enhance efficacy. Moreover, not only a synergistic anti-tumor effect might be induced, but also resistance can be delayed or avoided by combining agents.

This thesis highlights several combinations of kinase inhibitors targeting *BRAF* or *KRAS* mutant cancers. All phases of drug development are discussed, starting with preclinical experiments in cell lines and mouse models. Promising preclinical results led to investigational drug development in the clinic. Firstly, phase I trials were conducted to assess the safety of a certain single agent or drug combination and to determine the optimal dose and treatment regimen. With this recommended dose or regimen, phase II, III and/or IV trials were conducted to explore the safety and efficacy in a larger patient population. As mentioned above, the development of resistance is a major hurdle in targeted therapies. Possible mechanisms of resistance, challenges that have to be faced to overcome resistance and treatment strategies to delay or overcome resistance are also studied in this thesis.

**Chapter 1** focuses on introducing two approaches, synthetic lethality and collateral vulnerability for intervention to enhance efficacy and to overcome resistance to kinase inhibitors. Synthetic lethality is highlighted by the combination of two or more drugs or mutations that are together lethal to the cancer cell, but do not result in lethality by single treatment or appearance. Collateral vulnerability is characterized by newly developed vulnerabilities of cancer cells upon acquired resistance to an anti-cancer drug. Resistant cancer cells become sensitive to a drug that was not effective before development of resistance to the first given treatment. These approaches play a pivotal role in the novel treatment concepts of the trials described in this thesis.

**Chapter 2** highlights a novel treatment strategy for *BRAF*<sup>V600E</sup> mutant melanoma after development of resistance to BRAF inhibitors or a combination of BRAF- and MEK inhibitors.

**Chapter 2.1** describes the preclinical and first clinical results of treatment with the histone deacetylase inhibitor vorinostat. The trial protocol of the clinical proof of concept study is included in **chapter 2.2**. An interim analysis of this clinical trial, including safety, efficacy, pharmacokinetic, pharmacodynamic and pharmacogenetic results, is presented in **chapter 2.3**.

**Chapter 3** is focusing on a novel triplet regimen for *BRAF*<sup>V600E</sup> mutant metastatic colorectal cancer. The results of the Safety Lead-in investigation for the phase III trial with the EGFR inhibitor cetuximab, BRAF inhibitor encorafenib and MEK inhibitor binimetinib are provided in **chapter 3.1**. The clinical pharmacokinetics of this triplet combination are described and reviewed in **chapter 3.2**. **Chapter 3.3** describes a case-series in which secondary resistance mutations of triple and double inhibition of the MAPK pathway are highlighted, including recommendations for future treatment strategies and investigations.

In **chapter 4**, three phase I trials with combined targeted agents to treat tumors with *KRAS* mutations are presented. Results of three different combinations of EGFR/pan-HER inhibitors and MEK-inhibitors are described in **chapter 4.1, 4.2 and 4.3**.

In **chapter 5**, the research of this thesis is taken together in the conclusions and future perspectives section. Herein the gathered information is placed in a broader context including implications and recommendations for future research and treatment.

## References

1. World Health Organization. Fact sheet Cancer. 2019. <https://www.who.int/en/news-room/fact-sheets/detail/cancer> (Accessed 6 Januari 2019).
2. Singh RK, Kumar S, Prasad DN, Bhardwaj TR. Therapeutic journey of nitrogen mustard as alkylating anticancer agents: Historic to future perspectives. *European journal of medicinal chemistry*. 2018;151:401-33.
3. Lander ES, Linton LM, Birren B, Nusbaum C, Zody MC, Baldwin J, et al. Initial sequencing and analysis of the human genome. *Nature*. 2001;409(6822):860-921.
4. Torkamani A, Verkhivker G, Schork NJ. Cancer driver mutations in protein kinase genes. *Cancer letters*. 2009;281(2):117-27.
5. Beijnen JH, Schellens JHM. Personalized medicine in oncology: a personal view with myths and facts. *Current clinical pharmacology*. 2010;5(3):141-7.
6. Hanahan D, Weinberg RA. Hallmarks of cancer: the next generation. *Cell*. 2011;144(5):646-74.
7. Hanahan D, Weinberg RA. The hallmarks of cancer. *Cell*. 2000;100(1):57-70.
8. Sebolt-Leopold JS, Herrera R. Targeting the mitogen-activated protein kinase cascade to treat cancer. *Nature reviews cancer*. 2004;4(12):937-47.
9. Kim A, Cohen MS. The discovery of vemurafenib for the treatment of BRAF-mutated metastatic melanoma. *Expert opinion on drug discovery*. 2016;11(9):907-16.



# CHAPTER 1

General Introduction

## Two treatment strategies to interfere with vulnerabilities of resistance

Formerly, cancer was classified based on histological subtypes. However, genetic information is increasingly gaining importance for classification and treatment choices in oncology. More than 60 years ago, the first link between genetic alterations and cancer development was made by Nowell *et al.* and Rowley, who discovered the Philadelphia Chromosome in chronic myeloid leukemia.(1, 2) Approximately 95% of the patients with chronic myeloid leukemia harbor this mutation. The Philadelphia chromosome is formed by the reciprocal chromosomal translocation of parts of chromosomes 9 and 22 yielding the *BCR-ABL* fusion gene and synthesis of the BCR-ABL oncoprotein.(3, 4) The BCR-ABL protein is a tyrosine kinase, which activates downstream effector molecules upon phosphorylation via one of the tyrosine residues. The tyrosine kinase inhibitor (TKI) imatinib prevents kinase activity of the BCR-ABL protein by binding to the ATP-binding site and thereby blockade of the kinase pocket. It was the second small molecule TKI to be approved by the Food and Drug Administration (FDA) in 2001.(4) In the same year the initial sequencing of the human genome was performed after which new insights into the link between cancer and genetic alterations succeeded quickly.(5) Genome sequencing revealed that only approximately 200 of the some 20,000 genes can function as a driver gene in cancer. Furthermore, two to eight driver mutations are necessary for tumor outgrowth and metastases. Despite the multiple and complex changes in cancer cells, only one or a few oncogenes are necessary for proliferation and survival. Cancer cells can become addicted to these few oncogenes, also known as oncogene addiction.(6, 7) Somatic point mutations are frequently causing driver mutations in genes coding for protein kinases such as BCR-ABL, v-RAF murine sarcoma viral oncogene homolog B (*BRAF*), epidermal growth factor receptor (*EGFR*) or Kirsten rat sarcoma viral oncogene homolog (*KRAS*). It might therefore not be surprising that inhibition of the proteins harboring these driver mutations by selective inhibitors has led to clinically relevant improvements in patient outcome.(8) Unfortunately, these clinical benefits are restricted by intrinsic and acquired resistance to targeted agents. Even tumors revealing an initial complete response on targeted therapies can escape in only a few weeks by development of secondary mutations. The newly developed mutations lead to comprehensive rewiring of the cell signaling, causing resistance. This comprehensive rewiring results in the development of both sensitive and resistant clones within the same patient leading to heterogeneity and this increases the complexity of targeted treatments. As a consequence of this heterogeneity major intra- and interpatient differences are observed on response to targeted therapies. This is confirmed in the clinic by low response rates and short duration of response in patients treated with a single kinase inhibitor. On the other hand, by combining kinase inhibitors, the progression free survival and overall survival of patients might be prolonged. For example, the combination of a BRAF inhibitor plus a MEK inhibitor has led to improved outcomes in patients with *BRAF*<sup>V600E</sup> mutant melanoma. Although clinical benefit is enhanced with the combination of both drugs, the development of resistance is still limiting the duration of response. Development of resistance in *BRAF*<sup>V600E</sup> mutant melanoma occurs within six to eight months with single BRAF inhibition and within nine to fourteen months with the combination of BRAF- and MEK inhibition.(9, 10)



Comparable results are being observed for EGFR inhibitors in *EGFR* mutant lung cancer and trastuzumab in *HER2*-amplified breast cancer.(11)

Hitherto 52 small molecule protein kinase inhibitors with different targets are approved for an oncological indication by the FDA.(12) Today, the challenge is to rationally combine and time inhibitors to optimally interfere with resistance mechanisms. The current focus lies therefore not only on the development of new combinations, but also on optimizing treatment schedules of known combinations. Moreover, the fine-tuning of dose and treatment order may influence anti-tumor effect, duration of response and toxicity. Optimized treatment schedules might thus lead to a better benefit-risk ratio and improved treatment outcome. Therefore, the research described in this thesis is more focusing on the improvement of combinations and treatment order of available drugs, rather than the development of completely new compounds. This improvement might be reached via two approaches, called synthetic lethality and collateral vulnerability, to enhance efficacy and interplay with resistance.

### Synthetic lethality

Synthetic lethality refers to the combination of two or more drugs or mutations that are together lethal to the cancer cell, but do not result in lethality by single treatment or appearance.(13) Synthetic lethality can be achieved by the combination of mutations in two genes, the interaction of a mutation and an inhibitory drug or by a pharmacodynamic drug-drug interaction (figure 1). In the concept of synthetic lethality, the mutation that interacts with an inhibitory drug might be used as a biomarker for patient selection. Furthermore, in theory a lower dose of drugs is effective with lower toxicity of a drug and synthetic lethality can be feasible to all types of mutations.(13)

The first successful synthetic lethal gene-drug combination that made it to the clinic was discovered in 2005 by targeting the DNA repair defect in Breast Cancer 1 (*BRCA1*) or Breast Cancer 2 (*BRCA2*) deficient tumors.(14) *BRCA1* and *BRCA2* are important players in the repair of DNA double strand breaks during homologous recombination. Poly (ADP) ribose polymerase (PARP) is an enzyme that is required for repair of single strand breaks in the DNA.(15) The combination of *BRCA* and PARP mutations is synthetically lethal to a cell.(13) Moreover, the inhibition of PARP with targeted drugs such as olaparib or niraparib is an effective anti-cancer monotherapy for patients with *BRCA1* or *BRCA2* deficient tumors, including breast, ovarian and prostate cancer.(16)

Most treatment concepts in this thesis are based on a drug-drug synthetic lethality with the most promising treatment regimen included in **chapter 3**. Here, the combination of the EGFR inhibitor cetuximab, the BRAF inhibitor encorafenib and the MEK inhibitor binimetinib in *BRAF*<sup>V600E</sup> mutant metastatic colorectal cancer patients is described. In monotherapy trials with BRAF inhibition it became clear that the favorable responses observed in *BRAF*<sup>V600E</sup> mutant melanoma were not observed in colorectal cancer.(17) These disappointing results were clarified by Prahallad *et al.* with a synthetic lethality screen in *BRAF* mutant colon cancer cells. By inhibiting BRAF, upstream activation of EGFR occurred in the cells, which could be

overcome by combining a BRAF inhibitor with EGFR inhibition.(18) These emerging preclinical results were confirmed in clinical phase I and II trials (19, 20) and have led to the initiation of the BEACON CRC phase III trial. Furthermore, another drug-drug synthetic lethality is described in **chapter 4**. Here, three combinations of pan-HER and MEK inhibitors are investigated in *KRAS* mutant colorectal, lung and pancreatic cancer.

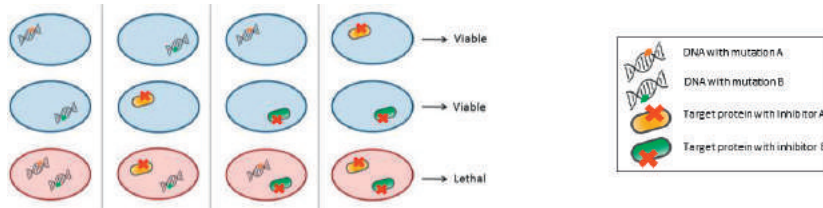


**Figure 1. Schematic view on the concept of synthetic lethality.**

### Collateral vulnerability

Collateral vulnerability is characterized by newly developed vulnerabilities of cancer cells upon development of acquired resistance to an anti-cancer drug. Resistant cancer cells may become sensitive to a drug that was not effective before development of resistance to the first given treatment (figure 2).(21, 22)

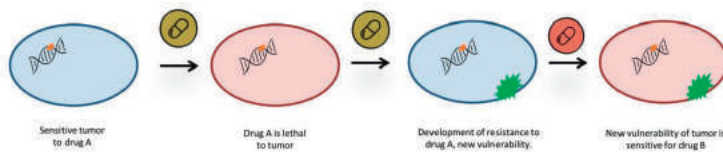


**Figure 2. Schematic view on the concept of collateral vulnerability.**

Simplistically, the development of resistance can create a new potent therapeutic target. Since the heterogeneous character of tumors, both sensitive and resistant clones might be present upon resistance as a result of comprehensive rewiring. To target both sensitive and resistant clones it might be beneficial to alternate treatment rather than to combine drugs simultaneously. The recently published “one-two punch” strategy in which the sequential order of drugs is key showed encouraging results. A new vulnerability of the cancer cell is induced by the first drug and thereafter a second drug is administered that exploits this vulnerability.(21) Moreover, response rates and duration of response might be improved by administering drugs in an alternating schedule.(11) In **chapter 2**, this alternating treatment approach is investigated in preclinical and clinical studies by targeting an acquired vulnerability with the histone deacetylase inhibitor vorinostat in patients with *BRAF*<sup>V600E</sup> mutant melanoma that developed resistance to BRAF and/or MEK inhibitors.

## References

1. Rowley JD. Letter: A new consistent chromosomal abnormality in chronic myelogenous leukaemia identified by quinacrine fluorescence and Giemsa staining. *Nature*. 1973;243(5405):290-3.
2. Nowell PC, Hungerford DA. Chromosome studies on normal and leukemic human leukocytes. *Journal of the National Cancer Institute*. 1960;25:85-109.
3. O'Brien SG, Guilhot F, Larson RA, Gathmann I, Baccarani M, Cervantes F, et al. Imatinib compared with interferon and low-dose cytarabine for newly diagnosed chronic-phase chronic myeloid leukemia. *The New England journal of medicine*. 2003;348(11):994-1004.
4. Savage DG, Antman KH. Imatinib mesylate--a new oral targeted therapy. *The New England journal of medicine*. 2002;346(9):683-93.
5. Lander ES, Linton LM, Birren B, Nusbaum C, Zody MC, Baldwin J, et al. Initial sequencing and analysis of the human genome. *Nature*. 2001;409(6822):860-921.
6. Vogelstein B, Kinzler KW. The path to cancer --Three strikes and you're out. *The New England journal of medicine*. 2015;373(20):1895-8.
7. Weinstein IB. Cancer. Addiction to oncogenes--the Achilles heal of cancer. *Science*. 2002;297(5578):63-4.
8. Torkamani A, Verkhivker G, Schork NJ. Cancer driver mutations in protein kinase genes. *Cancer letters*. 2009;281(2):117-27.
9. Michielin O, Hoeller C. Gaining momentum: New options and opportunities for the treatment of advanced melanoma. *Cancer treatment reviews*. 2015;41(8):660-70.
10. Zia Y, Chen L, Daud A. Future of combination therapy with dabrafenib and trametinib in metastatic melanoma. *Expert opinion on pharmacotherapy*. 2015;16(14):2257-63.
11. Wang L, Bernards R. Taking advantage of drug resistance, a new approach in the war on cancer. *Frontiers of medicine*. 2018;12(4):490-5.
12. Roskoski R, Jr. Properties of FDA-approved small molecule protein kinase inhibitors: A 2020 update. *Pharmacological research*. 2020;152:104609.
13. O'Neil NJ, Bailey ML, Hieter P. Synthetic lethality and cancer. *Nature reviews genetics*. 2017;18(10):613-23.
14. Farmer H, McCabe N, Lord CJ, Tutt AN, Johnson DA, Richardson TB, et al. Targeting the DNA repair defect in BRCA mutant cells as a therapeutic strategy. *Nature*. 2005;434(7035):917-21.
15. Evers B, Helleday T, Jonkers J. Targeting homologous recombination repair defects in cancer. *Trends in pharmacological sciences*. 2010;31(8):372-80.
16. Lord CJ, Ashworth A. PARP inhibitors: Synthetic lethality in the clinic. *Science*. 2017;355(6330):1152-8.
17. Kopetz S, Desai J, Chan E, Hecht JR, O'Dwyer PJ, Maru D, et al. Phase II pilot study of vemurafenib in patients with metastatic BRAF-mutated colorectal cancer. *Journal of clinical oncology*. 2015;33(34):4032-8.
18. Prahallad A, Sun C, Huang S, Di Nicolantonio F, Salazar R, Zecchin D, et al. Unresponsiveness of colon cancer to BRAF(V600E) inhibition through feedback activation of EGFR. *Nature*. 2012;483(7387):100-3.
19. van Geel R, Tabernero J, Elez E, Bendell JC, Spreafico A, Schuler M, et al. A phase Ib dose-escalation study of encorafenib and cetuximab with or without alpelisib in metastatic BRAF-mutant colorectal cancer. *Cancer discovery*. 2017;7(6):610-9.
20. Yaeger R, Cercek A, O'Reilly EM, Reidy DL, Kemeny N, Wolinsky T, et al. Pilot trial of combined BRAF and EGFR inhibition in BRAF-mutant metastatic colorectal cancer patients. *Clinical cancer research*. 2015;21(6):1313-20.
21. Leite de Oliveira R, Wang L, Bernards R. With great power comes great vulnerability. *Molecular & cellular oncology*. 2018;5(6):e1509488.
22. Hutchison DJ. Cross resistance and collateral sensitivity studies in cancer chemotherapy. *Advances in cancer research*. 1963;7:235-50.



# CHAPTER 2

Sequential treatment in  
resistant *BRAFV600*  
mutant melanoma



# CHAPTER 2.1

An acquired vulnerability  
of drug resistant melanoma  
with therapeutic potential

Liqin Wang, Rodrigo Leite de Oliveira, Sanne  
C.F.A. Huijberts, Evert Bosdriesz, Diede  
Brunen, Astrid Bosma, Ji-Ying Song, John  
Zevenhoven, Tjitske Los- de Vries, Hugo  
Horlings, Bastiaan Nuijen, Jos H. Beijnen,  
Jan H.M. Schellens, Rene Bernards

## Summary

*BRAF(V600E)* mutant melanomas treated with inhibitors of the BRAF and MEK kinases almost invariably develop resistance, which is frequently caused by reactivation of the Mitogen Activated Protein Kinase (MAPK) pathway. To identify novel treatment options for such patients, we searched for acquired vulnerabilities of MAPK inhibitor-resistant melanomas. We find that resistance to BRAF+MEK inhibitors is associated with increased levels of reactive oxygen species (ROS). Subsequent treatment with the histone deacetylase inhibitor vorinostat suppresses *SLC7A11*, leading to a lethal increase in the already elevated levels of ROS in drug-resistant cells. This causes selective apoptotic death of only the drug resistant tumor cells. Consistently, treatment of BRAF inhibitor-resistant melanoma with vorinostat in mice results in a dramatic tumor regression. In a study in patients with advanced BRAF+MEK inhibitor resistant melanoma, we find that vorinostat can selectively ablate drug-resistant tumor cells, providing clinical proof of concept for the novel therapy identified here.



## Introduction

Approximately half of melanoma skin cancers carry activating mutations in the *BRAF* oncogene, leading to activation of the Mitogen Activated Protein Kinase (MAPK) pathway. Inhibition of the BRAF oncoprotein with targeted drugs provides substantial benefit to patients, albeit that most patients ultimately relapse with resistant disease.(1) Dual inhibition of both BRAF and the downstream MEK kinases leads to more sustained clinical benefit, but resistance is still mostly inevitable.(2) Resistance to MAPK pathway inhibitors in melanoma is frequently caused by reactivation of signaling through this pathway in the presence of drug.(3, 4) Multiple mechanisms of MAPK reactivation have been described, including upregulation of Receptor Tyrosine Kinases (RTKs), mutations in *KRAS* and *NRAS*, splice site mutations in *BRAF*, amplification of *BRAF* and mutation of MEK kinases (reviewed by Manzano *et al.* (5)). Drug withdrawal in such drug-resistant patients often does not lead to an immediate disease flare up, but rather to a transient pause in tumor growth, known as the “drug holiday effect”.(6) This effect can be explained, at least in part, by hyper-activation of the MAPK pathway signaling following drug withdrawal, leading to a cellular state that has hallmarks of oncogene-induced senescence.(7) Downregulation of this hyper-active MAPK signaling marks the end of the drug holiday, resulting in re-initiation of tumor growth and regained drug sensitivity upon re-challenge with BRAF inhibitor.(6)

The transient proliferation arrest of BRAF inhibitor-resistant melanomas following drug withdrawal points towards an acquired vulnerability of drug-resistant cells that was not present in the parental drug-sensitive cells.(7) That drug resistance of cancer cells comes at a fitness cost that in turn can cause sensitivity to other drugs was already identified over 50 years ago and is referred to as “collateral sensitivity”.(8) Previous studies have pointed to alterations in mitochondrial oxidative metabolism when signaling through the MAPK pathway is modulated.(9-13) Here, we report a collateral sensitivity of BRAF inhibitor-resistant melanoma that takes advantage of increased levels of reactive oxygen species (ROS) in drug-resistant cells.

## Results

### A vulnerability of MAPKi-resistant melanoma

To explore new therapeutic strategies for melanomas having acquired resistance to inhibitors of the MAPK pathway, we generated drug-resistant derivatives of *BRAF* mutant A375 human melanoma cells by long-term culture in the presence of the BRAF inhibitor vemurafenib (A375R, resistant cells) or a combination of the BRAF inhibitor dabrafenib and the MEK inhibitor trametinib (A375DR, double-resistant cells). In a short-term proliferation assay A375R and A375DR cells proliferated in the presence of vemurafenib and the combination of dabrafenib plus trametinib, respectively, whereas parental A375 cells were sensitive to MAPK inhibition (Figure 1A). In the absence of MAPK inhibitors (MAPKi), A375R and A375DR cells displayed a slight proliferation impairment, modeling the drug holiday effect seen in the clinic.(6) Quantification of cell viability at the end of the proliferation assay confirmed the sustained viability of the MAPKi-resistant A375R and A375DR derivatives in

the presence of the drugs (Figure 1B). Further characterization of these derivatives revealed that A375R cells have gained platelet-derived growth factor receptor B (*PDGFRB*) expression (Figure 1C), while A375DR cells acquired a secondary *NRAS*<sup>Q61H</sup> mutation (Figure 1D). Similar results were obtained in Mel888 cells, another *BRAF*<sup>V600E</sup> mutated human melanoma model. After a similar long-term culture protocol in MAPKi, we isolated a variant resistant to vemurafenib (Mel888R) (Figures S1A and S1C) and a line resistant to the combination of dabrafenib plus trametinib (Mel888DR) (Figures S1B and S1C). Mel888R cells express a splice variant of *BRAF* (Figure S1D), whereas Mel888DR harbor a secondary *KRAS*<sup>G12C</sup> mutation (Figure S1E). These four resistance mutations commonly found in melanoma patients that develop resistance to drugs that target BRAF and/or MEK kinases converge on the hyperactivation of the MAPK pathway. These data also underscore that, although generated *in vitro*, our drug-resistant melanoma cell line derivatives faithfully recapitulate clinical drug resistance.

One of the features of increased RAS signaling is the abundant production of ROS, which serve as signaling molecules in multiple cellular pathways.(14-17) To test whether this is also the case in melanoma, we measured ROS levels using fluorescent flow cytometry. Indeed, basal levels of ROS were 2-fold higher in single drug-resistant cells (A375R and Mel888R) and increased even further in double drug-resistant cells (A375DR and Mel888DR) (Figures 1E, S1F). We hypothesized that this increase in ROS levels may represent an acquired vulnerability in the sense that a further increase in ROS levels could become detrimental to the drug-resistant cells. To test this, we exposed parental and drug-resistant melanoma cells to the ROS inducer paraquat. Indeed, paraquat treatment inhibited the proliferation of single-resistant A375R cells and double-resistant A375DR cells in a colony formation assay, while it induced only slight proliferation impairment in the parental cells (Figures 1F, 1G, S1G, S1H). The sensitivity to paraquat in resistant melanoma cells was proportional to the higher basal ROS levels (Figures 1E and S1F) and correlated with an increase of DNA damage and apoptosis, as evidenced by the presence of  $\gamma$ -H2AX and cleaved PARP, respectively (Figures 1I and S1J). The notion that increased sensitivity of MAPKi-resistant cells to paraquat is mediated by increased ROS levels is supported by the observation that treatment with the ROS scavenger N-acetyl-cysteine (NAC) reduced ROS levels negated the sensitivity negated the sensitivity of BRAFi-resistant cells to paraquat (Figures 1H and S1I) and reduced DNA damage and apoptosis (Figures 1I, 1J, S1J and S1K). These findings indicate that regardless of the type of mutation responsible for acquired MAPKi-resistance in melanomas, ROS induction is a common vulnerability that can be targeted with ROS inducers.

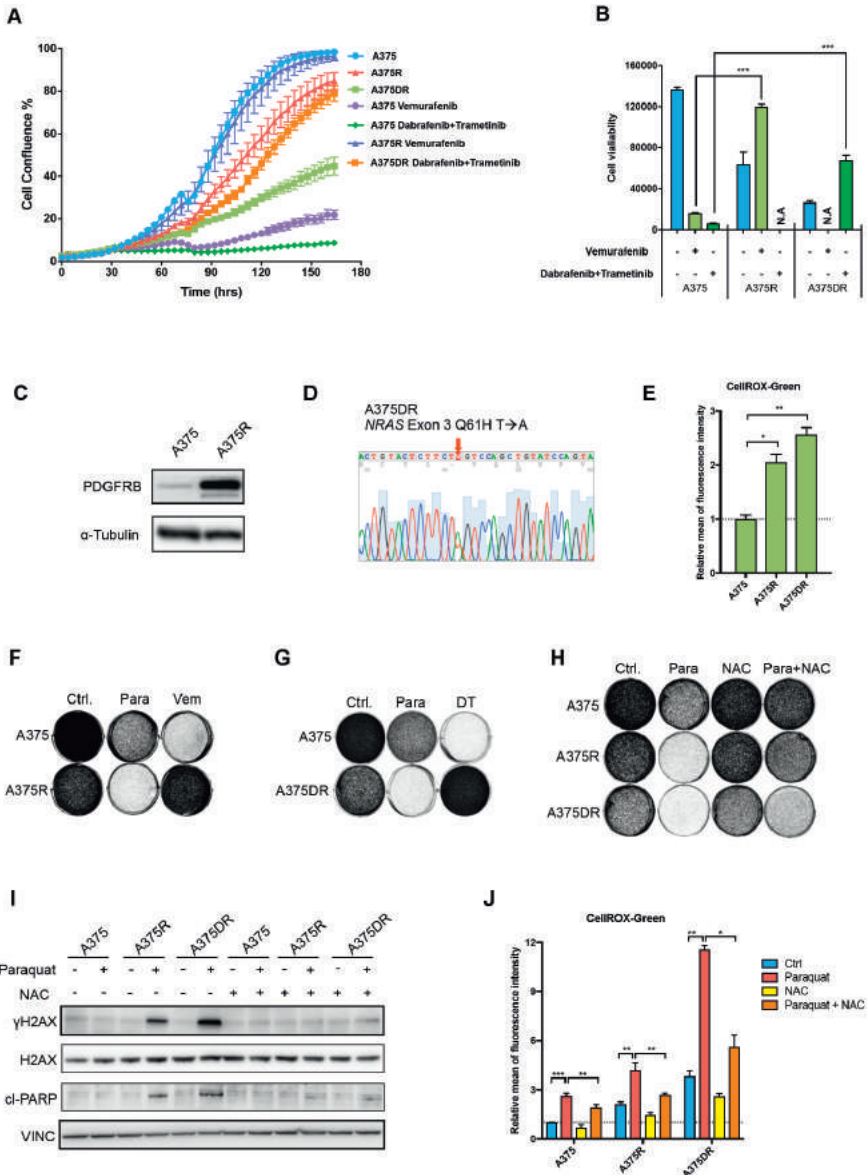


**Figure 1. ROS levels and ROS sensitivity of melanoma cells.**

(A) Incubate proliferation assays of parental (A375), BRAFi-resistant (A375R) and BRAFi/MEKi double-resistant (A375DR) melanoma cells in the presence or absence of 2  $\mu$ M vemurafenib or combination of 0.5  $\mu$ M dabrafenib and 10 nM trametinib.

(B) Quantification of cell viability assay of parental and drug-resistant cells cultured in the presence or absence of MAPK inhibitors shown in (A) at the end of the assay. Cell viability was quantified with CellTiter-Blue.

(C) Western blot analysis of PDGFRB expression in A375 cells and A375R cells.

(D) Sanger sequencing analysis of NRAS gene in A375DR cells showing gain of NRASQ61H mutation.

(E) ROS levels of A375R, A375DR and parental A375 cells measured after 72 hr of culturing without drugs. ROS levels were measured using CellROX-Green flow cytometry assay. Relative ROS levels are plotted.

(F and G) Long-term colony formation assays of A375R (panel F) and A375DR (panel G) compared to parental A375 cells treated with paraquat and/or MAPK inhibitors (Vem, vemurafenib; DT, dabrafenib+trametinib). Cells were seeded 50,000 cells per well in 6-well plates and treated with 20  $\mu$ M paraquat, 2  $\mu$ M vemurafenib or combination of 10 nM trametinib and 0.5  $\mu$ M dabrafenib for 10 days. Afterward, the cells were fixed, stained and photographed.

(H) Long-term colony formation assays of parental and MAPKi-resistant A375 cells treated with paraquat and/or NAC. Cells were seeded 50,000 cells per well in 6-well plates and treated with 20  $\mu$ M paraquat and/or 2.5 mM N-acetyl-L-cysteine (NAC) for 10 days. Afterward, the cells were fixed, stained and photographed.

(I) Protein lysates were harvested from the MAPKi-resistant (R and DR cells) and parental A375 cells were treated with 25  $\mu$ M paraquat and/or 2.5 mM NAC for 72 hr. Western blot analysis of  $\gamma$ H2AX as a DNA damage marker and cleaved-PARP (cl-PARP) as an apoptosis marker; vinculin (VINC) served as the loading control.

(J) Parental and MAPKi-resistant A375 cells were treated with 20 $\mu$ M paraquat and/or 2.5 mM NAC for 72 hr. ROS levels were measured using CellROX-Green flow cytometry assay.

Error bars represent the mean  $\pm$  SD from the biological triplicates (\* $p \leq 0.05$ , \*\* $p \leq 0.01$ , \*\*\* $p \leq 0.001$ , Student's t-test). See also figure S1.

### **MAPKi-resistant melanoma cells are sensitive to vorinostat**

To take this concept closer to a potential clinical use, we searched for approved drugs that also induce ROS. We selected histone deacetylase inhibitor (HDACi) vorinostat, because vorinostat has a safe pharmacological profile in the clinic and HDACi are known to induce ROS.(17-20) To test whether vorinostat also induces ROS in melanoma, we treated our two cell models with vorinostat for 72 hours and measured intracellular ROS. Indeed, vorinostat induced ROS levels in parental and resistant cells, which could be prevented by co-treatment with NAC (Figures 2A and S2A). In long-term proliferation assays, vorinostat treatment inhibited the growth of drug-resistant cells, but the combination of vorinostat and NAC rescued this effect in both melanoma models (Figures 2B and S2B). Again, the vorinostat effect was far more pronounced in MAPKi-resistant melanoma cells, as it only caused a mild proliferation impairment in parental cells, also in a short-term Incucyte assay (Figures 2C and S2C). The differential effect of vorinostat is most likely explained by the much higher ROS levels induced in MAPKi-resistant melanoma cells as compared to the ROS levels induced by vorinostat in parental cells (Figures 2A and S2A). Similar to paraquat treatment, vorinostat induced DNA damage and apoptosis in BRAFi-resistant, but not in parental A375 cells, which was rescued by NAC treatment (Figure 2D). In Mel888 cells, vorinostat treatment also induced apoptosis in MAPKi-resistant cells (Mel888R and Mel888DR) but not in the parental line (Figure S2D). The same results were essentially obtained with a second ROS scavenger glutathione ethyl ester (GEE) as GEE also reduced ROS levels induced by vorinostat and rescued the proliferation defect induced by vorinostat in MAPK inhibitor-resistant cells (Figures 2E, 2F, S2E and S2F). These observations suggest that a certain ROS level is required to inflict sufficient DNA damage and to activate cell death pathways, which is only achieved by vorinostat in drug-resistant, but not in parental, melanoma cells.

We also tested the vorinostat sensitivity in *NRAS* mutant melanoma cells, since this gene is the second most commonly mutated in melanoma patients. We generated *NRAS* mutant SK-MEL-147 melanoma cells resistant to MEK inhibitor by long-term culture in trametinib-containing medium. Vorinostat treatment of parental SK-MEL-147 cells and resistant derivatives (SK-MEL-147R) induced an increase in intracellular ROS levels that could be abrogated with co-treatment with NAC (Figure S2G). Accordingly, in a colony formation assay SK-MEL-147R cells showed increased sensitivity to vorinostat as compared to the parental line. This sensitivity was reversed by the concomitant treatment with NAC (Figure S2H).

### MAPK inhibition is antagonized by HDACi

It has been shown in short-term assays that combined HDAC and MAPK inhibition can prevent some forms of MAPK inhibitor resistance in melanoma.(21) It has also been shown, however, that increased ROS levels lead to activation of the MAPK pathway.(22) This would suggest that vorinostat, by virtue of its increase in ROS levels, could activate MAPK signaling and thereby counteract the effects of MAPK inhibitors. Indeed, also in melanoma, vorinostat activated MAPK signaling in A375, A375R and A375DR cells, as evidenced by an increase in phosphorylated MEK (pMEK) and p-P90RSK (Figure 3A and 3B). While MAPK inhibitors were able to reduce levels of pMEK and p-P90RSK in all three cells, combined treatment with MAPKi and vorinostat resulted in significant residual MAPK signaling (Figure 3A and 3B). Consistent with this, treatment of A375 or Mel888 cells with a combination of HDACi and MAPKi resulted in continued proliferation (Figure 3C and S3C). Conversely, whereas A375DR and A375R are hyper-sensitive to three different HDAC inhibitors, the combination of MAPKi and HDACi resulted in a poor response (Figure 3C and 3D). This finding is most readily explained by the reduced MAPK signaling caused by the MAPKi, resulting in lower ROS levels and hence a lesser effect of ROS increase by HDACi. Indeed, treatment of A375 and A375 DR cells with MAPK inhibitors reduced ROS levels and suppressed the increase in ROS caused by vorinostat (Figures 3E and 3F). The same results were essentially obtained in short-term proliferation assays (Figures 3G-3L), in additional *BRAF*<sup>V600E</sup> mutant melanomas (Figures S3C-S3G), and in the *NRAS* mutant melanoma models (Figure S3H).

To further study the antagonism of ROS and MAPK inhibition, we performed long-term colony formation on A375 cells treated with the BRAFi vemurafenib and/or the ROS inducer paraquat. Figure 3M and S3I show that the ROS inducers paraquat and DMNQ inhibit the proliferation of the cells in a dose dependent manner, but this was counteracted by vemurafenib. Moreover, paraquat and *tert*-butyl-hydroperoxide (tBHP, another ROS inducer) both caused an increase in RAS-GTP loading in A375 cells and prevented vemurafenib from effectively inhibiting MEK activity (Figures 3N and 3O). These results indicate that indeed ROS can positively regulate MAPK signaling, as previously shown by others (22). Consistently, vorinostat can increase RAS-GTP loading in A375, but this induction can be abrogated by co-treatment with the ROS scavenger NAC (Figure 3P). Taken together, these data indicate antagonistic effects of HDACi and MAPKi and emphasize the need to administer MAPK and

HDAC inhibitors sequentially in a therapeutic setting rather than simultaneously, a notion that is tested further below.

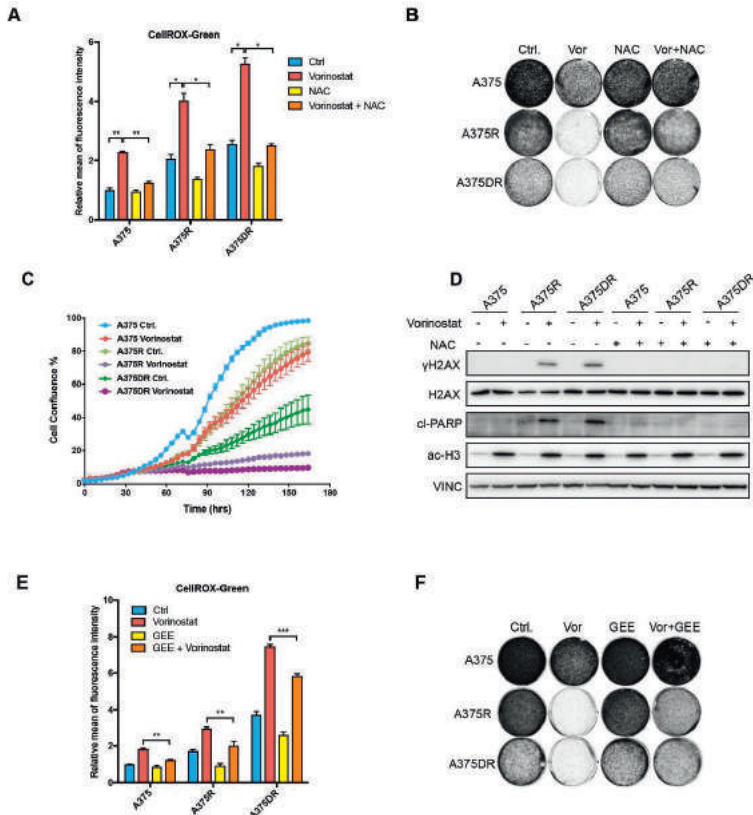


**Figure 2. HDACi is detrimental to MAPKi-resistant melanoma cells.**

(A) Parental and MAPKi-resistant A375 cells were treated with 2  $\mu$ M vorinostat and/or 2.5 mM NAC for 72 hours. ROS levels were measured using CellROX-Green flow cytometry assay. Relative ROS levels are indicated.

(B) Long-term colony formation assays of parental and MAPKi-resistant A375 cells treated with vorinostat and/or NAC. Cells were seeded 50,000 cells per well in 6-well plates and treated with 1  $\mu$ M vorinostat and/or 2.5 mM NAC for 8 days. Afterward, the cells were fixed, stained and photographed.

(C) Incucyte proliferation assay of parental and MAPKi-resistant A375 cells were seeded 400 cells per well in a 384-well plate and cultured in the presence or absence of 1  $\mu$ M vorinostat.

(D) Protein lysates were harvested from the MAPKi-resistant and parental A375 cells treated with 1  $\mu$ M vorinostat and/or 2.5 mM NAC for 72 hr and Western blot analysis performed for gamma-H2AX ( $\gamma$ H2AX) as a DNA damage marker and cleaved-PARP (cl-PARP) as an apoptosis marker. Ac-H3 was used as an indicator for levels of acetylated histone H3. Vinculin (VINC) served as the loading control.

(E) Parental and MAPKi-resistant A375 cells were treated with 2  $\mu$ M vorinostat and/or 2.5 mM reduced glutathione ethyl ester (GEE) for 72 hr. ROS levels were measured using CellROX-Green flow cytometry assay. Relative ROS levels are indicated.

(F) Long-term colony formation assays of parental and MAPKi-resistant A375 cells treated with vorinostat and/or GEE. Cells were seeded 50,000 cells per well in 6-well plates and treated with 1  $\mu$ M

*vorinostat and/or 2.5 mM GEE for 8 days. Afterward, the cells were fixed, stained and photographed. Error bars represent the mean  $\pm$  SD from the biological triplicates (\* $p \leq 0.05$ , \*\* $p \leq 0.01$ , \*\*\* $p \leq 0.001$ , Student's *t*-test). See also figure S2.*

### **HDACi confers a disadvantage to MAPKi resistant melanoma**

We have shown previously that acquisition of resistance to vemurafenib leads to a transient proliferation arrest upon drug withdrawal, phenocopying the transient arrest in tumor growth upon drug withdrawal seen in the clinic, known as the drug holiday effect.(6, 7) Biochemically, vemurafenib withdrawal in drug-resistant cells resulted in hyperactivation of the MAPK pathway and indeed such cells have hallmarks of “oncogene-induced senescence”.(7) Our present data indicate that treatment of MAPKi-resistant melanoma with HDACi results in active cell death, suggesting that this treatment is more effective in MAPKi-resistant melanoma than in drug-sensitive cells. We tested this prediction in a competition assay using a mixed population of parental and two MAPKi-resistant derivatives (R and DR) of A375 cells and Mel888 cells. Drug-sensitive and drug-resistant cells were labeled with green or red fluorescent proteins through transduction with lentiviral vectors encoding GFP and RFP. The two cell populations were mixed in a 1:9 or 1:8 ratio of drug-resistant cells over drug-sensitive cells and cultured with either no drug (drug holiday effect), MAPKi or HDACi, as schematically outlined in Figure 4A. Relative abundance of the two populations was followed over 17 days using quantification by flow cytometry. Figure 4B shows that MAPK inhibition efficiently depleted GFP+ parental cells and enriched RFP+ MAPKi-resistant cells. In contrast, RFP+ MAPKi-resistant cells were depleted by vorinostat treatment, while GFP+ parental cells were enriched. The drug holiday arm followed the same trend as the vorinostat arm; however, the changes were moderate and initiated at a later time point (Figure 4B, 4C, S4A and S4B). These results support the notion that a switch from MAPKi to HDACi can specifically deplete the drug-resistant cells in a heterogeneous melanoma population that harbors both drug sensitive and drug resistant cells. Moreover, the competition experiment indicates that a switch to HDACi upon development of resistance to MAPKi is more effective in eliminating drug-resistant cells than a drug holiday.

### **HDACi induces ROS through suppression of SLC7A11**

To systematically interrogate the molecular pathways governing ROS induction upon HDACi treatment, we performed transcriptome profiling by next-generation RNA sequencing (RNAseq) of A375 parental and MAPKi-resistant derivatives (A375R and A375DR) treated with and without vorinostat. This analysis identified a set of 12 genes commonly downregulated in the three cell lines upon HDACi treatment (Table S1). We focused our attention on *SLC7A11*, as it encodes the cystine-glutamate antiporter xCT.

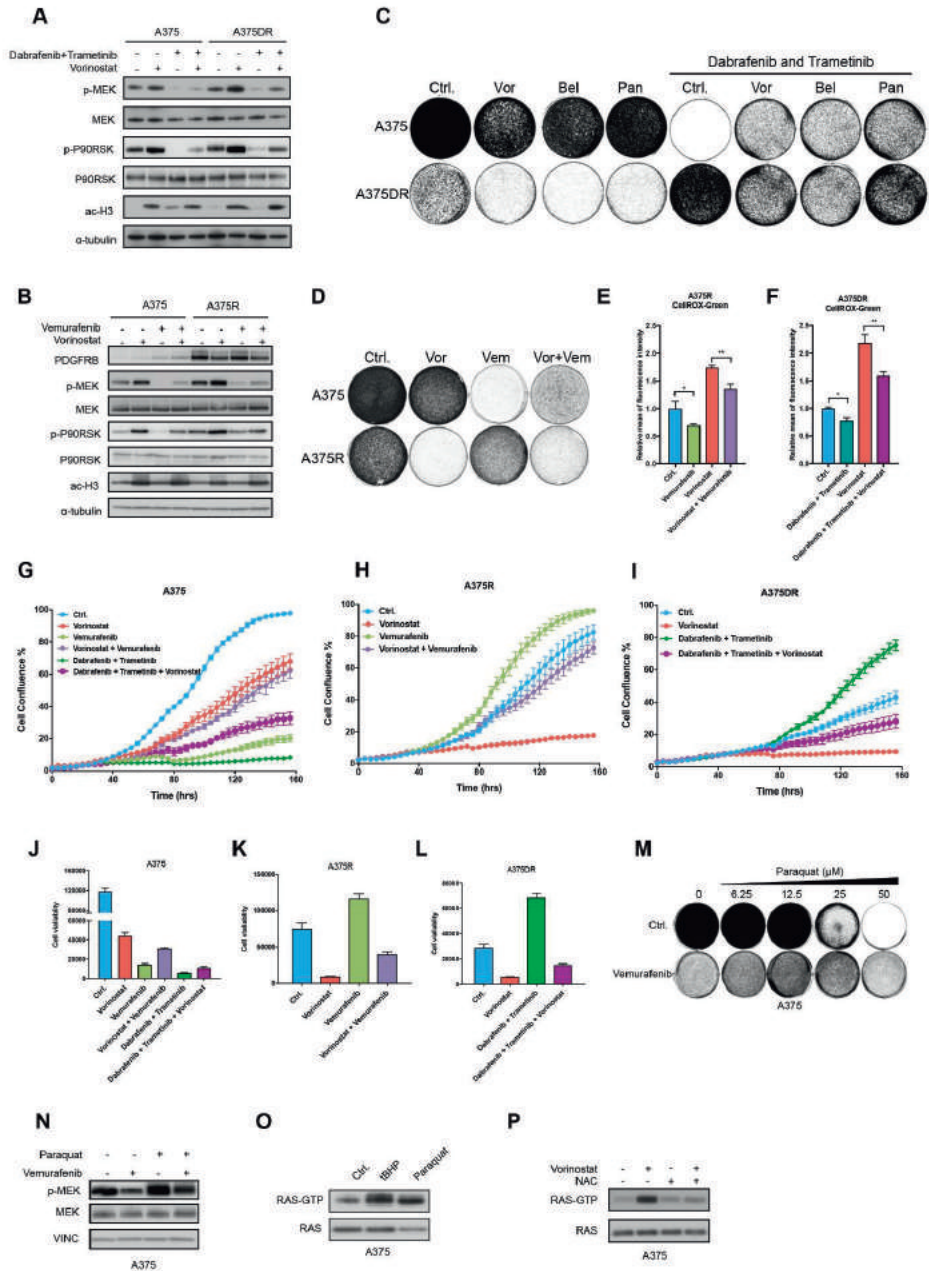




**Figure 3. MAPK inhibition is antagonistic with HDAC inhibition.**

(A) BRAFi/MEKi-resistant A375DR and the parental A375 cells were treated with 2  $\mu$ M vorinostat and/or the combination of 0.125  $\mu$ M dabrafenib and 5 nM trametinib. Protein lysates were harvested after 72 hr. Western blot analysis was carried out for p-MEK and p-P90RSK as indicators of activation of MAPK pathway, ac-H3 as indicator for levels of acetylated histone H3 and  $\alpha$ -tubulin as a loading control.

(B) A375R and the parental cells were treated with 2  $\mu$ M vorinostat and/or 0.5  $\mu$ M vemurafenib for 72 hr, and after which protein lysates were harvested. Western blot analysis was performed for p-MEK and p-P90RSK as activation of MAPK pathway, ac-H3 indicated levels of acetylated histone H3, PDGFRB,  $\alpha$ -tubulin served as the loading control.

(C) A375DR and parental cells were seeded 50,000 cells per well in 6-well plates and treated with 1  $\mu$ M vorinostat (Vor), 0.5  $\mu$ M belinostat (Bel), 5 nM panobinostat (Pan) and/or combination of 5 nM trametinib and 0.125  $\mu$ M dabrafenib.

(D) A375R and parental cells were seeded 50,000 cells per well in 6-well plates and treated with 1  $\mu$ M vorinostat and/or 1  $\mu$ M vemurafenib. After 10 days culturing, the cells were fixed, stained and photographed.

(E and F) Relative ROS level measurements of A375R treated with 2  $\mu$ M vorinostat and/or 2  $\mu$ M vemurafenib (E), A375DR cells with 2  $\mu$ M vorinostat, and/or the combination of 0.125  $\mu$ M dabrafenib and 5 nM trametinib (F).

(G-I) Incucyte proliferation assay of A375 cells (G), A375R cells (H) and A375DR (I) cells seeded at 400 cells per well in a 384-well plate cultured in the presence or absence of 1  $\mu$ M vorinostat, 1  $\mu$ M vemurafenib, and/or combination of 62.5 nM dabrafenib and 5 nM trametinib.

(J-L) At the end of the Incucyte assay, the cell viability of A375 cells. (J), A375R cells (K) and A375DR cells (L) were quantified. Cell viability was measured with CellTiter-Blue.

(M) Long-term colony formation assays of A375 cells treated with 0.25  $\mu$ M vemurafenib and indicated concentrations of paraquat for 10 days.

(N) A375 cells were treated with 50  $\mu$ M paraquat and/or 0.25  $\mu$ M vemurafenib, and protein lysates were harvested after 48 hours. Western blot analysis was performed for p-MEK and total MEK. inculin (VINC) served as the loading control.

(O) RAS-GTP loading measurement by western blot in A375 cells treated for 30 minutes with 125 mM tert-Butyl hydroperoxide (tBHP) or 48 hours of 50  $\mu$ M paraquat treatments.

(P) RAS-GTP loading measurement by western blot in A375 cells treated with 2  $\mu$ M vorinostat and/or 5mM NAC for 72 hr.

Error bars represent the mean  $\pm$  SD from the biological triplicates (\* $p \leq 0.05$ , \*\* $p \leq 0.01$ , \*\*\* $p \leq 0.001$ , Student's t-test). See also figure S3.

This transporter is responsible for the cellular intake of cystine, the precursor of the major antioxidant glutathione (GSH).<sup>(23, 24)</sup> Suppression of this antiporter can therefore lead to reduction of cellular GSH levels and, consequently, increased cellular ROS. It was shown previously that vorinostat suppresses *SLC7A11* expression in malignant gliomas.<sup>(20)</sup> To investigate whether HDACi can induce ROS through *SLC7A11* suppression in *BRAF* or *NRAS* mutant melanomas, we first quantitated changes in *SLC7A11* expression upon treatment of parental and resistant melanoma cells with HDACi using qRT-PCR. Vorinostat indeed transcriptionally suppresses *SLC7A11* in three melanoma models (Figures 5A, S5A and S5I) and reduced GSH levels in two melanoma models (Figures 5B and S5B). In addition, genetic silencing of *SLC7A11* using multiple short hairpin RNAs (shRNAs) increased melanoma ROS levels (Figures 5C and 5D). These shRNAs also suppressed proliferation in our melanoma models, in particular the double-resistant cells (Figures 5E and S5D). Next, we used the most

efficient shRNA (shSLC7A11-4) to study the effect of *SLC7A11* reduction on ROS induction. We observed that *SLC7A11* suppression correlated with increased ROS levels both in the parental cells and also in the MAPKi- resistant derivatives (Figures 5F, 5G, S5C and S5E).

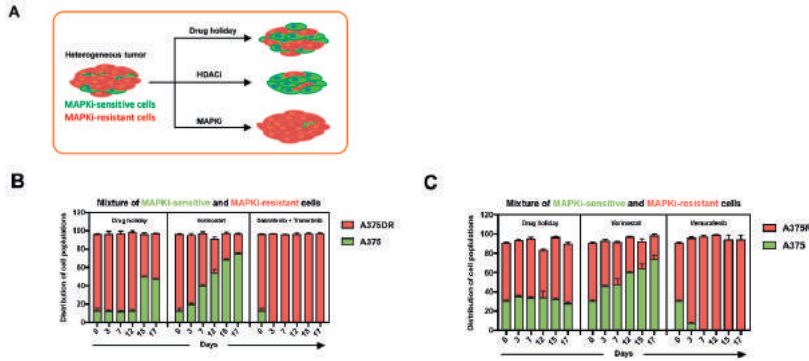


**Figure 4. HDACi is detrimental to MAPKi-resistant melanoma.**

(A) Schematic of the *in vitro* competition assay to study the effect of HDAC inhibition in a heterogeneous tumor containing both MAPKi-resistant and MAPKi-sensitive cells. MAPKi-resistant cells were labeled with red fluorescent protein (RFP) through stable infection with a lentiviral vector pLKO-H2B-RFP. MAPKi-sensitive cells were labeled with GFP by infection with lentiviral vector pLKO-H2B-GFP. After mixing the MAPKi-resistant and sensitive cell populations, the cells were followed after different treatments. MAPK inhibition served as a control. MAPKi treatment resulted in enrichment of RFP+ cells.

(B and C) MAPKi-resistant A375DR cells (RFP+) (B) or A375R cells (C) were mixed at a 9-to- 1 ratio with MAPKi-sensitive parental A375 cells (GFP+) and then 2,000,000 cells were seeded cells into 10-cm dishes and followed after different treatments. At each time point, the distribution of the cell populations was determined using flow cytometry. The ratio of two cell population is indicated at the starting of the experiment (day 0). The distribution changes of the two cell populations are plotted on the Y-axis against the time on the X-axis.

Error bars represent SD of the biological triplicates. See also Figure S4.

This suggests that the HDACi-mediated ROS induction is (at least in part) due to the reduction of *SLC7A11* expression in melanomas, leading to reduced GSH levels. The ROS scavenger trolox acts on the lipid peroxidation process only and does not affect ROS levels in A375R and A375DR cells and did not rescue the toxicity of vorinostat in these cells (Figure S5M and S5N).(25) Glutathione in contrast acts more broadly on oxygen radicals and therefore is more efficient in rescuing increased ROS in melanoma (see also Figure 2E and S2E). To further support the notion that *SLC7A11* suppression is responsible for ROS modulation by HDACi, we overexpressed *SLC7A11* using a lentiviral vector, leading to a 25- to 30-fold increase in *SLC7A11* mRNA levels (Figure 5I). Our data predict that *SLC7A11* overexpression should rescue the HDACi-mediated ROS induction and consequently also the anti-proliferation effect of vorinostat. The short-term IncuCyte proliferation assay (Figures 5J and 5K) and long-term colony formation assay (Figures 5L and S5G) indicate that the HDACi-mediated anti-proliferation effect is reduced by *SLC7A11* overexpression. Quantification of the short-term proliferation assays are shown in Figure S5O. Moreover, HDACi-mediated

ROS induction was abrogated by *SLC7A11* overexpression (Figures 5M and 5SH). This same mechanism was confirmed in additional *NRAS* mutant melanoma (SK-MEL-147) models (Figures S51-S5L).

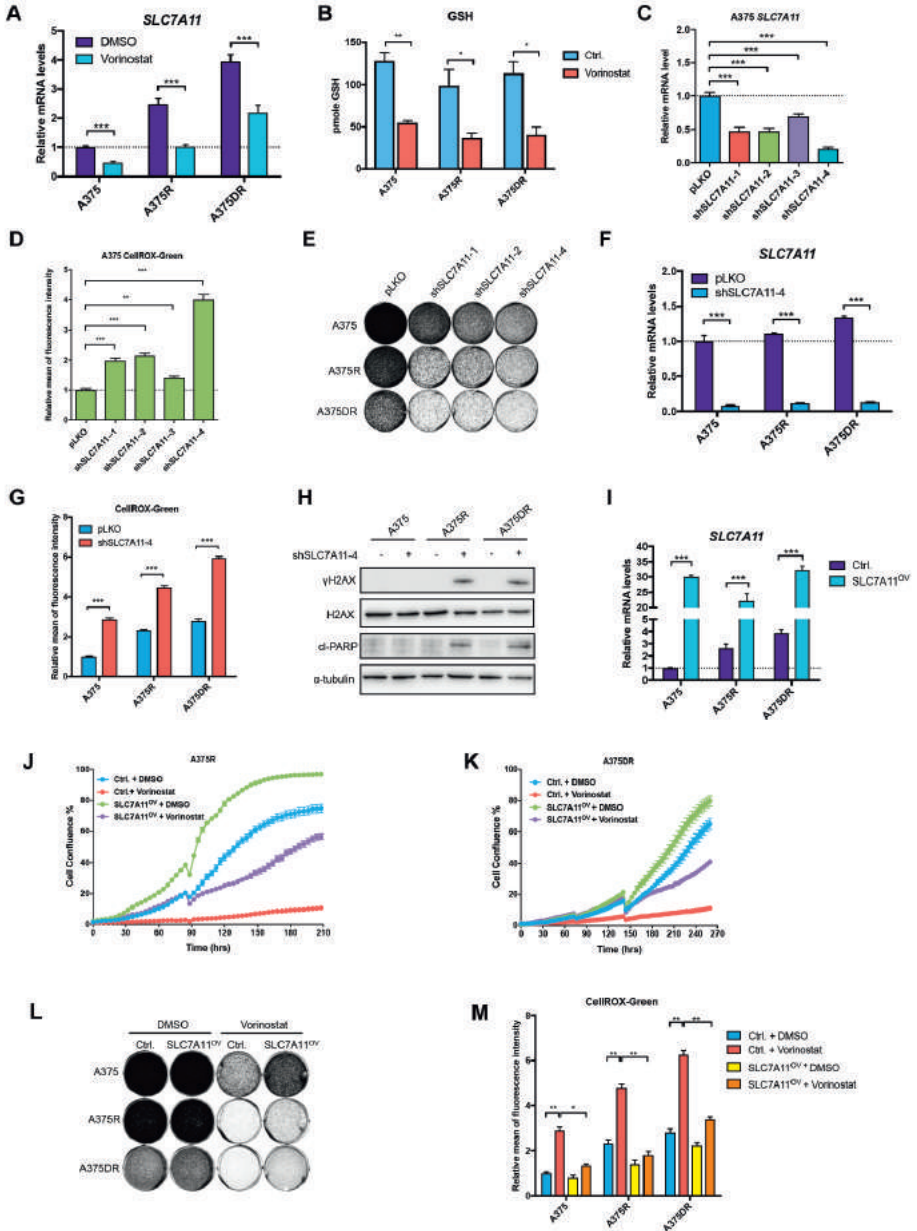


**Figure 5. HDACi suppresses *SLC7A11* resulting in ROS induction.**

(A) mRNA expression analysis of *SLC7A11* by qRT-PCR in parental and MAPK1-resistant A375 cells treated with 2  $\mu$ M vorinostat for 48 hours.

(B) Parental and MAPKi-resistant A375 cells were treated with 2  $\mu$ M vorinostat for 72 hours. Total intracellular glutathione (GSH) levels were measured using colorimetric based glutathione detection assay.

(C) Four independent shRNAs targeting SLC7A11 were individually introduced in A375 cells by lentiviral transduction. pLKO empty vector served as the control. Shown is the level of SLC7A11 knockdown by each shRNAs was measured by qRT-PCR.

(D) Relative ROS induction upon SLC7A11 knockdown as measured by flow cytometry.

(E) Long-term colony formation of parental and MAPKi-resistant A375 cells upon SLC7A11 knockdown. The cells were seeded 50,000 cells per well in 6-well plate and cultured 10 days. Afterwards, the cells were fixed, stained and photographed.

(F) The levels of SLC7A11 knockdown in parental and MAPKi-resistant A375 cells were measured by qRT-PCR.

(G) Relative ROS levels in parental and MAPKi-resistant A375 cells upon SLC7A11 knockdown were measured by CellROX-Green flow cytometry assay.

(H) Protein lysates were harvested from the MAPKi-resistant and parental A375 cells with/without SLC7A11 knockdown. Western blot analysis performed for gamma-H2AX ( $\gamma$ H2AX) as a DNA damage marker and cleaved-PARP (cl-PARP) as an apoptosis marker,  $\alpha$ -tubulin as a loading control.

(I) SLC7A11 was expressed in parental and MAPKi-resistant A375 cells by lentiviral transduction. pLX304 empty vector was used as the control (Ctrl). The level of SLC7A11 overexpression in parental and MAPKi-resistant cells was measured by qRT-PCR of SLC7A11 mRNA.

(J-K) Incucyte proliferation assays indicating the responsiveness to 1 $\mu$ M vorinostat treatment in A375R (J) and A375DR (K) cells with and without SLC7A11 overexpression.

(L) Long-term colony formation of SLC7A11 overexpressing parental and MAPKi-resistant A375 cells in the treatment of vorinostat. The cells were seeded 50,000 cells per well in 6-well plate and cultured 10 days with or without 1 $\mu$ M vorinostat. Afterwards, the cells were fixed, stained and photographed.

(M) SLC7A11 overexpressing parental and MAPKi-resistant A375 cells were treated with 2  $\mu$ M vorinostat for 72 hours. Afterwards, ROS levels were measured using CellROX-Green flow cytometry assay.

Error bars in this figure represent the mean  $\pm$  standard deviations from the biological triplicates (\* $p \leq 0.05$ , \*\* $p \leq 0.01$ , \*\*\* $p \leq 0.001$ , Student's t-test).

### **In vivo study of sequential drug treatment**

Next, we tested the effectiveness of sequential treatment of melanoma with BRAFi, followed by a switch to HDACi upon progression on BRAFi *in vivo*. We injected immunodeficient nude mice with A375 cells and after tumors reached 500 mm<sup>3</sup>, animals were fed a control chow, chow supplemented with PLX4720 (an analog of vemurafenib) or with vorinostat through daily intraperitoneal injection. Figure 6A shows that in the absence of drug or in the presence of vorinostat, A375 cells formed progressively growing tumors. In the presence of PLX4720 tumors regressed initially, but drug-resistant tumors started to emerge approximately 40-50 days after the start of PLX4720 treatment. To address which mechanisms of PLX4720 resistance operated *in vivo*, we re-established four drug-resistant A375 tumors in cell culture (*ex vivo* A1-A4: Exv. A1-A4). Figure 6G shows that each of these four tumor-derived cell lines was highly resistant to vemurafenib, but responded very strongly to vorinostat, belinostat and panobinostat. All four cell lines maintained elevated levels of p-MEK in the presence of vemurafenib (Figure 6C), which is explained by an amplification of BRAF in the case of Exv. A4 cells and a gain of an NRAS<sup>Q61K</sup> mutation in the case of Exv. A3 cells (Figures 6D and 6E). The other two drug-resistant tumor lines exhibited

increased expression of bona fide transforming growth factor  $\beta$  (TGF- $\beta$  target genes, suggestive of the possibility of activated TGF- $\beta$  signaling in these *ex vivo* clones (Figure 6F), which has also been linked to resistance to vemurafenib.(26) These data indicate that a range of different mechanisms can operate *in vivo* to confer resistance to BRAF inhibition and that, like in actual patients, in most cases drug resistance results from re-activation of MAPK signaling. Most importantly, these data also indicate that melanoma cells with reactivated MAPK signaling are very responsive to HDACi, regardless of how MAPK signaling was reactivated.

To test directly in an animal model whether BRAFi-resistant melanomas are responsive to HDACi, we allowed the PLX4720-treated tumors in our mouse cohort to acquire drug resistance (after tumors reached a volume of approximately 400 mm<sup>3</sup> in the presence of drug), which took on average 110 days (Figure 6A). After this, mice were randomized into four treatment cohorts: no drug, vorinostat only, PLX4720 only or the combination of vorinostat and PLX4720. Figure 6B shows the response of the PLX4720-resistant tumors to these four treatment regimens. Continuous PLX4720 treatment resulted in the most rapid tumor growth, consistent with the notion that these cells are fully drug-resistant. PLX4720 withdrawal resulted in a pausing of tumor growth followed by slow growth, analogous to the drug holiday effect seen in drug-resistant patients. A slow-growth phenotype was also seen for tumors treated with a combination of vorinostat and PLX4720, consistent with the notion that these two drugs are antagonistic. Most strikingly, a decline in tumor volume was seen when PLX4720-resistant tumors were switched to vorinostat alone, in agreement with the strong cytotoxic effects of HDACi on BRAFi-resistant melanoma cell lines seen *in vitro*.

### Clinical validation of sequential drug treatment

To investigate the MAPKi-HDACi sequential treatment efficacy in patients, we initiated a clinical study (NCT02836548) to evaluate the effects of vorinostat treatment in *BRAF*<sup>V600E</sup> mutated advanced melanoma patients that had progressed on dabrafenib+trametinib therapy. We synthesized vorinostat under GMP conditions in our own pharmacy (see the STAR methods). Since the *in vitro* studies demonstrated that HDACi and MAPKi act antagonistically, we used a 1-week MAPKi drug washout in patients before vorinostat administration. After this, patients received vorinostat in a safe single daily oral dose of 360 mg, slightly lower than the 400 mg dose approved for use in cutaneous T cell lymphoma.

Tumor measurements were performed every 8 weeks and tumor tissue was collected for exploratory analyses (Figure 7A). Pharmacokinetics of the drug in patients (Table S3) showed very good concordance with literature data.(27) Currently, six patients have been treated and an additional 15 patients will be enrolled in this ongoing study. A more detailed report of this trial will be published elsewhere. Relevant to the potential therapeutic application reported above, we present here molecular analyses from three patients (see Table S2 for patient details) from whom we were able to obtain pre-, during, and post-vorinostat treatment biopsies.

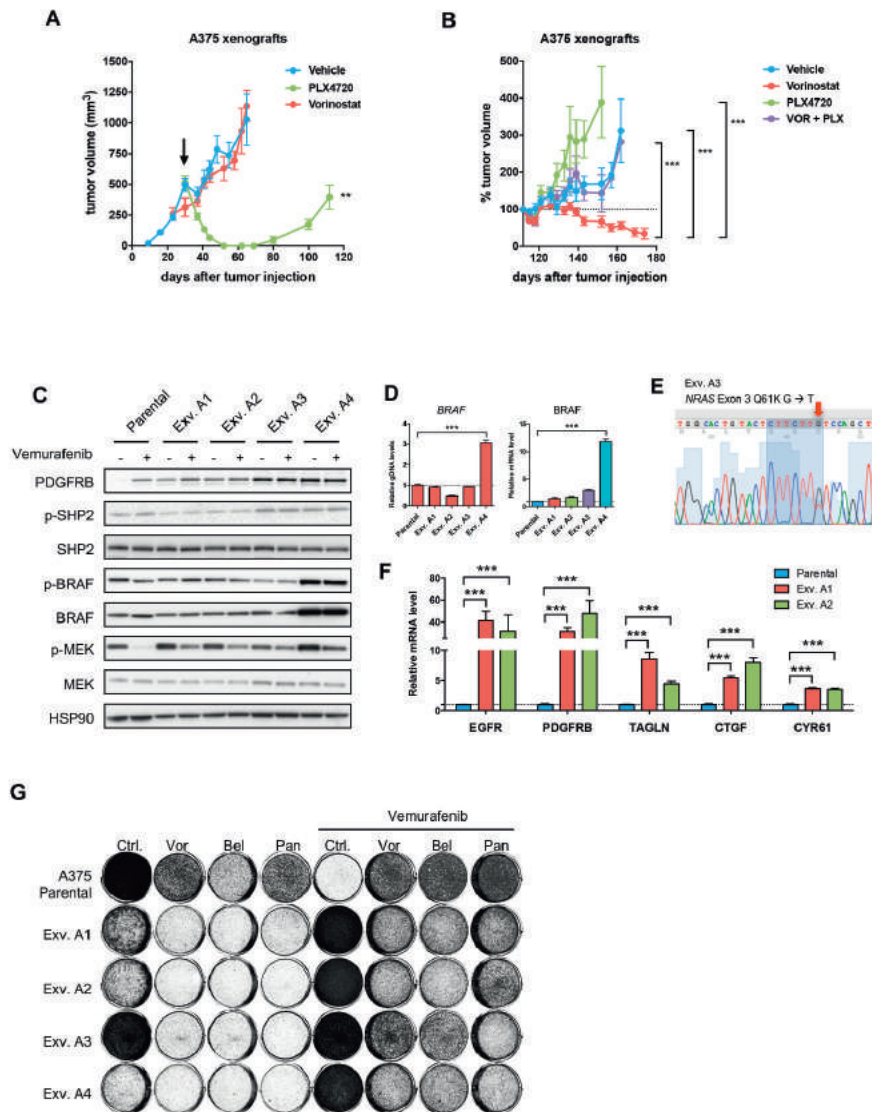


**Figure 6. In vivo responses of BRAF-mutant melanoma to HDAC inhibitors.**

(A) Tumor growth of A375 parental cells in the flanks of Balb/c nude mice subcutaneously injected with  $1 \times 10^6$  A375 cells and, when tumors reached approximately 500 mm<sup>3</sup> (black arrow), mice were assigned to control chow ( $n = 8$ ), PLX4720-supplemented chow (40 mg/kg/day,  $n = 30$ ), or vorinostat (100 mg/kg/day, intraperitoneal injection,  $n = 5$ ).

(B) On day 112 post-injection, PLX4720-treated mice were assigned to control chow ( $n = 7$ ), continuous PLX4720-supplemented chow (40 mg/kg/day,  $n=6$ ), vorinostat (100 mg/kg/day, intraperitoneal injection,  $n = 11$ ), or combination PLX4720-supplemented chow (40 mg/kg/day) and vorinostat (100 mg/kg/day, intraperitoneal injection,  $n=6$ ).

(C) Four BRAFi-resistant ex vivo clones (exv. A1, exv. A2, exv. A3 and exv. A4) were isolated from four different A375 tumors receiving continued PLX4720 treatment from the cohort shown in (B). The protein levels of phosphorylated PDGFRB, p-SHP2, SHP2, p-MEK, MEK and HSP90 were measured by

Western blotting, and A375 parental cell line was treated with 2  $\mu\text{M}$  vemurafenib for 24 hours. HSP90 served as the loading control.

(D) BRAF levels in the four BRAFi-resistant ex vivo clones and parental A375 line were determined by qRT-PCR on genomic DNA (left panel) and mRNA (right panel).

(E) Sanger sequencing analysis of NRAS exon 3 in A375 BRAFi-resistant exv. 3 clone.

(F) Fold changes in mean expression levels, measured by qRT-PCR, of TGF $\beta$  target genes EGFR, PDGFRB, TAGLN, CTGF and CYR61 in A375 BRAFi-resistant exv. 1 and exv. 2, and A375 parental line.

(G) A375 parental and BRAFi-resistant ex vivo clones were treated with a panel of HDACi (1  $\mu\text{M}$  vorinostat, 0.5  $\mu\text{M}$  belinostat and 6 nM panobinostat) in single treatment or in combination with 1 M vemurafenib in a long-term colony formation assay.

Error bars represent the mean  $\pm$  SD from the biological triplicates (\* $p \leq 0.05$ , \*\* $p \leq 0.01$ , \*\*\* $p \leq 0.001$ , Student's *t*-test).

Figures 7B-D show radiological volume measurements of multiple metastatic lesions for these three patients. The curves stop at progression, which is the end of treatment of vorinostat. The time points of biopsies are marked with a red triangle on the curve of the lesion from which the biopsy was taken. The red dotted vertical line marks the start of vorinostat therapy. We used the biopsy transcriptome (RNA-seq) data to assess *SLC7A11* levels in these pre-, during, and post-vorinostat treated tumor biopsies to ask whether HDACi also suppress this gene in patients. Consistent with our *in vitro* data, we observed that vorinostat repressed *SLC7A11* expression in the patient lesions (Figure 7I). We were particularly interested in whether vorinostat therapy could eradicate tumor cells that had gained resistance to BRAF+MEK inhibitor therapy. To assess this, we isolated DNA from these biopsies and searched for changes in the prevalence of drug resistance mutations in the tumors during vorinostat treatment. Intriguingly, patient A harbored the known MAPKi resistance mutation *KRAS*<sup>G12C</sup> before vorinostat treatment at an allele frequency of 44%, but this mutation was reduced to 0% after 3 weeks of vorinostat treatment (Figure 7E). Similarly, the analysis of biopsies from patient B who acquired the *NRAS*<sup>Q61H</sup> mutation at 10% allele frequency during the MAPKi treatment was reduced to 0% after vorinostat therapy (Figure 7F). Patient C developed an *NRAS* amplification as judged by the increased read count for the *NRAS* gene and mRNA expression as judged by RNA-seq (Figures 7G and 7H), but its level of amplification and expression was reduced upon vorinostat treatment (Figures 7G and 7H). These findings are in line with our *in vitro* and mouse data and demonstrate that BRAF+MEK inhibitor resistant melanoma cells can be preferentially eliminated by treatment with vorinostat. No significant effects of vorinostat were seen on infiltration of immune cells in the metastatic lesions (Figure S6).

## Discussion

We identify here a vulnerability of *BRAF* mutant melanomas that is specifically acquired upon development of resistance to inhibitors of the MAPK pathway. When patients progress on first line therapy, subsequent therapies have a tendency to become increasingly less effective. However, theoretically this does not have to be the case. It is a well-established principle that drug resistance comes at a “fitness cost” for the cancer cell that in turn can lead to novel vulnerabilities of the drug resistant cells.(8) Such acquired vulnerabilities have

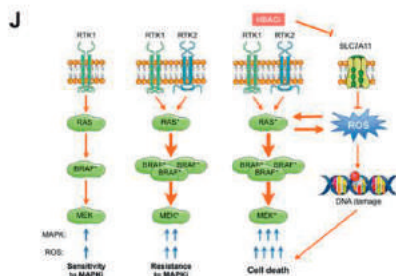
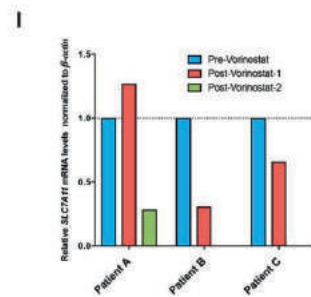
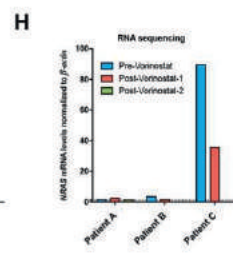
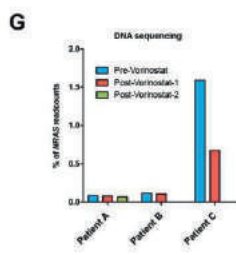
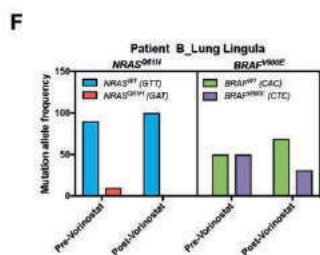
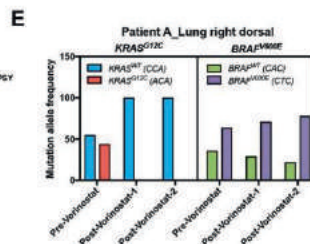
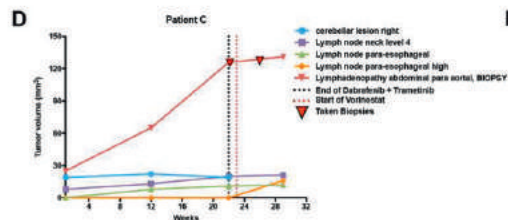
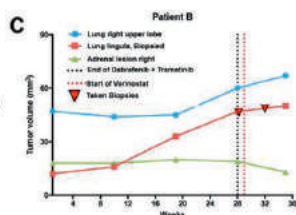
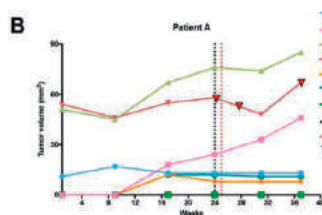
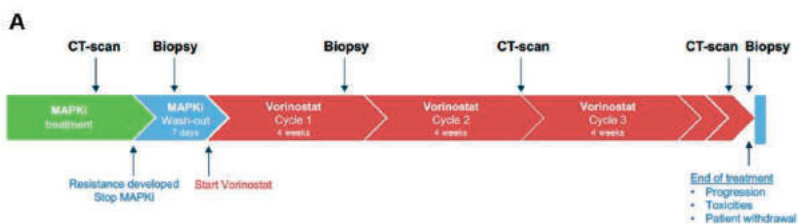




**Figure 7. HDACi responsiveness in MAPK inhibitor resistant melanoma patients.**

(A) Diagram of the design of clinical trial NCT02836548 proof-of-concept study of vorinostat treatment in MAPKi-resistant melanoma patients.

(B) Tumor responsiveness to vorinostat in MAPKi-resistant melanoma patient A evaluated by CT scan measurements. The tumor volume of multiple lesions was plotted on the y axes against time on the x axes.

(C) Like in (B), except for patient B.

(D) Like in (B), except for patient C. Biopsies were collected at indicated time points (inverted red triangles) on the curves of the target lesions (solid red lines).

(E and F) Genomic DNA isolated from the biopsied target lesions of patient A was analyzed using the NKI-178 gene panel using targeted NGS, as described.(28) Representation of the allele frequency of drug-resistance associated  $KRAS^{G12C}$  mutation in patient A (E) and  $NRAS^{Q61H}$  in patient B.

(F) Pre- and post-vorinostat treatment.  $BRAF^{V600E}$  mutation in each panel served as an indication of tumor cell percentage in the biopsy.

(G) DNA copy number level of  $NRAS$  gene, as measured by the percentage of NGS reads for this gene as percentage of total captured reads.

(H) Normalized transcript levels of  $NRAS$  analyzed by RNAseq in the patients' biopsies pre- and post-vorinostat treatment.  $\beta$ -actin served as a housekeeping gene for normalization.

(I) Fold change in expression levels of  $SLC7A11$  in patients' biopsies pre- and post-vorinostat treatment deduced from RNA-seq data.

(J) Model for the sequential treatment of melanomas.  $BRAF^{V600E}$  ( $BRAF^*$ ) melanoma cells with normal MAPK signaling and normal ROS levels are sensitive to MAPKi (left). Drug resistance develops through upregulation of RTKs, RAS mutations ( $RAS^*$ ),  $BRAF$  amplification or MEK mutations ( $MEK^*$ ), all of which result in enhanced signaling through the MAPK pathway and increased ROS levels (center). Switching therapy from a MAPKi to an HDACi in MAPKi-resistant cells induces ROS through downregulation of  $SLC7A11$ . The increased ROS also act on RAS to maintain high levels of MAPK signaling. Cellular ROS levels are already increased in MAPKi-resistant tumors and the further increase of ROS by HDACi leads to a massive DNA damage response that has a lethal effect on the cells (right).

See also Figure S6 and Tables S2 and S3.

in the past been searched for through compound screens in pairs of sensitive and chemotherapy resistant cancer cells.(29, 30) These efforts have been relatively unproductive from a clinical perspective, most likely because cancer cells have many avenues to become chemotherapy insensitive, making the collateral sensitivities of drug resistant cells equally heterogeneous and unpredictable. This issue is less relevant for  $BRAF$  mutant melanoma, as resistance to MAPK pathway inhibition more often than not leads to secondary mutations that re-activate the MAPK pathway in the presence of drug. This predictable resistance mechanism may also lead to more foreseeable collateral sensitivities as compared to the chemotherapy resistance models. Indeed, our data show that melanoma cells that have acquired resistance to MAPK inhibitors through different MAPK pathway reactivation mechanisms all become sensitive to HDACi, including  $PDGFRB$  overexpression (A375R cells) (Figure 1C),  $NRAS^{Q61H}$  mutation (A375DR cells) (Figure 1D),  $KRAS^{G12C}$  (Mel888DR cells) (Figure S1E),  $BRAF$  splice site mutations (Mel888R cells) (Figure 1D) and  $BRAF$  amplification (A375 Exv A4) (Figures 6C and 6D). The common vulnerability we identified in these MAPK resistant cells results from the induction of ROS by hyperactive MAPK pathway signaling. Consequently, further activation of these increased ROS levels by vorinostat leads to

significant DNA damage and apoptotic cell death only in the MAPK-resistant cells, but not in the drug-sensitive cells that have lower ROS levels. Consistent with this, we see no effect of vorinostat in MAPK inhibitor-sensitive melanoma cells.

Vorinostat has proven anticancer activity and was approved in 2006 for use in cutaneous T cell lymphoma. Our data indicate that ROS induction plays a major part in the killing of BRAF inhibitor-resistant melanoma cells by vorinostat, as the ROS scavengers NAC and GEE counteracted the vorinostat effects. The vorinostat effect on ROS induction is primarily caused by suppression of *SLC7A11*, as ectopic *SLC7A11* expression rescued ROS induction by vorinostat (Figure 5K and S5G). This gene encodes the importer of cystine, which serves as a precursor to the ROS scavenger glutathione. *SLC7A11* expression did not completely rescue the anti-proliferative effect of vorinostat in BRAF inhibitor-resistant melanoma, consistent with the notion that vorinostat also has ROS-independent effects on cancer cells (Figure 5J and S5F). Together, these data support a model in which the increased ROS level in BRAF-resistant melanoma becomes a liability when ROS levels are increased further by HDACi treatment, leading to DNA damage and apoptotic cell death (Figure 7J).

We find that vorinostat treatment in mouse xenograft tumors that have developed resistance to BRAF inhibitor *in vivo* leads to tumor regressions. This was not seen when BRAFi-resistant tumor cells were treated with a combination of BRAFi+HDACi, in agreement with our *in vitro* findings showing that the two drugs are antagonistic. The molecular basis for the notion that BRAFi and HDACi must not be used simultaneously is provided by our finding that increased MAPK signaling resulting from BRAF inhibitor resistance leads to an increase in ROS levels that are increased to toxic levels by subsequent treatment with vorinostat. Conversely, MAPK inhibition with selective drugs diminishes ROS levels. While vorinostat can increase these lower ROS levels in the presence of MAPK inhibitors also, they do not reach toxic concentrations that result in DNA damage and cell death (Figures 3D-3F). The finding that BRAF and HDAC inhibitors must be used sequentially was unexpected as a recent publication demonstrated that combination of BRAF and HDAC inhibitors upfront can prevent emergence of resistant melanoma cells in a short-term assay.(21) This difference most likely has its origin in the notion that the effects of epigenetic drugs like vorinostat take considerable time to develop. That lethal ROS levels can be used to kill cancer cells was recently also shown by others using a combination of mTOR and HDAC inhibitors in *NF1* and *RAS* mutant cancers.(31) The fundamental difference between this observation and ours is that Malone *et al.* used simultaneous treatment with two drugs to increase ROS levels to lethal levels, whereas in our melanoma model, it is mandatory to use the drugs sequentially to reach toxic ROS levels. Indeed, most other recent publications that identify combinations of drugs to prevent resistance development use upfront combinations to accomplish this.(32, 33) The sequential treatment we identify here has the advantage that it avoids toxicity arising from simultaneous use of drugs. Therefore, sequential drug therapy enables the use of a much larger drug repertoire than simultaneous use. In a pilot study in patients with advanced *BRAF* mutant melanoma that progressed on BRAF+MEK inhibitor therapy we see that tumor cells harboring a drug-resistance mutation are quickly depleted by vorinostat,

consistent with the sensitivity of these cells to vorinostat seen *in vitro* and in mouse models. In patients, tumors initially stabilize upon switch to vorinostat therapy, but then progression occurs. This is not unexpected, given that parental, MAPK inhibitor sensitive, tumor cells fail to respond to vorinostat. After initial depletion of the drug-resistant clones in the tumor by vorinostat therapy, the BRAF+MEK inhibitor sensitive clones continue to proliferate, leading to progression. To avoid this problem, we plan to adapt the protocol for the ongoing trial NCT02836548 to include monitoring of patients on BRAF+MEK inhibitor therapy for early signs of drug resistance through analysis of cell free tumor DNA in blood.(34) Such mutations are often detectable before radiological progression is evident.(35) By pulsatile treatment with vorinostat to eradicate emergent drug-resistant cells, followed by a switch back to BRAF+MEK inhibition, we expect to get longer progression free survival benefit for patients as compared to an intermittent BRAF inhibitor only regimen(36), which in the context of *EGFR* mutant lung cancer does not seem very effective in the clinic.(37, 38) Indeed, our *in vitro* data indicate that switching from MAPK inhibitor therapy to vorinostat is more effective in eradicating drug-resistant cells than a drug holiday (Figures 4 and S4). We cannot exclude that drug-resistance mechanisms occur in patients that are not associated with reactivation of the MAPK pathway. If they occur, such drug-resistant variants may not respond to vorinostat therapy. We note that all melanoma cells that acquired resistance *in vitro* or *in vivo*, including the three patients analyzed here, upregulated the MAPK pathway to gain resistance and thereby gained susceptibility to HDAC inhibition. More generally, our data highlight that studying how cancer cells acquire resistance to targeted cancer drugs may be fruitful to identify novel vulnerabilities that can be exploited therapeutically.

### Acknowledgements

We thank Plexxikon Inc. (Berkeley, CA, USA) for providing PLX4720. This work was funded by a grant from the Dutch Cancer Society (KWF, grant number NNKI2012-5401), the European Research Council (ERC, grant number 250043) and the Center for Cancer Genomics (CGC.nl, grant number 024.001.028). The clinical study was supported by a proof of concept ERC grant, grant number 712951.

### Author contributions

L.W., R.L.d.O, co-designed the study, performed experiments and wrote the manuscript. E.B., N.P., D.B., A.B., J-Y.S., J.Z., T.L-d.V., H.H. performed and interpreted the experiments. B.N., J.H.B. synthesized and formulated the vorinostat. S.H., J.H.M.S. designed and performed the clinical study. R.B. co-designed the study, wrote the manuscript and supervised the project. All authors contributed to the manuscript text.

### Declaration of interests

L.W., R.L.d.O., and R.B. are listed as investors on a patent application on the use of HDAC inhibitors in MAPKi-resistant melanoma. All other authors declare no competing interest.

## References

1. Sosman JA, Kim KB, Schuchter L, Gonzalez R, Pavlick AC, Weber JS, et al. Survival in BRAF V600-mutant advanced melanoma treated with vemurafenib. *The New England journal of medicine*. 2012;366(8):707-14.
2. Robert C, Karaszewska B, Schachter J, Rutkowski P, Mackiewicz A, Stroiakovski D, et al. Improved overall survival in melanoma with combined dabrafenib and trametinib. *The New England journal of medicine*. 2014;372(1):30-9.
3. Van Allen EM, Wagle N, Sucker A, Treacy DJ, Johannessen CM, Goetz EM, et al. The genetic landscape of clinical resistance to RAF inhibition in metastatic melanoma. *Cancer discovery*. 2014;4(1):94-109.
4. Wagle N, Van Allen EM, Treacy DJ, Frederick DT, Cooper ZA, Taylor-Weiner A, et al. MAP kinase pathway alterations in BRAF-mutant melanoma patients with acquired resistance to combined RAF/MEK inhibition. *Cancer discovery*. 2014;4(1):61-8.
5. Manzano JL, Layos L, Bugés C, de Los Llanos Gil M, Vila L, Martínez-Balibrea E, et al. Resistant mechanisms to BRAF inhibitors in melanoma. *Annals of translational medicine*. 2016;4(12):237.
6. Seghers AC, Wilgenhof S, Lebbé C, Neyns B. Successful rechallenge in two patients with BRAF-V600-mutant melanoma who experienced previous progression during treatment with a selective BRAF inhibitor. *Melanoma research*. 2012;22(6):466-72.
7. Sun C, Wang L, Huang S, Heynen GJJE, Prahallad A, Robert C, et al. Reversible and adaptive resistance to BRAF(V600E) inhibition in melanoma. *Nature*. 2014;508(7494):118-22.
8. Hutchison DJ, Haddow A, Weinhouse S, et al. Cross resistance and collateral sensitivity studies in cancer chemotherapy. *Advances in cancer research*. 1963;7: 235-350.
9. Vazquez F, Lim JH, Chim H, Bhalla K, Girnun G, Pierce K, et al. PGC1alpha expression defines a subset of human melanoma tumors with increased mitochondrial capacity and resistance to oxidative stress. *Cancer Cell*. 2013;23(3):287-301.
10. Haq R, Shoag J, Andreu-Perez P, Yokoyama S, Edelman H, Rowe GC, et al. Oncogenic BRAF regulates oxidative metabolism via PGC1alpha and MITF. *Cancer Cell*. 2013;23(3):302-15.
11. Corazao-Rozas P, Guerreschi P, Jendoubi M, André F, Jonneaux A, Scalbert C, et al. Mitochondrial oxidative stress is the Achilles' heel of melanoma cells resistant to Braf-mutant inhibitor. *Oncotarget*. 2013;4(11):1986-98.
12. Hernandez-Davies JE, Tran TQ, Reid MA, Rosales KR, Lowman XH, Pan M, et al. Vemurafenib resistance reprograms melanoma cells towards glutamine dependence. *Journal of translational medicine*. 2015;13:210.
13. Baenke F, Chaneton B, Smith M, Van Den Broek N, Hogan K, Tang H, et al. Resistance to BRAF inhibitors induces glutamine dependency in melanoma cells. *Molecular oncology*. 2016;10(1):73-84.
14. Lee AC, Fenster BE, Ito H, Takeda K, Bae NS, Hirai T, et al. Ras proteins induce senescence by altering the intracellular levels of reactive oxygen species. *The Journal of biological chemistry*. 1999;274(12):7936-40.
15. Reczek CR, Chandel NS. The two faces of reactive oxygen species in cancer. *Annual review of cancer biology*. 2017;1(1):79-98.
16. Chio IIC, Tuveson DA. ROS in cancer: The burning question. *Trends in molecular medicine*. 2017;23(5):411-29.
17. Ruefli AA, Ausserlechner MJ, Bernhard D, Sutton VR, Tainton KM, Kofler R, et al. The histone deacetylase inhibitor and chemotherapeutic agent suberoylanilide hydroxamic acid (SAHA) induces a cell-death pathway characterized by cleavage of Bid and production of reactive oxygen species. *Proceedings of the National Academy of Sciences*. 2001;98(19):10833-8.
18. Ungerstedt JS, Sowa Y, Xu WS, Shao Y, Dokmanovic M, Perez G, et al. Role of thioredoxin in the response of normal and transformed cells to histone deacetylase inhibitors. *Proceedings of the National Academy of Sciences*. 2005;102(3):673-8.

19. Petruccelli LA, Dupéré-Richer D, Pettersson F, Retrouvey H, Skoulikas S, Miller WH, Jr. Vorinostat induces reactive oxygen species and DNA damage in acute myeloid leukemia cells. *PLoS one*. 2011;6(6):e20987.
20. Wolf IM, Fan Z, Rauh M, Seufert S, Hore N, Buchfelder M, et al. Histone deacetylases inhibition by SAHA/Vorinostat normalizes the glioma microenvironment via xCT equilibration. *Scientific reports*. 2014;4:6226.
21. Johannessen CM, Johnson LA, Piccioni F, Townes A, Frederick DT, Donahue MK, et al. A melanocyte lineage program confers resistance to MAP kinase pathway inhibition. *Nature*. 2013;504(7478):138-42.
22. Son Y, Cheong YK, Kim NH, Chung HT, Kang DG, Pae HO. Mitogen-activated protein kinases and reactive oxygen species: How can ROS activate MAPK pathways? *Journal of signal transduction*. 2011;2011:792639.
23. Bannai S, Tateishi N. Role of membrane transport in metabolism and function of glutathione in mammals. *The Journal of membrane biology*. 1986;89(1):1-8.
24. Gout PW, Kang YJ, Buckley DJ, Bruchoovsky N, Buckley AR. Increased cystine uptake capability associated with malignant progression of Nb2 lymphoma cells. *Leukemia*. 1997;11(8):1329-37.
25. Valko M, Leibfritz D, Moncol J, Cronin MT, Mazur M, Telser J. Free radicals and antioxidants in normal physiological functions and human disease. *The international journal of biochemistry & cell biology*. 2007;39(1):44-84.
26. Huang S, Holzel M, Knijnenburg T, Schlicker A, Roepman P, McDermott U, et al. MED12 controls the response to multiple cancer drugs through regulation of TGF-beta receptor signaling. *Cell*. 2012;151(5):937-50.
27. Iwamoto M, Friedman EJ, Sandhu P, Agrawal NG, Rubin EH, Wagner JA. Clinical pharmacology profile of vorinostat, a histone deacetylase inhibitor. *Cancer chemotherapy and pharmacology*. 2013;72(3):493-508.
28. Groenendijk FH, de Jong J, Franssen van de Putte EE, Michaut M, Schlicker A, Peters D, et al. ERBB2 mutations characterize a subgroup of muscle-invasive bladder cancers with excellent response to neoadjuvant chemotherapy. *European urology*. 2016;69:384-8.
29. Jensen PB, Holm B, Sorensen M, Christensen IJ, Sehested M. In vitro cross-resistance and collateral sensitivity in seven resistant small-cell lung cancer cell lines: preclinical identification of suitable drug partners to taxotere, taxol, topotecan and gemcitabine. *British journal of cancer*. 1997;75(6):869-77.
30. Rickardson L, Fryknäs M, Haglund C, Lövborg H, Nygren P, Gustafsson MG, et al. Screening of an annotated compound library for drug activity in a resistant myeloma cell line. *Cancer chemotherapy and pharmacology*. 2006;58(6):749.
31. Malone CF, Emerson C, Ingraham R, Barbosa W, Guerra S, Yoon H, et al. mTOR and HDAC inhibitors converge on the TXNIP/Thioredoxin pathway to cause catastrophic oxidative stress and regression of RAS-driven tumors. *Cancer discovery*. 2017;7(12):1450-63.
32. Hangauer MJ, Viswanathan VS, Ryan MJ, Bole D, Eaton JK, Matov A, et al. Drug-tolerant persister cancer cells are vulnerable to GPX4 inhibition. *Nature*. 2017;551(7679):247-50.
33. Sharma SV, Lee DY, Li B, Quinlan MP, Takahashi F, Maheswaran S, et al. A chromatin-mediated reversible drug-tolerant state in cancer cell subpopulations. *Cell*. 2010;141(1):69-80.
34. Murtaza M, Dawson SJ, Tsui DW, Gale D, Forshew T, Piskorz AM, et al. Non-invasive analysis of acquired resistance to cancer therapy by sequencing of plasma DNA. *Nature*. 2013;497(7447):108-12.
35. Misale S, Yaeger R, Hobor S, Scala E, Janakiraman M, Liska D, et al. Emergence of KRAS mutations and acquired resistance to anti-EGFR therapy in colorectal cancer. *Nature*. 2012;486:532-6.

36. Das Thakur M, Salangsang F, Landman AS, Sellers WR, Pryer NK, Levesque MP, et al. Modelling vemurafenib resistance in melanoma reveals a strategy to forestall drug resistance. *Nature*. 2013;494(7436):251-5.
37. Yu HA, Sima C, Feldman D, Liu LL, Vaitheesvaran B, Cross J, et al. Phase 1 study of twice weekly pulse dose and daily low-dose erlotinib as initial treatment for patients with EGFR-mutant lung cancers. *Annals of oncology*. 2017;28(2):278-84.
38. Kaiser J. When less is more. *Science*. 2017;355(6330):1144.

## Materials and methods

### METHOD DETAILS

#### Long-term colony formation assay and IncuCyte cell proliferation assays

Cells were seeded into 6-well plates (50,000 cells per well) or 12-well plates (30,000 cells per well) and cultured both in the absence and presence of drugs as indicated for 10-15 days. At the end of the assay, cells were fixed with 4% of formaldehyde (#1.04002, Millipore) diluted in PBS, stained with 2% of crystal violet (#HT90132 Sigma-Aldrich) diluted in water and photographed. For IncuCyte proliferation assays, cells were seeded in 384-well plate (400 cells per well) and cultured in absence or presence of drugs as indicated. Cell confluence was measured and quantified by the IncuCyte imaging system (Essen Bioscience).

#### Cell viability measurement

Cell viability was detected using CellTiter-Blue® Cell Viability Assay Kit (G8081, Promega) according to the manufacturer's instructions. The assay measurement was performed using EnVision multi-label plate reader (PerkinElmer).

#### Protein lysate preparation and immunoblotting

Cells were seeded in DMEM-based medium containing 10% fetal bovine serum (FBS) in the absence or presence of drug for 48 or 72 hours. The drugs were daily refreshed. Afterwards, the cells were washed with PBS and lysed with RIPA buffer supplemented with protease inhibitors (cOmplete, Roche) and phosphatase inhibitor cocktails II and III (Sigma). All lysates were freshly prepared and processed with Novex NuPAGE Gel Electrophoresis Systems (Invitrogen). The detection was performed after 48 or 72 hours drug treatment.

#### ROS detection

The cells were treated in the absence or presence of drugs for 72 hours, daily refreshed. ROS level in cells was detected using CellROX® Green Flow Cytometry Assay Kit (C10492, Life Technologies) according to the manufacturer's instructions. Drugs remained present during the assay.

#### Glutathione detection

The cells were treated in the absence or presence of drugs for 72 hours, daily refreshed. Total GSH level in cells was detected using Glutathione detection kit (ADI-900-160, Enzo) according to the manufacturer's instructions.

#### Competition assay

The MAPKi-resistant cells were stably transfected with pLKO-H2B-RFP. The MAPKi-sensitive parental cells were stably transfected with pLKO-H2B-GFP. Afterwards, two cell populations were mixed and then seeded 2,000,000 cells into 10-cm dishes for biological replicates and different 6 treatment arms. At each time point, the distribution of the cell populations was determined using flow cytometry (The BD LSRFortessa™ cell analyzer, BD Biosciences). The ratio of two cell populations was indicated. Day 0 is the starting of the assay; this also indicates the ratio of the seeded GFP and RFP cells. The medium containing drugs were refreshed during each time point. During the experiment, when cells reach 80% confluency in the plates, the cells were re-seeded 2,000,000 cells into a new 10-cm dish.

### **qRT-PCR**

Total RNA was extracted from cells using TRIzol reagent from Invitrogen or Quick-RNA™ MiniPrep (# R1055) from Zymo Research. cDNA synthesis was performed using Maxima Universal First Strand cDNA Synthesis Kit (#K1661) from Thermo scientific. qPCR reactions were performed with FastStart Universal SYBR Green Master (Rox) from Roche. The experiments were performed according to the manufacturer's instructions. The sequences of the primers used for qRT-PCR analyses are described in the key resource table. All reactions were run in triplicate. The CT values were calculated using the Standard Curve Method.

### **Detection of genomic DNA alterations**

Genomic DNA was isolated using DNeasy® Blood&Tissue kit (#6950, Qiagen) according to the manufacture's instructions. 40ng gDNA was inputted for 40 cycles of PCR. Next, the PCR products were cleaned with ExoSAP-IT® (#78200, Affymetrix) and capillary sequenced using the BigDye terminator V3.1 sequencing Kit (Applied Biosystems). The sequences of the primers used to detect the genomic alternations in NRAS, KRAS and BRAF are described in Supplementary Table 1. All the sequencing was verified with Forward and Reverse primers.

### **Lentiviral transduction**

A third-generation lentivirus packaging system consisting of pCMV-VSV-G (addgene#8454), pRSV-Rev (Addgene#12253) and pMDLg/pRRE (Addgene#12251) was used to create virus particles of the modified reporter plasmids. A transient transfection was performed in 293T cells and lentiviral supernatants were produced. Destination cells were infected with lentiviral supernatants, using 8µg/ml Polybrene and low virus titer. After 48h of incubation, the supernatant was replaced by medium containing 10 µg/ml Blasticidin or 2 µg/ml Puromycin. After 48h, selection of viral transduced cell lines was completed. All the lentiviral vectors in the study are described in supplemental experiment procedure.

### **Relative growth rate calculation**

The growth rate of each replicate was calculated as the slope a curve fitted through the linear range of the log-transformed confluence measurements (the first 84 hours for A375R and 76 hours for A375DR) of the Incucyte proliferation experiment. For each cell line, the growth rates were normalized to the mean of the untreated controls. The growth rate of untreated control was considered as a basal line and normalized to 1. The relative growth rates of all growth rates of the drug-treated and genetic manipulated arms were compared with the untreated control arm. Error bars indicate standard deviation of 4 replicates.

### **Active RAS Pull-Down detection**

Melanoma cells were treated in the absence or presence of drugs for 72 hours, daily refreshed. RAS-GTP levels were detected using RAS Assay Reagent (RAF-1 RBD, agarose, Merck Millipore according to the manufacturer's instructions.

### **Vorinostat synthesis**

Vorinostat (N-hydroxy-N'-phenyloctanediamide) has been synthesized with suberic acid as starting material. The method is based on the procedure described by Mai and co-workers (Mai et al., 2001). Suberic acid was treated with acetic anhydride to form its cyclic anhydride. By stirring in tert- butylmethylether rather pure cyclized anhydride is obtained. The second



step is the reaction of the cyclized anhydride with aniline. This yields three products: suberic acid, mono-anilide (desired product) and bis-anilide. The mono-anilide is isolated in relatively high purity from the mixture. A final trituration in tert-butylmethylether will give 93-96% pure mono-anilide. Last step is the formation of the hydroxylamide to form vorinostat. After multiple crystallizations the desired purity of 99% is obtained. All conversions, after each step, are followed by <sup>1</sup>H NMR spectroscopy and liquid chromatography with mass spectrometric (LC-MS) detection. Vorinostat capsules have been manufactured under GMP conditions by mixing vorinostat drug substance with microcrystalline cellulose PH102 followed by semi-automatic filling into red, hard gelatin capsules (size 0). Each capsule contains an amount of 90 mg vorinostat. Vorinostat capsules are packed per 28 capsules in HD-PE containers and labeled according to GMP EU Annex 13. Vorinostat capsules are stable for at least 1 year at room temperature. Quality control of vorinostat capsules encompasses determination of identity, content, purity and uniformity of dosage units, using a validated reversed phase high performance liquid chromatography method with UV detection at 241 nm. Column: Symmetry Shield RP8 150 x 2.1 mm ID and particle size 3.5 μm. Mobile phase: A, 0.5 % acetic acid in water; B, 0.5% acetic acid in acetonitrile (90/10). Flow: 300 μL/min. Temperature: 30 °C.

#### **NKI 178 gene panel exosome next generation DNA sequencing**

DNA were isolated from the fresh frozen tumour biopsies. Target enrichment DNA nextgeneration sequencing was performed with a custom SureSelect XT2 bait library (Agilent Technologies) covering a selected panel of 178 genes, consisting of (indirect or direct) clinically relevant genes. The experimental details are described (Groenendijk et al., 2016).

#### **Immunohistochemistry**

Immunohistochemistry of the FFPE tumor samples was performed on a BenchMark Ultra (CD3, CD4, CD8, CD20, CD56 and CD68) automated stainer (Ventana Medical Systems). Briefly, paraffin sections were cut at 3 μm, heated at 75°C for 28 minutes and deparaffinized in the instrument with EZ prep solution (Ventana Medical Systems). Heat-induced antigen retrieval was carried out using Cell Conditioning 1 (CC1, Ventana Medical Systems) for 32 minutes at 950C (CD3, CD4, CD8, CD20, CD56 and CD68). CD3 was detected using clone SP7 (1/100 dilution, 32 minutes at 370C, Spring / ITK), CD4 clone SP35 (1/50 dilution, 32 minutes at 370C, Cell Marque), CD8 clone C8/144B (Dako / Agilent) using 1/200 dilution 32 minutes at 370C, CD20 using clone L26 (1/800 dilution, 32 minutes at 370C, Dako / Agilent), CD56 clone MRQ-75 (1/2000 dilution, 32 minutes at 370C, Cell Marque), CD68 clone KP1 (Dako / Agilent) using 1/20000 dilution 32 minutes at 370C. detection for CD markers were visualized using the OptiView DAB Detection Kit (Ventana Medical Systems). Slides were counterstained with Hematoxylin and Bluing Reagent (Ventana Medical Systems).

#### **QUANTIFICATION AND STATISTICAL ANALYSIS**

Statistical significance was calculated by Student's t test with two tails. Prism and Microsoft Excel were used to generate graphs and statistical analyses. \*p-value <0.05, \*\*p-value <0.01, \*\*\*p-value <0.001. For animal experiments, no statistics methods were used to predetermine sample size; we used the generally accepted number of tumors per treatment group.

## DATA AND SOFTWARE AVAILABILITY

Raw and processed data from the next generation RNA sequencing of patient biopsies before and after therapy with HDAC inhibitors have been deposited to NCBI Gene Expression Omnibus (GEO) under accession number GSE111140.

## ADDITIONAL RESOURCES

The clinical study described in this manuscript was registered under number NCT02836548 and can be accessed at <https://clinicaltrials.gov/show/NCT02836548>.

## STAR Methods

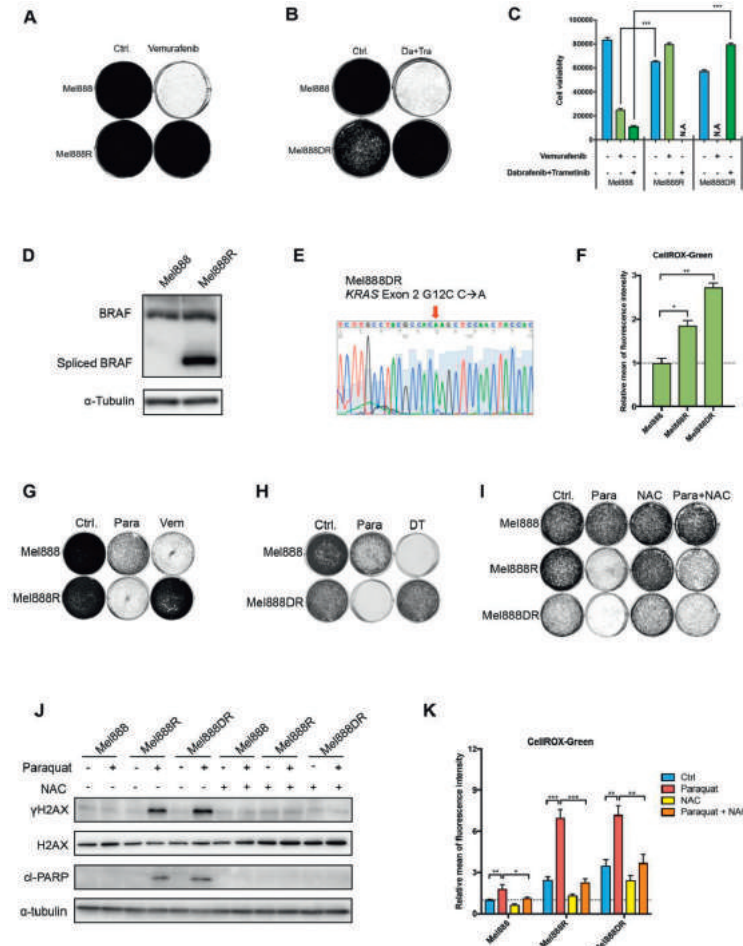
### Key resources table

REAGENT or RESOURCE	SOURCE	IDENTIFIER
<b>Antibodies</b>		
HSP 90 (H-114) Rabbit polyclonal antibody	Santa Cruz Biotechnology	Cat#: sc-7947 RRID: AB_2121235
Vinculin / VINC Mouse monoclonal antibody	Sigma-Aldrich	Cat#: V9131 RRID: AB_477629
$\alpha$ -tubulin (CP06) Mouse monoclonal antibody	Millipore	Cat#: CP06 RRID: AB_2617116
$\beta$ -actin (C-2) Mouse monoclonal antibody	Santa Cruz Biotechnology	Cat#: sc-8432 RRID: AB_626630
Histone 3 / H3 Rabbit polyclonal antibody	Cell Signaling Technology	Cat#: 9715 RRID: AB_331563
acetyl-Histone 3 / ac-H3 Rabbit polyclonal antibody	Millipore	Cat#: 06-599 RRID: AB_2115283
Phospho-Rb (Ser780) Rabbit polyclonal antibody	Cell Signaling Technology	Cat#: 39033 RRID: AB_330015
Phospho-MEK1/2 (Ser217/221) (41G9) Rabbit monoclonal antibody	Cell Signaling Technology	Cat#: 9154S RRID: AB_2138017
MEK1/2 (L38C12) Mouse monoclonal antibody	Cell Signaling Technology	Cat#: 4694S RRID: AB_10695868
SHP2 (C-18) Rabbit polyclonal antibody	Santa Cruz Biotechnology	Cat#: SC-280 RRID: AB_632401
p-SHP2 Rabbit monoclonal antibody	Abcam	Cat#: ab62322 RRID: AB_945452
Pan-Ras (Ras10) Mouse monoclonal antibody	Thermo Scientific	Cat#: MA1-012X RRID: AB_2536665
PDGFRB (C82A3) Rabbit monoclonal antibody	Cell Signaling Technology	Cat#: 4564 RRID: AB_2236927
p-BRAF (Ser445) Rabbit polyclonal antibody	Cell Signaling Technology	Cat#: #2696 RRID: AB_390721
BRAF (F-7) Mouse monoclonal antibody	Santa Cruz Biotechnology	Cat#: sc-5284 RRID: AB_626760
Cleaved PARP (Asp214) (D64E10) XP Rabbit monoclonal antibody	Cell Signaling Technology	Cat#: #5625 RRID: AB_10699459
phospho-Rsk1 (Thr359/Ser363) Rabbit monoclonal antibody	Millipore	Cat#: 04-419 RRID: AB_11213444
RSK1 (D6D5) Rabbit monoclonal antibody	Cell Signaling Technology	Cat#: 8408S RRID: AB_10828594

γH2AX Mouse monoclonal antibody	Millipore	Cat # 05-636 RRID: AB_309864
CD3 (SP7) for IHC Rabbit monoclonal antibody	Spring Bioscience	Cat # M3071 RRID: 1660770
CD4 (SP35) for IHC Rabbit monoclonal antibody	Cell Marque	Cat # 104R-14, RRID: 1516770
CD8 (C8/144B) for IHC Mouse monoclonal antibody	Dako/Agilent	Cat # M7103 RRID: 2075537
CD20 (L26) for IHC Mouse monoclonal antibody	Dako/Agilent	Cat # N/A RRID: N/A
CD68 (KP1) for IHC Mouse monoclonal antibody	Dako/Agilent	Cat # GA60961-2 RRID: 2661840
<b>Chemicals, Peptides, and Recombinant Proteins</b>		
Vorinostat	Selleck Chemicals	Cat#: S1047
Dabrafenib	Selleck Chemicals	Cat#: S2807
Trametinib	Selleck Chemicals	Cat#: S2673
Vemurafenib	Selleck Chemicals	Cat#: S1267
Entinostat	Selleck Chemicals	Cat#: S1053
Panobinostat	Selleck Chemicals	Cat#: S1030
Belinostat	Selleck Chemicals	Cat#: S1085
Paraquat	Sigma-Aldrich	Cat#: 36541
N-Acetyl-L-cysteine (NAC)	Sigma-Aldrich	Cat#: A0150000
tert-Butyl hydroperoxide	Sigma-Aldrich	Cat#: 416665
Vorinostat (used in <i>in vivo</i> )	LC Laboratories	Cat#: V-8477
Vorinostat (used in clinic)	Synthesized by J. Beijnen	N/A
PLX4720 chow	Produced by Research Diets Inc PLX4720 was provided by Plexxikon	N/A
Glutathione reduced ethyl ester (GEE)	Sigma-Aldrich	Cat#: G1404
6-Hydroxy-2,5,7,8-tetramethylchromane-2-carboxylic acid (Trolox)	Sigma-Aldrich	238813-1G
<b>Critical Commercial Assays</b>		
RAF-1 RBD Agarose	Merck Millipore	Cat#: 14-278
FastStart Universal SYBR Green Master (Rox)	Roche	Cat#: 04913850001
Quick-RNA™ MiniPrep	Zymo Research	Cat#: R1055
CellTiter-Blue® Cell Viability Assay	Promega	Cat#: G8081
Maxima First Strand cDNA Synthesis Kit for RT-qPCR	Thermo Fisher	Cat#: K1641
Glutathione detection kit	Enzo	Cat#: ADI-900-160
CellROX® Green Flow Cytometry Assay Kit	Life Technologies	Cat#: C10492
<b>Deposited Data</b>		
NKI 178-gene panel exosome DNA sequencing from tumor biopsies	NKI-AVL, The Genomics Core Facility	N/A
<b>Experimental Models: Cell Lines</b>		
A375, SK-MEL-2, SK-MEL-147	ATCC	NA
Colo741	R. Marais (Manchester, UK)	NA
Mel888	D. Peeper (NKI, Amsterdam, The Netherlands)	NA
A375 ex vivo BRAFi-resistant clones	This paper	NA
<b>Plasmids and Recombinant DNA</b>		
pLKO 0.1 (TRC)	Sigma-Aldrich TRC shRNA collection	NA
pLKO-shSLC7A11 shRNAs	Sigma-Aldrich TRC shRNA collection	NA
pLKO-H2A-GFP	K. Lint (NKI, Amsterdam, The Netherlands)	
pLKO-H2A-RFP	K. Lint (NKI, Amsterdam, The Netherlands)	

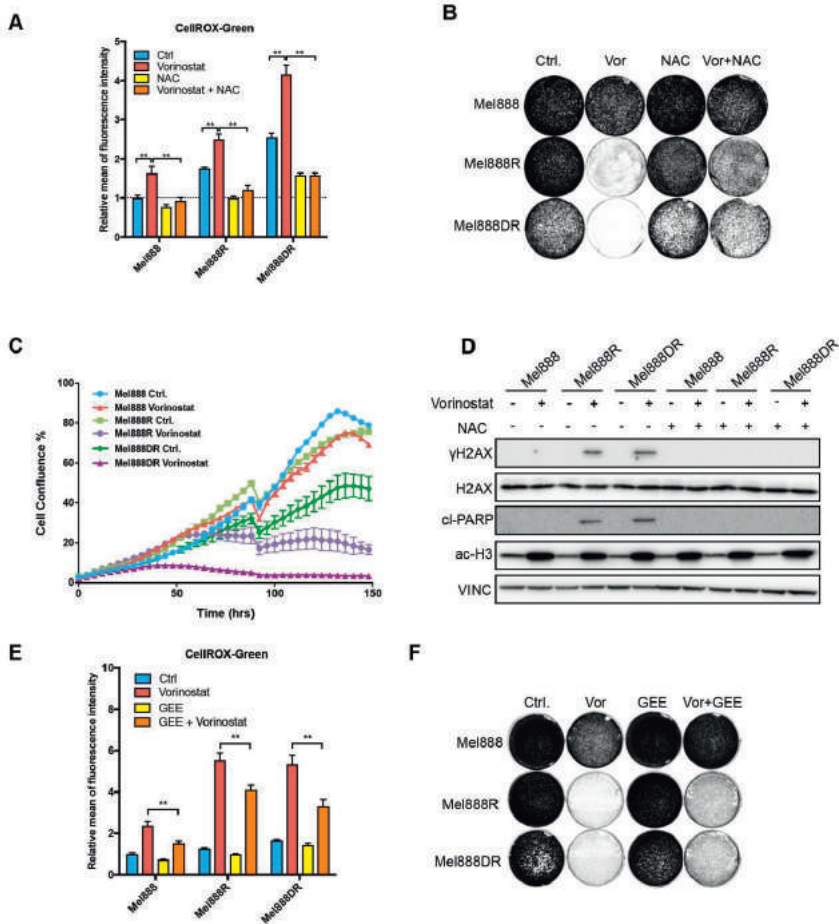
pLX304-empty	Addgene	Cat#: #25890
pLX304-SLC7A11	SSCB Broad ORF lentiviral expression collection	NA
<b>Sequence-Based Reagents</b>		
<b>shRNA target sequences</b>		
shSLC7A11#1 CCGGCCTGCTACTATTTGGAGCTTTCTCGAGAA AGCTCAAATAGTGACAGGTTTTTG	Sigma-Aldrich TRC shRNA collection	TRCN0000043123
shSLC7A11#2 CCGGGCTGATTTATCTTCGATACAACCTCGAGTT GTATCGAAGATAAATCAGCTTTTTG	Sigma-Aldrich TRC shRNA collection	TRCN0000043127
shSLC7A11#3 CCGGCCTGCGTATTATCTCTTTATTCTCGAGAAT AAAGAGATAATACGCAGGTTTTTG	Sigma-Aldrich TRC shRNA collection	TRCN0000288865
shSLC7A11#4 GTACCGGCCCTCTATTTCGACCCATTTACTCGA GTAATGGGTCCGAATAGAGGGTTTTTG	Sigma-Aldrich TRC shRNA collection	TRCN0000380471
<b>Primers of Genomic DNA mutation detection</b>		
<i>gGAPDH</i> Forward: 5'-CCACCCAGAAGACTGTGGAT-3'	Invitrogen	NA
<i>gGAPDH</i> Reverse: 5'-TTCAGCTCAGGGATGACCTT-3'	Invitrogen	NA
<i>gNRAS</i> exon3 Forward: 5'-TGCAAATACACAGAGGAAGC-3'	Invitrogen	NA
<i>gNRAS</i> exon3 Reverse: 5'-CACACCCAGGATTCTTAC-3'	Invitrogen	NA
<i>gKRAS</i> exon2 Forward: 5'-AGAATGGTCTGCACCAGTAA-3'	Invitrogen	NA
<i>gKRAS</i> exon2 Reverse: 5'-TTAACCTTATGTGTGACATGTTCTAA-3'	Invitrogen	NA
<i>gBRAF</i> Forward: 5'-CAAGTACCACAAAACTATCGT-3'	Invitrogen	NA
<i>gBRAF</i> Reverse: 5'-AACTGACTCACCCTGTCTCTGTT-3'	Invitrogen	NA
<b>Gene expression qPCR primer sequences</b>		
<i>GAPDH</i> Forward: 5'-AAGGTGAAGGTCGGAGTCAA-3'	Invitrogen	NA
<i>GAPDH</i> Reverse: 5'-AATGAAGGGGTCATTGATGG-3'	Invitrogen	NA
<i>PDGFRB</i> Forward: 5'-CAGGAGACAGCAACAGCA-3'	Invitrogen	NA
<i>PDGFRB</i> Reverse: 5'-TGTCCAGAGCCTGGAAGTGT-3'	Invitrogen	NA
<i>EGFR</i> Forward: 5'-TCCTCTGGAGGCTGAGAAAA-3'	Invitrogen	NA
<i>EGFR</i> Reverse: 5'-GGGCTCTGGAGAAAAGAAA-3'	Invitrogen	NA
<i>TAGLN</i> Forward: 5'-GTCCGAACCCAGACACAAGT-3'	Invitrogen	NA
<i>TAGLN</i> Reverse: 5'-CTCATGCCATAGGAAGGACC-3'	Invitrogen	NA
<i>CYR61</i> Reverse: 5'-GCTGGAATGCAACTTCGG-3'	Invitrogen	NA
<i>CYR61</i> Forward: 5'-CCCCTTTGGTAGATTCTGG-3'	Invitrogen	NA
<i>CTGF</i> Reverse: 5'-TACCAATGACAACGCCTCT-3'	Invitrogen	NA
<i>CTGF</i> Forward: 5'-TGGAGATTTTGGGAGTACGG-3'	Invitrogen	NA
<i>BRAF</i> Forward: 5'-GTGGATTATGCTCCCCACC-3'	Invitrogen	NA
<i>BRAF</i> Reverse: 5'-CTGCCATTCCGGAGGAG-3'	Invitrogen	NA
<i>SLC7A11</i> Forward: 5'-AGCACATAGCCAAATGGTGAC-3'	Invitrogen	NA
<i>SLC7A11</i> Reverse: 5'-GCTGGCTGGTTTTACCTCAA-3'	Invitrogen	NA
<b>Software and Algorithms</b>		
Prism version 7.0	GraphPad Software	NA
FlowJo version 7.6.5	FlowJo, LLC	NA
qPrimerDepot	<a href="https://primerdepot.nci.nih.gov/">https://primerdepot.nci.nih.gov/</a>	NA
IncuCyte ZOOM® system	ESSEN Bioscience	NA
4 Peaks version 1.7.2	Nucleobytes	NA
IGV version 2.3.61 (88)	Broad Institute	NA

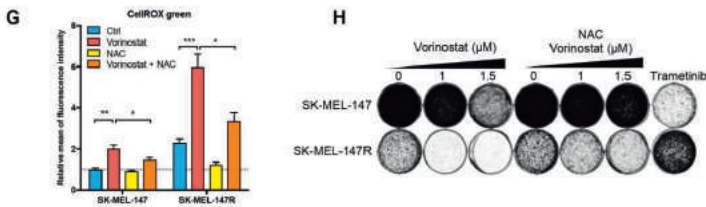
## Supplemental data



**Figure S1. ROS levels and ROS sensitivity of additional melanoma cells, related to Figure 1.** (A) Long-term colony formation assay of parental (Mel888) and BRAFi-resistant (Mel888R) melanoma cells were seeded 50,000 cells per well in a 6-well plate and cultured in the presence or absence of 2  $\mu$ M vemurafenib for 10 days. (B) Long-term colony formation assay of parental (Mel888) and BRAFi/MEKi-double drug resistant (Mel888DR) melanoma cells were seeded 50,000 cells per well in a 6-well plate and cultured in the presence or absence of 0.5  $\mu$ M dabrafenib and 10 nM trametinib. (C) Cell viability assay of parental and drug-resistant cells were seeded 3,000 cells per well in a 96-well plate and cultured in the presence or absence of MAPK inhibitors for 96 hours, and then measured with CellTiter-Blue. (D) Protein Western blot analysis for BRAF indicating that Mel888R cells harbor a 61 kDa BRAF variant. (E) Sanger sequencing of the KRAS gene in Mel888DR cells showing a KRASG12C mutation. (F) ROS levels of Mel888R, Mel888DR and their parental cells were measured after 72 hr culturing without drugs. ROS levels were measured using CellROX-Green flow cytometry assay. Relative ROS inductions are plotted. (G, H) Long-term colony formation assay of Mel888R (G), Mel888DR (H) and their parental cells in the treatment of paraquat and/or MAPK inhibitors. Cells

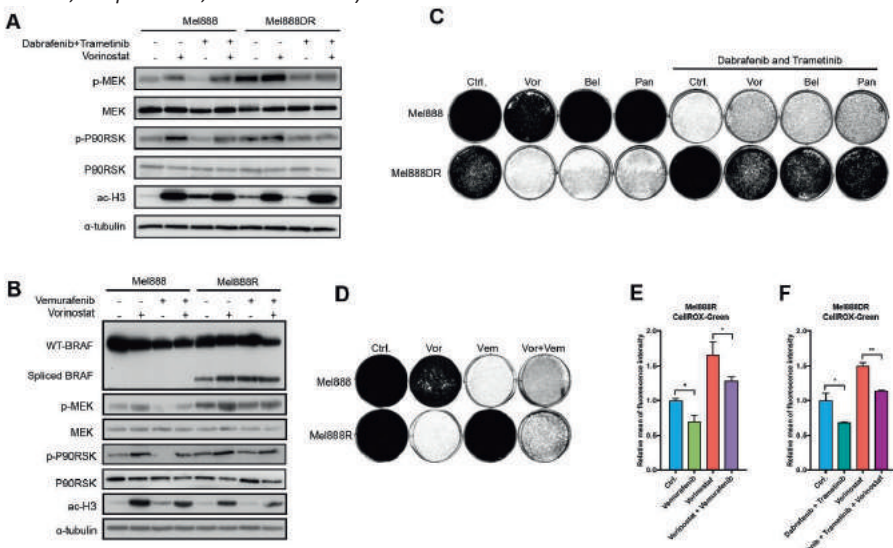
were seeded 50,000 cells per well in 6-well plates and treated with 20  $\mu$ M paraquat, 2  $\mu$ M vemurafenib or combination of 10nM trametinib and 0.5  $\mu$ M dabrafenib for 10 days. Afterward, the cells were fixed, stained and photographed. (I) Long-term colony formation assays of parental and MAPKi-resistant Mel888 cells in the treatment of paraquat and/or NAC. Cells were seeded 50,000 cells per well in 6-well plates and treated with 20  $\mu$ M paraquat and/or 2.5 mM N-acetylcysteine (NAC) for 10 days. Afterwards, the cells were fixed, stained and photographed. (J) Protein lysates were harvest from the MAPKi-resistant (R and DR) and parental Mel888 cells treated with 25  $\mu$ M paraquat and/or 2.5mM NAC for 72 hours. Western blot analysis showing  $\gamma$ H2AX as a DNA damage marker and cleaved-PARP (cl-PARP) as an apoptosis marker;  $\alpha$ -tubulin served as the loading control. (K) Parental and MAPKi-resistant Mel888 cells were treated with 20 $\mu$ M paraquat and/or 2.5 mM NAC for 72 hr. ROS levels were measured using CellROX-Green flow cytometry assay. Relative ROS inductions are plotted. Error bars in this figure represent as mean  $\pm$  standard deviations from biological triplicates (\* $p \leq 0.05$ , \*\* $p \leq 0.01$ , \*\*\* $p \leq 0.001$ , Student's t-test).





**Figure S2. HDACi is detrimental to MAPKi-resistant BRAF and NRAS mutant melanoma cells, related to Figure 2.**

(A) Parental and MAPKi-resistant Mel888 cells were treated with 2  $\mu$ M vorinostat and/or 2.5 mM NAC for 72 hr. ROS levels were measured using CellROX-Green flow cytometry assay. Relative ROS inductions are plotted. (B) Long-term colony formation assays of parental and MAPKi-resistant Mel888 cells treated with vorinostat and/or NAC. Cells were seeded 50,000 cells per well in 6-well plates and treated with 1  $\mu$ M vorinostat and/or 2.5 mM NAC for 8 days. Afterward, the cells were fixed, stained and photographed. (C) Incucyte proliferation assay of parental and MAPKi-resistant Mel888 cells, seeded 2,000 cells per well in a 96-well plate and cultured in the presence or absence of 1  $\mu$ M vorinostat. (D) Protein lysates were harvest from the MAPKi-resistant and parental Mel888 cells treated with 1  $\mu$ M vorinostat and/or 2.5 mM NAC for 72 hr. Western blot analysis shows  $\gamma$ H2AX as a DNA damage marker and cleaved-PARP (cl-PARP) as an apoptosis marker;  $\alpha$ -tubulin served as the loading control. (E) Parental and MAPKi-resistant Mel888 cells were treated with 2  $\mu$ M vorinostat and/or 2.5 mM reduced glutathione ethyl ester (GEE) for 72 hr. ROS levels were measured using CellROX-Green flow cytometry assay. Relative ROS levels are indicated. (F) Long-term colony formation assays of parental and MAPKi-resistant Mel888 cells treated with vorinostat and/or GEE. Cells were seeded 50,000 cells per well in 6-well plates and treated with 1  $\mu$ M vorinostat and/or 2.5 mM GEE for 8 days. Afterward, the cells were fixed, stained and photographed. (G) NRAS mutant melanoma cells SK-MEL-147 and its MEKi-resistant variant SK-MEL-147R cells were treated with 2  $\mu$ M vorinostat and/or 2.5 mM NAC for 72 hours. ROS levels were measured using CellROX-Green flow cytometry assay. Relative ROS inductions are plotted. (H) Long-term colony formation assays of parental and MEKi-resistant SK-MEL-147 cells treated with vorinostat and/or NAC. Cells were seeded 50,000 cells per well in 6-well plates and treated with 1  $\mu$ M or 1.5  $\mu$ M vorinostat, 2.5 mM NAC and/or 100 nM trametinib for 8 days. Afterward, the cells were fixed, stained and photographed. Error bars in this figure represent as mean  $\pm$  standard deviations from biological triplicates (\* $p \leq 0.05$ , \*\* $p \leq 0.01$ , \*\*\* $p \leq 0.001$ , Student's t-test).



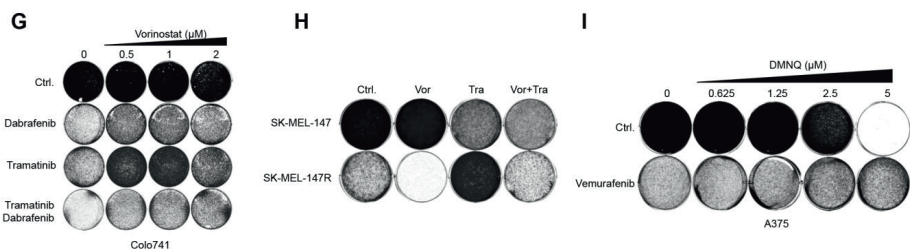


**Figure S3. MAPK inhibition is antagonistic with HDAC inhibition in additional BRAF and NRAS mutant melanomas, related to Figure 3.**

(A) Mel888DR and parental Mel888 cells were treated with 2  $\mu\text{M}$  vorinostat and/or the combination of 0.125  $\mu\text{M}$  dabrafenib and 5 nM trametinib. Protein lysates were harvested after 72 hr. Western blot analysis was performed for p-MEK and p-P90RSK as indicators of activation of MAPK pathway, ac-H3 indicated levels of acetylated histone H3;  $\alpha$ -tubulin served as the loading control. (B) Mel888R and the parental cells were treated with 2  $\mu\text{M}$  vorinostat and/or 0.5  $\mu\text{M}$  vemurafenib for 72 hr. Protein lysates were harvested after 72 hr. Western blot analysis was performed for p-MEK and p-P90RSK as activation of MAPK pathway, ac-H3 indicated levels of acetylated histone H3, Alternative splice variant 61kDa BRAF as the BRAFi-resistance mechanism;  $\alpha$ -tubulin served as the loading control. (C, D) Long-term colony formation assays of parental and MAPKi-resistant Mel888 cells treated with vorinostat and/or MAPKi. (C) Mel888DR and parental cells were seeded 50,000 cells per well in 6-well plates and treated with 1  $\mu\text{M}$  vorinostat (Vor), 0.5  $\mu\text{M}$  belinostat (Bel), 5 nM panobinostat (Pan) and/or combination of 5 nM trametinib and 0.125  $\mu\text{M}$  dabrafenib. (D) Mel888R and parental cells were seeded 50,000 cells per well in 6-well plates and treated with 1  $\mu\text{M}$  vorinostat and/or 1  $\mu\text{M}$  vemurafenib. After 10 days culturing, the cells were fixed, stained and photographed. (E-F) Relative ROS level measurements of Mel888R treated with 2  $\mu\text{M}$  vorinostat and/or 2  $\mu\text{M}$  vemurafenib (E), Mel888DR cells with 2  $\mu\text{M}$  vorinostat and/or the combination of 0.125  $\mu\text{M}$  dabrafenib and 5 nM trametinib (F). (G) Long-term colony formation assays of BRAF mutant melanoma cells (Colo741). The cells were seeded 50,000 cells per well in 6-well plates and treated with vorinostat, 5 nM trametinib, 0.125  $\mu\text{M}$  dabrafenib and/or the combinations for 10 days. Afterward, the cells were fixed, stained and photographed. (H) Long-term colony formation assays of parental and MEKi-resistant SK-MEL-147 cells treated with vorinostat and/or MAPKi. The cells were seeded 50,000 cells per well in 6-well plates and treated with 1  $\mu\text{M}$  vorinostat and/or 50nM trametinib. (I) Long-term colony formation assays of A375 cells treated with 0.25  $\mu\text{M}$  vemurafenib and indicated concentrations of 2,3-dimethoxy-1,4-naphthoquinone (DMNQ) for 10 days. Error bars in this figure represent as mean  $\pm$  standard deviations from biological triplicates (\* $p \leq 0.05$ , \*\* $p \leq 0.01$ , \*\*\* $p \leq 0.001$ , Student's t-test).

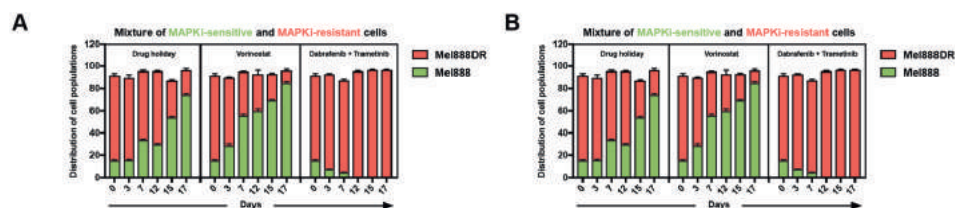
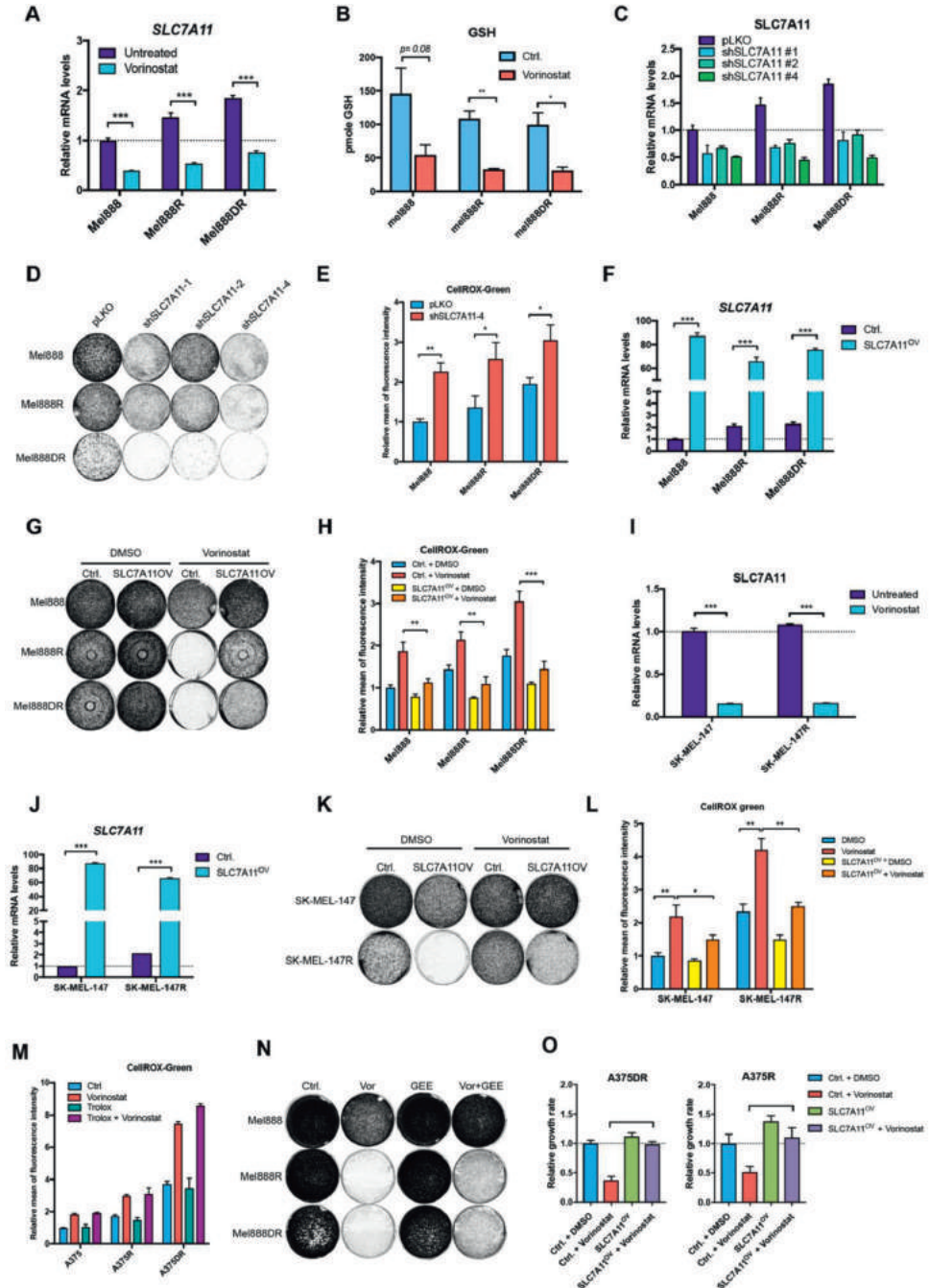


**Figure S4. HDACi is detrimental to MAPKi-resistant Mel888 melanoma, related to Figure 4.**

(A-B) MAPKi-resistant cells (RFP+) and their MAPKi-sensitive parental cells (GFP+) were mixed in a 9-to-1 ratio. 2,000,000 cells were seeded in a 10-cm dish and subjected to different treatments. At each time point, the distribution of the cell population was determined using flow cytometry. The ratio of two cell populations at the starting of the experiment (day 0) is indicated. The distribution changes of mixed two cell populations are plotted on the Y-axes against the time on the X-axes. Error bars in this

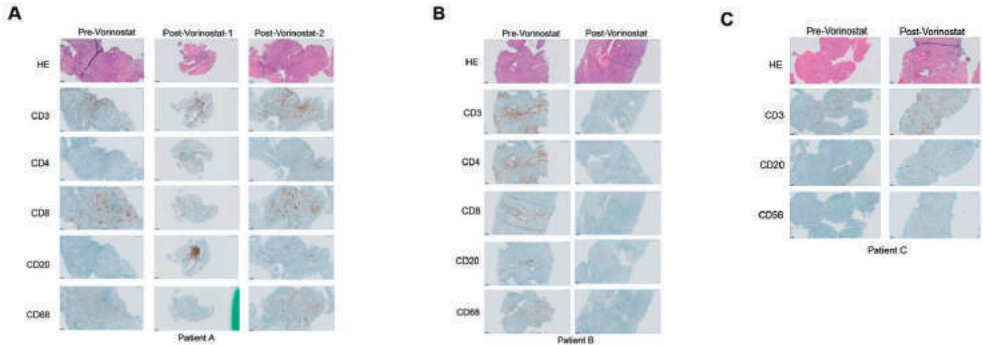


figure panel denoted standard deviations of biological triplicates. Panel (A) presents the mixture of Mel888DR and Mel888. Panel (B) presented mixture of Mel888R and Mel888. Error bars in this figure denoted standard deviations of biological triplicates.



**Figure S5. HDACi suppresses SLC7A11 resulting in ROS induction in additional BRAF and NRAS mutant melanoma, related to Figure 5.**

(A) mRNA expression analysis of SLC7A11 measured by qRT-PCR in parental and MAPKi-resistant Mel888 cells treated with 2  $\mu$ M vorinostat for 48 hr. (B) Parental and MAPKi-resistant Mel888 cells were treated with 2  $\mu$ M vorinostat for 72 hr. Total intracellular glutathione (GSH) levels were measured using colorimetric based glutathione detection assay. (C-E) Three independent shRNAs targeting SLC7A11 were individually introduced in parental and MAPKi-resistant Mel888 cells by lentiviral transduction. pLKO empty vector served as the control. (C) The level of SLC7A11 knockdown by each shRNAs was measured by qRT-PCR. (D) Long-term colony formation of parental and MAPKi-resistant Mel888 cells upon SLC7A11 knockdown. The cells were seeded 50,000 cells per well in 6-well plate and cultured 10 days. Afterward, the cells were fixed, stained and photographed. (E) Relative ROS levels in parental and MAPKi-resistant A375 cells upon SLC7A11 knockdown were measured by CellROX-Green flow cytometry assay. (F-H) SLC7A11 was expressed in parental and MAPKi-resistant Mel888 cells by lentiviral transduction. pLX304 empty vector was used as the control (Ctrl.). (F) The levels of SLC7A11 overexpression in parental and MAPKi-resistant Mel888 cells was measured by qRT-PCR of SLC7A11 mRNA levels. (G) Long-term colony formation of SLC7A11 overexpressing parental and MAPKi-resistant Mel888 cells treated with vorinostat. The cells were seeded 50,000 cells per well in 6-well plate and cultured 10 days with or without 1 $\mu$ M vorinostat. Afterward, the cells were fixed, stained and photographed. (H) SLC7A11 overexpressing parental and MAPKi-resistant Mel888 cells were treated with 2  $\mu$ M vorinostat for 72 hours. Afterwards, ROS levels were measured using CellROX-Green flow cytometry assay. Relative ROS inductions are plotted. (I) mRNA expression analysis of SLC7A11 by qRT-PCR in parental and MEKi-resistant SK-MEL-147 cells treated with 2  $\mu$ M vorinostat for 48 hr. (J-L) SLC7A11 cDNA was expressed in parental and MEKi-resistant SK-MEL-147 cells by lentiviral transduction. pLX304 empty vector was used as the control (Ctrl.). (J) The levels of SLC7A11 overexpression in parental and MEKi-resistant SK-MEL-147 cells were measured by examining the SLC7A11 mRNA levels by qRT-PCR. (K) Long-term colony formation of SLC7A11 overexpressed parental and MEKi-resistant SK-MEL-147 cells treated with vorinostat. The cells were seeded 50,000 cells per well in 6-well plate and cultured 10 days with or without 1 $\mu$ M vorinostat. Afterward, the cells were fixed, stained and photographed. (L) SLC7A11 overexpressing parental and MEKi-resistant SK-MEL-147 cells were treated with 2  $\mu$ M vorinostat for 72 hr. Afterward, ROS levels were measured using CellROX-Green flow cytometry assay. Relative ROS inductions are plotted. (M) Parental and MAPKi-resistant A375 cells were treated with 2  $\mu$ M vorinostat and/or 0.25 mM 6-hydroxy-2,5,7,8-tetramethylchroman-2-Carboxylic Acid (Trolox) for 72 hr. ROS levels were measured using CellROX-Green flow cytometry assay. Relative ROS levels are indicated. (N) Long-term colony formation assays of parental and MAPKi-resistant A375 cells treated with vorinostat and/or Trolox. Cells were seeded 50,000 cells per well in 6-well plates and treated with 1  $\mu$ M vorinostat and/or 0.25 mM Trolox for 8 days. (O) The relative growth rate of the responsiveness to 1  $\mu$ M vorinostat treatment in MAPKi-resistant A375 cells with and without SLC7A11 overexpression. The growth rates were calculated based on the slope a curve fitted through the linear range of the log-transformed confluence measurements from Incucyte data of figure 5 J-5K. For each cell line, the growth rates were normalized to the mean of the untreated controls. The growth rate of untreated control was considered as a basal line and normalized to 1. The relative growth rates of all growth rates of the drug-treated and genetic manipulated arms were compared with the untreated control arm. Error bars in this figure represent as mean  $\pm$  standard deviations from biological triplicates (\* $p$   $\leq$  0.05, \*\* $p$   $\leq$  0.01, \*\*\* $p$   $\leq$  0.001, Student's t-test).



**Figure S6. Immune cells staining on the biopsies from vorinostat treated MAPKi-resistant melanoma patients, related to Figure 7.**

(A-C) Immunohistochemical staining of immune cells in melanoma tissue section from MAPKi-resistant melanoma patients (A-C) pre- and post-treated with vorinostat as indicated. CD3 served as a pan-T cell marker. CD4 served as a T helper cell marker. CD8 served as killer T cells. CD20 served as a B cell marker. CD68 served as a macrophage marker. The black bar in the lower left corner represents 50  $\mu$ m.

**Table S1. The commonly down-regulated genes upon vorinostat treatment in A375, A375R, A375DR cells, related to figure 5.**

CENPV	LMLNB1	SLC7A11	FXD3
HMG2	ACP5	SERPINF1	FAM169A
FAIM	BCAT1	SERTAD4	MMP8

**Table S2. Characteristics of three patients in the clinical study, Related to Figure 7.**

Characteristics	Patient A
Demographic information	
Sex	Female
Age (years)	58
Disease information	
Melanoma stage	IV
ECOG performance status	0
Previous treatment lines	
Total	4
Immunotherapy	2 (ipilimumab, pembrolizumab)
Chemotherapy	0
Targeted therapy (MAPKi)	2 (dabrafenib, dabrafenib+trametinib)
Total time on treatment before resistance to MAPKi (months)	43
Time on treatment previous MAPKi before enrollment (months)	6
Information regarding biopsies	
Site of the biopsies	Lung, right dorsal

Characteristics	Patient B
Demographic information	
Sex	Male
Age (years)	48
Disease information	
Melanoma stage	IV
ECOG performance status	0
Previous treatment lines	
Total	3
Immunotherapy	1 (nivolumab)
Chemotherapy	0
Targeted therapy (MAPKi)	2 (vemurafenib, dabrafenib+trametinib)
Total time on treatment before resistance to MAPKi (months)	15
Time on treatment previous MAPKi before enrollment (months)	11
Information regarding biopsies	
Site of the biopsies	Lung lingula

Characteristics	Patient C
Demographic information	
Sex	Male
Age (years)	54
Disease information	
Melanoma stage	IV
ECOG performance status	1
Previous treatment lines	
Total	4
Immunotherapy	3 (TIL*, ipilimumab, pembrolizumab)
Chemotherapy	0
Targeted therapy (MAPKi)	1 (dabrafenib+trametinib)
Total time on treatment before resistance to MAPKi (months)	18
Time on treatment previous MAPKi before enrollment (months)	6
Information regarding biopsies	
Site of the biopsies	Abdominal, para-aortal lymph nodes

\* TIL = tumor infiltrating lymphocytes

Characteristics	All patients (n = 3)
Demographic information	
Male (%)	67
Age, years (median; range)	53; 48-58
Disease information	
Melanoma stage IV (%)	100
ECOG performance status (median; range)	1; 0-1
Previous treatment lines	
Total (median; range)	4; 3-4
Immunotherapy (median; range)	2; 1-3
Chemotherapy (median; range)	0; 0
Targeted therapy (MAPKi) (median; range)	2; 1-2
Total time on treatment before resistance to MAPKi, months (median; range)	25; 15-43
Time on treatment previous MAPKi before enrollment, months (median; range)	8; 6-11
Information regarding biopsies	
Site of the biopsies	Lung, right dorsal (pt A) Lung lingual (pt B) Abdominal, para-aortal lymph nodes (pt C)

**Table S3. Pharmacodynamics of vorinostat, related to Figure 7.**

Study/Source	Dosing schedule	C <sub>max</sub> (ng/ml)	AUC <sub>0-∞</sub> (ng/ml•h)	t <sub>1/2</sub>
Day 1, patient A	1 d 360 mg, fed state	376	1720	3.1
Day 1, patient B	1d 260 mg fed stat	416	1450	1.1
Day 1, literature (Iwamoto, M et al. 2013)	1d 400 mg, fed state	296.6 (42.2-292.2)	1403 (898-2455)	1.44 (0.79-3.77)

Measurements on vorinostat levels in blood of a patient in the clinical study.



# CHAPTER 2.2

Vorinostat in patients with resistant *BRAFV600E* mutated advanced melanoma: a proof of concept study

Sanne Huijberts, Liqin Wang, Rodrigo Leite de Oliveira, Hilde Rosing, Bastiaan Nuijen, Jos Beijnen, Rene Bernards, Jan Schellens, Sofie Wilgenhof

## **Abstract**

The clinical benefit of treatment with BRAF- and MEK-inhibitors in melanoma is limited due to resistance associated with emerging secondary mutations. Preclinical and clinical studies have shown that short-term treatment with the histone deacetylase inhibitor vorinostat can eliminate cells harboring these secondary mutations causing resistance. This proof of concept study is to determine the efficacy of sequential treatment with vorinostat and BRAFi/MEKi in resistant *BRAF<sup>V600</sup>* mutant melanoma. The primary aim is demonstrating anti-tumor response of progressive lesions according to RECIST 1.1. Secondary endpoints are to determine that emerging resistant clones with a secondary mutation in the MAPK pathway can be detected in circulating tumor DNA and purged by short-term vorinostat treatment. Exploratory endpoints include pharmacokinetic, pharmacodynamic and pharmacogenetic analyses (NCT02836548).

## **Introduction to the trial**

Here we describe an ongoing, proof of concept study of sequential treatment with vorinostat and BRAF and/or MEK inhibition in patients with BRAF inhibitor (BRAFi) resistant *BRAF<sup>V600</sup>* mutant melanoma, assessing the anti-tumor response of progressive lesions and exploring if emerging resistant clones with a secondary mutation in the mitogen-activated protein kinases signalling (MAPK) pathway can be detected in circulating tumor DNA and purged by short-term vorinostat treatment.



## Background & rationale

The prevalence of melanoma and its associated mortality increases rapidly worldwide. In the European Union the 1-year prevalence of melanoma was 6.5 per 10,000 people in 2015. (1, 2) The last decade, the introduction of checkpoint inhibitors and targeted therapy has significantly improved the outcome of advanced melanoma patients.

Activating mutations in the *BRAF* gene are present in about half of the melanomas. BRAFi inhibit the serine-threonine protein kinase BRAF, which plays a dominant role in the MAPK pathway influencing cell growth. MEK inhibitors (MEKi) inhibit MEK1 and MEK2, two regulatory proteins downstream of BRAF.(3) Combination of both drugs improved both the progression-free (PFS) and overall survival (OS) of patients with advanced *BRAF*<sup>V600</sup> mutated (BRAFi) melanoma, compared to BRAF inhibition alone.(4-6) More recently, also the adjuvant use of BRAFi dabrafenib and MEKi trametinib resulted in a significantly lower risk of recurrence in stage III BRAFi melanoma patients.(7)

However, the clinical benefit of this treatment in metastatic patients is limited due to development of drug resistance to a BRAFi in 6-8 months and in 9-14 months for treatment with a BRAFi combined with a MEKi.(3, 8) This is often associated with secondary mutations in the MAPK pathway leading to re-activation of the pathway.(9, 10) Currently, there are no effective treatment options for advanced BRAFi melanoma patients that progressed on treatment with BRAF (+/- MEK) inhibitor and immunotherapy.(11)

Withholding treatment with BRAFi and/or BRAFi/MEKi leads to reversible hyperactivation of the MAPK pathway, causing a transient growth arrest. When melanoma cells that have acquired resistance to the combination of BRAF and MEK inhibitors are released from drug treatment, a transient proliferation arrest occurs due to hyperactivation of the MAPK pathway, which has hallmarks of oncogene-induced senescence.(12) More recently, it has been shown that treatment of such drug-resistant cells with vorinostat, a histone deacetylase inhibitor (HDACi), leads to further hyperactivation of the MAPK pathway leading to cell death, see figure 1.(10) Importantly, no cell death was observed if parental melanoma cells were exposed to vorinostat, showing that vorinostat selectively kills only the melanoma cells that have acquired resistance to BRAF and MEK inhibitors.(10)

Histone deacetylases (HDACs) are enzymes that catalyse the removal of acetyl groups from the lysine residues of histones and transcription factors. A condensed chromatin structure and repression of gene transcription occur when histones are hypo-acetylated. In previous studies HDACi were identified as an important new class of anti-cancer drugs for selected hematologic and solid tumor malignancies, despite incomplete knowledge about the mechanism of action.(13-15)

Vorinostat is an FDA approved HDACi for the treatment of cutaneous T-cell lymphoma (CTCL) in patients who have progressive, persistent or recurrent disease on or following two systemic therapies. Most common adverse events include fatigue, gastro-intestinal toxicity and thrombocytopenia. Severe adverse events consisted of lung embolism, severe anaemia and squamous cell carcinoma observed in a phase 1 study with 86 patients.(16)

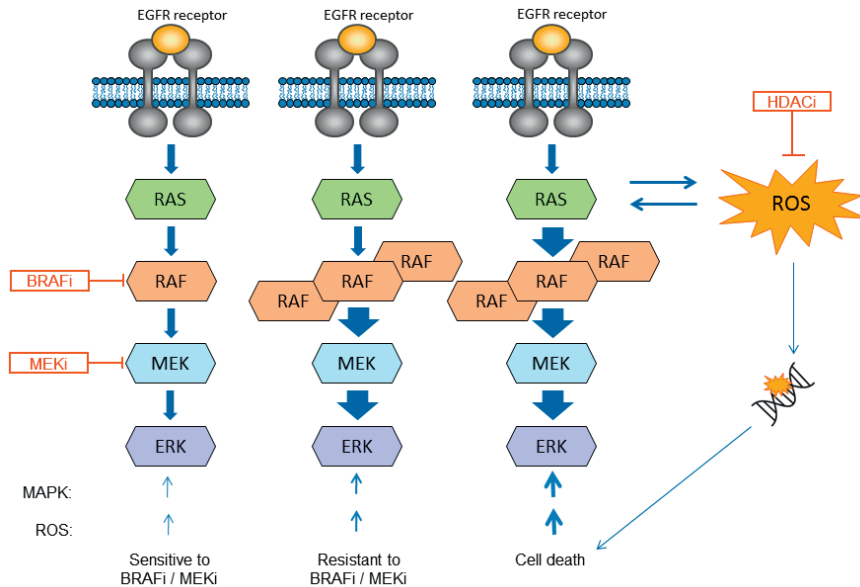


**Figure 1. Systematic view on the alternating treatment of BRAF<sup>V600E</sup> melanomas.**

BRAFi/MEKi are effective in BRAF<sup>V600E</sup> melanoma cells with normal MAPK signaling (left). Enhanced signaling through the MAPK pathway as a result of acquired resistance mutations or upregulation of Tyrosine Kinase receptors (RTKs), induces drug resistance. Switching treatment from BRAFi/MEKi to an HDACi in resistant cells leads to upregulation of ROS. High levels of MAPK signaling are maintained by the interaction of ROS on RAS. In resistant BRAF<sup>V600E</sup> melanoma cellular ROS levels are already high, and further increase of ROS by HDACi leads to a lethal effect on the cells through massive DNA damage.

Vorinostat has specific action on the enzymatic activity of HDAC 1,2,3 and 6 by interacting with the catalytic site. It leads to the accumulation of acetylated histones and this causes apoptosis and cell cycle arrest, *in vitro*.(16)

Vorinostat treatment in mice with BRAFi resistant BRAFm melanoma resulted in complete disappearance of the tumor after two months of treatment.(10)

A clinical study was designed to investigate the abovementioned preclinical results in which patients with BRAFi/MEKi resistant BRAFm melanoma received vorinostat 360 mg once daily (QD) continuously. In total 6 patients were treated and showed mixed responses with both tumor progression of some metastatic lesions and regression of other lesions at the first tumor evaluation after 6 weeks of investigational treatment. Based on the pre-clinical data, we postulated that vorinostat treatment leads to regression of progressive lesions harboring a resistant clone, but would have little effect on metastases dominated by BRAFi/MEKi sensitive clones. This was validated in the first patient study, in which we found that tumor biopsies which showed newly developed secondary MAPK pathway mutations, e.g. NRAS<sup>Q61H</sup> and KRAS<sup>G12C</sup> at baseline, had a complete absence of these resistance mutations after 2 weeks of vorinostat treatment. See figure 2 for the mutation allele frequencies analysed in tumor tissue of 2 patients treated with vorinostat 360 mg QD continuously.

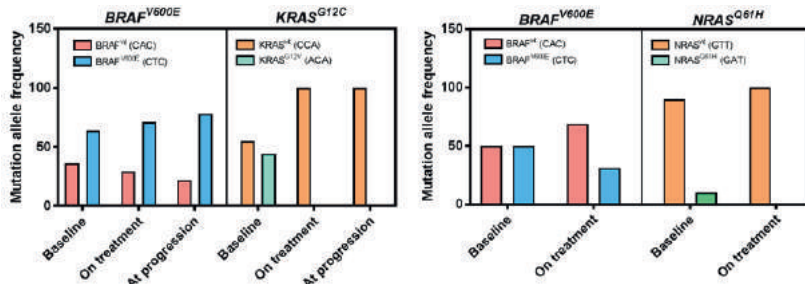


**Figure 2. Results of genomic DNA isolation from paired biopsies of target lesions of two patients (left and right) treated vorinostat 360 mg QD continuously.**

Tumor biopsies were taken on baseline, on cycle 1 day 14 of vorinostat treatment and for the patient on the left at progression of disease. The NKI-178 gene panel using targeted NGS (17) showed changes in acquired resistance mutations of the MAPK-pathway. The mutation allele frequency of *KRAS*<sup>G12C</sup> was high before vorinostat treatment and lowered to a non-detectable level during vorinostat treatment. For the patient on the right, the allele frequency of *NRAS*<sup>Q61H</sup> was around 10 before vorinostat treatment and decreased to 0 during treatment. *BRAF*<sup>V600E</sup> mutation was used as an indication of tumor cell percentage in the biopsy.

Based on these preclinical and clinical results we postulate that BRAFi-resistant BRAFm melanoma cells can be eliminated by a short-term treatment with HDACi vorinostat due to killing of tumor cells harboring a secondary mutation in the MAPK-pathway.

Abovementioned insights have led to an amendment of our study protocol. Future patients will be treated with BRAFi and/or MEKi until development of resistance by monitoring circulating tumor DNA (ctDNA) on top of standard clinical and radiological tumor evaluations. In case of resistance, vorinostat treatment for a total duration of 2 weeks will be initiated to purge the resistant clones and thereafter medication will be switched back to BRAFi and/or MEKi to improve outcome of treatment.

Rechallenge with BRAFi/MEKi (dabrafenib and trametinib) showed clinical activity with an objective response rate of 32% in patients who had previously progressed on BRAFi in a prospective phase 2 trial. All patients in this study had a treatment interval of more than 12 weeks and received immunotherapy in between both BRAFi/MEKi treatments.(18) As such, this rechallenge treatment strategy can only be used in patients with first-line targeted therapy. Moreover, in patients with early progression upon BRAFi/MEKi, retrospective clinical data suggest that treatment beyond progression might result in prolonged palliation of symptoms and survival, although the observed benefit was of a very short duration.(11) Therefore, there remains an unmet need to develop new treatment strategies to further improve the efficacy of this targeted therapy and significantly improve BRAFm melanoma patient's outcome.

## Study design

This investigator-initiated trial is a two-stage, single arm, mono-center, open-label, clinical, pharmacological, proof of concept study conducted in the Netherlands Cancer Institute/Antoni van Leeuwenhoek Hospital (NKI-AVL), located in Amsterdam, The Netherlands. Patients with BRAF<sub>m</sub> melanoma will be included in this trial upon progression on BRAFi and/or BRAFi/MEKi, mostly the combination of dabrafenib/trametinib. After a wash-out period of 3 days vorinostat 360 mg QD will be administered for 14 days to purge out the resistant clones. On day 15 BRAFi and/or BRAFi/MEKi treatment will be reintroduced according to standard care. If in the best interest of the patient a subsequent 14 days treatment cycle can be given upon newly developed resistance against BRAFi/MEKi. Patients will be screened for baseline inclusion criteria and, after informed consent is obtained, all baseline assessments will be performed. During vorinostat treatment patients will be weekly followed for safety assessments and drug accountability. During BRAFi/MEKi treatment patients will be followed for safety assessments according to standard care. If indicated, more safety assessments will be planned. Every 6 weeks radiological tumor assessments will be scheduled.

## Objectives

The primary objective of this proof of concept trial is to demonstrate an anti-tumor response rate of progressive lesions of at least 30% of alternating treatment with the HDACi vorinostat and BRAFi/MEKi in advanced resistant BRAF<sub>m</sub> melanoma. Secondary objectives are: to demonstrate that emerging resistant clones with a secondary mutation in the MAPK pathway can be detected by ctDNA analyses and purged by short term treatment with vorinostat; to characterize the safety and tolerability of intermittent treatment of vorinostat before and after treatment with BRAFi/MEKi in this population assessed by the incidence and severity of adverse events; and to determine progression free survival and overall survival of alternating treatment with vorinostat and BRAFi/MEKi. During this trial additional blood and tissue sampling will be done for exploratory pharmacokinetic (PK), pharmacodynamic (PD) and pharmacogenetic (PG) analyses.

## Inclusion criteria

Patients are eligible for this trial if they have a histological proven advanced melanoma with BRAF<sup>V600</sup> mutation and previous documented response of at least 4 weeks to treatment with BRAFi and/or BRAFi/MEKi. Eligible patients have an age of at least 18 years, a World Health Organization (WHO) performance status of 0, 1 or 2 and a life expectancy of at least 3 months. Minimal acceptable safety laboratory values include ANC  $\geq 1.5 \times 10^9$  /L, Platelet count  $\geq 100 \times 10^9$  /L, Hemoglobin  $\geq 6.0$  mmol/L, serum bilirubin  $\leq 1.5 \times$  ULN, ALAT and ASAT  $\leq 2.5 \times$  ULN (in case of liver metastases ALAT and ASAT  $\leq 5 \times$  ULN), serum creatinine  $\leq 1.5 \times$  ULN or creatinine clearance  $\geq 50$  ml/min (by Cockcroft-Gault formula or MDRD). Pregnancy test must be negative within 72 hours before receiving the first dose of study drug. At least one progressive target lesion according to RECIST 1.1. must be measurable on radiological

assessments. Patients will only be included if they consent to undergo blood sampling and tumor sampling of a progressive target lesion if technically feasible for exploratory analyses.

### **Exclusion criteria**

Excluded from this trial are patients that are pregnant or breast feeding, use unreliable contraceptive methods, have symptomatic brain metastasis, have leptomeningeal disease or a myocardial infarction < 6 months before receiving the first dose of investigational treatment. Any treatment with investigational drugs, except BRAFi and MEKi within 28 days or any standard chemotherapy or immunotherapy within 21 days. Previous treatment with vorinostat or other HDACi prior to receiving the first dose of investigational treatment is not allowed. Other conditions leading to exclusion of patients in this trial are uncontrolled infectious disease or known Human Immunodeficiency Virus HIV-1 or HIV-2 type or a known history of hepatitis B or C. Radiotherapy within the last 4 weeks prior to receiving the first dose of investigational treatment is only accepted if 1 x 8 Gray for pain palliation is given.

### **Study medication: manufacturing**

The investigational drug, vorinostat, has been pharmaceutically formulated in the pharmacy of the NKI-AVL under Good Manufacturing Practice (GMP) conditions. Vorinostat 90 mg is formulated as a capsule for oral use. Vorinostat drug substance is manufactured by Syncom B.V. (Groningen, The Netherlands). The quality of vorinostat final product was confirmed by complementary analytical methods.

### **Study medication: treatment schedule**

The registered posology by the FDA is 400 mg vorinostat oral QD, continuously to be taken as 4 capsules of 100 mg each.<sup>(16)</sup> The newly developed capsules used in this study contain 90 mg vorinostat per capsule. The daily dose will be 360 mg, slightly lower than registered for treatment of CTCL for safety reasons.

Vorinostat 360 mg QD treatment will start within a minimum period of 3 days after discontinuation of BRAFi and/or BRAFi/MEKi. A wash-out period is necessary, since the hypothesis is that BRAFi/MEKi and vorinostat work antagonistic as seen in preclinical research and to minimize the risk of overlapping adverse events. BRAFi and/or BRAFi/MEKi can be continued after progression to provide sufficient time to perform baseline assessments. Vorinostat will be given for 14 days, thereafter treatment is switched back to BRAFi/MEKi according to standard care. See figure 3 for a schematic view of the treatment schedule, including most important study assessments. The timing of this alternating treatment is based on the results of biopsy analyses in earlier patients, who were treated with continuous vorinostat 360 mg QD after progression on BRAFi/MEKi treatment. These results showed that after 14 days of vorinostat treatment the acquired mutations leading to resistance are purged out. If in best interest of the patient and by judgement of the treating oncologist subsequent cycles of vorinostat can be administered.

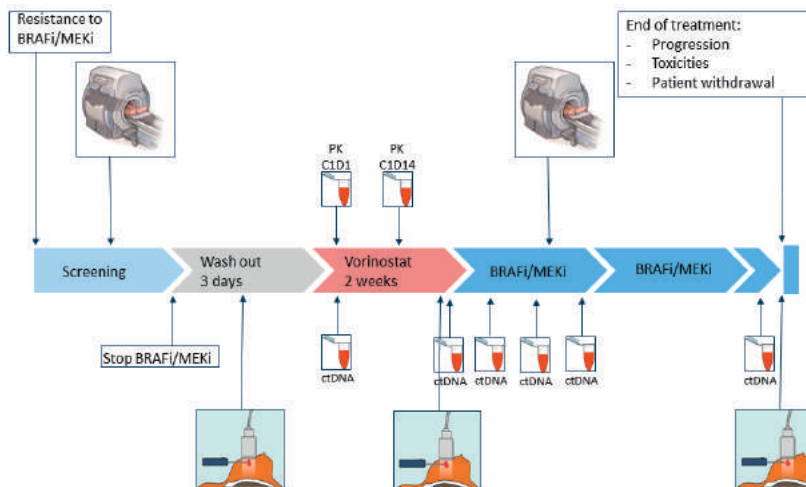


**Figure 3. Schematic view of the treatment schedule.**

After progression on BRAFi/MEKi, vorinostat 360 mg QD will be administered for 14 days after a wash-out period of 3 days. Thereafter, BRAFi/MEKi will be reintroduced according to standard care. On baseline and every 6 weeks radiological tumor assessment will take place. For pharmacogenetic analysis, tumor biopsies are included in the protocol on baseline, on vorinostat cycle 1 day 14 and at end of treatment. Also blood sampling will be performed every 2 weeks for circulating tumor DNA analyses. The study will continue until disease progression, toxicities or patient withdrawal. If in best interest of the patient, a subsequent cycle of vorinostat can be administered.

### Dose modifications

Patients experiencing grade 3 or 4 vorinostat related toxicity or intolerable grade 2 toxicity despite optimal supportive care can resume treatment after a dose reduction. A maximum of two dose reductions is allowed according to the following steps; starting dose of vorinostat is 360 mg QD, first dose reduction 270 mg QD, second dose reduction 180 mg QD. If patients experience BRAFi/MEKi related toxicity the dose can be resumed according to the described dose reduction steps in the label of the specific drug.

### Concomitant treatment

Patients will be permitted to receive appropriate supportive care measures as deemed necessary by the treating physician, including analgesic medication and single dose radiation therapy in case of pain. Switching from a coumarin-derivate anticoagulant to a low molecular weight heparin is advised as previous research showed an interaction between coumarin-derivate anticoagulants and vorinostat, leading to prolonged prothrombin time and International Normalized Ratio. If switching to LMWH is not desirable, careful monitoring is recommended with a minimal control of INR once a week.(16, 19)

### Safety assessments

To evaluate safety of vorinostat in this alternating treatment schedule different measurements will be used, including assessments of performance status, signs and

symptoms/adverse events, vital signs, physical examination, laboratory testing (hematology and clinical chemistry) and 12-lead electrocardiography. All patients that received at least one administration of vorinostat are evaluable for safety and will be followed for safety assessments until 28 days after the last dose of treatment.

### **Tumor response evaluation**

Tumor response is assessed either in measurable or evaluable tumor lesions according to modified RECIST criteria, version 1.1.(20) Evaluation will be performed 6 weeks after cycle 1 day 1 of vorinostat with CT and/or MRI and/or PET scans to measure the progressive target lesion(s). Patients are evaluable for response to study treatment if at least one tumor response follow-up examination was performed within 4 weeks after study entry. Target lesions progressive under BRAFi/MEKi will be evaluated with the first CT-scan as assessment of vorinostat treatment. At the next tumor assessments all lesions will be evaluated. Radiological tumor evaluations have to be planned every 6 weeks for at least 3 evaluations after every day 1 of vorinostat (not only after cycle 1, but also after subsequent cycles). After these first 3 radiological evaluations the planning will be determined by the patient's own medical oncologist.

All patients will be followed for survival every 8 weeks per phone call until death.

### **Pharmacokinetics, pharmacodynamics and pharmacogenetics**

Blood samples for vorinostat PK measurements will be drawn on cycle 1 day 1 and day 14 of vorinostat treatment to determine the single-dose and steady state PK curves of vorinostat, 4-anilino-4-oxobutanoic acid and vorinostat-glucuronide and using a validated liquid chromatography-tandem mass spectrometry (LC-MS/MS) method.

Tumor biopsies of progressive target lesions will be taken before vorinostat treatment, on cycle 1 day 14 and at disease progression. PD assessments, including phosphorylated MEK, phosphorylated ERK levels and the cysteine-glutamate antiporter SLC7A11 will be performed on these tumor biopsies to confirm the above-mentioned rationale of the mechanism of action of alternating HDACi and BRAFi/MEKi. For PG assessments both tumor biopsies and blood samples will be used. In tumor biopsies secondary mutations causing resistance will be explored by Next-generation sequencing of the NKI-178-gene panel. (17) With ctDNA analysis acquired driver mutations for resistance to BRAFi/MEKi can be detected and increasing ctDNA levels can reveal acquired resistance to targeted therapy and precede radiological evidence of disease progression.(21-23) For example, NRAS mutations might be detected earlier than radiological progression.(21, 22) In this trial every 2 weeks a blood sample will be drawn to analyse ctDNA. ctDNA will be performed to search for acquired resistance mutations and if these mutations can be purged with short term vorinostat treatment. Moreover, it will be used to investigate if ctDNA changes precede radiological progression. Since ctDNA is not implemented in standard care for melanoma patients, it will only be used as exploratory analysis.

### **Statistics: sample size calculation**

Simon's minimax two-stage design will be used. The smallest clinically relevant response rate is 30%, which is our alternative hypothesis. Based on the literature of vorinostat in solid tumors the null hypothesis is a response rate of 13%. (24-28) Thus, the largest response probability which would clearly not warrant further investigation was set at 13% ( $\pi_0 = 0.13$ ) and a probability of 30% was considered desirable ( $\pi_1 = 0.3$ ). For 70% power ( $\beta = 0.3$ ) at a significance level of 5% ( $\alpha = 0.05$ ), the first part will consist of 18 evaluable patients. If a response occurs in 2 or fewer of these 18 patients, the study will be stopped and the efficacy of the treatment will be declared insufficient. If 3 or more of these 18 patients have a response, 8 additional evaluable patients will be recruited. This means that the total sample size will include 26 evaluable patients. The final conclusion will be made by the principal investigator in discussion with the study personal at the NKI-AVL and will be as follows: with 7 or more patients with a response, the treatment is considered sufficiently effective and with 6 or fewer it will be declared insufficient. If the true probability of response is 13%, then the probability that the study will stop after the first 18 patients will be 58%.

### **Statistics: methods**

The data cut-off date for the final analyses for the study will be when all patients continuing treatment have been followed for at least 6 months after the last intake of vorinostat or have been discontinued from the trial.

The full analysis set includes all patients who received at least one dose of study drug. Patient will only be considered evaluable for PK analyses if they have undergone PK blood sampling during day 1 and day 14 of the first vorinostat cycle. To be considered evaluable for safety, patients should have received at least one administration of study treatment. Patients should have at least one measurable lesion to be evaluable for response. A pre-dose and at least one post-dose measurement after completion of the first vorinostat cycle are required to assess the response to treatment. Patients who discontinue for reasons unrelated to the study drug or malignancy will be replaced as required for the study to meet its objectives.

The PK will be determined using non-compartmental methods. The mean, median, coefficient of variation and range of the following PK parameters of vorinostat and its metabolites 4-anilino-4-oxobutanoic acid and vorinostat-glucuronide, will be calculated: Time to maximal plasma concentration ( $t_{max}$ ), maximum plasma concentration ( $C_{max}$ ), area under the time versus concentration curve from zero to the last data point ( $AUC_{0-t}$ ), area under the time versus concentration curve from zero to infinity ( $AUC_{inf}$ ), half-life ( $t_{1/2}$ ), mean residence time (MRT), volume of distribution (Vd), and clearance (Cl).

Summary statistics will be provided with frequency counts and percentages for categorical variables, and mean with standard deviation or median with range or IQR for continuous variables. Associations with treatment groups of unordered categorical variables will be assessed with Fisher's exact test or the Chi-square test and of numeric variables with



Wilcoxon's rank sum test. Time to event endpoints will be evaluated using Kaplan-Meier methods. Hazard ratio's will be calculated with proportional hazard models.

### **Logistics and administrative arrangements**

This study was approved by the accredited Medical Ethics Committee of the NKI-AVL on 27 May 2016. The principles of the Declaration of Helsinki and the Medical Research Involving Human Subject Act (WMO) are followed in this protocol and it is compliant to ICH-GCP. To ensure compliance with ICH-GCP and all applicable regulatory requirements, as part of the quality system, a quality assurance audit may be conducted by an independent quality assurance officer.

Patients are registered by the trial office of the NKI-AVL after written informed consent is given. Electronical Case Report Forms (eCRF) are by data managers and the Clinical Research Associate (CRA) of the trial office in collaboration with SH. Data will be collected as described in the study assessments. The eCRF will be completed by the study personnel and monitoring of this data will be performed by a CRA of the trial office according to the data management plan and data monitoring plan. Safety data will be collected according to the CTCAE 4.03 criteria and response data will be collected according to RECIST 1.1 criteria. Patients will go off study in the case of disease progression, unacceptable toxicity or withdrawal of consent by the patient.

### **Conclusion and discussion**

Although a major improvement in survival has been observed in recent years for patients with BRAFm melanoma, there are currently no effective treatment options for patients who failed both BRAFi/MEKi and immunotherapy. Albeit BRAFi/MEKi therapy is highly active with objective response rates between 66 and 70%, resistance to therapy will occur in almost all patients. In contrast, combination immunotherapy with ipilimumab and nivolumab can induce very durable tumor responses, but this is only observed in half of the patients.(29, 30)

Resistance to BRAFi/MEKi is frequently caused by reactivation of the MAPK signaling pathway and multiple mechanisms of reactivation have been described. Preclinical insights have shown that resistance to BRAFi/MEKi is associated with increased levels of ROS following drug withdrawal and subsequent treatment with the histone deacetylase inhibitor vorinostat further increases ROS levels in drug-resistant cells, resulting in apoptosis.

We here report a proof of concept clinical trial design to investigate the clinical activity of short term vorinostat treatment in BRAFm melanoma patients with progressive disease upon BRAFi/MEKi therapy.

Furthermore, we will explore the manufacturing of study medication by our institutes own pharmacy. Vorinostat 90 mg capsules will be manufactured in the pharmacy of the Antoni van Leeuwenhoek hospital, which will give several advantages. Most important is that start of the trial will not be delayed by study contracts and drug shipments from pharmaceutical companies. Another advantage is that the daily dose of 360 mg will be slightly lower than

the approved dose of 400 mg, probable leading to less toxic treatment. The last benefit of this concept is that costs per 90 mg capsule are only € 2,50 instead of € 91,65 per commercially available capsule of 100 mg. (31)

Secondary objectives also include safety and tolerability of intermittent treatment of vorinostat before and after treatment with BRAFi/MEKi . The decreased dose of 360 mg vorinostat in combination with a treatment duration of only 14 days might reduce the risk on vorinostat related toxicity. We attempt to further reduce the toxicity risk of combined vorinostat and BRAFi/MEKi by introducing a 3 day wash-out period for clearance of at least two half-lives of BRAFi/MEKi before the start of vorinostat. Because of the short half-life of vorinostat wash-out will not be necessary before switching back to BRAFi/MEKi.

Moreover, we want to analyze if emerging resistant clones with a secondary mutation in the MAPK pathway can be detected by ctDNA analysis and purged by short treatment with vorinostat. ctDNA analysis could possibly serve as an additional monitoring tool for advanced melanoma patients treated with BRAFi/MEKi. Because of the aggressive course of disease in metastatic melanoma, early detection of progression is of importance and might allow for a timely switch to other therapies.

Recently, more potent inhibitors of the MAPK pathway, such as encorafenib and binimetinib, are approved by the FDA and EMA. (32, 33) The more potent inhibition of proteins as BRAF or MEK can theoretically lead to different mechanisms of acquired resistance. For example, more amplification of the genes targeted by the drugs might be seen or mutations in components of pathways that mediate other crosstalk with the MAPK pathway might occur. Patients treated with these more potent inhibitors will probably be included in this trial, which may create an opportunity to detect different secondary mutation mechanisms and a different response on vorinostat during treatment with more and less potent BRAFi/MEKi.

This is a small single arm (proof of concept) study in a patient population with no standard and active treatment options. A larger and randomized follow-up trial will be necessary to obtain reliable conclusions on efficacy. For that reason, we will propose a larger confirmatory trial in patients with resistant advanced BRAFm melanoma, if proof of concept can be obtained in the small patient population of this clinical trial. The first arm of the confirmatory trial will consist of alternating treatment with BRAFi/MEKi and vorinostat and the second arm will contain only BRAFi/MEKi treatment beyond progression. If ctDNA analysis shows that resistant clones can be detected earlier than can be seen on radiological assessments, ctDNA instead of radiological assessment may be a potential biomarker to optimize the timing of alternation between vorinostat and BRAFi/MEKi.

## Executive summary

### Background and rationale

- Activating mutations of the *BRAF* gene are present in about half of the melanomas.
- The clinical benefit of treatment with BRAF and MEK inhibitors (BRAFi; MEKi) is limited due to the development of drug resistance within 6-14 months.
- Resistance is often associated with secondary mutations in the MAPK pathway leading to re-activation of the pathway.
- Preclinical and clinical studies have shown that short-term treatment with vorinostat can eliminate cells harboring secondary resistance mutations.
- Vorinostat is a histone deacetylase inhibitor that is FDA approved for the treatment of cutaneous T-cell lymphoma.

### Design

- This is a two-stage, single arm, mono-center proof of concept study to demonstrate the efficacy of sequential treatment with vorinostat and BRAFi/MEKi in resistant *BRAF*<sup>V600</sup> mutant melanoma.
- Patients with *BRAF*<sup>V600</sup> mutant melanoma will be included in this trial upon progression on BRAFi or BRAFi/MEKi.
- After a wash-out period of 3 days vorinostat 360 mg QD will be administered for 14 days to purge out the resistant clones. On day 15 BRAFi or BRAFi/MEKi treatment will be reintroduced according to standard care.
- If in the best interest of the patient a subsequent 14 days treatment cycle can be given upon newly developed resistance against BRAFi/MEKi.

### Objectives

- The primary objective is to demonstrate an anti-tumor response rate of progressive lesions of at least 30% of alternating treatment with the vorinostat and BRAFi/MEKi in advanced resistant BRAFm melanoma.
- Secondary objectives are:
  - to demonstrate that emerging resistant clones with a secondary mutation in the MAPK pathway can be detected by ctDNA analyses and purged by short term treatment with vorinostat
  - to characterize the safety and tolerability of intermittent treatment of vorinostat before and after treatment with BRAFi/MEKi in this population assessed by the incidence and severity of adverse events
  - to determine progression free survival and overall survival of alternating treatment with vorinostat and BRAFi/MEKi.
- During this trial additional blood and tissue sampling will be done for exploratory pharmacokinetic (PK), pharmacodynamic (PD) and pharmacogenetic (PG) analyses.

### Statistics

- Simon's minimax two-stage design is used with a power of 70% and a significance level of 5%.
- The first part will consist of 18 patients and if 3 or more favorable responses, 8 additional patients will be recruited in the second part. This makes a total sample size of 26 patients.
- If a response occurs in 2 or fewer patients in the first part, the study will be stopped and the efficacy of the treatment will be declared insufficient.

### Conclusion

- There remains an unmet need to develop new treatment strategies to further improve the efficacy of targeted therapy and significantly improve *BRAF*<sup>V600</sup> mutant melanoma patient's outcome.
- We here report a proof of concept clinical trial design to investigate the clinical activity of short term vorinostat treatment in BRAFm melanoma patients with progressive disease upon BRAFi/MEKi therapy.
- If proof of concept can be obtained, we will propose a confirmatory randomized trial with in the first arm alternating treatment with BRAFi/MEKi and vorinostat and in the second arm only BRAFi/MEKi treatment beyond progression.

## References

Papers of special note have been highlighted as: • of interest.

1. ECIS - European Cancer Information System. European Cancer Information System. <http://eco.iarc.fr/EUCAN/CancerOne.aspx?Cancer=46&Gender=2>. Accessed on 1 November 2019.
2. Wolter Kluwer. Molecularly targeted therapies for metastatic melanoma. [www.UpToDate.com](http://www.UpToDate.com). Accessed on 1 November 2019.
3. Zia Y, Chen L, Daud A. Future of combination therapy with dabrafenib and trametinib in metastatic melanoma. Expert opinion on pharmacotherapy. 2015;16(14):2257-63.
  - Review highlighting the pharmacology, efficacy, and toxicity of clinical trials with dabrafenib and trametinib in patients with *BRAF*<sup>V600E</sup> mutant melanoma. Half of the melanoma harbor a *BRAF*<sup>V600E</sup> mutation. A major problem of combined dabrafenib and trametinib is the development of resistant, mainly caused by secondary mutations in the MAPK pathway.
4. Chapman PB, Hauschild A, Robert C, Haanen JB, Ascierto P, Larkin J, et al. Improved survival with vemurafenib in melanoma with BRAF V600E mutation. The New England journal of medicine. 2011;364(26):2507-16.
5. Sosman JA, Kim KB, Schuchter L, Gonzalez R, Pavlick AC, Weber JS, et al. Survival in BRAF V600-mutant advanced melanoma treated with vemurafenib. The New England journal of medicine. 2012;366(8):707-14.
6. Werkgroep Nm. Concept richtlijn melanoom. [www.oncoline.nl/uploaded/docs/melanoom/CONCEPT%20richtlijn20melanoom.doc.pdf](http://www.oncoline.nl/uploaded/docs/melanoom/CONCEPT%20richtlijn20melanoom.doc.pdf). Accessed on 1 November 2019.
7. Long GV, Hauschild A, Santinami M, Atkinson V, Mandala M, Chiarion-Sileni V, et al. Adjuvant Dabrafenib plus Trametinib in Stage III BRAF-Mutated Melanoma. The New England journal of medicine. 2017;377(19):1813-23.
8. Michielin O, Hoeller C. Gaining momentum: New options and opportunities for the treatment of advanced melanoma. Cancer treatment reviews. 2015;41(8):660-70.
9. Nazarian R, Shi H, Wang Q, Kong X, Koya RC, Lee H, et al. Melanomas acquire resistance to BRAF(V600E) inhibition by RTK or N-RAS upregulation. Nature. 2010;468(7326):973-7.
10. Wang L, Leite de Oliveira R, Huijberts S, Bosdriesz E, Pencheva N, Brunen D, et al. An Acquired Vulnerability of Drug-Resistant Melanoma with Therapeutic Potential. Cell. 2018;173(6):1413-25.e14.
  - Resistance to BRAF and MEK inhibitors in *BRAF*<sup>V600E</sup> mutant melanoma is associated with increased levels of reactive oxygen species. Treating drug-resistant cells with the histone deacetylase inhibitor vorinostat results in an upregulation of the already high reactive oxygen species levels and leads to cell death. This is confirmed in mice. In a study in patients was found that vorinostat selectively purged out the resistant tumor clones harboring secondary mutations in the MAPK pathway.
11. Scholtens A, Geukes Foppen MH, Blank CU, van Thienen JV, van Tinteren H, Haanen JB. Vemurafenib for BRAF V600 mutated advanced melanoma: results of treatment beyond progression. European journal of cancer. 2015;51(5):642-52.
12. Sun C, Hobor S, Bertotti A, Zecchin D, Huang S, Galimi F, et al. Intrinsic resistance to MEK inhibition in KRAS mutant lung and colon cancer through transcriptional induction of ERBB3. Cell reports. 2014;7(1):86-93.
13. Ververis K, Hiong A, Karagiannis TC, Licciardi PV. Histone deacetylase inhibitors (HDACIs): multitargeted anticancer agents. Biologics : targets & therapy. 2013;7:47-60.
14. New M, Olzscha H, La Thangue NB. HDAC inhibitor-based therapies: can we interpret the code? Molecular oncology. 2012;6(6):637-56.
15. Lane AA, Chabner BA. Histone deacetylase inhibitors in cancer therapy. Journal of clinical oncology. 2009;27(32):5459-68.
16. US FDA. FDA approval Zolinza (vorinostat), prescribing information (2008).

17. Groenendijk FH, de Jong J, Fransen van de Putte EE, Michaut M, Schlicker A, Peters D, et al. ERBB2 mutations characterize a subgroup of muscle-invasive bladder cancers with excellent response to neoadjuvant chemotherapy. *European urology*. 2016;69(3):384-8.
18. Schreuer M, Jansen Y, Planken S, Chevolet I, Seremet T, Kruse V, et al. Combination of dabrafenib plus trametinib for BRAF and MEK inhibitor pretreated patients with advanced BRAF(V600)-mutant melanoma: an open-label, single arm, dual-centre, phase 2 clinical trial. *The Lancet oncology*. 2017;18(4):464-72.
19. Iwamoto M, Friedman EJ, Sandhu P, Agrawal NG, Rubin EH, Wagner JA. Clinical pharmacology profile of vorinostat, a histone deacetylase inhibitor. *Cancer chemotherapy and pharmacology*. 2013;72(3):493-508.
20. Eisenhauer EA, Therasse P, Bogaerts J, Schwartz LH, Sargent D, Ford R, et al. New response evaluation criteria in solid tumours: revised RECIST guideline (version 1.1). *European journal of cancer*. 2009;45(2):228-47.
21. Gray ES, Rizos H, Reid AL, Boyd SC, Pereira MR, Lo J, et al. Circulating tumor DNA to monitor treatment response and detect acquired resistance in patients with metastatic melanoma. *Oncotarget*. 2015;6(39):42008-18.
  - Circulating Tumor DNA is a non-invasive method to assess genetic changes during anti-cancer therapy. In 35 of the 48 patients with metastatic melanoma was circulating tumor DNA measurable. ctDNA levels lowered in response to treatment and a NRAS mutation, which might cause resistance to BRAF inhibitors, was detected in 43% of the patients. These data demonstrate that ctDNA is a valuable biomarker to monitor response on targeted therapies.
22. Calapre L, Warburton L, Millward M, Ziman M, Gray ES. Circulating tumour DNA (ctDNA) as a liquid biopsy for melanoma. *Cancer letters*. 2017;404:62-9.
23. Tsao SC, Weiss J, Hudson C, Christophi C, Cebon J, Behren A, et al. Monitoring response to therapy in melanoma by quantifying circulating tumour DNA with droplet digital PCR for BRAF and NRAS mutations. *Scientific reports*. 2015;5:11198.
24. Kelly WK, O'Connor OA, Krug LM, Chiao JH, Heaney M, Curley T, et al. Phase I study of an oral histone deacetylase inhibitor, suberoylanilide hydroxamic acid, in patients with advanced cancer. *Journal of clinical oncology*. 2005;23(17):3923-31.
  - In this phase I study, 73 patients with solid tumors were treated with different doses of vorinostat orally. Vorinostat could be safely administered in these patients. Pharmacokinetics were linear and pharmacodynamic analyses showed inhibition of histone deacetylase in peripheral-blood mononuclear cells.
25. Fujiwara Y, Yamamoto N, Yamada Y, Yamada K, Otsuki T, Kanazu S, et al. Phase I and pharmacokinetic study of vorinostat (suberoylanilide hydroxamic acid) in Japanese patients with solid tumors. *Cancer science*. 2009;100(9):1728-34.
26. Ramalingam SS, Kummar S, Sarantopoulos J, Shibata S, LoRusso P, Yerk M, et al. Phase I study of vorinostat in patients with advanced solid tumors and hepatic dysfunction: a National Cancer Institute Organ Dysfunction Working Group study. *Journal of clinical oncology*. 2010;28(29):4507-12.
27. Kelly WK, Richon VM, O'Connor O, Curley T, MacGregor-Curtelli B, Tong W, et al. Phase I clinical trial of histone deacetylase inhibitor: suberoylanilide hydroxamic acid administered intravenously. *Clinical cancer research*. 2003;9(10):3578-88.
28. Doi T, Hamaguchi T, Shirao K, Chin K, Hatake K, Noguchi K, et al. Evaluation of safety, pharmacokinetics, and efficacy of vorinostat, a histone deacetylase inhibitor, in the treatment of gastrointestinal (GI) cancer in a phase I clinical trial. *International journal of clinical oncology*. 2013;18(1):87-95.
29. Atkinson V. Recent advances in malignant melanoma. *Internal medicine journal*. 2017;47(10):1114-21.

30. Yu C, Liu X, Yang J, Zhang M, Jin H, Ma X, et al. Combination of immunotherapy with targeted therapy: Theory and practice in metastatic melanoma. *Frontiers in immunology*. 2019;10:990.
31. Geskin L, Malone DC. An exploratory cost-effectiveness analysis of systemic treatments for cutaneous T-cell lymphoma. *The Journal of dermatological treatment*. 2018;29(5):522-30.
32. Delord JP, Robert C, Nyakas M, McArthur GA, Kudchakar R, Mahipal A, et al. Phase I dose-escalation and -expansion study of the BRAF inhibitor encorafenib (LGX818) in metastatic BRAF-mutant melanoma. *Clinical cancer research*. 2017;23(18):5339-48.
33. Bendell JC, Javle M, Bekaii-Saab TS, Finn RS, Wainberg ZA, Laheru DA, et al. A phase 1 dose-escalation and expansion study of binimetinib (MEK162), a potent and selective oral MEK1/2 inhibitor. *British journal of cancer*. 2017;116(5):575-83.





# CHAPTER 2.3

A proof of concept study of sequential treatment with the histone deacetylase inhibitor vorinostat plus BRAF and/or MEK inhibitors in patients with resistant *BRAFV600* mutated advanced melanoma

Sanne Huijberts, Liqin Wang,  
Rodrigo Leite de Oliveira, Hilde Rosing,  
Bastiaan Nuijen, Jos Beijnen, Rene Bernards,  
Jan Schellens, Sofie Wilgenhof

*Interim analysis*

## **Abstract**

### **Background**

Development of resistance to BRAF- and MEK-inhibitors (BRAFi; MEKi) limits the clinical benefit in *BRAF*<sup>V600</sup> mutant melanoma. Switching from a BRAFi to vorinostat resulted in a decline in tumor volume in resistant *BRAF*<sup>V600</sup> mutant melanoma in preclinical models. Tumor assessments of six patients treated with continuously vorinostat (360 mg once daily) showed progression of BRAFi sensitive clones but regression of BRAFi resistant clones. Tumor biopsies revealed acquired mutations, e.g. *NRAS*<sup>Q61H</sup> and *KRAS*<sup>G12C</sup>, at baseline and a complete elimination after 14 days of vorinostat. Based on these results, it was postulated that elimination of resistant *BRAF*<sup>V600</sup> melanoma cells can be achieved by short treatment of vorinostat due to killing of resistant tumor cells.

### **Methods**

In this two-stage, proof of concept study, 26 *BRAF*<sup>V600</sup> mutant melanoma patients with resistance to BRAFi/MEKi will be treated with vorinostat for 14 days and thereafter BRAFi/MEKi will be reintroduced. The primary aim is to demonstrate a response rate of progressive lesions of  $\geq 30\%$ . Secondary endpoints are to investigate whether emerging resistant clones harboring secondary mutations in the MAPK pathway (e.g. *NRAS* or *KRAS* mutations) can be eliminated by short-term treatment with vorinostat and if these mutations can be detected by ctDNA analysis. Pharmacokinetic and pharmacogenetic analyses will be performed in blood and tumor tissue.

### **Results**

At data cut-off (26 March 2020), an overall response rate of progressive target lesions of 25% was achieved in 11 evaluable patients. Overall confirmed response rate of all target lesions was 9% in 8 evaluable patients. The median time to progression was 50 days, three patients were on treatment for at least 5 months. No safety issues were observed. Emerging secondary mutations in *NRAS* were detectable in ctDNA of three patients at the time of BRAFi resistance. *NRAS* mutations were not eliminated in all patients.

### **Conclusions**

In the patients analyzed to date, we observed clinical benefit in three out of 11 patients. *NRAS* mutations were detectable in ctDNA, but not eliminated in all patients by vorinostat. Although the outcome in some patients is encouraging, it is too early to draw a conclusion on efficacy. Currently, recruitment in phase I of the Simon two-stage design is ongoing.

## Introduction

In recent years, prevalence of melanoma and its associated mortality is rising rapidly.(1) In 2018 almost 300.000 new cases of melanoma were diagnosed worldwide. Significant improvement in prognosis for advanced melanoma patients has been made by introduction of targeted therapies and checkpoint inhibitors in the last decade.(2)

Approximately 50% of melanomas harbor activating mutations in the *BRAF* gene, which encodes the serine-threonine protein kinase BRAF. This protein plays a prominent role in the mitogen-activated protein kinases signaling (MAPK) pathway causing cell proliferation and tumor growth. BRAF can be inhibited with a BRAF inhibitor (BRAFi) and the two kinases that act downstream of BRAF, MEK1 and MEK2, which can be inhibited with drugs known as MEK inhibitors (MEKi).(3) Progression-free survival (PFS) and overall survival (OS) of patients with advanced *BRAF*<sup>V600</sup> mutant melanomas are improved by combined treatment with a BRAFi and MEKi, compared to monotherapy with a BRAFi.(4-6) More recent, a clinical study demonstrated that also a significantly lower risk of recurrence in stage III *BRAF*<sup>V600</sup> melanoma patients can be achieved with adjuvant BRAF and MEK inhibition during one year.(7)

Nevertheless, *BRAF*<sup>V600</sup> mutant melanoma develop resistance to BRAF and MEK inhibition in 9-14 months.(3, 8) This resistance is mostly caused by acquired secondary mutations in the MAPK pathway, such as *NRAS* or *KRAS* mutations, which lead to re-activation of this pathway.(9, 10) Currently, the prognosis for patients that failed immunotherapy and also develop resistance to BRAFi and/or BRAFi/MEKi is disappointing without any effective treatment options.(11)

Sun et al. demonstrated that withholding of BRAFi and/or BRAFi/MEKi in resistant melanoma cells causes reversible hyperactivation of the MAPK pathway, leading to a transient growth arrest with hallmarks of oncogene-induced senescence.(12) In more recent cell line experiments it has been shown that the hyperactivation of the MAPK pathway results in an increase in reactive oxygen species (ROS). The histone deacetylase inhibitor vorinostat further increases these ROS levels, leading to cell death in resistant *BRAF*<sup>V600</sup> mutant melanoma cells.(10) In mice with BRAFi resistant *BRAF* mutant melanoma, complete disappearance of the tumor was obtained after treatment with vorinostat.(10)

Vorinostat is approved by the Food and Drug Administration for the treatment of cutaneous T-cell lymphoma (CTCL) in patients whose disease was progressive, persistent or recurrent on or after two lines of systemic therapies.(13) Vorinostat inhibits histone deacetylases 1, 2, 3 and 6, which are enzymes that work on the lysine residues of histones and transcription factors by catalyzing the removal of acetyl groups. Repression of gene transcription and a condense chromatin structure are the result of this acetyl group removal.(14-16) The inhibitory activity of vorinostat leads to the accumulation of acetylated histones, causing cell cycle arrest and apoptosis.(13)

As a result of these preclinical findings, a proof of concept study was designed in patients with advanced *BRAF*<sup>V600</sup> mutant melanoma resistant to BRAFi/MEKi. A total of six patients were treated with continuously administered vorinostat 360 mg daily. The patients showed

regression of some metastasis but also progression of other metastatic lesions at the first tumor assessment after 6 weeks of treatment with vorinostat. The tumor biopsies and circulating tumor DNA (ctDNA) samples of these patients revealed acquired mutations in the MAPK pathway causing resistance, e.g. at baseline *KRAS*<sup>G12C</sup> and *NRAS*<sup>Q11H</sup>, and had a complete disappearance of these mutations in tumor biopsies and at least a decrease of the percentage of the resistance mutations in ctDNA after two weeks of treatment with vorinostat.

Based on these clinical and preclinical results we hypothesized that vorinostat treatment leads to regression of BRAFi/MEKi resistant clones and has only minor effect on BRAFi/MEKi sensitive clones. Moreover, we postulate that short-term treatment with vorinostat can eliminate BRAFi/MEKi resistant *BRAF*<sup>V600</sup> melanoma cells harboring a secondary mutation in the MAPK-pathway.

Based on this hypothesis the study protocol was amended to change the treatment schedule. Patients with advanced *BRAF*<sup>V600</sup> mutant melanoma progressive on BRAFi/MEKi treatment were treated with vorinostat 360 mg daily for 14 days to eliminate the resistant clones, and thereafter BRAFi/MEKi treatment was reintroduced to treat the remaining BRAFi/MEKi sensitive population.

In this proof of concept study, we aimed to reach an overall response rate of progressive target lesions of at least 30% with the sequential of vorinostat and BRAFi/MEKi. Secondary aims are to characterize safety and tolerability of vorinostat in this patient population, to assess the pharmacokinetic profile of vorinostat and to investigate if secondary mutations causing resistance can be detected by ctDNA analysis and be eliminated by two weeks of vorinostat treatment. In this report, we provide an interim analysis of the ongoing clinical trial.

## Patients and methods

### Patient population

This ongoing, investigator-initiated, monocenter, two-stage, open-label, proof of concept study enrolled patients at the Netherlands Cancer Institute/Antoni van Leeuwenhoek hospital. Patients with *BRAF*<sup>V600</sup> mutant melanoma are eligible after response on BRAFi/MEKi treatment of at least 4 weeks and thereafter the development of resistance to BRAFi or BRAFi/MEKi. To eliminate the resistant cells, patients will be treated with vorinostat 360 mg daily for 14 days after a BRAFi/MEKi washout period of 3 days (figure 1). Other inclusion criteria are age  $\geq 18$  years, WHO performance status of 0-2 and a life expectancy of  $\geq 3$  months. Laboratory safety values include, Hemoglobin  $\geq 6.0$  mmol/L, ANC  $\geq 1.5 \times 10^9$  /L, Platelet count  $\geq 100 \times 10^9$  /L, serum creatinine  $\leq 1.5 \times$  ULN or creatinine clearance  $\geq 50$  ml/min (by Cockcroft-Gault formula or MDRD), serum bilirubine  $\leq 1.5 \times$  ULN, ALAT and ASAT  $\leq 2.5 \times$  ULN (in case of liver metastases ALAT and ASAT  $\leq 5 \times$  ULN). At least one progressive target lesion must be measurable on radiological assessments according to RECIST 1.1. Patients must consent to undergo tumor biopsies if technically feasible and willing to undergo blood draws for exploratory analyses. Pregnant patients and patients that

use unreliable contraceptive methods are excluded from this trial. Also excluded are patients with symptomatic brain metastasis, leptomeningeal disease or a myocard infarction within 6 months before start in the study. Previous treatment with vorinostat or other HDAC inhibitors is not allowed. Chemotherapy, immunotherapy or any investigational drugs, except BRAFi and MEKi, are forbidden within 21 days before receiving the first dose of vorinostat. Radiotherapy is only accepted for pain palliation in a dose of 1 x 8 Gray. Human Immunodeficiency Virus HIV-1 or HIV-2 type or a known history of hepatitis B or C or other uncontrolled infectious disease leads to exclusion for this trial.

The study was conducted in accordance with guidelines for Good Clinical Practice as defined by the International Conference on Harmonization. The study protocol and all amendments were approved by the Dutch competent authority (CCMO) and the ethics committee of the NKI-AVL (METC AVL). This study is registered on ClinicalTrials.gov (NCT02836548) and funded by Oncode and an ERC proof of concept grant.

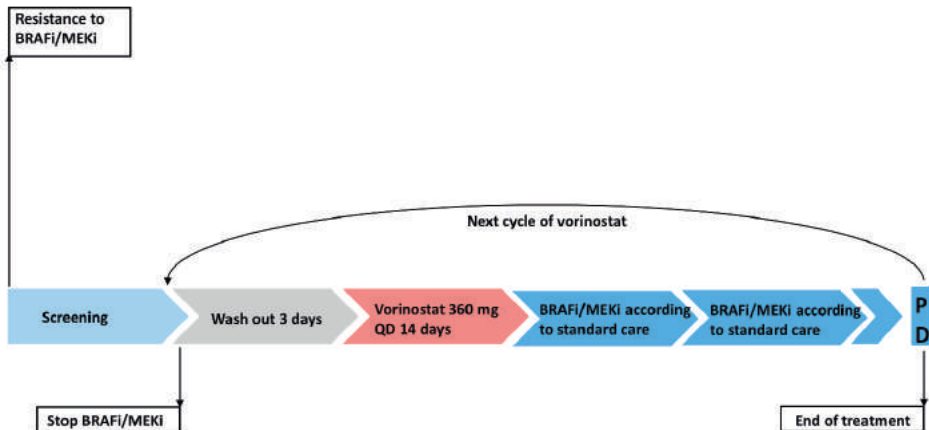


**Figure 1. Schematic view of treatment schedule.**

*At progressive disease, a next cycle of vorinostat will be administered if in best interest of the patient or patients will be declared end of treatment.*

*Abbreviations: PD, progressive disease; BRAFi, BRAF inhibitor; MEKi, MEK inhibitor; QD, once daily.*

### Study design and procedures

Patients were treated with orally administered vorinostat 360 mg once daily (QD) for 14 days upon progression on BRAFi/MEKi. One cycle of vorinostat is defined as vorinostat 360 mg QD for 14 days. This dose is slightly lower than the registered dose of 400 mg for CTCL. On day 15, patients switched back to a BRAFi or combination of BRAFi/MEKi according to standard care. A subsequent cycle of vorinostat treatment could be given if in best interest of the patient and upon newly developed BRAFi resistance. Patients continued in the study until disease progression, unacceptable toxicity, or investigator/patient decision to discontinue.

CT-scans and if indicated MRI-scans were scheduled at baseline and every 6 weeks to evaluate response according to Response Evaluation Criteria in Solid Tumors (RECIST) version 1.1.(17) After three tumor assessments from day one of every cycle of vorinostat radiological assessments were planned according to the treating oncologist's discretion. Patients were evaluable for tumor response if at least one dose of vorinostat was administered. To proof the concept of this study, only at baseline defined progressive target lesions were measured during the first tumor assessment after the start of every new cycle of vorinostat. After the first CT-scan all lesions were included in the response analyses. Monitoring of safety was done throughout the treatment by physical examination including vital signs, electrocardiography and laboratory assessments. Adverse events related to vorinostat were collected and recorded according to Common Terminology Criteria for Adverse Events version 4.3.

### **Pharmacokinetic, pharmacodynamic and pharmacogenetic analyses**

During the first cycle of vorinostat on day 1 and day 14 serial blood samples were drawn pre-dose, 0.5, 1, 1.5, 2, 3, 4, 6, 8, 10, 11 and 24 hours post-dose of vorinostat intake. The pharmacokinetic analyses of vorinostat, and its metabolites, 4-anilino-4-oxobutanoic acid and vorinostat-glucuronide was performed by using a validated high performance liquid chromatography-tandem mass spectrometry method (HPLC-MS/MS). Furthermore, blood was sampled at baseline and every two weeks for the exploratory analysis of ctDNA, conducted by Inivata. This analysis is performed through a qualitative DNA sequencing technology that detects single nucleotide variants, copy number variations, insertions and deletions in a selected 36-gene panel (InVisionSeq, Inivata, NC, USA). The aim is to analyse ctDNA for acquired resistance mutations and to proof if these mutations can be eliminated with a 14-day cycle of vorinostat. Moreover, ctDNA changes might precede radiological progression which will also be investigated in this study.(18-20) At baseline, on cycle 1 day 14 and at disease progression tumor biopsies were taken, preferably from progressive target lesions. To proof the scientific rationale of the mechanism of action of alternating treatment with vorinostat and BRAFi/MEKi, pharmacodynamic and pharmacogenetic assessments were performed on these biopsies.

### **Statistical analysis**

Assuming a true response rate of progressive lesions of 30%, 26 patients yield 70% power to reject the null hypothesis of a 13% response rate with a one-sided alpha of 0.05. The first part of the Simon's minimax two-stage design consists of 18 patients. If three or more patients show a response an additional 8 patients will be included in the second part of the two-stage design. The true probability of response was set on 13%, which means that the probability of study discontinuation after part 1 will be 58%.

The overall response rate was performed by investigator assessment and analyses was done with a standard logistic regression model. Pharmacokinetics, pharmacodynamics, pharmacogenetics and safety were reported descriptively.

## Results

### Patient disposition and characteristics

At data cut-off (26 March 2020), 12 patients with resistant *BRAF*<sup>V600</sup> mutant advanced melanoma were enrolled onto this trial between September 2018 and February 2020. All patients developed resistance to BRAF inhibition with or without MEK inhibition after a documented anti-tumor response of at least four weeks. The majority of patients was pretreated with at least three prior antineoplastic treatment lines for advanced disease. A total of 11 patients were evaluable for response, one patient was considered not evaluable due to rapidly progressive disease before the start of vorinostat treatment. At data cut-off, two patients were ongoing and ten patients had discontinued treatment due to progressive disease (n=9) or clinical deterioration (n=1).

**Table 1. Baseline and disease characteristics.**

	Patients (n=12)
Sex, n (%)	
Male	8
Female	4
Age, median (range), years	57 (41 – 70)
ECOG PS, n (%)	
0	10
1	2
Number of prior treatment lines, n (%)	
1	0
2	1
≥ 3	11

Abbreviation: ECOG, Eastern Cooperative Oncology Group performance status.

### Anti-tumor activity

Eleven patients were evaluable for anti-tumor activity (figure 2); most patients received one cycle of vorinostat (n=6), one patient received two cycles and two patients received three vorinostat cycles. Vorinostat was discontinued before completion of cycle one (vorinostat 360 mg QD for 14 days) in three patients due to rapidly progressive brain metastases (n=2) or abdominal metastasis (n=1).

The primary aim of this trial is an overall response rate of at least 30% of progressive target lesions. Consequently, the first analysis was only done in the before defined progressive target lesions and the second analysis included all lesions (table 2). Response of the progressive target lesion is based on the first radiological assessment or in case of partial response the first and second radiological assessment for confirmation of partial response. In three patients, the response of the progressive target lesion could not be determined due to lack of follow-up radiological assessments because of rapidly progressive disease. The overall response rate based on progressive target lesions was 25% (n=2) and three patients showed a stable disease.

Response of all target lesions could be determined in 11 patients. The majority of patients (n=7) revealed progressive disease as best response, three patients had stable disease including one non-confirmed partial response and one patient showed a confirmed partial response.

At data cut-off, the overall median duration of treatment was 50 days. The two ongoing patients had the longest treatment duration of 498 and 468 days (figure 3). Both patients revealed stable disease as best response.

**Table 2. Clinical activity of subsequent treatment with vorinostat and BRAFi/MEKi.**

	Progressive target lesion (n=8)	All lesions (n=11)
PR, n (%)	2 (25)	1 (9)
SD, n (%)	3 (38)	3 (27)
PD, n (%)	3 (38)	7 (64)
ORR, n (%)	2 (25)	1 (9)

Abbreviations: PR, partial response; SD, stable disease; PD, progressive disease; ORR, overall response rate.

**Table 3. Vorinostat-related adverse events.**

Adverse event, n (%)	Grade 1	Grade 2	Total
Nausea	4 (36)	1 (9)	5 (45)
Fatigue	3 (27)	1 (9)	4 (36)
Vomiting	3 (27)		3 (27)
Anorexia	2 (18)	1 (9)	3 (27)
Headache		1 (9)	1 (9)
Diarrhea	1 (9)		1 (9)
Dry cuticles skin	1 (9)		1 (9)
Muscle stiffness	1 (9)		1 (9)
Weight loss	1 (9)		1 (9)
Dry mouth	1(9)		1 (9)
Dyspnea		1 (9)	1 (9)
Cough		1 (9)	1 (9)

All adverse events that are definite, probable or possible related to vorinostat were considered as study drug related.

## Safety

Adverse events related to vorinostat were reported in the eleven patients that started vorinostat treatment, only grade 1 or 2 adverse events occurred. No adverse events were reported that caused treatment interruption of vorinostat. In all cases, supportive care was sufficient to decrease the severity of the event to grade 1 or less. The most common events were nausea (45%), fatigue (36%), vomiting (27%) and anorexia (27%) (table 3). Supportive care, including metoclopramide was sufficient to manage nausea.

Since toxicities related to BRAFi and/or MEKi were managed according to standard care, no adverse events were collected for these drugs.



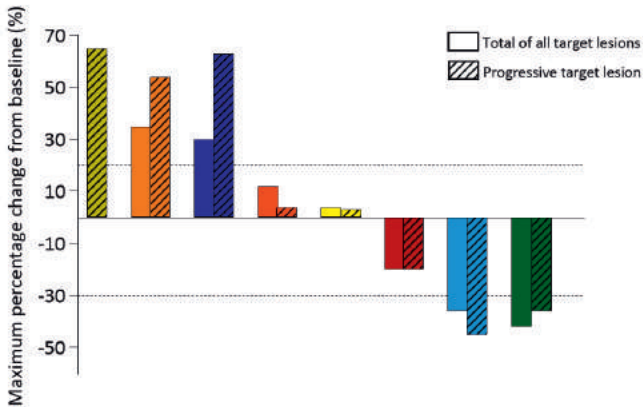


**Figure 2. Maximum percentage change in sum of progressive and all target lesion size from baseline, including response assessed by RECIST.**  
Every color represents a patient, two bars per patient are shown for the total of all target lesions and the progressive target lesion only.

2

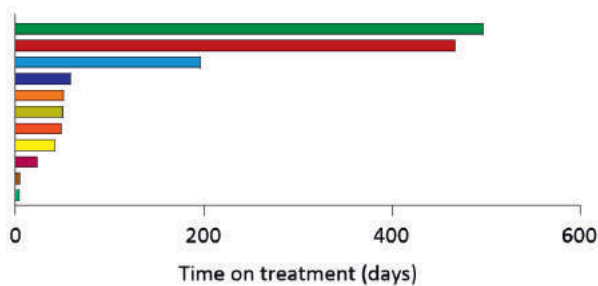


**Figure 3. Swimmer plot of treatment duration.**  
Every bar represents one patient.

### Pharmacokinetic analyses

Pharmacokinetic parameters of vorinostat and its pharmacologically inactive metabolites, 4-anilino-4-oxobutanoic acid and vorinostat-glucuronide are summarized in table 4 and the mean plasma concentration-time curves, including error bars, are shown in figure 4. The mean vorinostat peak plasma concentration ( $C_{max}$ ) and area under the plasma concentration-time curve from time 0 to 24 hours ( $AUC_{0-24h}$ ) were similar after one single administration and at steady state, which indicates that no drug accumulation occurs after multiple dosing. Vorinostat trough concentrations were below the lower limit of quantification (2.0 ng/ml), which corresponds with the short half-life of vorinostat of approximately 2 hours.(21, 22)

The  $C_{max}$  and  $AUC_{0-24h}$  of both metabolites were higher than for vorinostat, including a 4-6 fold higher  $C_{max}$  and 2-3 times higher  $AUC_{0-24h}$ . Vorinostat showed moderate to high interpatient variability in our study with concentrations ranging from 963-2807 ng/ml at steady state.

**Table 4. Pharmacokinetic parameters of vorinostat and its active metabolites 4-anilino-4-oxobutanoic acid and vorinostat-glucuronide, at the first day of administration (C1D1) and at steady state (C1D14).**

Timepoint	Vorinostat		4A4O acid		Vorinostat-glucuronide	
	C1D1	C1D14	C1D1	C1D14	C1D1	C1D14
Mean	n = 11	n = 7	n = 11	n = 7	n = 11	n = 7
C <sub>max</sub> (ng/ml)	497	424	883	960	1519	1420
T <sub>max</sub> (h)	1.6	1.5	3.1	2.5	2.1	1.8
AUC <sub>0-24h</sub> (ng*h/ml)	1858	1489	6895	8319	7198	5696

Abbreviations: C1D1, cycle 1 day 1; C1D14, cycle 1 day 14; 4A4O acid, 4-anilino-4-oxobutanoic acid; vor-glu; C<sub>max</sub>, peak plasma concentration; t<sub>max</sub>, time of maximum plasma concentration observed; AUC<sub>0-24h</sub>, area under the plasma concentration-time curve from time zero to 24 hours; T<sub>1/2</sub>, elimination half-life.

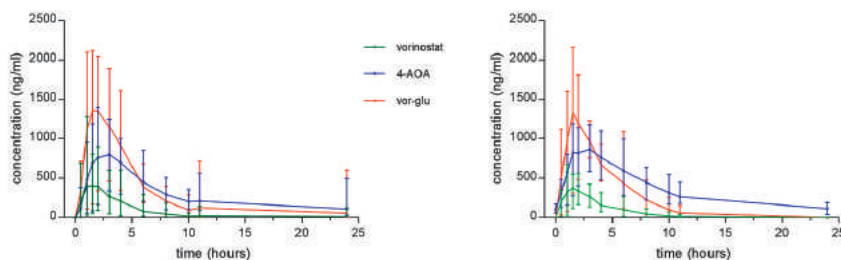


**Figure 4. Pharmacokinetic profiles of vorinostat and its metabolites 4-anilino-4-oxobutanoic acid and vorinostat-glucuronide.**

Left: Plasma concentration time curve of mean plasma levels on cycle 1 day 1 with error bars.(n=11)

Right: Plasma concentration time curve of mean plasma levels at steady state (cycle 1 day 14) with error bars.(n=7)

Abbreviations: 4-AOA, 4-anilino-4-oxobutanoic acid; vor-glu, vorinostat-glucuronide

### Pharmacogenetic analyses

Blood samples for ctDNA analysis were collected for nine patients and ctDNA was evaluable in six patients. For the three non-evaluable patients ctDNA was only collected at baseline (n=2) and for the other patient the quality of the DNA in the sample was not sufficient to draw a conclusion.

Emerging secondary mutations causing resistance to BRAFi and/or MEKi were detected in two patients, including *NRAS*<sup>Q61K</sup>, *NRAS*<sup>Q61L</sup> and *NRAS*<sup>G13R</sup> in one patient and *NRAS*<sup>Q61L</sup> in the other patient. The best response for the progressive target lesion and overall best response was progressive disease for both patients. Although the *NRAS*<sup>Q61L</sup> mutation was initially eliminated by vorinostat treatment in one of the two patients, this mutation was again detectable 2 weeks thereafter.

For one patient, no resistance mutations were found at baseline, nor after the first two cycles of vorinostat. This patient developed progressive disease after cycle two and a newly developed *NRAS*<sup>Q61K</sup> mutation was detected in ctDNA, therefore vorinostat was reintroduced. After the first two vorinostat cycles a partial response of the total of target

lesions was observed, but no tumor response was seen after the third vorinostat cycle and the *NRAS*<sup>Q61K</sup> mutation was not eliminated.

For the two ongoing patients with the longest treatment response, no emerging mutations were detected at baseline, nor during the treatment course.

## Discussion

The aim of this study was to evaluate the anti-tumor activity of alternating treatment with vorinostat and BRAFi/MEKi in patients with resistant *BRAF*<sup>V600</sup> mutant advanced melanoma. At date cut-off, the overall response rate of progressive target lesions was 25% and of all lesions was 9% in the eleven evaluable patients. Besides the two patients with a partial response of the progressive target lesion, stable disease was observed in three patients. Moreover, three patients showed a time to progression of >5.2 months, which was described as the median progression free survival for patients treated with the BRAFi vemurafenib beyond progression.(11) Although the primary aim of this proof of concept study is currently not met, we assume that sequential treatment of vorinostat and BRAFi/MEKi might improve patient outcome because of the relatively long treatment duration in some patients. In 2 patients, tumor regression was also observed upon a second cycle of vorinostat after initial progression, suggesting a cyclic-alternating approach might be beneficial in some patients.

The second important goal of this proof of concept study was to demonstrate whether emerging resistant clones with a secondary mutation in the MAPK pathway could be detected by ctDNA analyses and eliminated by two weeks of vorinostat treatment. The ctDNA results showed that *NRAS* mutations were detectable at baseline in two patients and during treatment in one patient. These *NRAS* mutations, such as *NRAS*<sup>Q61L</sup>, *NRAS*<sup>G13R</sup> and *NRAS*<sup>Q61K</sup> are all pathogenic according to the COSMIC database and the *NRAS*<sup>Q61K</sup> mutation is a known resistance mutation for the BRAF inhibitors vemurafenib and dabrafenib.(23) Due to the small sample size, no clear correlation could be made between the detection of resistance mutations in ctDNA and response. For the two ongoing patients with a stable disease of 498 and 468 days, no emerging mutations causing resistance were detected at baseline, nor during study treatment. For the other patient with a time to progression of > 5.2 months, we have observed that a *NRAS* mutation could be detected after two cycles of vorinostat and that this mutation was not eliminated by vorinostat treatment. In line with the development of this *NRAS* mutation was the poor response to the third cycle of vorinostat, despite the partial response earlier observed after the first two cycles of vorinostat. This implies that another resistance and response mechanism may play a role in this patient. Hopefully, we will gain more insights into these mechanisms during the official interim analysis, including exploratory analyses of pharmacodynamics and pharmacogenetics after part 1 of the Simon Two-stage design of this trial. Pharmacogenetic analyses will include DNA/RNA sequencing of tumor biopsies and ctDNA analysis in blood. Pharmacodynamic biomarkers to be investigated include but are not limited to the ROS antiporter SLC7A11, the signaling markers phosphorylated ERK and EGFR, the DNA damage

marker  $\gamma$ H2AX, the apoptosis marker cleaved-PARP and immune markers. The pharmacodynamic biomarkers are based on the results of the in vitro and in vivo studies of vorinostat in resistant *BRAF*<sup>V600</sup> mutated melanoma cell lines.(10)

Most common adverse events were fatigue and gastro-intestinal toxicities, which is comparable to earlier reported adverse events of vorinostat. In contrast to literature, no grade three or higher events were observed.(13) The milder toxicity profile might be the result of the slightly lower dose of 360 mg once daily instead of the registered posology of 400 mg once daily and the short treatment duration of only 14 days. Furthermore, no significant risk of overlapping toxicities between vorinostat and BRAFi/MEKi was expected due to the washout period of three days in which at least three half-lives were washed out for BRAFi and/or MEKi. Since the short half-life of vorinostat (approximately two hours), only one day of washout was necessary before the re-introduction of BRAF and/or MEK inhibition. Indeed, our pharmacokinetic results show trough levels equal to zero at 24 hours after vorinostat administration, which confirms that one washout day might be sufficient to prevent overlapping toxicity of vorinostat and BRAFi and/or MEKi.

The majority of the pharmacokinetic results in our study were in line with previously reported data. Although AUC<sub>0-24h</sub> was similar to literature for vorinostat and its metabolites, the C<sub>max</sub> of vorinostat was almost 2-fold higher than in earlier reported data.(22, 24) However, this might be caused by the known moderate to high interpatient variability in combination with the small patient population of this interim analysis. The higher C<sub>max</sub> might also be influenced as a result of breakfast intake together with vorinostat administration, since vorinostat absorption is influenced by food.(22)

As described in the introduction, the current sequential treatment schedule is based on results of the first patients that were treated with continuous vorinostat. Based on the observations in the current study, the treatment schedule might be further optimized after completion of the first part of the Simon Two-stage design. The monitoring of ctDNA might give more insights into the time until development and elimination of secondary mutations causing resistance and the best timing of vorinostat treatment will preferably be determined based on this exploratory analysis. Moreover, optimization of patient selection is pivotal to make this sequential treatment a successful strategy. Currently, a significant part of the enrolled patients developed rapidly progressive disease and no beneficial effect of vorinostat treatment. This progression is probable caused by the heterogeneity of the heavily pretreated advanced disease. Sensitive clones for BRAF inhibition can grow out after BRAFi/MEKi is temporarily discontinued to administer vorinostat. This heterogeneity is a difficult factor in melanoma treatment and might also be the limiting factor for the anti-tumor response in this proof of concept trial. Nevertheless, the here described time on treatment and pharmacogenetic results are encouraging. Currently, patient enrollment is ongoing in the first part of the Simon Two-stage design. The planned interim analyses might give more relevant information on the feasibility, anti-tumor activity and mechanisms of resistance and response of sequential treatment of vorinostat and BRAFi/MEKi in resistant *BRAF*<sup>V600</sup> mutant melanoma.



## References

1. Sosman JA, Atkins MB, Shah S. Overview of the management of advanced cutaneous melanoma. Up to Date Wolters Kluwer;2019. <http://www.UpToDate.com>. Accessed on 14 March 2020.
2. World Cancer Research Fund International. <https://www.wcrf.org/dietandcancer/cancer-trends/skin-cancer-statistics>. Accessed on 20 Nov 2019.
3. Zia Y, Chen L, Daud A. Future of combination therapy with dabrafenib and trametinib in metastatic melanoma. *Expert opinion on pharmacotherapy*. 2015;16(14):2257-63.
4. Chapman PB, Hauschild A, Robert C, Haanen JB, Ascierto P, Larkin J, et al. Improved survival with vemurafenib in melanoma with BRAF V600E mutation. *The New England journal of medicine*. 2011;364(26):2507-16.
5. Sosman JA, Kim KB, Schuchter L, Gonzalez R, Pavlick AC, Weber JS, et al. Survival in BRAF V600-mutant advanced melanoma treated with vemurafenib. *The New England journal of medicine*. 2012;366(8):707-14.
6. Werkgroep Nm, IKNL. Concept richtlijn melanoom 2012. <http://www.oncoline.nl>. Accessed on 10 March 2020.
7. Long GV, Hauschild A, Santinami M, Atkinson V, Mandala M, Chiarion-Sileni V, et al. Adjuvant dabrafenib plus trametinib in stage III BRAF-mutated melanoma. *The New England journal of medicine*. 2017;377(19):1813-23.
8. Michielin O, Hoeller C. Gaining momentum: New options and opportunities for the treatment of advanced melanoma. *Cancer treatment reviews*. 2015;41(8):660-70.
9. Nazarian R, Shi H, Wang Q, Kong X, Koya RC, Lee H, et al. Melanomas acquire resistance to B-RAF(V600E) inhibition by RTK or N-RAS upregulation. *Nature*. 2010;468(7326):973-7.
10. Wang L, Leite de Oliveira R, Huijberts S, Bosdriesz E, Pencheva N, Brunen D, et al. An acquired vulnerability of drug-resistant melanoma with therapeutic potential. *Cell*. 2018;173(6):1413-25.e14.
11. Scholtens A, Geukes Foppen MH, Blank CU, van Thienen JV, van Tinteren H, Haanen JB. Vemurafenib for BRAF V600 mutated advanced melanoma: results of treatment beyond progression. *European journal of cancer*. 2015;51(5):642-52.
12. Sun C, Hobor S, Bertotti A, Zecchin D, Huang S, Galimi F, et al. Intrinsic resistance to MEK inhibition in KRAS mutant lung and colon cancer through transcriptional induction of ERBB3. *Cell reports*. 2014;7(1):86-93.
13. Food and Drug Administration. FDA approval Zolinza (vorinostat). 2006, revised 2008. <http://accessdata.fda.gov>. Accessed on 12 December 2020.
14. Ververis K, Hiong A, Karagiannis TC, Licciardi PV. Histone deacetylase inhibitors (HDACIs): multitargeted anticancer agents. *Biologics : targets & therapy*. 2013;7:47-60.
15. Lane AA, Chabner BA. Histone deacetylase inhibitors in cancer therapy. *Journal of clinical oncology*. 2009;27(32):5459-68.
16. New M, Olzscha H, La Thangue NB. HDAC inhibitor-based therapies: can we interpret the code? *Molecular oncology*. 2012;6(6):637-56.
17. Eisenhauer EA, Therasse P, Bogaerts J, Schwartz LH, Sargent D, Ford R, et al. New response evaluation criteria in solid tumours: revised RECIST guideline (version 1.1). *European journal of cancer*. 2009;45(2):228-47.
18. Gray ES, Rizos H, Reid AL, Boyd SC, Pereira MR, Lo J, et al. Circulating tumor DNA to monitor treatment response and detect acquired resistance in patients with metastatic melanoma. *Oncotarget*. 2015;6(39):42008-18.
19. Calapre L, Warburton L, Millward M, Ziman M, Gray ES. Circulating tumour DNA (ctDNA) as a liquid biopsy for melanoma. *Cancer letters*. 2017;404:62-9.
20. Tsao SC, Weiss J, Hudson C, Christophi C, Cebon J, Behren A, et al. Monitoring response to therapy in melanoma by quantifying circulating tumour DNA with droplet digital PCR for BRAF and NRAS mutations. *Scientific reports*. 2015;5:11198.

21. Fujiwara Y, Yamamoto N, Yamada Y, Yamada K, Otsuki T, Kanazu S, et al. Phase I and pharmacokinetic study of vorinostat (suberoylanilide hydroxamic acid) in Japanese patients with solid tumors. *Cancer science*. 2009;100(9):1728-34.
22. Rubin EH, Agrawal NG, Friedman EJ, Scott P, Mazina KE, Sun L, et al. A study to determine the effects of food and multiple dosing on the pharmacokinetics of vorinostat given orally to patients with advanced cancer. *Clinical cancer research*. 2006;12(23):7039-45.
23. Tate JG, Bamford S, Jubb HC, Sondka Z, Beare DM, Bindal N, et al. COSMIC: the Catalogue Of Somatic Mutations In Cancer. *Nucleic acids research*. 2019;47(D1):D941-d7.
24. Fujiwara Y, Nokihara H, Yamada Y, Yamamoto N, Sunami K, Utsumi H, et al. Phase 1 study of galunisertib, a TGF-beta receptor I kinase inhibitor, in Japanese patients with advanced solid tumors. *Cancer chemotherapy and pharmacology*. 2015;76(6):1143-52.





# CHAPTER 3

Double or triple targeted combinations for the treatment of *BRAFV600E* mutant colorectal cancer



# CHAPTER 3.1

Binimetinib, encorafenib and cetuximab triplet therapy for patients with *BRAFV600E*-mutant metastatic colorectal cancer: Safety lead-in results from the phase III BEACON colorectal cancer study

Eric van Cutsem, Sanne Huijberts, Axel Grothey, Rona Yaeger, Pieter-Jan Cuyle, Elena Elez, Markan Fakih, Clara Montagut, Marc Peeters, Takayuki Yoshino, Harpreet Wasan, Jayesh Desai, Fortunato Ciardiello, Ashwin Gollerkeri, Janna Christy-Bittel, Kati Maharry, Victor Sandor, Jan H.M. Schellens, Scott Kopetz, Josep Tabernero

*Journal of Clinical Oncology*. 2019 Jun;37(17):1460-1469

## **Abstract**

### **Purpose**

To determine the safety and preliminary efficacy of selective combination targeted therapy for *BRAF* V600E-mutant metastatic colorectal cancer (mCRC) in the safety lead-in phase of the open-label, randomized, three-arm, phase III BEACON Colorectal Cancer trial (ClinicalTrials.gov identifier: NCT02928224; European Union Clinical Trials Register identifier: EudraCT2015-005805-35).

### **Patients and Methods**

Before initiation of the randomized portion of the BEACON Colorectal Cancer trial, 30 patients with *BRAF* V600E-mutant mCRC who had experienced treatment failure with one or two prior regimens were to be recruited to a safety lead-in of encorafenib 300 mg daily, binimetinib 45 mg twice daily, plus standard weekly cetuximab. The primary endpoint was safety, including the incidence of dose-limiting toxicities. Efficacy endpoints included overall response rate, progression-free survival, and overall survival.

### **Results**

Among the 30 treated patients, dose-limiting toxicities occurred in five patients and included serous retinopathy (n=2), reversible decreased left ventricular ejection fraction (n=1) and cetuximab-related infusion reactions (n=2). The most common grade 3 or 4 adverse events were fatigue (13%), anemia (10%), increased creatine phosphokinase (10%), increased aspartate aminotransferase (10%), and urinary tract infections (10%). In 29 patients with *BRAF* V600E-mutant tumors (one patient had a non-*BRAF* V600E mutant tumor and was not included in the efficacy analysis), the confirmed overall response rate was 48% (95% CI, 29.4% to 67.5%), median progression free survival was 8.0 months (95% CI, 5.6 to 9.3 months), and median overall survival was 15.3 months (95% CI, 9.6 months to not reached), with median duration of follow-up of 18.2 months (range, 16.6 to 19.8 months).

### **Conclusions**

In the safety lead-in, the safety and tolerability of the encorafenib, binimetinib, and cetuximab regimen is manageable and acceptable for initiation of the randomized portion of the study. The observed efficacy is promising compared to available therapies and, if confirmed in the randomized portion of the trial, could establish this regimen as a new standard of care for previously treated *BRAF* V600E-mutant mCRC.

## Introduction

*BRAF* V600E mutation is found in approximately 8-15% of patients with metastatic colorectal cancer (mCRC), and is a marker of poor prognosis.(1-4)

Because *BRAF* V600E and *RAS* mutations are nearly always mutually exclusive (5), patients with *BRAF* V600-mutant mCRC have typically been treated with standard-of-care regimens for *RAS*-wild type mCRC.(6-9) Standard first-line therapy, even with intensified regimens, produces poorer results in patients with *BRAF* V600E-mutant mCRC than in patients with wild-type disease (10-12), and after standard first-line therapy, subsequent treatment provides limited benefits, with reported overall response rates (ORRs) of less than 10%, median progression free survival (PFS) times of approximately 2 months and median overall survival (OS) times ranging from 4 to 6 months.(2, 13-19) Immunotherapies such as nivolumab and pembrolizumab are active in patients with microsatellite instability-high or mismatch repair-deficient solid tumors, including mCRC.(20, 21) Although the rate of mismatch repair-deficiency is higher in *BRAF* V600E-mutant CRC than in *BRAF* wild-type disease, recent retrospective data and a pooled analysis of four clinical trials indicated that less than 20% of patients with *BRAF* V600E-mutant mCRC have microsatellite instability-high or mismatch repair-deficient tumors, thus limiting this option to a minority of patients.(19, 22-24)

Unlike in other tumor histologies with *BRAF* V600 mutations such as melanoma and non-small cell lung cancer, where *BRAF* inhibition is clinically highly active (25-36), *BRAF* inhibition in *BRAF* V600E-mutant mCRC produced only marginal clinical activity.(35, 37-39) In vitro studies later demonstrated that in *BRAF* V600E-mutant colorectal cancer (CRC) cells, *BRAF* inhibition results in rapid feedback activation of epidermal growth factor receptor (EGFR), permitting sustained MAPK activation and continued cell proliferation; however, combined inhibition of *BRAF* and EGFR resulted in synergistic inhibition of tumor growth in *BRAF* V600E-mutant CRC xenograft models.(40, 41) Subsequent clinical studies of EGFR-targeted monoclonal antibodies combined with *BRAF* inhibition using the *BRAF* inhibitors vemurafenib or dabrafenib confirmed that addition of an EGFR-targeted therapy can improve the activity of *BRAF*-inhibition in *BRAF* V600E-mutant CRC.(42-44) In addition, preclinical studies indicated that profound inhibition of the MAPK pathway and greater antitumor activity could be achieved with the addition of a MEK inhibitor to *BRAF* inhibition, and this was also validated clinically.(41, 45, 46) Despite improvements in the activity of these regimens, to date, triplet combinations of *BRAF* inhibition with EGFR-targeted therapy and either a MEK inhibitor or irinotecan have demonstrated response rates of approximately 20%, in contrast to response rates of 60% to 70% for combined dual *BRAF*/MEK inhibition alone in melanoma and non-small cell lung cancer.(19, 33, 36, 44, 47)

The combination of encorafenib, a *BRAF* inhibitor, and binimetinib, a MEK inhibitor, has recently been approved in the United States and Europe for the first-line treatment of patients with *BRAF* V600-mutant melanoma.(48, 49) Results from a recent phase 2 study in patients with *BRAF* V600E-mutant mCRC who received at least one prior regimen, showed that the doublet of encorafenib plus cetuximab resulted in a confirmed ORR of 24%, a PFS of

4.2 months, and an OS of 9.3 months with a tolerable safety profile.(50) Relative to the standard of care, and to other BRAF, MEK, and EGFR inhibitor triplet combinations, the promising results with the encorafenib and cetuximab doublet supported the initiation of the phase III BEACON CRC study. (ClinicalTrials.gov identifier: NCT02928224; European Union Clinical Trials Register identifier: EudraCT2015-005805-35).

BEACON CRC is an open-label, randomized, three-arm, phase III study evaluating the efficacy and safety of encorafenib plus cetuximab with or without binimetinib versus investigators' choice of cetuximab combined with either irinotecan or fluorouracil, folinic acid, and irinotecan in patients with *BRAF* V600E-mutant mCRC whose disease has progressed after one or two prior regimens (ClinicalTrials.gov Identifier NCT02928224; EudraCT Number 2015-005805-35).

At the time BEACON CRC was initiated, the triplet combination of binimetinib, encorafenib, and cetuximab had not been clinically evaluated. Therefore, a 30-patient safety lead-in (SLI) was conducted to determine the safety, tolerability, and preliminary efficacy of the triplet combination at the doses planned for the randomized portion of the trial. Here, we describe results of the BEACON CRC SLI. At the time of this analysis, the randomized portion of the trial was ongoing.

## Patients and methods

Patients were required to be 18 years of age or older with histologically or cytologically confirmed mCRC, with the presence of *BRAF* V600E mutation in tumor tissue. Patients could enroll based on local determination of *BRAF* V600E mutation; however, confirmation by a central laboratory was required for all patients within 30 days of starting treatment. Patients must have had progression of disease on at least one and no more than two prior treatment regimens in the metastatic setting; have had evidence of measurable or evaluable, nonmeasurable disease per Response Evaluation Criteria in Solid Tumors (RECIST) version 1.1; have had an Eastern Cooperative Oncology Group performance status 0 or 1; have been eligible to receive cetuximab per their local label; and have had adequate bone marrow, renal, hepatic, and cardiac function. Patients were excluded if they had previous treatment with any RAF or MEK inhibitor, cetuximab, panitumumab, or other EGFR inhibitor or had symptomatic brain metastasis or leptomeningeal disease. Additional details regarding inclusion and exclusion criteria are provided in the Data Supplement.

The SLI was performed at seven sites in four countries (two in Belgium, one in the Netherlands, two in Spain, and two in the United States). The study was approved by the ethics committee for each study site. All clinical work was conducted in compliance with current Good Clinical Practices as referenced in the International Conference on Harmonisation of Technical Requirements for Registration of Pharmaceuticals for Human Use. All patients enrolled in the study provided written, informed consent prior to their participation.

## Study procedures

The first nine patients were enrolled in the SLI on a rolling basis. These patients received encorafenib 300 mg every day plus binimetinib 45 mg twice a day plus cetuximab 400 mg/m<sup>2</sup> followed by 250 mg/m<sup>2</sup> intravenously weekly in 28-day cycles. The cohort was to be expanded to a total of 30 patients in the dose-expansion cohort based on assessments of the safety data in the first nine patients by the Data Monitoring Committee.

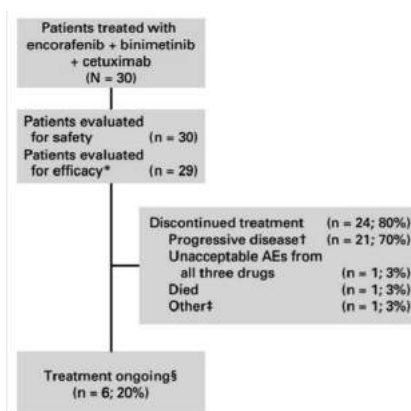


**Figure 1. Patient Disposition.**

(\*) One treated patient had a non-V600 BRAF mutation (BRAF G466V). (†) Includes two patients with changes in condition or development of intercurrent illness. (‡) Dose interruption for more than 28 consecutive days. (§) As of the data cutoff date of September 2, 2018. AE, adverse event.

## Outcome Measures

Safety was evaluated by ongoing monitoring of adverse events, clinical laboratory tests, vital signs, physical examinations, ophthalmic examinations, dermatologic examinations, ECGs, and echocardiography or multigated acquisition scans.

Tumors were assessed using radiologic imaging (eg, computed tomography, magnetic resonance imaging, X-ray, whole body bone scans), with tumor response determined locally by the investigator and by blinded independent central review according to RECIST, version 1.1. Tumor assessments were performed every 6 weeks for the first 24 weeks, then every 12 weeks until disease progression, withdrawal of consent, or initiation of subsequent anticancer therapy.

## Statistical Methods

**Study Population.** All patients who received at least one dose of study drug were included in the safety analyses (N = 30). For efficacy analyses, all patients with a BRAF V600E mutation (confirmed by local assessment, central assessment, or both) who received at least one dose of study drug were included.

**Endpoints.** The primary end point of the SLI was the assessment of safety and tolerability, which included dose-limiting toxicities (DLTs; defined as any adverse event [AE] or abnormal laboratory values assessed as unrelated to disease, disease progression, intercurrent illness, or concomitant medications or therapies occurring within the first 28 days of treatment that met criteria that were established before the start of the study; Data Supplement); the incidence and severity of AEs and changes in clinical laboratory parameters, vital signs, ECGs, echocardiography or multigated acquisition scans, and ophthalmic examinations; and the incidence of dose interruptions, dose modifications, and discontinuations.

Efficacy end points included confirmed ORR (per RECIST version 1.1), duration of response (DOR), PFS (per RECIST version 1.1), time to response and OS. Radiographic assessment of tumor response and progression was determined locally by the investigator. Blinded central review of radiographically determined tumor response and progression was also conducted retrospectively and reported. Pharmacokinetic end points were also evaluated and will be presented elsewhere.

**Statistical Analysis.** Descriptive statistics were used to summarize pretreatment characteristics and to evaluate DLTs, frequency of AEs, and best overall response. PFS was defined as the time from first dose of study drug to the earliest documented date of disease progression, per RECIST version 1.1, or death from any cause. OS was defined as the time from first dose of study drug to death from any cause. The survival status of all patients was assessed as of the cutoff date based on ongoing survival follow-up and public records where permitted. Data for patients who did not die by the data cutoff date were censored for OS at their last contact date. DOR was defined as time from first radiographic evidence of response to the earliest documented disease progression or death. Time to progression was defined as time from first dose of study treatment to first radiographic evidence of response. The Kaplan-Meier method was used to estimate PFS and OS rates. This was also used to assess DOR.

## Results

Thirty patients were enrolled in the SLI of BEACON CRC between November 1, 2016, and April 24, 2017; as of September 2, 2018, treatment remained ongoing for 6 patients (20%; Fig 1). A total of 24 patients (80%) discontinued from the study, with the primary reason for study discontinuation being disease progression (n = 21, 70%).

### Patient Disposition and Characteristics

Patient demographics and baseline tumor characteristics are listed in Table 1. Patients were characteristic of a population of patients with *BRAF* V600E-mutant metastatic CRC with predominantly right sided disease and high frequency of nodal and peritoneal metastasis, although the liver was the most frequent site of metastasis. One patient had a non-V600 mutation of *BRAF* (G466V) and was included in the safety analysis but excluded from the efficacy analysis.



## Safety

**DLTs.** DLTs were reported in five of 30 patients and included two patients with cetuximab-related drug hypersensitivity (grade 2 and grade 3, both patients remained in the study on binimetinib and encorafenib), two patients with grade 2 serous retinopathy (both patients remained in the study after an interruption of binimetinib dosing), and one patient with decreased left ventricular ejection fraction (grade 2) that resolved with the interruption of binimetinib dosing (the patient continued in the study on a reduced dose of binimetinib).

**Table 1. Baseline patient and tumor characteristics (safety population).**

Characteristic	Patients* (N = 30)
BRAF V600E mutation†	29 (97)
Male	13 (43)
Race	
White	29 (97)
Black or African American	1 (3)
Median age, years (range)	59 (38–77)
ECOG PS of 0	17 (57)
Location of primary tumor	
Left side	9 (30)
Right side	18 (60)
Unknown	3 (10)
No. of organs with metastases ≥ 2	22 (73)
Metastatic site locations	
Liver	20 (67)
Lymph nodes	15 (50)
Peritoneum	11 (37)
Lung	9 (30)
Other	15 (50)
Resection of primary tumor	
Yes	21 (70)
No	9 (30)
No. of prior systemic therapies‡	
1	18 (60)
2	12 (40)
Received prior irinotecan	13 (43)
MSI-H§	1 (3)
Median CEA at baseline, µg/mL (range)	28 (1–3,434)

Abbreviations: CEA, carcinoembryonic antigen; ECOG PS, Eastern Cooperative Oncology Group performance status; MSI-H, microsatellite instability high. \* Values are number and percentages, unless otherwise noted. † One patient treated had a non-BRAF V600E mutation. ‡ Includes prior systemic therapies in the metastatic setting only. § Based on immunohistochemical assessment of MLH1 and MSH6.

**AEs.** Two patients (6.7%) experienced grade 1 toxicities; seven (23.3%) experienced grade 2 toxicities; 16 (53.3%) experienced grade 3 toxicities; and five (16.7%) experienced grade 4 toxicities. The most frequently reported treatment-emergent AEs (any grade) included diarrhea (77%), dermatitis acneiform (67%), fatigue (63%), and nausea (63%). The most frequently reported grade 3 or 4 treatment-emergent AEs included fatigue (13%; all grade 3),

anemia (10%; two grade 3 and one grade 4), increased AST (10%; one grade 3 and two grade 4), increased creatine phosphokinase (10%; all grade 3), and urinary tract infections [10%]; all grade 3; Table 2 and 3).

**Table 2. Adverse events, regardless of causality, reported in five or more patients (safety population).**

Event	No. of patients (%) with adverse event of any grade (N = 30)*
Total Patients With Any Adverse Event†	30 (100.0)
Diarrhea	23 (76.7)
Dermatitis acneiform	20 (66.7)
Fatigue	19 (63.3)
Nausea	19 (63.3)
Dry skin	15 (50.0)
Vomiting	15 (50.0)
Anemia	12 (40.0)
Decreased appetite	12 (40.0)
Abdominal pain	11 (36.7)
Blood creatine phosphokinase increased	11 (36.7)
Pyrexia	11 (36.7)
Dyspnea	10 (33.3)
Constipation	9 (30.0)
Arthralgia	8 (26.7)
Blood creatinine increased	8 (26.7)
Skin fissures	8 (26.7)
Vision blurred	8 (26.7)
AST increased	6 (20.0)
Asthenia	6 (20.0)
Malaise	6 (20.0)
Myalgia	6 (20.0)
Palmar-plantar erythrodysesthesia syndrome	6 (20.0)
Rash maculo-papular	6 (20.0)
Back pain	5 (16.7)
Dizziness	5 (16.7)
Ejection fraction decreased	5 (16.7)
Edema peripheral	5 (16.7)
Peripheral sensory neuropathy	5 (16.7)
Rash	5 (16.7)
Rash pustular	5 (16.7)
Urinary tract infection	5 (16.7)

NOTE. Grade is based on National Cancer Institution Common Terminology Criteria for Adverse Event version 4.03. \*Any single patient may have experienced adverse events under multiple terms (ie, not mutually exclusive). †Reported using standard Medical Dictionary for Regulatory Activities dictionary coding.

**Drug Discontinuations as a result of AEs.** A total of six patients (20%) had at least one study drug discontinued as a result of AEs. Among these, one patient (3.3%) discontinued all three drugs as a result of grade 2 fatigue; two patients (6.7%) discontinued binimetinib alone as a

result of increased blood creatinine (n = 1) and retinal detachment (n = 1); two patients (6.7%)

discontinued cetuximab alone as a result of an allergic reaction; and one patient (3.3%) discontinued both encorafenib and binimetinib as a result of increased blood bilirubin. At the time of the increased blood bilirubin, there was radiographic evidence of extrinsic obstruction of the gallbladder. The patient received a dose of cetuximab 2 weeks after discontinuation of encorafenib and binimetinib and then discontinued study treatment completely 2 weeks later as a result of clinical progression. There were five on-treatment deaths (17%), all as a result of disease progression.

**Table 3. Grade 3 or 4 adverse events, regardless of causality, reported in two or more patients (safety population).**

Preferred Term	No. of patients (%) with grade 3 or 4 event (N = 30)*
Total Patients With Any Grade 3 or 4 Adverse Event†	21 (70.0)
Fatigue	4 (13.3)
AST increased	3 (10.0)
Urinary tract infection	3 (10.0)
Anemia	3 (10.0)
Blood creatine phosphokinase increased	3 (10.0)
Decreased appetite	2 (6.7)
Dyspnea	2 (6.7)
Nausea	2 (6.7)
Vomiting	2 (6.7)
Alanine aminotransferase increased	2 (6.7)
Hypokalaemia	2 (6.7)
Hypophosphatemia	2 (6.7)

NOTE. Grade is based on National Cancer Institute Common Terminology Criteria for Adverse Events version 4.03. \* Any single patient may have experienced adverse events under multiple terms (ie, not mutually exclusive). † Reported using standard Medical Dictionary for Regulatory Activities dictionary coding.

### Efficacy

Efficacy was assessed in the 29 patients with *BRAF* V600E mutation-containing tumors. The median time on study drug was 7.9 months (range, 1.0–21.4), and median follow-up for survival was 18.2 months (range, 16.6 to 19.8 months).

**Overall Response.** Confirmed best overall responses are listed in Table 4. The ORR per local assessment was 48% (95% CI, 29.4% to 67.5%). Fourteen patients had a confirmed response; three patients (10%) had complete responses and 11 patients (38%) had partial responses. The ORR, as determined by retrospective central assessment, was 41% (95% CI, 23.5% to 61.1%), with two complete responses (7%) and 10 partial responses (34%). Changes in tumor measurements from baseline are presented in Figure 2.

Among the 17 patients treated with one prior therapy, ORRs per local and central assessment were 59% (95% CI, 32.9% to 81.6%) and 53% (95% CI, 27.8% to 77.0%), respectively. Among the 12 patients treated with two prior therapies, the local ORR was 33% (95% CI, 9.9% to 65.1%), with corresponding rates from central assessment of 25% (95% CI, 5.5% to 57.2%).

**Time to Response.** Per local assessment, 78.6% of responding patients achieving response within 2 months, 92.9% within 4 months, and all patients within 6 months of treatment initiation. On the basis of central assessment, 75.0% of responding patients achieved response within 2 months, 91.7% within 4 months, and all patients within 12 months of treatment initiation.

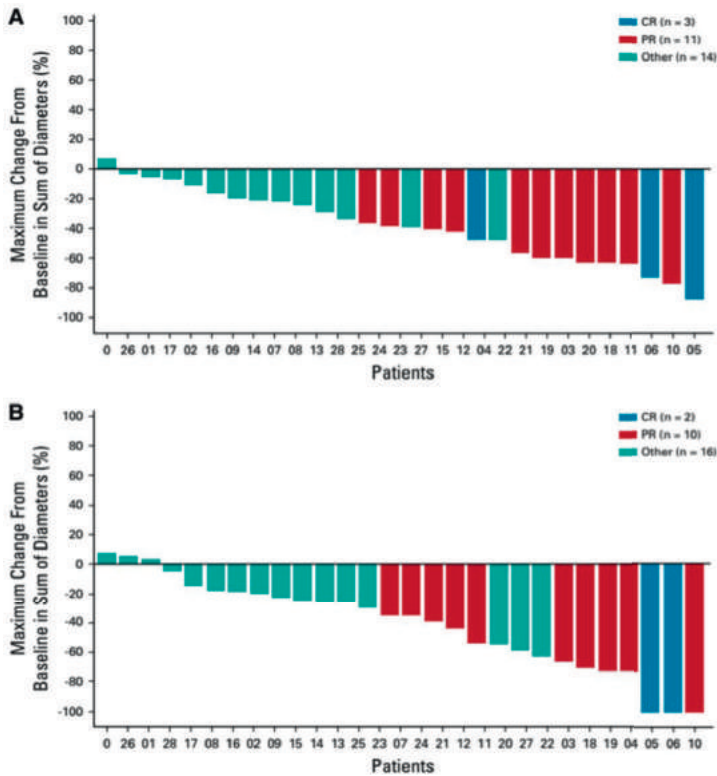


**Figure 2. Best percent change from baseline in sum of tumor diameters based on (A) local assessment and (B) central assessment.**

One patient was without postbaseline sum of diameters (not presented). Colors represent best response (confirmed) of partial response (PR) or complete response (CR). The category other represents stable disease (SD) or not evaluable (NE). Patients with CR, defined as the disappearance of all target lesions, could have pathological lymph node metastases present; target or nontarget lymph node metastases must have had reduction in short axis to less than 10 mm.

**DOR.** Among responders (n = 14), the median DOR per local assessment was 5.5 months (95% CI, 4.1 months to not reached [NR]); 85.7% of patients achieved a DOR of 3 months, 42.9% achieved a DOR of 6 months, and 25.7% achieved a DOR of 15 months. Median DOR among the 12 responders confirmed by central assessment was 8.1 months (95% CI, 2.8 months to NR); 73% of patients achieved a DOR of 6 months or longer (Data Supplement).

**PFS and OS.** Median PFS was 8.0 months (95% CI, 5.6 to 9.3 months; Fig 3A) per local assessment and 5.5 months (95% CI, 4.2 to 9.3 months) per central assessment. Median PFS (by local assessment) by number of prior regimens was similar: 8.0 months (95% CI, 5.6 to 9.7 months) for patients who received one prior regimen compared with 7.7 months (95% CI, 4.1 to 10.8 months) for patients who received two prior regimens. The median OS time was 15.3 months (95% CI, 9.3 months to NR; Fig 3B) with median follow-up of 18.2 months (range, 16.6 to 19.8 months). The 12-month OS rate was 62% (95% CI, 42.1% to 76.9%).

**Table 4. Best overall response to treatment.**

Confirmed Best Overall Response	Patients (N=29)†
<b>Local Assessment*</b>	
ORR (CR + PR), n (%)	14 (48%) (95% CI, 29–68)
CR	3 (10%)
PR	11 (38%)
SD	13 (45%)
PD	0
Not evaluable for response	2 (7%)
<b>Central Assessment*</b>	
ORR (CR + PR), n (%)	12 (41%) (95% CI, 24–61)
CR	2 (7%)
PR	10 (34%)
SD	13 (45%)
PD	0
Not evaluable for response	4 (14%)

Abbreviations: CR, complete response; ORR, overall response rate; PD, progressive disease; PR, partial response; SD, stable disease. \* Confirmed responses per RECIST 1.1. † Patients with BRAF V600E mutations.

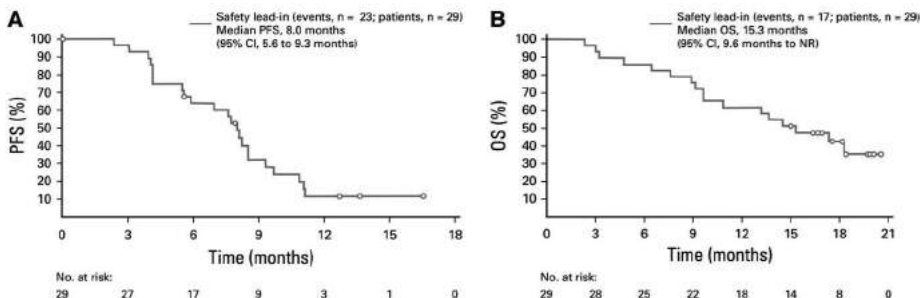


**Figure 3. Kaplan-Meier plots of (A) progression-free survival (PFS; local assessment) and (B) overall survival (OS).**

NR, not reached.

## Discussion

On the basis of the safety and efficacy results of the SLI phase of the BEACON CRC study, the randomized phase of the study was initiated and is ongoing. The safety profile of the triplet combination regimen of binimetinib, encorafenib, and cetuximab was similar to that

previously reported for the individual agents and included predominantly GI and skin toxicities. Higher grade (grade 3 or 4) skin toxicities were rare and were less common than the 12% rate of grade 3 or 4 rash reported for cetuximab monotherapy(48), suggesting that *BRAF* inhibition may ameliorate this cetuximab-related AE. Although the overall rates of grade 3 and grade 4 toxicity were 53.3% and 16.7%, respectively, there was no single predominant toxicity driving these rates, with only the event of fatigue (13%) reported at a rate higher than 10%. The regimen appeared to be well tolerated and the safety profile manageable; a few patients (six patients [20%]) required dose discontinuation of at least one of the study drugs as a result of an AE and only one patient discontinued treatment with all three agents as a result of a drug-related AE. Patients requiring dose discontinuation included two patients who required discontinuation of cetuximab as a result of infusion reactions, a rate consistent with prior reports for cetuximab infusion reactions.(51) Addition of the MEK inhibitor binimetinib did result in some patients experiencing MEK inhibitor class-related AEs including serous retinopathy, increased creatine phosphokinase, and decreases in left ventricular ejection fraction. Serous retinopathy (also referred to as retinal pigment epithelial detachment) is a known MEK inhibitor-associated toxicity and was observed as a grade 2 DLT in two patients. It was documented to reverse in all patients who underwent repeat ophthalmologic examination; in one patient, ophthalmologic examination was not repeated but the patient continued on study treatment without loss of visual acuity. Serous retinopathy is most often asymptomatic, and reported rates depend on the frequency of monitoring.(29) Symptomatic serous retinopathy is generally reversible and manageable with dose interruption, with or without subsequent dose reduction.(52) Increased creatine phosphokinase was also observed (37%) but is rarely associated with significant myopathy, and it led to dose modification in only one patient. Clinically significant MEK inhibitor-associated left ventricular dysfunction is uncommon and is generally reversible with interruption and dose modification. Grade 2 left ventricular dysfunction was reported as a DLT in one patient, was reversed with binimetinib interruption, and did not lead to treatment discontinuation.

Benchmarked against both prior standards of care for RAS wild-type metastatic CRC as well as more recent experience with other BRAF inhibitor combinations, including triplet combinations with cetuximab and either irinotecan or the MEK inhibitor trametinib(19, 44), the efficacy findings from the SLI are promising. The confirmed ORR was 48%, with 43% of responses lasting for more than 6 months. The median PFS time was 8 months and median OS time was 15.3 months, with a median follow-up of 18.2 months. Results by central review were, in general, consistent with local review findings. By comparison, expected outcomes for historical second- and third-line standards of care, similar to the control arm of the randomized portion of the trial, included an ORR of less than 10%, median PFS of 2 to 3 months and median OS of 4 to 6 months.(2, 13-19) Similarly, other triplet therapy regimens incorporating a BRAF inhibitor and an EGFR-targeted monoclonal antibody (dabrafenib, trametinib, and panitumumab and vemurafenib, irinotecan, and cetuximab) have shown improved but limited efficacy, with ORRs of 16% to 21%, median PFS of approximately 4.2 to

5.6 months and median OS of 9.1 to 9.6 months.(19, 39) Although the mechanisms underlying the outcomes associated with encorafenib and binimetinib combined with cetuximab remain to be fully characterized, preclinical data suggest that encorafenib has target binding characteristics that differ from both vemurafenib and dabrafenib, with a prolonged target dissociation half-life and higher potency.(53) Clinically, although never compared head-to-head with other BRAF/MEK inhibitor combinations, in the COLUMBUS trial (ClinicalTrials.gov identifier: NCT01909453) in patients with advanced *BRAF* V600K or V600E melanoma(36, 54), the combination of binimetinib and encorafenib produced new benchmarks for efficacy as measured by PFS (median, 14.9 months; 95% CI, 11.0 to 18.5 months) and OS (median, 33.6 months; 95%CI 24.4 to 39.2 months). Vemurafenib monotherapy, the control arm in the COMLUMBUS study, performed almost identically to its activity in pivotal trials of other BRAF/MEK inhibitor combinations. In addition, the COLUMBUS trial did include a head-to-head comparison of encorafenib monotherapy at 300 mg daily and vemurafenib monotherapy and demonstrated improved PFS (hazard ratio, 0.68; 95% CI, 0.52 to 0.88) and OS (hazard ratio, 0.76; 95%CI 0.58 to 0.98) for encorafenib relative to vemurafenib in patients with *BRAF* V600E- or *BRAF* V600K-mutated advanced melanoma.(36) Thus, the data suggest that the differences between encorafenib and other BRAF inhibitors in terms of target binding may underlie the observed differences clinically, including efficacy in *BRAF* V600E-mutated CRC, which in terms of the ability to modulate the MAPK-pathway is inherently less sensitive to BRAF inhibition than melanoma.(40, 41)

The randomized portion of the BEACON CRC study is ongoing, and if results approximate those from the SLI, the combination of binimetinib, encorafenib, and cetuximab may become a new standard of care for patients with *BRAF* V600E-mutated CRC. To maximize the potential for benefit to patients, results warrant additional investigation of this regimen in the first-line and potentially in the adjuvant settings. A trial to investigate the regimen in the first-line setting (ANCHOR-CRC [Encorafenib, binimetinib, and cetuximab in subjects with previously untreated *BRAF*-mutant colorectal cancer]; ClinicalTrials.gov identifier: NCT03693170) was recently initiated.

**Author Contributions**

**Conception and design:** Eric Van Cutsem, Axel Grothey, Pieter-Jan Cuyle, Elena Elez, Harpreet Wasan, Fortunato Ciardiello, Ashwin Gollerkeri, Janna Christy-Bittel, Kati Maharry, Victor Sandor, Jan H.M. Schellens, Scott Kopetz, Josep Tabernero

**Administrative support:** Harpreet Wasan

**Provision of study materials or patients:** Eric Van Cutsem, Sanne Huijberts, Pieter-Jan Cuyle, Elena Elez, Harpreet Wasan, Fortunato Ciardiello, Ashwin Gollerkeri, Josep Tabernero

**Collection and assembly of data:** Eric Van Cutsem, Sanne Huijberts, Axel Grothey, Rona Yaeger, Elena Elez, Marwan Fakh, Clara Montagut, Marc Peeters, Ashwin Gollerkeri, Janna Christy-Bittel, Kati Maharry, Victor Sandor, Jan H.M. Schellens, Scott Kopetz, Josep Tabernero

**Data analysis and interpretation:** Eric Van Cutsem, Sanne Huijberts, Axel Grothey, Rona Yaeger, Pieter-Jan Cuyle, Elena Elez, Marwan Fakh, Marc Peeters, Takayuki Yoshino, Harpreet Wasan, Jayesh Desai, Fortunato Ciardiello, Ashwin Gollerkeri, Janna Christy-Bittel, Kati Maharry, Victor Sandor, Jan H.M. Schellens, Scott Kopetz, Josep Tabernero

**Manuscript writing and final approval, and accountable for all aspects of work:** All authors

**Acknowledgement**

We thank the patients, their families, and the sites that participated in this study. For editorial support, funded by Array Biopharm, we thank Philip Sjostedt from the Medine Group LLC, a Division of Bespoke Communications.



## References

1. Davies H, Bignell GR, Cox C, Stephens P, Edkins S, Clegg S, et al. Mutations of the BRAF gene in human cancer. *Nature*. 2002;417(6892):949-54.
2. Loupakis F, Ruzzo A, Cremolini C, Vincenzi B, Salvatore L, Santini D, et al. KRAS codon 61, 146 and BRAF mutations predict resistance to cetuximab plus irinotecan in KRAS codon 12 and 13 wild-type metastatic colorectal cancer. *British journal of cancer*. 2009;101(4):715-21.
3. Tie J, Gibbs P, Lipton L, Christie M, Jorissen RN, Burgess AW, et al. Optimizing targeted therapeutic development: analysis of a colorectal cancer patient population with the BRAF(V600E) mutation. *International journal of cancer*. 2011;128(9):2075-84.
4. Clarke CN, Kopetz ES. BRAF mutant colorectal cancer as a distinct subset of colorectal cancer: clinical characteristics, clinical behavior, and response to targeted therapies. *Journal of gastrointestinal oncology*. 2015;6(6):660-7.
5. De Roock W, Claes B, Bernasconi D, De Schutter J, Biesmans B, Fountzilias G, et al. Effects of KRAS, BRAF, NRAS, and PIK3CA mutations on the efficacy of cetuximab plus chemotherapy in chemotherapy-refractory metastatic colorectal cancer: a retrospective consortium analysis. *The Lancet oncology*. 2010;11(8):753-62.
6. Van Cutsem E, Cervantes A, Adam R, Sobrero A, Van Krieken JH, Aderka D, et al. ESMO consensus guidelines for the management of patients with metastatic colorectal cancer. *Annals of oncology*. 2016;27(8):1386-422.
7. Falcone A, Ricci S, Brunetti I, Pfanner E, Allegrini G, Barbara C, et al. Phase III trial of infusional fluorouracil, leucovorin, oxaliplatin, and irinotecan (FOLFOXIRI) compared with infusional fluorouracil, leucovorin, and irinotecan (FOLFIRI) as first-line treatment for metastatic colorectal cancer: the Gruppo Oncologico Nord Ovest. *Journal of clinical oncology*. 2007;25(13):1670-6.
8. Souglakos J, Androulakis N, Syrigos K, Polyzos A, Ziras N, Athanasiadis A, et al. FOLFOXIRI (folinic acid, 5-fluorouracil, oxaliplatin and irinotecan) vs FOLFIRI (folinic acid, 5-fluorouracil and irinotecan) as first-line treatment in metastatic colorectal cancer (MCC): a multicentre randomised phase III trial from the Hellenic Oncology Research Group (HORG). *British journal of cancer*. 2006;94(6):798-805.
9. Cremolini C, Loupakis F, Masi G, Lonardi S, Granetto C, Mancini ML, et al. FOLFOXIRI or FOLFIRI plus bevacizumab as first-line treatment of metastatic colorectal cancer: a propensity score-adjusted analysis from two randomized clinical trials. *Annals of oncology*. 2016;27(5):843-9.
10. Loupakis F, Cremolini C, Masi G, Lonardi S, Zagonel V, Salvatore L, et al. Initial therapy with FOLFOXIRI and bevacizumab for metastatic colorectal cancer. *The New England journal of medicine*. 2014;371(17):1609-18.
11. Cremolini C, Loupakis F, Antoniotti C, Lupi C, Sensi E, Lonardi S, et al. FOLFOXIRI plus bevacizumab versus FOLFIRI plus bevacizumab as first-line treatment of patients with metastatic colorectal cancer: updated overall survival and molecular subgroup analyses of the open-label, phase 3 TRIBE study. *The Lancet oncology*. 2015;16(13):1306-15.
12. Ursem C, Atreya CE, Van Loon K. Emerging treatment options for BRAF-mutant colorectal cancer. *Gastrointestinal cancer : targets and therapy*. 2018;8:13-23.
13. Ulivi P, Capelli L, Valgiusti M, Zoli W, Scarpi E, Chiadini E, et al. Predictive role of multiple gene alterations in response to cetuximab in metastatic colorectal cancer: a single center study. *Journal of translational medicine*. 2012;10:87.
14. Saridaki Z, Tzardi M, Sfakianaki M, Papadaki C, Voutsina A, Kalykaki A, et al. BRAFV600E mutation analysis in patients with metastatic colorectal cancer (mCRC) in daily clinical practice: correlations with clinical characteristics, and its impact on patients' outcome. *PLoS one*. 2013;8(12):e84604.
15. Seymour MT, Brown SR, Middleton G, Maughan T, Richman S, Gwyther S, et al. Panitumumab and irinotecan versus irinotecan alone for patients with KRAS wild-type, fluorouracil-resistant

- advanced colorectal cancer (PICCOLO): a prospectively stratified randomised trial. *The Lancet oncology*. 2013;14(8):749-59.
16. Morris V, Overman MJ, Jiang ZQ, Garrett C, Agarwal S, Eng C, et al. Progression-free survival remains poor over sequential lines of systemic therapy in patients with BRAF-mutated colorectal cancer. *Clinical colorectal cancer*. 2014;13(3):164-71.
  17. Peeters M, Oliner KS, Price T. Updated analysis of KRAS/NRAS and BRAF mutations in study 20050181 of panitumumab (pmab) plus FOLFIRI for second-line treatment (tx) of metastatic colorectal cancer (mCRC). *Journal of clinical oncology*. 2014;32 (suppl 5s; abstr 3568).
  18. Mitani S, Taniguchi H, Honda K, Masuishi T, Narita Y, Kadowaki S, et al. Analysis of efficacy and prognostic factors in second-line chemotherapy for BRAF V600E mutant metastatic colorectal cancer. *Annals of oncology*. 2017;28.
  19. Kopetz S, McDonough SL, Morris VK, et al. Randomized trial of irinotecan and cetuximab with or without vemurafenib in BRAF-mutant metastatic colorectal cancer (SWOG 1406). *Journal of clinical oncology*. 2017;35:520.
  20. Bristol-Myers Squibb: Opdivo USPI. [https://packageinserts.bms.com/pi/pi\\_opdivo.pdf](https://packageinserts.bms.com/pi/pi_opdivo.pdf).
  21. Merck: Keytruda USPI. [https://www.merck.com/product/usa/pi\\_circulars/k/keytruda/keytruda\\_pi.pdf](https://www.merck.com/product/usa/pi_circulars/k/keytruda/keytruda_pi.pdf).
  22. Venderbosch S, Nagtegaal ID, Maughan TS, Smith CG, Cheadle JP, Fisher D, et al. Mismatch repair status and BRAF mutation status in metastatic colorectal cancer patients: a pooled analysis of the CAIRO, CAIRO2, COIN, and FOCUS studies. *Clinical cancer research*. 2014;20(20):5322-30.
  23. Lochhead P, Kuchiba A, Imamura Y, Liao X, Yamauchi M, Nishihara R, et al. Microsatellite instability and BRAF mutation testing in colorectal cancer prognostication. *Journal of the National Cancer Institute*. 2013;105(15):1151-6.
  24. Roma C, Rachiglio AM, Pasquale R, Fenizia F, Iannaccone A, Tatangelo F, et al. BRAF V600E mutation in metastatic colorectal cancer: Methods of detection and correlation with clinical and pathologic features. *Cancer biology & therapy*. 2016;17(8):840-8.
  25. Flaherty KT, Infante JR, Daud A, Gonzalez R, Kefford RF, Sosman J, et al. Combined BRAF and MEK inhibition in melanoma with BRAF V600 mutations. *The New England journal of medicine*. 2012;367(18):1694-703.
  26. Flaherty KT, Puzanov I, Kim KB, Ribas A, McArthur GA, Sosman JA, et al. Inhibition of mutated, activated BRAF in metastatic melanoma. *The New England journal of medicine*. 2010;363(9):809-19.
  27. Boni A, Cogdill AP, Dang P, Udayakumar D, Njauw CN, Sloss CM, et al. Selective BRAFV600E inhibition enhances T-cell recognition of melanoma without affecting lymphocyte function. *Cancer research*. 2010;70(13):5213-9.
  28. Wilmott JS, Long GV, Howle JR, Haydu LE, Sharma RN, Thompson JF, et al. Selective BRAF inhibitors induce marked T-cell infiltration into human metastatic melanoma. *Clinical cancer research*. 2012;18(5):1386-94.
  29. Dummer R, Ascierto PA, Gogas HJ, Arance A, Mandala M, Liskay G, et al. Overall survival in patients with BRAF-mutant melanoma receiving encorafenib plus binimetinib versus vemurafenib or encorafenib (COLUMBUS): a multicentre, open-label, randomised, phase 3 trial. *The Lancet oncology*. 2018;19(10):1315-27.
  30. Long GV, Stroyakovskiy D, Gogas H, Levchenko E, de Braud F, Larkin J, et al. Dabrafenib and trametinib versus dabrafenib and placebo for Val600 BRAF-mutant melanoma: a multicentre, double-blind, phase 3 randomised controlled trial. *Lancet*. 2015;386(9992):444-51.
  31. Chapman PB, Hauschild A, Robert C, Haanen JB, Ascierto P, Larkin J, et al. Improved survival with vemurafenib in melanoma with BRAF V600E mutation. *The New England journal of medicine*. 2011;364(26):2507-16.
  32. Chapman PB, Solit DB, Rosen N. Combination of RAF and MEK inhibition for the treatment of BRAF-mutated melanoma: feedback is not encouraged. *Cancer cell*. 2014;26(5):603-4.

33. Planchard D, Besse B, Groen HJM, Souquet PJ, Quoix E, Baik CS, et al. Dabrafenib plus trametinib in patients with previously treated BRAF(V600E)-mutant metastatic non-small cell lung cancer: an open-label, multicentre phase 2 trial. *The Lancet oncology*. 2016;17(7):984-93.
34. Long GV, Hauschild A, Santinami M, Atkinson V, Mandalà M, Chiarion-Sileni V, et al. Adjuvant dabrafenib plus trametinib in stage III BRAF-mutated melanoma. *The New England journal of medicine*. 2017;377(19):1813-23.
35. Hyman DM, Puzanov I, Subbiah V, Faris JE, Chau I, Blay JY, et al. Vemurafenib in multiple nonmelanoma cancers with BRAF V600 mutations. *The New England journal of medicine*. 2015;373(8):726-36.
36. Loupakis F, Cremolini C, Salvatore L, Masi G, Sensi E, Schirripa M, et al. FOLFOXIRI plus bevacizumab as first-line treatment in BRAF mutant metastatic colorectal cancer. *European journal of cancer*. 2014;50(1):57-63.
37. Kopetz S, Desai J, Chan E, Hecht JR, O'Dwyer PJ, Maru D, et al. Phase II pilot study of vemurafenib in patients with metastatic BRAF-mutated colorectal cancer. *Journal of clinical oncology*. 2015;33(34):4032-8.
38. Seligmann JF, Fisher D, Smith CG, Richman SD, Elliott F, Brown S, et al. Investigating the poor outcomes of BRAF-mutant advanced colorectal cancer: analysis from 2530 patients in randomised clinical trials. *Annals of oncology*. 2017;28(3):562-8.
39. Prahallad A, Sun C, Huang S, Di Nicolantonio F, Salazar R, Zecchin D, et al. Unresponsiveness of colon cancer to BRAF(V600E) inhibition through feedback activation of EGFR. *Nature*. 2012;483(7387):100-3.
40. Corcoran RB, Ebi H, Turke AB, Coffee EM, Nishino M, Cogdill AP, et al. EGFR-mediated reactivation of MAPK signaling contributes to insensitivity of BRAF mutant colorectal cancers to RAF inhibition with vemurafenib. *Cancer discovery*. 2012;2(3):227-35.
41. Hong DS, Morris VK, El Osta B, Sorokin AV, Janku F, Fu S, et al. Phase IB study of vemurafenib in combination with irinotecan and cetuximab in patients with metastatic colorectal cancer with BRAFV600E mutation. *Cancer discovery*. 2016;6(12):1352-65.
42. Connolly K, Brungs D, Szeto E, Epstein RJ. Anticancer activity of combination targeted therapy using cetuximab plus vemurafenib for refractory BRAF (V600E)-mutant metastatic colorectal carcinoma. *Current oncology*. 2014;21(1):e151-4.
43. Corcoran RB, André T, Atreya CE, Schellens JHM, Yoshino T, Bendell JC, et al. Combined BRAF, EGFR, and MEK inhibition in patients with BRAF(V600E)-mutant colorectal cancer. *Cancer discovery*. 2018;8(4):428-43.
44. Corcoran RB, Dias-Santagata D, Bergethon K, Iafrate AJ, Settleman J, Engelman JA. BRAF gene amplification can promote acquired resistance to MEK inhibitors in cancer cells harboring the BRAF V600E mutation. *Science signaling*. 2010;3(149):ra84.
45. Corcoran RB, Atreya CE, Falchook GS, Kwak EL, Ryan DP, Bendell JC, et al. Combined BRAF and MEK inhibition with dabrafenib and trametinib in BRAF V600-mutant colorectal cancer. *Journal of clinical oncology*. 2015;33(34):4023-31.
46. Robert C, Karaszewska B, Schachter J, et al: Two year estimate of overall survival in COMBI-v, a randomized, open-label, phase III study comparing the combination of dabrafenib (D) and trametinib (T) with vemurafenib (Vem) as first-line therapy in patients (pts) with unresectable or metastatic BRAF V600E/K mutation-positive cutaneous melanoma. *European journal of cancer* 51:S663, 2015 (abstr 3301).
47. Dummer R, Ascierto PA, Gogas H, et al: Overall survival in COLUMBUS: A phase 3 trial of encorafenib (ENCO) plus binimetinib (BINI) vs vemurafenib (VEM) or enco in BRAF-mutant melanoma. *Journal of clinical oncology* 36, 2018 (suppl 15; abstr 9504).
48. Array BioPharma: Braftovi USPI. [http://www.arraybiopharma.com/documents/Braftovi\\_Prescribing\\_information.pdf](http://www.arraybiopharma.com/documents/Braftovi_Prescribing_information.pdf).
49. Array BioPharma: Mektovi USPI. [http://www.arraybiopharma.com/documents/Mektovi\\_Prescribing\\_information.pdf](http://www.arraybiopharma.com/documents/Mektovi_Prescribing_information.pdf).

50. Van Cutsem E, Cuyle P, Huijberts S, et al: BEACON CRC study safety lead-in: Assessment of the BRAF inhibitor encorafenib + MEK inhibitor binimetinib + anti-epidermal growth factor receptor antibody cetuximab for BRAF V600E metastatic colorectal cancer. *Annals of oncology* 29, 2018 (suppl 5; abstr mdy149.026).
51. Eli Lilly: Erbitux USPI. <http://pi.lilly.com/us/erbitux-uspi.pdf>.
52. Urner-Bloch U, Urner M, Jaberg-Bentele N, Frauchiger AL, Dummer R, Goldinger SM. MEK inhibitor-associated retinopathy (MEKAR) in metastatic melanoma: Long-term ophthalmic effects. *European journal of cancer*. 2016;65:130-8.
53. Delord JP, Robert C, Nyakas M, McArthur GA, Kudchakar R, Mahipal A, et al. Phase I dose-escalation and -expansion study of the BRAF inhibitor encorafenib (LGX818) in metastatic BRAF-mutant melanoma. *Clinical cancer research*. 2017;23(18):5339-48.
54. Dummer R, Ascierto PA, Gogas HJ, Arance A, Mandala M, Liskay G, et al. Overall survival in patients with BRAF-mutant melanoma receiving encorafenib plus binimetinib versus vemurafenib or encorafenib (COLUMBUS): a multicentre, open-label, randomised, phase 3 trial. *The Lancet oncology*. 2018;19(10):1315-27.

## Supplemental data

**Table S1. Inclusion and exclusion screening and patient eligibility criteria for BEACON safety lead-in.**

Patient Eligibility
<p><b>Inclusion Criteria</b></p> <p>All the following inclusion criteria must be met for a patient to be included in the study:</p> <ol style="list-style-type: none"> <li>1. Provide a signed and dated Screening informed consent document</li> <li>2. Age <math>\geq 18</math> years at time of informed consent</li> <li>3. Histologically or cytologically confirmed CRC that is metastatic</li> <li>4. Presence of <i>BRAF V600E</i> in tumor tissue previously determined by a local assay at any time prior to Screening or by the central laboratory</li> </ol> <p>Notes:</p> <ol style="list-style-type: none"> <li>a. Only PCR and NGS-based local assays results will be acceptable.</li> <li>b. Central testing cannot be repeated to resolve discordances with a local result once the central laboratory delivers a definitive result (positive or negative).</li> <li>c. If the result from the central laboratory is indeterminate or the sample is deemed inadequate for testing, a second sample may be submitted.</li> <li>d. If at any time there is discordance in the results between the local assay and the central laboratory (potential false-positive local result), or lack of <i>BRAF V600E</i> confirmation in 18 patients, all subsequent patients will be required to have <i>BRAF V600E</i> determined by the central laboratory prior to enrollment.</li> <li>e. Results from local laboratories with more than 1 discordant result leading to patient enrollment will not be accepted for further patient enrollment.</li> </ol> <p>5. Able to provide a sufficient amount of representative tumor specimen (primary or metastatic, archival or newly obtained) for confirmatory central laboratory testing of <i>BRAF</i> and <i>KRAS</i> mutation status (minimum of 6 slides; optimally up to 15 slides)</p> <p>Note: Tumor samples must be submitted to the central laboratory for <i>BRAF</i> testing as soon as possible following the signing of the Molecular Prescreening informed consent. The <i>BRAF</i> status must be confirmed no later than 30 days following first dose of study drug.</p> <ol style="list-style-type: none"> <li>6. Eligible to receive cetuximab per locally approved label with regard to tumor <i>RAS</i> status</li> <li>7. Progression of disease after one or two prior regimens in the metastatic setting</li> </ol> <p>Notes:</p> <ol style="list-style-type: none"> <li>a. Disease relapse during treatment or within 6 months following adjuvant therapy will be considered metastatic disease.</li> <li>b. Patients who have received two prior regimens (ie, those entering the study in the third-line setting), must have received or have been offered and refused prior oxaliplatin unless it was contraindicated due to underlying conditions.</li> <li>c. Maintenance therapy given in the metastatic setting will not be considered a separate regimen.</li> <li>d. In the phase III portion of study, the number of patients having received two prior regimens will be limited to 215 (35% of the total randomized). Patients with two prior regimens who have entered Screening at the time that the limit has been reached will be permitted to continue into the study if they are otherwise determined to be eligible.</li> </ol> <ol style="list-style-type: none"> <li>8. Evidence of measurable or evaluable non-measurable disease per RECIST, v1.1</li> <li>9. ECOG PS of 0 or 1</li> <li>10. Adequate bone marrow function characterized by the following at screening: <ol style="list-style-type: none"> <li>a. Absolute neutrophil count (ANC) <math>\geq 1.5 \times 10^9/L</math>;</li> <li>b. Platelets <math>\geq 100 \times 10^9/L</math>;</li> <li>c. Hemoglobin <math>\geq 9.0</math> g/dL</li> </ol> <p>Note: Transfusions will be allowed to achieve this. Transfusions will be permitted provided the patient has not received more than 2 units of red blood cells in the prior 4 weeks to achieve these criteria.</p> </li> <li>11. Adequate renal function characterized by serum creatinine <math>\leq 1.5 \times</math> upper limit of normal (ULN), or calculated by Cockcroft-Gault formula or directly measured creatinine clearance <math>\geq 50</math> mL/min at screening</li> <li>12. Adequate electrolytes at Baseline, defined as serum potassium and magnesium levels within institutional normal limits (Note: replacement treatment to achieve adequate electrolytes will be allowed)</li> <li>13. Adequate hepatic function characterized by the following at screening: <ol style="list-style-type: none"> <li>a. Serum total bilirubin <math>\leq 1.5 \times</math> ULN and <math>&lt; 2</math> mg/dL</li> </ol> </li> </ol>

Note: Patients who have a total bilirubin level  $> 1.5 \times \text{ULN}$  will be allowed if their indirect bilirubin level is  $\leq 1.5 \times \text{ULN}$ .

b. Alanine aminotransferase (ALT) and/or aspartate aminotransferase (AST)  $\leq 2.5 \times \text{ULN}$ , or  $\leq 5 \times \text{ULN}$  in presence of liver metastases

14. Adequate cardiac function characterized by the following at screening:

a. Left ventricular ejection fraction (LVEF)  $\geq 50\%$  as determined by a MUGA scan or ECHO;

b. Mean triplicate QT interval corrected for heart rate using Fridericia's formula (QTcF) value  $\leq 480$  msec

15. Able to take oral medications

16. Willing and able to comply with scheduled visits, treatment plan, laboratory tests, and other study procedures

17. Female patients are either postmenopausal for at least 1 year, are surgically sterile for at least 6 weeks, or must agree to take appropriate precautions to avoid pregnancy from screening through follow-up if of childbearing potential

Note: Permitted contraceptive methods should be communicated to the patients and their understanding confirmed. For all females, the pregnancy test result must be negative at screening.

18. Males must agree to take appropriate precautions to avoid fathering a child from screening through 90 days following end of therapy.

Note: Permitted contraceptive methods should be communicated to the patients and their understanding confirmed.

19. Patients under guardianship or partial guardianship will be eligible unless prohibited by local laws or by local/central ethic committees (eg, France). Where allowed, all procedures prescribed by law must be followed.

#### Exclusion Criteria

Patients meeting any of the following criteria will not be included in the study:

1. Prior treatment with any RAF inhibitor, MEK inhibitor, cetuximab, panitumumab, or other EGFR inhibitors

2. Prior irinotecan hypersensitivity or toxicity that would suggest an inability to tolerate irinotecan  $180 \text{ mg/m}^2$  every 2 weeks

3. Symptomatic brain metastasis

Notes: Patients previously treated or untreated for this condition who are asymptomatic in the absence of corticosteroid and anti-epileptic therapy are allowed. Brain metastases must be stable for  $\geq 4$  weeks, with imaging (eg, magnetic resonance imaging [MRI] or computed tomography [CT]) demonstrating no current evidence of progressive brain metastases at screening.

4. Leptomeningeal disease

5. History or current evidence of RVO or current risk factors for RVO (eg, uncontrolled glaucoma or ocular hypertension, history of hyperviscosity or hypercoagulability syndromes)

6. Use of any herbal medications/supplements or any medications or foods that are strong inhibitors or inducers of cytochrome P450 (CYP) 3A4/5  $\leq 1$  week prior to the start of study treatment

7. Known history of acute or chronic pancreatitis

8. History of chronic inflammatory bowel disease or Crohn's disease requiring medical intervention (immunomodulatory or immunosuppressive medications or surgery)  $\leq 12$  months prior to randomization

9. Impaired cardiovascular function or clinically significant cardiovascular diseases, including any of the following:

a. History of acute myocardial infarction, acute coronary syndromes (including unstable angina, coronary artery bypass graft [CABG], coronary angioplasty or stenting)  $\leq 6$  months prior to start of study treatment;

b. Symptomatic congestive heart failure (ie, grade 2 or higher), history or current evidence of clinically significant cardiac arrhythmia and/or conduction abnormality  $\leq 6$  months prior to start of study treatment, except atrial fibrillation and paroxysmal supraventricular tachycardia

10. Uncontrolled hypertension defined as persistent systolic blood pressure  $\geq 150$  mmHg or diastolic blood pressure  $\geq 100$  mmHg despite current therapy

11. Impaired hepatic function, defined as Child-Pugh class B or C

12. Impaired gastrointestinal (GI) function or disease that may significantly alter the absorption of encorafenib or binimetinib (eg, ulcerative diseases, uncontrolled vomiting, malabsorption syndrome, small bowel resection with decreased intestinal absorption)

13. Concurrent or previous other malignancy within 5 years of study entry, except cured basal or squamous cell skin cancer, superficial bladder cancer, prostate intraepithelial neoplasm, carcinoma in-situ of the cervix, or other noninvasive or indolent malignancy without Sponsor approval

14. History of thromboembolic or cerebrovascular events  $\leq$  6 months prior to starting study treatment, including transient ischemic attacks, cerebrovascular accidents, deep vein thrombosis or pulmonary emboli
15. Concurrent neuromuscular disorder that is associated with the potential of elevated CK (eg, inflammatory myopathies, muscular dystrophy, amyotrophic lateral sclerosis, spinal muscular atrophy)
16. Treatment with any of the following:
  - a. Cyclical chemotherapy within a period of time that was shorter than the cycle length used for that treatment (eg, 6 weeks for nitrosourea, mitomycin-C) prior to starting study treatment
  - b. Biologic therapy (eg, antibodies) except bevacizumab or aflibercept, continuous or intermittent small molecule therapeutics, or any other investigational agents within a period of time that is  $\leq$  5 half-lives ( $t_{1/2}$ ) or  $\leq$  4 weeks (whichever is shorter) prior to starting study treatment
  - c. Bevacizumab or aflibercept therapy  $\leq$  3 weeks prior to starting study treatment
  - d. Radiation therapy that included  $>$  30% of the bone marrow
17. Residual CTCAE  $\geq$  grade 2 toxicity from any prior anticancer therapy, with the exception of grade 2 alopecia or grade 2 neuropathy
18. Known history of HIV infection
19. Active hepatitis B or hepatitis C infection
20. Known history of Gilbert's syndrome or is known to have any of the following genotypes: UGT1A1\*6/\*6, UGT1A1\*28/\*28, or UGT1A1\*6/\*28
21. Known contraindication to receive cetuximab or irinotecan at the planned doses; refer to the most recent cetuximab and irinotecan SPC or local label as applicable
22. Current treatment with a non-topical medication known to be a strong inhibitor of CYP3A4. However, patients who either discontinue this treatment or switch to another medication at least 7 days prior to starting study treatment are eligible.
23. Concomitant use of St. John's wort (*hypericum perforatum*)
24. Other severe, acute, or chronic medical or psychiatric condition or laboratory abnormality that may increase the risk associated with study participation or study drug administration or that may interfere with the interpretation of study results and, in the judgment of the Investigator, would make the patient an inappropriate candidate for the study
25. Pregnant, confirmed by a positive human chorionic gonadotropin (hCG) laboratory test result, or nursing (lactating)
26. Prior enrollment into this clinical study

**Table S2. Dose-limiting toxicity criteria for BEACON safety lead-in.**

- Any AE or laboratory value considered unrelated to underlying disease, disease progression, intercurrent illness, or concomitant medications/therapies resulting in the inability to tolerate at least 75% dose intensity ( $[\text{administered dose in mg}/\text{planned dose in mg}] \times 100$ ) of binimetinib, encorafenib, or cetuximab during cycle 1
- Cardiac disorders**
- Absolute decrease of LVEF  $>$  10% compared to Baseline and the LVEF is below the institution's LLN
  - Left ventricular systolic dysfunction grade  $\geq$  3
  - Other cardiac disorders grade  $\geq$  3
- Vascular disorders**
- Grade 3 hypertension for  $>$  14 consecutive days
  - Grade 4 hypertension
- General disorders and administration site conditions**
- Fatigue grade 3 for  $>$  14 consecutive days
- Respiratory disorders**
- Interstitial lung disease/pneumonitis grade  $\geq$  2
- Skin and subcutaneous tissue disorders\***
- Rash, hand foot skin reaction (HFSR), or photosensitivity CTCAE grade 3 for  $>$  14 consecutive days despite maximal skin toxicity treatment (as per local practice)
  - Rash, HFSR, or photosensitivity CTCAE grade 4
- Gastrointestinal disorders\***
- Diarrhea grade 3 for  $\geq$  48 hours despite optimal use of antidiarrheal therapy
  - Diarrhea grade 4

- Nausea/vomiting grade 3 for  $\geq 48$  hours despite optimal use of antiemetic therapy
- Nausea/vomiting grade 4

#### Investigations

- Total bilirubin grade  $\geq 3$
- AST or ALT grade  $\geq 3$  in conjunction with total bilirubin grade  $\geq 2$  of any duration
- AST or ALT grade 3 for  $> 7$  consecutive days
- AST or ALT grade 4
- Serum creatinine grade  $\geq 3$
- CK elevation  $\geq$  grade 3 associated with an increase in creatinine  $\geq 1.5 \times$  the patient's Baseline screening creatinine
- ANC grade 4 for  $> 7$  consecutive days
- Platelet count grade 3 with signs of clinically significant bleeding
- Platelet count grade 4
- ECG QTcF prolonged  $\geq$  grade 3<sup>†</sup>

#### Eye disorders – Retinal

- Retinopathy or retinal detachment grade  $\geq 3$ , confirmed by ophthalmic examination
- Retinal vascular disorder including retinal vein occlusion (RVO), confirmed by ophthalmic examination

#### Eye disorders – Visual disturbances without ocular (retinal) changes

- Blurred vision, flashing lights, floaters: Grade  $\geq 3$

#### Eye disorders – (other; specify)

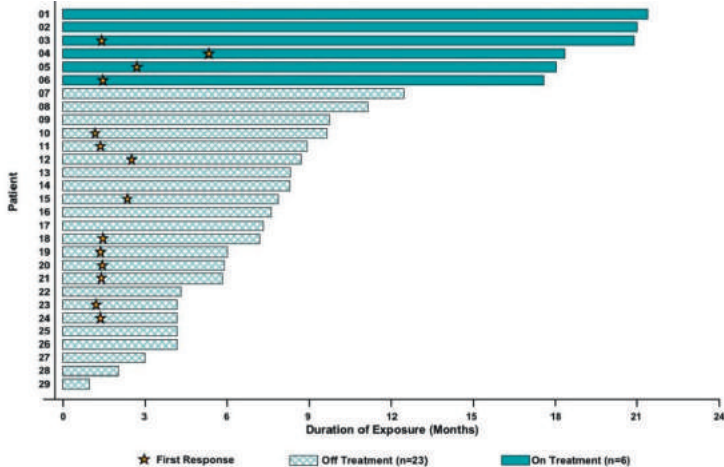
- Grade  $\geq 3$  for  $> 21$  consecutive days
- Grade 4 confirmed by ophthalmic examination

#### Other hematologic and nonhematologic toxicities<sup>‡</sup>

- Any other grade  $\geq 3$  AE except:
- Lymphocyte count decreased (lymphopenia) grade  $\geq 3$  unless clinically significant

Abbreviations: AE, adverse event; ALT, alanine aminotransferase; ANC, absolute neutrophil count; AST, aspartate aminotransferase; CK, creatine kinase; DLT, dose-limiting toxicity; ECG, electrocardiogram; LLN, lower limit of normal; LVEF, left ventricular ejection fraction; QTcF, QT interval corrected for heart rate using Fridericia's formula. \* Prophylactic treatment for nausea/vomiting or skin AEs grade  $\geq$ . <sup>†</sup> QTc must be prolonged on two separate ECGs. <sup>‡</sup> Isolated laboratory changes (eg, alkaline phosphatase, cholesterol, lipase, serum amylase) or those due to sampling or laboratory errors without associated clinical signs or symptoms may be determined to not be DLTs upon review and agreement by the Investigator and Sponsor's Medical Monitor.

Figure S1. Duration on treatment in patients with BRAF V600E mCRC.









# CHAPTER 3.2

Encorafenib, binimetinib  
and cetuximab combined  
therapy for patients with  
*BRAFV600E* mutant  
metastatic colorectal cancer

Sanne C.F.A. Huijberts, Robin M.J.M. van Geel,  
Rene Bernards, Jos. H. Beijnen, Neeltje Steeghs

**Abstract**

Approximately 10 - 15% of colorectal cancers (CRC) harbor an activating *BRAF* mutation, leading to tumor growth promotion by activation of the mitogen-activated protein kinases pathway. *BRAFV600E* mutations are prognostic for treatment failure after first-line systemic therapy in the metastatic setting. In contrast to the efficacy of combined BRAF and MEK inhibition in melanoma, *BRAFV600E* mutant CRC is intrinsically unresponsive due to upregulation of HER/EGFR. However, combining the EGFR inhibitor cetuximab, the BRAF inhibitor encorafenib and the MEK inhibitor binimetinib improves overall survival. This review discusses the current treatment field for patients with *BRAFV600E* mutant metastatic CRC and summarizes the pharmacology, efficacy and safety of the novel doublet and triplet therapies consisting of encorafenib and cetuximab with or without binimetinib.

## Introduction

Colorectal cancer (CRC) was accountable for 880,792 deaths in 2018 worldwide, making it the third leading cause of cancer related deaths.(1) Some 13% of all cancer related deaths in women and 12% of all cancer related deaths in men are attributed to CRC.(2, 3) Approximately 50% of all patients with CRC will develop metastases and in 25% of the patients CRC is already metastasized at initial diagnosis.

CRC is a highly heterogeneous disease with a diverse tumor biology and response to therapy per CRC subtype. Predictive and prognostic biomarkers, based on the genomic landscape of the tumor, are necessary to define subgroups and to develop precision treatment for each individual patient.(4)

About 10-15% of metastatic colorectal cancers (mCRC) harbor an activating mutation in the v-Raf murine sarcoma viral oncogene homolog B (*BRAF*) gene, encoding a protein kinase in the mitogen-activated protein kinases (MAPK) pathway.(5) The most common *BRAF* mutation is the *BRAF valine 600 (BRAfV600)* mutation and occurs when valine is substituted by glutamic acid on codon 600 in the *BRAF* gene.(6) The activating *BRAfV600E* mutation drives proliferation and tumor cell growth. *BRAfV600E* mutations are more frequently found in right-sided tumors, Caucasians, females, and older patients.(7, 8) *BRAfV600E* mutations can be used as both a prognostic and predictive biomarker.(9, 10)

The 5-year survival for mCRC was around 60% in 2014.(3) The prognosis of mCRC has dramatically improved over the past decades due to treatment optimization and early detection. The optimization of systemic anti-cancer therapies includes new chemotherapeutic agents, immunotherapy and targeted therapies. (3) However, efficacy of widely used treatment containing fluoropyrimidine, oxaliplatin and bevacizumab with or without irinotecan is significantly better in *BRAF* and Kirsten rat sarcoma viral oncogene homolog (*KRAS*) wildtype mCRC than in *KRAS* or *BRAF* mutant mCRC, as indicated by overall survival (OS) times of 37.1 months for *BRAF* and *KRAS* wildtype mCRC, 25.6 months in *KRAS* mutant mCRC and 13.4 months in *BRAfV600E* mutant(*BRAfM*) mCRC.(11)

In several clinical trials the response to epidermal growth factor receptor (EGFR) inhibition with an EGFR inhibitor (EGFRi) in combination with chemotherapy is investigated in molecular subgroups.(12, 13) Unfortunately, EGFRi co-administered with chemotherapy resulted in disappointing clinical activity in patients with *KRAS* or *BRAfM* mCRC. The response rate (RR) of *BRAfM* mCRC was 8.3% versus 38% in *BRAF* wildtype tumors, median progression free survival (PFS) of *BRAfM* mCRC was only 2.5 months and median OS less than 6 months.(6, 14) Indeed, a meta-analysis by Cui *et al.* confirmed that *BRAF* mutation presence dramatically decreased tumor response and worsened prognosis.(15)

An important signature for *BRAfM* mCRC is microsatellite instability (MSI), which is based on high-levels of the CpG island methylator phenotype and methylation of the MLH1 promoter.(16) The reported incidence of *BRAfV600E* mutations in MSI CRC differs among studies. Analyses performed on resection material of primary tumors show that the incidence of concurrent *BRAfV600E* mutations and MSI ranges between 5 and 42%.

Moreover, in retrospective and prospective analyses the combination of *BRAF*m and MSI is prognostic for a shorter disease free and OS. (16-22) In the recently published KEYNOTE 164 phase II trial, this specific subpopulation of mCRC was treated with the PD-1 inhibitor pembrolizumab. A response was observed in five out of nine patients, who were previously treated with two or more therapies, and one out of five patients with one prior standard treatment line.(20) These results may provide a rationale to further explore the effect of PD-1 blockade in this population.

Nevertheless, most *BRAF*m mCRC are microsatellite stable and therefore no favorable results of immunotherapy might be expected.

Above-mentioned results imply that *BRAFV600E* mutations are a predictive marker for poor prognosis and failure on conventional chemotherapeutic treatment in the metastatic setting. (8, 14, 23) Moreover, in a retrospective analysis PFS of the first three lines of palliative chemotherapy was only 6.3, 2.5 and 2.6 months in patients with *BRAF*m mCRC, respectively.(24) Due to the poor prognosis and limited treatment options, a better understanding of tumor biology and the development of more effective systemic therapies for *BRAF*m mCRC is of great importance.(25)

This review highlights the current treatment field for *BRAF*m mCRC and summarizes the pharmacology, efficacy and safety of the novel doublet and triplet combinations of the BRAF inhibitor (BRAFi) encorafenib and the EGFRi cetuximab with or without the MEK inhibitor (MEKi) binimetinib in patients with *BRAF*m mCRC.

### **Targeted therapies for BRAFm mCRC**

Several combinations of inhibitors of the MAPK pathway have been investigated in clinical trials with variable results. Not only targeted therapies are combined together, but also combinations with immunotherapy and/or chemotherapy have been explored.(26-30)

The first efforts in the targeted treatment of *BRAF*m mCRC were made in a phase II trial with the BRAFi vemurafenib. Although the earlier determined optimal dose of 960 mg BID was tolerable in this patient population, the anti-tumor results were disappointing with a median PFS of 2.1 months.(31)

Moreover, treatment with BRAFi monotherapy is effective in only 5% of the patients with *BRAF*m mCRC which is in strong contrast to the RR of 50% in *BRAF*m melanoma.(31) Remarkably, suppression of the phosphorylation of ERK, one of the downstream kinases in the MAPK pathway, was not sustained in *BRAF*m CRC cells during BRAFi treatment. *In vitro* and *in vivo*, upregulation of EGFR and rapid reactivation of ERK through EGFR-mediated activation of RAS and CRAF was seen in *BRAF*m CRC cell lines in response to treatment with a BRAFi.(32, 33) Efficacy was improved when EGFR and BRAF blockade were combined.(32) These findings suggest that colon cancer is unresponsive to single BRAF inhibition through feedback activation of EGFR and implies that combined treatment with a BRAFi and an EGFRi will work synergistic in *BRAF*m CRC.(32, 33) Several double combinations of BRAFi and EGFRi in clinical trials validated this hypothesis, but clinical benefits are only of short term.(27, 28) For this reason, doublet and triplet combinations with the addition of a MEK

inhibitor (MEKi), which blocks signaling in the MAPK pathway downstream of BRAF, were explored. These combinations showed favorable anti-tumor activity in preclinical research, which was confirmed in the clinic as well.(34, 35) Moreover, the addition of vemurafenib to the vascular endothelial growth factor receptor inhibitor bevacizumab and capecitabine with or without irinotecan in xenograft models resulted in enhanced tumor growth inhibition and improved OS.(36) This was the bases for the combination of MAPK inhibition and chemotherapy in clinical studies. Below the different combination treatments investigated in the clinic are described.

The combination of vemurafenib and EGFRi panitumumab demonstrated a modest RR of 16% in a pilot study with 12 evaluable patients with *BRAF*<sub>m</sub>, *KRAS* wildtype mCRC.(37) Additionally, a patient with *BRAF*<sub>m</sub> mCRC that received off-label vemurafenib combined with cetuximab experienced stable disease for six to seven months.(38) A pilot study of vemurafenib and cetuximab in non-melanoma *BRAF*<sub>m</sub> cancers showed favorable results.(29) For the doublets of the MEKi trametinib and the EGFRi panitumumab or the BRAFi dabrafenib and panitumumab disappointing objective response rates (ORR) of 0% and 10%, respectively, were reported. However, combining the three drugs, trametinib, dabrafenib and panitumumab together improved the ORR to 21% and the efficacy was correlated with a decreased presence of mutant BRAF alleles in cell free DNA.(28)

Moreover, preclinical trials provided a rationale for adding irinotecan to vemurafenib and cetuximab. BRAF inhibition with vemurafenib leads to activation of EGFR, which causes tumor progression by signaling through multiple downstream pathways. *In vitro*, a higher RR and prolonged survival were observed by the addition of irinotecan. Based on this finding, a phase IB and randomized trial with vemurafenib, irinotecan and cetuximab were conducted in patients with *BRAF*<sub>m</sub> mCRC. It showed an ORR of 16-35% and a median PFS of 4.4-7.7 months. In the randomized trial the favorable disease control rate was 67% for the triplet treatment with vemurafenib, irinotecan and cetuximab versus 22% in the doublet treatment of irinotecan and cetuximab.(30, 39) Co-administration of the MEKi binimetinib and chemotherapy, such as 5-fluoropyrimidine/oxaliplatin (FOLFOX), revealed stable disease in 10 patients and manageable toxicity in 23 evaluable patients with *BRAF*<sub>m</sub> mCRC in a phase I dose-escalation study.(40) Another combination investigated in a phase II trial is dabrafenib and trametinib. This treatment was administered in 43 patients with *BRAF*<sub>m</sub> mCRC and resulted in a moderate ORR of 14% and stable disease in 56% of the patients. Median duration of response was promising and above 36 months.(27)

Despite auspicious results in these different trials, resistance is a recurring problem in *BRAF*<sub>m</sub> cancers. One of the mechanisms of resistance to BRAFi is activation of the PI3K/AKT signaling pathway. To overcome this resistance mechanism a combination of inhibitors of the MAPK pathway and PI3K inhibition was investigated.(41, 42) Two studies were performed: a phase IB dose-escalation study and a phase II trial with 2 treatment arms, consisting of the BRAFi encorafenib and EGFRi cetuximab with or without the PI3K inhibitor alpelisib.(43, 44) The results of the combination of encorafenib and cetuximab in these trials were promising and led to initiation of the BEACON CRC phase III trial with the combination

of encorafenib and cetuximab with or without the addition of binimetinib (ClinicalTrials.gov identifier: NCT02928224).(22) The primary aim of this phase III study was to compare the activity of the triplet combination to standard treatment as measured by OS and ORR. Secondary objectives included the comparison between doublet arm and standard therapy as measured by OS and ORR. Another important secondary aim was to compare OS and ORR of the triplet and doublet arm. More insights into the anti-tumor activity and safety of the double and triple combinations, investigated in these phase IB, II and III trials are given in paragraph 4 and 5 of this review.

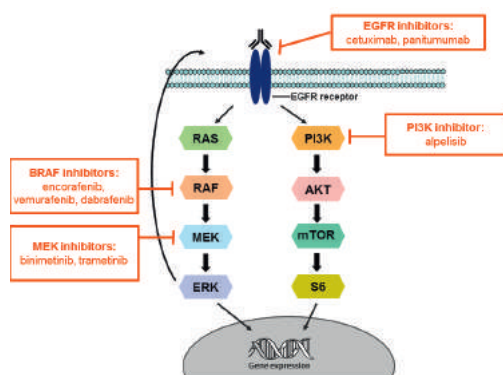


**Figure 1. Mechanism of action triplet therapy of targeted inhibitors of the MAPK and PI3K pathway.(45)**

Since activation of the PI3K/AKT pathway is a known resistance mechanism in BRAFm CRC, it is also included in this figure.

## Pharmacology of the novel triplet combination

The triplet combination comprises encorafenib, binimetinib and cetuximab. Encorafenib is an orally available highly selective adenosine triphosphate (ATP)-competitive small molecule BRAF inhibitor. Binimetinib is an orally available potent and selective allosteric ATP-uncompetitive small molecule inhibitor of MEK1/2. Cetuximab is a recombinant, human/mouse chimeric monoclonal antibody that binds specifically to the extracellular domain of human EGFR. Those three drugs thus inhibit different components of the MAPK pathway.(46-48) Combining the three drugs in a triplet treatment causes a synergistic and robust inhibitory effect on the MAPK pathway, leading to more potent anti-tumor activity in BRAFm CRC.(5) Figure 1 shows the combined mechanism of action of the three drugs.

Chemistry, pharmacokinetic (PK), and pharmacodynamic (PD) properties of the three individual drugs are described below. See figure 2 for the chemical structures of the three drugs.



### Encorafenib

Encorafenib pharmacology has been investigated in healthy subjects and patients with solid tumors. PK is approximately dose-linear after single and multiple dosing and steady state concentrations were reached within 15 days with an accumulation ratio of 0.5, due to CYP3A4 auto-induction.(47) Absorption of encorafenib rapidly occurs after oral dosing with a median time to maximum concentration ( $t_{max}$ ) of 1.5 to 2 hours. The bioavailability of encorafenib was 86% after a single oral administration of 100 mg encorafenib. Maximum plasma concentration ( $C_{max}$ ) was highest in fasted state, while the area under the plasma concentration-time curve (AUC) was not influenced by administration with food.(47) In the phase IB study of van Geel *et al.* the mean AUC at steady state was 7,172 h•ng/mL to 15,300 h•ng/mL among the different doses between 200 and 400 mg QD.(43) The dissociation half-life of encorafenib is more than 30 hours and leads to prolongation of phosphorylated ERK inhibition.(47) This may lead to an increased potency for encorafenib compared to other BRAF inhibitors.(49) Metabolism results in 86% of clearance of encorafenib with N-dealkylation as primary metabolic pathway. In healthy volunteers, administration of strong and moderate CYP3A4 inhibitors in combination with encorafenib resulted in 45 – 68% higher encorafenib plasma concentration and a 2 – 3 fold increase in AUC.(47) Encorafenib elimination is equally distributed between urine and feces. Encorafenib has a median terminal half-life ( $t_{1/2}$ ) of 6.3 h and mean (CV%) apparent clearance (CL/F) was 27.9 L/h.(47) The dose of encorafenib must be lowered in patients with mild to severe hepatic impairment, as this may lead to increased exposure. No data are available for the treatment of patients with severe renal impairment and encorafenib must be used with caution in these cases.(47)

### Binimetinib

Binimetinib pharmacology was investigated in healthy subjects and patients with solid tumors. Steady state is reached within 15 days after twice-daily dosing administered in combination with encorafenib, with a mean AUC of 2.35  $\mu\text{g}\cdot\text{h}/\text{ml}$  according to population PK modeling. PK is dose-linear. (48) Approximately 50% of the dose was absorbed in healthy subjects after an oral single dose of 45 mg. Absorption rapidly occurs after oral administration with a median  $t_{max}$  of 1.5 hours. The  $C_{max}$  was highest in fasted state, while the AUC was not influenced by administration with food. (48, 50) The active metabolite of binimetinib is catalyzed by CYP1A2 and CYP2C19 *in vitro*.(48) Binimetinib has a median  $t_{1/2}$  of 8.66h and CL/F of 28.2 L/h.(48) No dose adjustments are recommended for the treatment of patients with hepatic or renal impairment.(48)

### Cetuximab

PK of cetuximab has been clinically investigated in various trials as single agent and in combination with other systemic anti-cancer therapies or radiotherapy in which cetuximab

doses ranged from 5 to 500 mg/m<sup>2</sup> body surface area (BSA). Following an initial dose of 400 mg/m<sup>2</sup> BSA the mean C<sub>max</sub> was 185 ug/mL.<sup>2</sup> After 3 weeks, steady state was reached for cetuximab monotherapy with mean peak concentrations of 155.8 µg/mL and mean trough concentrations of 41.3 µg/mL.

T<sub>1/2</sub> of cetuximab is long and ranging from 70 to 100 hours.(46) Like other antibodies, cetuximab undergoes biodegradation of the antibody into smaller molecules, i.e. amino acids or small peptides.(46) Only data from patients with adequate renal and hepatic function are available at the moment. Since this lack of data, the treatment of patients with severe hepatic or renal failure must be reconsidered.(46) The affinity for cetuximab to bind EGFR is 5- to 10-fold higher than the binding capacity of endogenous ligands. It blocks binding of endogenous ligands, leading to inhibition of the function of the EGFR receptor, *in vitro* and *in vivo*. (46)

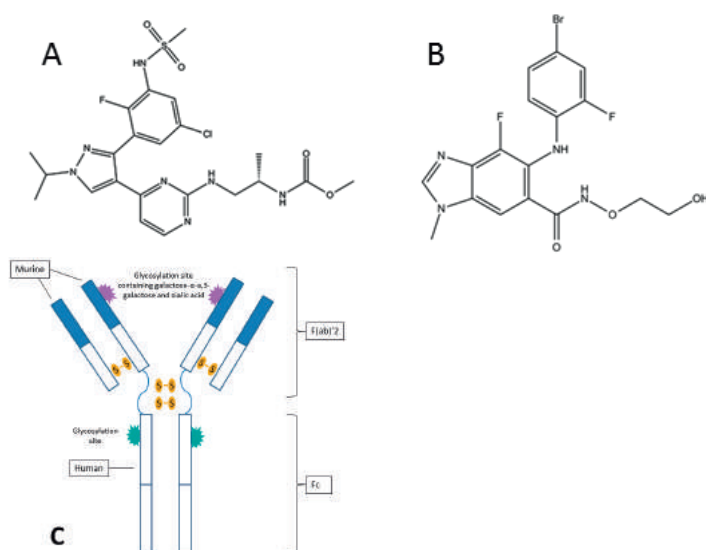


**Figure 2. Chemical structures of encorafenib (A)and binimetinib(B).(47, 48) Structure of cetuximab(C).**

### Combination of encorafenib, binimetinib and cetuximab

The encorafenib plus binimetinib combination resulted in a higher anti-tumor effect, *in vitro* and *in vivo*. Development of resistance was also prevented with combination treatment in BRAFm melanoma xenografts.(48)

Evaluation of the pharmacologic parameters of the triplet combination is included in the recently completed BEACON phase III trial in which encorafenib, binimetinib and cetuximab are administered to patients with BRAFm mCRC. The recommended dose for the triple combination is 300 mg encorafenib QD continuously, 45 mg binimetinib BID continuously and cetuximab at the registered dose, i.e. initial infusion of 400 mg/m<sup>2</sup> followed by 250

mg/m<sup>2</sup> weekly. The PK results have not yet been published at the moment. In a previous study, co-administration of cetuximab did not change the PK of encorafenib as indicated by a similar AUC compared to single agent encorafenib.(43)

Although encorafenib is a potent reversible inhibitor of UGT1A1, no differences were observed in binimetinib exposure if co-administered with encorafenib.(47) Theoretically, no interactions are to be expected regarding the metabolism of the three drugs. However, overlapping toxicities were seen in the safety lead-in and randomized part of the BEACON CRC phase III trial.(5, 22)

### Clinical efficacy of the doublet and triplet combination

Fifty-four patients, who progressed on at least one prior line of therapy for metastatic disease, were enrolled in the phase IB dose-escalation trial with cetuximab and encorafenib with or without alpelisib. The ORR of 18-19% was not significantly different between both treatment groups with a longer duration of response in the doublet group (46 weeks for doublet versus 12 weeks for triplet).(43) In phase II of this trial a total of 102 patients were randomized to the doublet or triplet arm. Adding alpelisib to encorafenib and cetuximab resulted in an improved PFS compared to the doublet therapy, but the toxicity profile was less favorable and OS was not increased.(44)

The BEACON CRC trial was an open-label randomized, three-arm, phase III study that evaluated the safety and efficacy of encorafenib and cetuximab with or without binimetinib compared to the control arm with standard therapy. The standard therapy was a physician's choice between irinotecan/cetuximab or FOLFIRI/cetuximab.(5) Patients with *BRAF*m mCRC progressive on one or two prior regimens were included with an age of 18 years or older, an Eastern Cooperative Oncology Groups (ECOG) performance status of 0 or 1, adequate organ function and prior administration of irinotecan-based therapy was allowed. All patients were treated with continuously, orally administered encorafenib, cetuximab intravenously weekly in cycles of 28 days with or without continuously administered oral binimetinib or standard chemotherapy in the control arm.(22) The efficacy results of this phase III trial showed an ORR of 26% for the triplet therapy and 20% for the doublet, compared to an ORR of 2% in the control arm. PFS was 4.3 months, 4.2 months and 1.5 months for the triplet, doublet and control arm, respectively. Both the triplet and the doublet arm showed a better OS compared to the control arm. The mean OS of the triplet was 9.0 months compared to 5.4 months in the control arm. For the doublet arm the OS was 8.4 months. No difference in hazard ratio (HR) was found for OS in the triplet regimen vs. control for patients that had received prior irinotecan (HR 0.55) or irinotecan naïve patients (HR 0.53).(22) It is important to notice that the triplet and doublet arm are compared in the BEACON CRC phase III trial, but the study was only powered for comparison of the investigational combinations versus the control arm, and not for efficacy differences between the doublet and triplet combination.(5, 22) In table 1, the response data for the phase IB, phase II and phase III trials are summarized.

**Table 1. Clinical activity of the combination of encorafenib (Enco) and cetuximab (CTX) +/- binimetinib (Bin) and or Irinotecan-based chemotherapy (Iri) + CTX.**

Clinical trial phase Treatment regimen	III(5, 22) Enco+CTX+Bin (n=111)	III(22) Enco+CTX (n=113)	II(44) Enco+CTX (n=50)	IB(43) Enco+CTX (n=26)	III(22) Iri+CTX (n=107)
ORR (CR + PR), n (%)	29 (26)	23 (20)	11 (22)	5 (19.2)	2 (2)
CR, n (%)	4 (4)	6 (5)	-	1 (3.8)	0
PR, n (%)	25 (23)	17 (15)	-	4 (15.4)	2 (2)
SD, n (%)	47 (23)	61 (54)	-	15 (57.7)	31 (29)
PD, n (%)	11 (10)	8 (7)	-	4 (15.4)	36 (34)
Not evaluable for response, n (%)	24 (22)	21 (19)	-	2 (7.7)	38 (36)
PFS (months)	4.3	4.2	4.2	3.7	1.5
OS (months)	9.0	8.4	> 15.2*	-	5.4

Abbreviations: CR complete response, PR partial response, SD stable disease, PD progressive disease, ORR overall response rate, PFS progression free survival, OS overall survival.

\* Only data available stating that OS of Enco+CTX was not reached at data cut-off, median OS of triplet Enco+CTX+alpelisib in the same trial was 15.2 months.(44)

- = missing data

## Safety and tolerability

In BRAFm melanoma, the safety of the combination of encorafenib and binimetinib was tested in 274 patients in two phase II trials and in 257 BRAFm melanoma patients in one phase III trial. The recommended phase 2 dose of orally administered binimetinib 45 mg BID and encorafenib 450 mg QD (in phase II) or encorafenib 300 mg QD (in phase III) caused the following adverse events in more than 30% of the patients: nausea, vomiting, fatigue, abdominal pain and dyspnea. In contrast to adverse events of encorafenib monotherapy, less skin toxicities were observed in combination.(47) In later trials with encorafenib and binimetinib in BRAFm mCRC patients, the RP2D determined in BRAFm melanoma was used. The first insight into the safety profile of cetuximab and encorafenib in BRAFm mCRC was given in the phase IB trial with encorafenib, cetuximab +/- alpelisib. All patients treated in the phase IB study experienced at least one adverse event. In 69% of the patients grade 3/4 toxicities were observed.(43) As stated before the benefit-risk ratio for this triplet regimen was negative and for this reason not further developed.

Since the addition of binimetinib to the combination of cetuximab and encorafenib was never investigated in patients before, the BEACON CRC phase III trial started with a safety lead-in to explore the safety and tolerability of the triplet.(5) In this safety lead-in a total of 30 patients received the same dose as in the phase III portion of the trial, as described above. All patients experienced adverse events.(5) In table 2, the adverse events of encorafenib and cetuximab +/- binimetinib that occurred in the phase III trial in more than 20% of the patients are listed. Grade 3 and 4 adverse events are shown separately. Adverse events of grade 3 or higher were observed in 61% of the patients in the control group, in 50% of the patients in the doublet group and in 58% in the triplet group. No grade 5 adverse events are described in the phase IB trial, but 3 deaths related to study medication were observed in the phase III trial, i.e. colonic perforation in the triplet arm, anaphylactic reaction and respiratory failure in the control group.(5, 22, 43) Most common adverse

events with the triplet combination were diarrhea (62%), dermatitis acneiform (49%), nausea (45%), vomiting (38%) and fatigue (33%). All adverse events occurred with a higher frequency in the triplet arm than the doublet arm. Mainly, skin and gastrointestinal toxicities were more frequent and more severe with the triplet combination compared to the doublet combination of encorafenib and cetuximab.(5, 43)

The median relative dose intensities were high in the triplet and doublet group: 91% in the triplet and 98% in the doublet arm for encorafenib, for cetuximab 91% in the triplet and 93% in the doublet arm and for binimetinib 91% in the triplet arm.(22)

All three drugs have less common occurring, but worth noticing adverse events. For MEK inhibitors, ocular toxicity is a known class effect.(51) Binimetinib-associated retinopathy correlates with inhibition of the MAPK pathway in multiple retinal components.(52) In a clinical trial with 51 patients treated with binimetinib visual symptoms were mild and mainly reversible. Around 90% of patients developed sub-retinal fluid with only 20% of the patients experiencing symptoms. In a retrospective cohort study with 25 patients, MEKi-associated retinopathy did not cause irreversible loss of vision or serious eye damage. Treatment interruption is not necessary in case of absence of severe symptoms and if no retinal detachment or vein occlusion is present.(53-55) In the Safety lead-in of the BEACON CRC phase III trial 27% of the patients experienced transient blurred vision and only 1 patient developed retinal detachment.(5) Encorafenib may also lead to ocular toxicities, such as uveitis, iritis and iridocyclitis. Patients should therefore be assessed at each visit for ocular symptoms.(47)

Compared to other BRAF inhibitors, encorafenib has increased specificity which may result in a better tolerability and less off-target effects, such as photosensitivity and pyrexia.(49) Besides the skin toxicities stated in table 2, development of cutaneous malignancies may also occur during treatment with encorafenib. Dermatological evaluations are recommended before start of treatment and every two months on treatment.(47)

### Regulatory affairs

Based on the COLUMBUS trial, the double combination of encorafenib and binimetinib was approved for *BRAF*<sup>v600E</sup> unresectable or metastasized melanoma by the U.S. Food and Drug Administration (FDA) in June 2018 and in July 2019 by the European Medicines Agency (EMA).(34, 47, 48, 56) For *NRAS* mutant advanced melanoma, registration application of the combination was submitted, but withdrawn based on risk-benefit assessment of the regulatory authorities, which made approval unlikely.(57) In September 2018, the FDA granted a Breakthrough Therapy Designation for encorafenib, binimetinib and cetuximab for the treatment of patients with *BRAF*<sup>v600E</sup> mCRC who have failed 1 or 2 prior lines of palliative therapies.(58) The Breakthrough Therapy Designation is designed to expedite development and review of drugs for serious conditions and with very favorable preliminary trial results.(58) It can be expected that the combination of encorafenib, binimetinib and cetuximab will be approved by both FDA and EMA in the near future for *BRAF*<sup>v600E</sup> mCRC based on the positive BEACON CRC phase III results.(22)

**Table 2. Adverse events in 20% or more of the patients treated with combined encorafenib (Enco) and cetuximab (CTX) +- binimetinib (Bin).**

Clinical trial phase Treatment regimen	III(5, 22) Enco+CTX+Bin (n=222)		III(22) Enco+CTX (n=216)		IB(43) Enco+CTX (n=26)	
	All grades n (%)	Grade 3/4 n (%)	All grades n (%)	Grade 3/4 n (%)	All grades n (%)	Grade 3/4 n (%)
Diarrhea	137 (62)	22 (10)	72 (33)	4 (2)	5 (19.2)	1 (3.8)
Dermatitis acneiform	108 (49)	5 (2)	63 (29)	1(<1)	3 (11.5)	0
Nausea	100 (45)	10 (5)	63 (29)	1(<1)	8 (30.8)	0
Vomiting	85 (38)	9(4)	46 (21)	3 (1)	12 (46.2)	2 (7.7)
Fatigue	73 (33)	5 (2)	65 (30)	9(4)	13 (50.0)	3 (11.5)
Abdominal pain	65 (29)	13 (6)	49 (23)	5 (2)	8 (30.8)	3 (11.5)
Decreased appetite	63 (28)	4 (2)	58 (27)	3 (1)	7 (26.9)	0
Asthenia	55 (25)	7 (3)	46 (21)	7 (3)	-	-
Constipation	55 (25)	0 (0)	33 (15)	0 (0)	7 (26.9)	1 (3.8)
Dry skin	46 (21)	2 (<1)	24 (11)	0 (0)	5 (19.2)	0
Pyrexia	45 (20)	4 (2)	35 (16)	2 (<1)	3 (11.5)	0

Grade is based on the National Cancer Institute Common Terminology Criteria for Adverse Events version 4.03. - = missing data. CPK = creatine phosphokinase

## Future perspectives

The combination of cetuximab and encorafenib with or without binimetinib slightly improved progression free survival and OS in patients with *BRAF*m mCRC. For this reason the search for other treatment combinations in this patient population continues. For example, the MEKi binimetinib is used in several ongoing trials with various combination regimens, including immunotherapy and chemotherapy.

Preclinical- and clinical trials have reported that a BRAFi and/or MEKi might have immunomodulatory effects, among other effects leading to increased infiltration of immune cells into the tumor and a better functionality of immune effector cells.(59-61) To optimize synergy of BRAFi and/or MEKi and immunotherapy, a better understanding of PK, PD and pharmacogenetics is of importance in future research.(62) Currently, binimetinib is combined with pembrolizumab and bevacizumab in a phase II trial with patients with refractory mCRC, including *BRAF*m mCRC [clinicaltrials.gov identifier NCT03475004]. The recruitment of a phase I and II trial in which binimetinib is combined with immunotherapy in *KRAS* mutant, microsatellite stable, mCRC has been completed [NCT03271047]. The results of this trial may expand indications for the use and combination of binimetinib. The combination of encorafenib and binimetinib is studied in advanced non-V600 activated *BRAF*m cancers and this phase I/II trial is currently recruiting patients [clinicaltrials.gov identifier NCT03843775].

Another approach to optimize treatment strategies is to explore different timing of treatment. A sub-analysis of the BEACON CRC phase III trial did not show a difference in anti-tumor response between patients treated with 1 or 2 prior treatment lines. Additionally, a study in treatment-naïve patients has not been performed so far and therefore it remains uncertain if treatment-naïve patients with *BRAF*m mCRC will benefit from this triplet regimen.(22) Therefore, a trial investigating encorafenib, binimetinib and

cetuximab in first-line palliative setting is ongoing to explore the efficacy in treatment-naïve patients [clinicaltrials.gov identifier NCT03693170].

Lastly, the development of resistance against targeted agents remains an emerging problem that impairs the duration of clinical benefit. The resistance mechanisms are based on acquired mutations in the MAPK pathway or alternative pathways, such as the PI3K-AKT-mTOR pathway.(63) For example, the analyses of paired biopsies from patients treated with inhibitors of the MAPK pathway revealed acquired KRAS amplifications, BRAF amplifications and MET1 mutation.(64, 65) Even though the development of resistance may be delayed by combining encorafenib, binimetinib and cetuximab in *BRAFm* mCRC, overcoming resistance is still not feasible. A detailed understanding of tumor biology, heterogeneity and resistance mechanisms therefore remains pivotal for the optimal treatment of *BRAFm* mCRC. Based on genetics and intracellular signaling pathways, which may change during treatment with MAPK pathway inhibitors, different treatment approaches might be needed. For example, by monitoring development of secondary resistance mutations in cell free DNA, sequential treatment with different targeted agents to overcome resistance may become feasible.(28, 66)

## Conclusion

*BRAFV600E* mutations in mCRC are predictive for treatment failure after first-line systemic therapy in the metastatic setting. In contrast to the efficacy of combined BRAF and MEK inhibition in melanoma, *BRAFm* CRC is unresponsive to these drugs, due to upregulation of HER/EGFR. The triplet combination of encorafenib, binimetinib and cetuximab has shown to be effective and to improve ORR, PFS and OS in second line palliative treatment as compared to standard chemotherapeutic regimens. Toxicity is extensive, but manageable with sufficient supportive care in this patient population. However, based on the currently available data, the addition of binimetinib seems to increase the severity of toxicity without improving OS significantly. Therefore, treatment with the doublet regimen may be a justifiable strategy in clinical practice for patients with *BRAFm* mCRC. Secondary resistance remains an issue and median OS after progression on first line treatment is unfortunately still under one year. This treatment will give patients with a poor prognosis and an often high symptom burden an extra few months with an acceptable quality of life as compared to chemotherapy. Regulatory approval of the combination of encorafenib and cetuximab with or without binimetinib for *BRAFm* mCRC is eagerly awaited.

## Executive summary

### Introduction

- *BRAFV600E* mutations are prognostic for treatment failure after first-line systemic therapy in CRC in the metastatic setting.
- In contrast to the efficacy of combined BRAF and MEK inhibition in melanoma, upregulation of HER/EGFR leads in *BRAFV600E* mutant CRC to unresponsiveness.
- Addition of an EGFR inhibitor to BRAF and MEK inhibition showed favorable anti-tumor activity.

### Targeted therapies for BRAFm mCRC

- Different combinations of MAPK inhibitory drugs were investigated in BRAFm mCRC:
  - Dabrafenib and trametinib combined resulted in ORR 14% and duration of response >36 months.
  - Dabrafenib and trametinib in combination with panitumumab demonstrated ORR of 21%.
  - Vemurafenib, irinotecan and cetuximab showed ORR of 16-25% and disease control rate of 67%.

### Pharmacology of the novel triplet combination

- Recommended dose for triple treatment is based on monotherapy RP2D; 300 mg encorafenib QD, 45 mg binimetinib BID and cetuximab in an initial infusion of 400 mg/m<sup>2</sup> and thereafter 250 mg/m<sup>2</sup> weekly.
- No known PK or metabolic interaction between the individual drugs is known.
- Overlapping adverse events have to be expected based on the toxicity profiles of the drugs.

### Clinical efficacy of the doublet and triplet combination

- In the BEACON CRC phase III trial, investigating encorafenib, cetuximab with or without binimetinib compared to a control arm of irinotecan-based chemotherapy and cetuximab, an interim analysis showed following results:
  - ORR of 26%, 20% and 2% for the triplet, doublet regimen and control arm.
  - PFS of 4.3, 4.5 and 1.5 months respectively.
  - OS of 9.0, 8.4 and 5.4 months respectively.

### Safety and tolerability

- Most common adverse events with the triplet combination were diarrhea (62%), dermatitis acneiform (49%), nausea (45%), vomiting (38%) and fatigue (33%).
- All adverse events were manageable with adequate supportive care.



### Conclusion

- The combination of encorafenib and cetuximab with or without binimetinib significantly improved survival and response rate compared to standard of care in *BRAF*m mCRC.
- The triplet and doublet combination have an acceptable safety profile.

## References

1. International Agency for Research on Cancer. Colorectal cancer fact sheet. [http://gco.iarc.fr/today/data/factsheets/cancers/10\\_8\\_9-Colorectum-fact-sheet.pdf](http://gco.iarc.fr/today/data/factsheets/cancers/10_8_9-Colorectum-fact-sheet.pdf) (accessed on 10 Oct 2019).
2. Regional Office for World Health Organization Europe. Colorectal cancer. <http://www.euro.who.int/en/health-topics/noncommunicable-diseases/cancer/news/news/2012/2/early-detection-of-common-cancers/colorectal-cancer> (assessed on 1 Aug 2019)
3. Van Cutsem E, Cervantes A, Nordlinger B, Arnold D. Metastatic colorectal cancer: ESMO Clinical practice guidelines for diagnosis, treatment and follow-up. *Annals of oncology*. 2014;25 Suppl 3:iii1-9.
4. Punt CJ, Koopman M, Vermeulen L. From tumour heterogeneity to advances in precision treatment of colorectal cancer. *Nature reviews clinical oncology*. 2017;14(4):235-46.
5. Van Cutsem E, Huijberts S, Grothey A, Yaeger R, Cuyler PJ, Elez E, et al. Binimetinib, encorafenib, and cetuximab triplet therapy for patients with BRAF V600E-mutant metastatic colorectal cancer: Safety lead-in results from the phase III BEACON colorectal cancer study. *Journal of clinical oncology*. 2019;37(17):1460-9.
6. Bahrami A, Hesari A, Khazaei M, Hassanian SM, Ferns GA, Avan A. The therapeutic potential of targeting the BRAF mutation in patients with colorectal cancer. *Journal of cellular physiology*. 2018;233(3):2162-9.
7. Loupakis F, Moretto R, Aprile G, Muntoni M, Cremolini C, Iacono D, et al. Clinico-pathological nomogram for predicting BRAF mutational status of metastatic colorectal cancer. *British journal of cancer*. 2016;114(1):30-6.
8. Tie J, Gibbs P, Lipton L, Christie M, Jorissen RN, Burgess AW, et al. Optimizing targeted therapeutic development: analysis of a colorectal cancer patient population with the BRAF(V600E) mutation. *International journal of cancer*. 2011;128(9):2075-84.
9. Yalcin S, Trad D, Kader YA, Halawani H, Demir OG, Mall R, et al. Personalized treatment is better than one treatment fits all in the management of patients with mCRC: a consensus statement. *Future oncology*. 2014;10(16):2643-57.
10. Saridakis Z, Tzardi M, Papadaki C, Sfakianaki M, Pega F, Kalikaki A, et al. Impact of KRAS, BRAF, PIK3CA mutations, PTEN, AREG, EREG expression and skin rash in  $\geq 2$  line cetuximab-based therapy of colorectal cancer patients. *PloS one*. 2011;6(1):e15980.
11. Cremolini C, Loupakis F, Antoniotti C, Lupi C, Sensi E, Lonardi S, et al. FOLFOXIRI plus bevacizumab versus FOLFIRI plus bevacizumab as first-line treatment of patients with metastatic colorectal cancer: updated overall survival and molecular subgroup analyses of the open-label, phase 3 TRIBE study. *The Lancet oncology*. 2015;16(13):1306-15.
12. Hsu HC, Thiam TK, Lu YJ, Yeh CY, Tsai WS, You JF, et al. Mutations of KRAS/NRAS/BRAF predict cetuximab resistance in metastatic colorectal cancer patients. *Oncotarget*. 2016;7(16):22257-70.
13. Kaczirek K, Ciuleanu TE, Vrbanec D, Marton E, Messinger D, Liegl-Atzwanger B, et al. FOLFOX4 plus cetuximab for patients with previously untreated metastatic colorectal cancer according to tumor RAS and BRAF mutation status: Updated analysis of the CECOG/CORE 1.2.002 study. *Clinical colorectal cancer*. 2015;14(2):91-8.
14. De Roock W, Claes B, Bernasconi D, De Schutter J, Biesmans B, Fountzilas G, et al. Effects of KRAS, BRAF, NRAS, and PIK3CA mutations on the efficacy of cetuximab plus chemotherapy in chemotherapy-refractory metastatic colorectal cancer: a retrospective consortium analysis. *The Lancet oncology*. 2010;11(8):753-62.
15. Cui D, Cao D, Yang Y, Qiu M, Huang Y, Yi C. Effect of BRAF V600E mutation on tumor response of anti-EGFR monoclonal antibodies for first-line metastatic colorectal cancer treatment: a meta-analysis of randomized studies. *Molecular biology reports*. 2014;41(3):1291-8.

16. Lochhead P, Kuchiba A, Imamura Y, et al: Microsatellite instability and BRAF mutation testing in colorectal cancer prognostication. *Journal of the National Cancer Institute*. 2013;105:1151-1156.
17. Taieb J, Le Malicot K, Shi Q, Penault-Llorca F, Bouche O, Taberero J, et al. Prognostic value of BRAF and KRAS mutations in MSI and MSS stage III colon cancer. *Journal of the National Cancer Institute*. 2016;138(5):1139-1145.
18. Chen D, Huang JF, Liu K, Zhang LQ, Yang Z, Chuai ZR, et al. BRAFV600E mutation and its association with clinicopathological features of colorectal cancer: a systematic review and meta-analysis. *PloS one*. 2014;9(3):e90607.
19. Blaker H, Alwers E, Arnold A, Herpel E, Tagscherer KE, Roth W, et al. The association between mutations in BRAF and colorectal cancer-specific survival depends on microsatellite status and tumor stage. *Clinical gastroenterology and hepatology*. 2019;17(3):455-62.e6.
20. Le DT, Kim TW, Van Cutsem E, Geva R, Jager D, Hara H, et al. Phase II open-label study of pembrolizumab in treatment-refractory, microsatellite instability-high/mismatch repair-deficient metastatic colorectal cancer: KEYNOTE-164. *Journal of clinical oncology*. 2020;38(1):11-19.
21. Venderbosch S, Nagtegaal ID, Maughan TS, Smith CG, Cheadle JP, Fisher D, et al. Mismatch repair status and BRAF mutation status in metastatic colorectal cancer patients: a pooled analysis of the CAIRO, CAIRO2, COIN, and FOCUS studies. *Clinical cancer research*. 2014;20(20):5322-30.
22. Kopetz S, Grothey A, Yaeger R, Van Cutsem E, Desai J, Yoshino T, et al. Encorafenib, binimetinib, and cetuximab in BRAF V600E-mutated colorectal cancer. *The New England journal of medicine*. 2019;381(17):1632-1643.
23. Ulivi P, Capelli L, Valgiusti M, Zoli W, Scarpi E, Chiadini E, et al. Predictive role of multiple gene alterations in response to cetuximab in metastatic colorectal cancer: a single center study. *Journal of translational medicine*. 2012;10:87.
24. Morris V, Overman MJ, Jiang ZQ, Garrett C, Agarwal S, Eng C, et al. Progression-free survival remains poor over sequential lines of systemic therapy in patients with BRAF-mutated colorectal cancer. *Clinical colorectal cancer*. 2014;13(3):164-71.
25. Sorbye H, Dragomir A, Sundstrom M, Pfeiffer P, Thunberg U, Bergfors M, et al. High BRAF mutation frequency and marked survival differences in subgroups according to KRAS/BRAF mutation status and tumor tissue availability in a prospective population-based metastatic colorectal cancer cohort. *PloS one*. 2015;10(6):e0131046.
26. Pancione M, Giordano G, Parcesepe P, Cerulo L, Coppola L, Curatolo AD, et al. Emerging insight into MAPK inhibitors and immunotherapy in colorectal cancer. *Current medicinal chemistry*. 2017;24(14):1383-402.
27. Corcoran RB, Atreya CE, Falchook GS, Kwak EL, Ryan DP, Bendell JC, et al. Combined BRAF and MEK inhibition with dabrafenib and trametinib in BRAF V600-mutant colorectal cancer. *Journal of clinical oncology*. 2015;33(34):4023-31.
28. Corcoran RB, Andre T, Atreya CE, Schellens JHM, Yoshino T, Bendell JC, et al. Combined BRAF, EGFR, and MEK inhibition in patients with BRAF(V600E)-mutant colorectal cancer. *Cancer discovery*. 2018;8(4):428-43.
29. Hyman DM, Puzanov I, Subbiah V, Faris JE, Chau I, Blay JY, et al. Vemurafenib in multiple nonmelanoma cancers with BRAF V600 mutations. *The New England journal of medicine*. 2015;373(8):726-36.
30. Hong DS, Morris VK, El Osta B, Sorokin AV, Janku F, Fu S, et al. Phase IB study of vemurafenib in combination with irinotecan and cetuximab in patients with metastatic colorectal cancer with BRAFV600E mutation. *Cancer discovery*. 2016;6(12):1352-65.
31. Kopetz S, Desai J, Chan E, Hecht JR, O'Dwyer PJ, Maru D, et al. Phase II pilot study of vemurafenib in patients with metastatic BRAF-mutated colorectal cancer. *Journal of clinical oncology*. 2015;33(34):4032-8.

32. Corcoran RB, Ebi H, Turke AB, Coffee EM, Nishino M, Cogdill AP, et al. EGFR-mediated reactivation of MAPK signaling contributes to insensitivity of BRAF mutant colorectal cancers to RAF inhibition with vemurafenib. *Cancer discovery*. 2012;2(3):227-35.
33. Prahallad A, Sun C, Huang S, Di Nicolantonio F, Salazar R, Zecchin D, et al. Unresponsiveness of colon cancer to BRAF(V600E) inhibition through feedback activation of EGFR. *Nature*. 2012;483(7387):100-3.
34. Dummer R, Ascierto PA, Gogas HJ, Arance A, Mandala M, Liskay G, et al. Encorafenib plus binimetinib versus vemurafenib or encorafenib in patients with BRAF-mutant melanoma (COLUMBUS): a multicentre, open-label, randomised phase 3 trial. *The Lancet oncology*. 2018;19(5):603-15.
35. Dummer R, Ascierto PA, Gogas HJ, Arance A, Mandala M, Liskay G, et al. Overall survival in patients with BRAF-mutant melanoma receiving encorafenib plus binimetinib versus vemurafenib or encorafenib (COLUMBUS): a multicentre, open-label, randomised, phase 3 trial. *The Lancet oncology*. 2018;19(10):1315-27.
36. Yang H, Higgins B, Kolinsky K, Packman K, Bradley WD, Lee RJ, et al. Antitumor activity of BRAF inhibitor vemurafenib in preclinical models of BRAF-mutant colorectal cancer. *Cancer research*. 2012;72(3):779-89.
37. Yaeger R, Cercek A, O'Reilly EM, Reidy DL, Kemeny N, Wolinsky T, et al. Pilot trial of combined BRAF and EGFR inhibition in BRAF-mutant metastatic colorectal cancer patients. *Clinical cancer research*. 2015;21(6):1313-20.
38. Connolly K, Brungs D, Szeto E, Epstein RJ. Anticancer activity of combination targeted therapy using cetuximab plus vemurafenib for refractory BRAF (V600E)-mutant metastatic colorectal carcinoma. *Current oncology*. 2014;21(1):e151-4.
39. Kopetz S, McDonough SL, Morris VK, Lenz H-J, Magliocco AM, Atreya CE, et al. Randomized trial of irinotecan and cetuximab with or without vemurafenib in BRAF-mutant metastatic colorectal cancer (SWOG 1406). *Journal of clinical oncology*. 2017;35(4\_suppl):520-520.
40. Cho M, Gong J, Frankel P, Synold TW, Lim D, Chung V, et al. A phase I clinical trial of binimetinib in combination with FOLFOX in patients with advanced metastatic colorectal cancer who failed prior standard therapy. *Oncotarget*. 2017;8(45):79750-60.
41. Mao M, Tian F, Mariadason JM, Tsao CC, Lemos R, Jr., Dayyani F, et al. Resistance to BRAF inhibition in BRAF-mutant colon cancer can be overcome with PI3K inhibition or demethylating agents. *Clinical cancer research*. 2013;19(3):657-67.
42. Jeong WJ, Cha PH, Choi KY. Strategies to overcome resistance to epidermal growth factor receptor monoclonal antibody therapy in metastatic colorectal cancer. *World journal of gastroenterology*. 2014;20(29):9862-71.
43. van Geel R, Tabernero J, Elez E, Bendell JC, Spreafico A, Schuler M, et al. A phase Ib dose-escalation study of encorafenib and cetuximab with or without alpelisib in metastatic BRAF-mutant colorectal cancer. *Cancer discovery*. 2017;7(6):610-9.
44. Tabernero JRVG, Guren TK, Schellens JHM, et al. Phase 2 results: encorafenib (ENCO) and cetuximab (CETUX) with or without alpelisib (ALP) in patients with advanced BRAFmutant colorectal cancer (BRAFM CRC). *Journal of clinical oncology*. 2016;34(15\_suppl):3544.
45. van Geel RM, Beijnen JH, Bernards R, Schellens JH. Treatment Individualization in Colorectal Cancer. *Current colorectal cancer reports*. 2015;11(6):335-44.
46. Eli Lilly: Erbitux USPI. <http://pi.lilly.com/us/erbitux-uspi.pdf>.
47. Array Biopharm: Braftovi USPI. [http://www.arraybiopharma.com/documents/Braftovi\\_Prescribing\\_information.pdf](http://www.arraybiopharma.com/documents/Braftovi_Prescribing_information.pdf).
48. Ogino S, Meyerhardt JA, Cantor M, Brahmandam M, Clark JW, Namgyal C, et al. Molecular alterations in tumors and response to combination chemotherapy with gefitinib for advanced colorectal cancer. *Clinical cancer research*. 2005;11(18):6650-6.

49. Trojaniello C, Festino L, Vanella V, Ascierto PA. Encorafenib in combination with binimetinib for unresectable or metastatic melanoma with BRAF mutations. *Expert review of clinical pharmacology*. 2019;12(3):259-66.
50. Bendell JC, Javle M, Bekaii-Saab TS, Finn RS, Wainberg ZA, Laheru DA, et al. A phase 1 dose-escalation and expansion study of binimetinib (MEK162), a potent and selective oral MEK1/2 inhibitor. *British journal of cancer*. 2017;116(5):575-83.
51. Heinzerling L, Eigentler TK, Fluck M, Hassel JC, Heller-Schenck D, Leipe J, et al. Tolerability of BRAF/MEK inhibitor combinations: adverse event evaluation and management. *ESMO open*. 2019;4(3):e000491.
52. van Dijk EH, Duits DE, Versluis M, Luyten GP, Bergen AA, Kapiteijn EW, et al. Loss of MAPK pathway activation in post-mitotic retinal cells as mechanism in MEK inhibition-related retinopathy in cancer patients. *Medicine*. 2016;95(18):e3457.
53. Weber ML, Liang MC, Flaherty KT, Heier JS. Subretinal fluid associated with MEK inhibitor use in the treatment of systemic cancer. *JAMA ophthalmology*. 2016;134(8):855-62.
54. Francis JH, Habib LA, Abramson DH, Yannuzzi LA, Heinemann M, Gounder MM, et al. Clinical and morphologic characteristics of MEK inhibitor-associated retinopathy: differences from central serous chorioretinopathy. *Ophthalmology*. 2017;124(12):1788-98.
55. Urner-Bloch U, Urner M, Jaberg-Bentele N, Frauchiger AL, Dummer R, Goldinger SM. MEK inhibitor-associated retinopathy (MEKAR) in metastatic melanoma: Long-term ophthalmic effects. *European journal of cancer*. 2016;65:130-8.
56. Shirley M. Encorafenib and Binimetinib: First Global Approvals. *Drugs*. 2018;78(12):1277-84.
57. Array BioPharma Inc. Array BioPharma provides NEMO update [media release]. 2017. <http://investor.arraybiopharma.com/newsreleases/news-release-detail/array-biopharma-provides-nemoupdate>. Accessed 2 September 2019.
58. <https://www.ascopost.com/News/59160> (assessed on 2 September 2019).
59. Liu C, Peng W, Xu C, Lou Y, Zhang M, Wargo JA, et al. BRAF inhibition increases tumor infiltration by T cells and enhances the antitumor activity of adoptive immunotherapy in mice. *Clinical cancer research*. 2013;19(2):393-403.
60. Boni A, Cogdill AP, Dang P, Udayakumar D, Njauw CN, Sloss CM, et al. Selective BRAFV600E inhibition enhances T-cell recognition of melanoma without affecting lymphocyte function. *Cancer research*. 2010;70(13):5213-9.
61. Frederick DT, Piris A, Cogdill AP, Cooper ZA, Lezcano C, Ferrone CR, et al. BRAF inhibition is associated with enhanced melanoma antigen expression and a more favorable tumor microenvironment in patients with metastatic melanoma. *Clinical cancer research*. 2013;19(5):1225-31.
62. Kim HY, Upadhyay PJ, Fahmy A, Liu X, Duong JK, Boddy AV. Clinical pharmacokinetic and pharmacodynamic considerations in the (Modern) treatment of melanoma. *Clinical pharmacokinetics*. 2019;58(8):1029-43.
63. Boussemart L, Malka-Mahieu H, Girault I, Allard D, Hemmingsson O, Tomasic G, et al. eIF4F is a nexus of resistance to anti-BRAF and anti-MEK cancer therapies. *Nature*. 2014;513(7516):105-9.
64. Ahronian LG, Sennott EM, Van Allen EM, Wagle N, Kwak EL, Faris JE, et al. Clinical acquired resistance to RAF inhibitor combinations in BRAF-mutant colorectal cancer through MAPK pathway alterations. *Cancer discovery*. 2015;5(4):358-67.
65. Pietrantonio F, Oddo D, Gloghini A, Valtorta E, Berenato R, Barault L, et al. MET-driven resistance to dual EGFR and BRAF blockade may be overcome by switching from EGFR to MET inhibition in BRAF-mutated colorectal cancer. *Cancer discovery*. 2016;6(9):963-71.
66. Das Thakur M, Stuart DD. Molecular pathways: response and resistance to BRAF and MEK inhibitors in BRAF(V600E) tumors. *Clinical cancer research*. 2014;20(5):1074-80.









# CHAPTER 3.3

Mutational profiles associated with resistance in patients with *BRAFV600E* mutant colorectal cancer treated with cetuximab and encorafenib +/- binimetinib or alpelisib

Sanne C.F.A. Huijberts, Mirjam C. Boelens,  
Rene Bernards, Frans L. Opdam

*Submitted for publication*

## **Abstract**

### **Background**

Treatment strategies inhibiting BRAF in combination with EGFR have been developed in patients with *BRAF*<sup>V600E</sup> mutant metastatic colorectal cancer, but intrinsic and secondary resistance remains a challenge. We aimed to investigate which genetic alterations cause intrinsic non-response and/or acquired resistance in these patients receiving therapies consisting of a backbone of BRAF and EGFR inhibition.

### **Methods**

This was a cohort study on genetic alterations in patients with *BRAF*<sup>V600E</sup> mutant advanced colorectal cancer treated with inhibitors of the MAPK pathway. We examined tumor tissue for genetic alterations at baseline, during treatment and at progression.

### **Results**

In total, 37 patients were included in this cohort. Genetic alterations in *EGFR* and in *PIK3CA* are associated with non-response. A greater fraction of non-responders (75%) versus responders (46%) had at least one genetic alteration in other genes than *TP53*, *APC* or *BRAF*. Secondary resistance mutations (n=16 patients) were observed most frequently in the PI3K pathway (n=6) and in receptor tyrosine kinases (n=4), leading to increased upstream signaling.

### **Conclusions**

Genetic alterations in the PI3K and upstream receptor tyrosine kinases were mostly associated with intrinsic and acquired resistance. By understanding these alterations, simultaneous or alternating treatments with targeted inhibitors might improve response duration.

## Background

Colorectal cancer (CRC) is one of the leading causes of mortality in the world and was responsible for almost 900,000 deaths worldwide in 2018.(1) At initial diagnosis, metastasized disease is found in 25% of the patients and 50% of all patient will develop metastases during their disease course.(2) Approximately 8-15% of metastatic CRC harbor a *BRAF*<sup>V600E</sup> mutation, which results in failure of standard chemotherapy and a dismal prognosis.(3)

The *BRAF* gene encodes a serine/threonine protein kinase, which is part of the signal transduction pathway RAS-RAF-MEK-ERK, also known as the mitogen-activated protein kinase (MAPK) pathway. Activating *BRAF* mutations are leading to signaling via this pathway by phosphorylation of the downstream MEK 1/2 proteins. MEK 1/2 subsequently phosphorylates the ERK1/2 kinases, resulting in gene transcription that drives cell proliferation and survival.(4)

The *BRAF*<sup>V600E</sup> mutation is the most common mutation among different tumor types and is caused by the substitution of valine to glutamic acid within codon 600.(5) *BRAF*<sup>V600E</sup> mutations were initially reported by Davies *et al.* in 2002. They discovered that these mutations in melanoma led to an overactive MAPK pathway and could therefore be an interesting drug target.(6) During the past decades, researchers intensively studied the *BRAF*<sup>V600E</sup> mutation to understand its role in tumor development and to explore possible treatment strategies for *BRAF*<sup>V600E</sup> mutated carcinoma, including CRC. Initially, the BRAF inhibitor vemurafenib had been investigated with observed responses in only 5% of the patients with *BRAF*<sup>V600E</sup> mutated metastatic CRC.(7) This lack of response was found to be the result of feedback reactivation of EGFR after BRAF inhibition, thereby limiting the response to BRAF inhibitors.(8, 9) To optimize response rates, BRAF inhibitors have been combined with EGFR inhibitors and other targeted agents in doublet and triplet regimens.(10-13) So far the combination of the BRAF inhibitor encorafenib and the EGFR inhibitor cetuximab with or without the MEK inhibitor binimetinib showed the best outcome with an overall response rate of 23 % (doublet) and 29 % (triplet) with manageable toxicity. Progression free survival was 4.2 months for the doublet and 4.3 months for the triplet regimen.(11) The combination of encorafenib and cetuximab was recently approved by the Food and Drug Administration (FDA). (14) <sup>14</sup> Although response rates are improved and acquired resistance delayed, progression free survival remains short and resistance is still a major challenge.(15)

Since not all *BRAF*<sup>V600E</sup> mutant tumors are responsive to MAPK inhibitors and resistance patterns differ among preclinical studies, it is likely that *BRAF*<sup>V600E</sup> mutated tumors are highly heterogeneous.(16) Moreover, two gene expression subtypes were earlier identified in a clustered analysis of 218 biopsies from *BRAF*<sup>V600E</sup> mutant tumors. *BRAF*<sup>V600E</sup> mutant subtype 1 (BM1) harbored KRAS/mTOR/AKT/4EBP1 activation with high levels of immune infiltration and epithelial-mesenchymal transition (EMT) and *BRAF*<sup>V600E</sup> mutant subtype 2 (BM2) was mainly dysregulated in cell-cycle checkpoints. (17) A higher sensitivity for BRAF, MEK and EGFR inhibition with dabrafenib, trametinib and panitumumab was found in BM1.(18) These

results suggest that *BRAF*<sup>V600E</sup> mutated CRC is indeed a heterogeneous disease with different molecular patterns, responses to and targets for therapy.

Improvement in understanding this heterogeneity, resistance and moderate response rates of MAPK inhibitors in *BRAF*<sup>V600E</sup> mutated CRC is pivotal to optimize treatment outcomes. We here provide an overview of intrinsic and acquired mutations before and during treatment with targeted agents in patients with *BRAF*<sup>V600E</sup> mutant CRC. We present a cohort study of *BRAF*<sup>V600E</sup> mutant CRC patients treated with combinations of MAPK inhibitors in the Netherlands Cancer Institute-Antoni van Leeuwenhoek hospital (NKI-AVL). The research questions we aim to address are; 1. Which biomarkers are associated with non-responders? 2. Which secondary mutations causing acquired resistance are developed during targeted treatment of the MAPK pathway? 3. Can we take advantage of this secondary mutations for optimization of subsequent treatment?

## Methods

### Cohort study

This retrospective cohort study was conducted in the NKI-AVL in patients with *BRAF*<sup>V600E</sup> mutated metastatic CRC between January 2012 and December 2019. All patients gave permission for the use of their residual material and data for research purposes.

All patients included in the analyses were treated with targeted therapies, including the following combinations; encorafenib/cetuximab, encorafenib/cetuximab/alpelisib or encorafenib/cetuximab/ binimetinib. Encorafenib is an orally administered small molecule that inhibits BRAF.(19) Cetuximab is an intravenously administered monoclonal antibody that binds specifically to the extracellular domain of EGFR. Binimetinib is an orally available small molecule and inhibits MEK 1/2.(20) Alpelisib is an orally administered small molecule that inhibits PI3-kinase.(10) The drugs were administered in the following doses: encorafenib 100-450 mg once daily continuously, cetuximab in an initial dose of 400 mg/m<sup>2</sup> and thereafter 250 mg/m<sup>2</sup> weekly, binimetinib 45 mg twice daily continuously and alpelisib 100-300 mg once daily continuously.

We reviewed electronic medical records for information on demographics, anti-tumor response and mutational status. Results from histopathological reports of tumor biopsies before, during treatment or at progressive disease were collected, if available. On treatment tumor biopsies were collected after at least two weeks of treatment, which means that all drugs were on steady state concentrations.

Results from different sequencing methods were included (supplementary table S1). If paired biopsies were available for patients, we carefully reviewed the sequencing methods used for overlap in genes present in the panels of the different sequencing methods. All results presented are restricted to genetic alterations of known clinical significance. This means that variants of unknown clinical significance (VUS) were excluded from this analysis.

## Statistical methods

Descriptive statistics, including median along with percentages and frequencies for categorical variables were tabulated and presented in this paper. Responses were defined according to RECIST version 1.1. criteria.(21) Time to progression was defined as the time from start of targeted treatment to date of first mentioning of progressive disease.

**Table 1. Baseline characteristics of patients included in the analyses.**

	Patients n = 37
Sex, n (%)	
Female	24 (65%)
Male	13 (35%)
Age, median (range), years	59 (38 – 74)
Number of prior treatment lines, n (%)	
1	14 (38%)
2	17 (46%)
≥3	6 (16%)
Treatment arm, n (%)	
Encorafenib + cetuximab	17 (46%)
Encorafenib + cetuximab + binimetinib	7 (19%)
Encorafenib + cetuximab + alpelisib	13 (35%)
Micro satellite stability, n (%)	
MSI	1 (3%)
MSS	20 (54%)
Unknown	16 (43%)
Time points molecular analysis, n (%)	
Single: BL	16 (43%)
Single: OT	2 (5%)
Paired: BL and OT	5 (14%)
Paired: BL and PD	6 (16%)
Paired: OT and PD	4 (11%)
Paired: BL, OT and PD	4 (11%)

Abbreviations: n, number; MSI, micro satellite instable; MSS, micro satellite stable; BL, baseline; OT, on treatment; PD, progressive disease.

## Results

### Overall baseline characteristics

A total of 53 patients with BRAF<sup>V600E</sup> mutated metastatic CRC were screened for mutational status at baseline, on treatment and at progressive disease. The genetic alterations, including the variant of the mutation (e.g. KRAS<sup>G12V</sup>), anti-tumor response and sequencing method per patient are summarized in supplementary table S2 for the total set of 53 patients. The current analysis is performed in 37 patients with at least one other detected genetic alteration at one time point, besides the known BRAF<sup>V600E</sup> mutation.

The majority of patients was pretreated with no more than two lines of anticancer therapy for advanced disease, including one patient with one line of immunotherapy, before the start of double or triple combined targeted agents. Seventeen patients were treated with encorafenib and cetuximab, seven patients with the combination of encorafenib, cetuximab and binimetinib and 13 patients with encorafenib, cetuximab and alpelisib. More than half of the tumors were microsatellite stable (table 1).

Best response on treatment and time to progression were collected for the total patient population and per treatment arm to correlate genetic alterations and anti-tumor activity (table 2). The overall response rate was 46%, including one patient with a complete response (CR) and 16 patients with a partial response (PR). The median time to progression (TTP) was 9 months (range 1-26 months).

Although significant correlations between mutational status and clinical outcomes were not found in this small sample size, some interesting trends were observed as described below. The genetic alterations per patient and anti-tumor response, including best response (BR) and TTP, is schematically shown in figure 1.

Paired biopsies were available for 19 patients, of which 16 double paired biopsies and three triple paired biopsies. However, three patients were excluded from the analyses of paired biopsies, because of the lack of overlap in genes tested in the different sequencing methods per time point. In summary, baseline assessment was conducted in 16 non-responding and 15 responding patients and paired analyses comparing different time points in 16 patients.

**Table 2. Anti-tumor activity.**

	Encorafenib + cetuximab n = 17	Encorafenib+ cetuximab+ binimetinib n = 7	Encorafenib+ cetuximab+ alpelisib n = 13	Total n = 37
Best response, n (%)				
CR	1 (6%)	0 (0%)	0 (0%)	1 (3%)
PR	8 (47%)	3 (43%)	5 (38%)	16 (43%)
SD	6 (35%)	3 (43%)	7 (54%)	16 (43%)
PD	2 (12%)	1 (14%)	1 (8%)	4 (10%)
TTP, median (range), months	8 (1-26)	14 (3-26)	7 (2-16)	9 (1-26)

Abbreviations: CR, complete response; PR, partial response; SD, stable disease; PD, progressive disease; TTP, time to progression; n, number of patients.

### Biomarkers that predict non-response

The baseline samples of 16 patients with stable (n=13) or progressive disease (n=3) were analyzed with the sequencing panels indicated in table S1 to understand the genetic alterations that predict non-response. These 16 patients were compared to 15 patients with response, including 14 patients with a PR and one patient with a CR (figure 2). No mutations other than *BRAF*<sup>V600E</sup> were found in eight patients, 4 non-responders and 4 responders. Six mutations were observed in the phosphoinositide-3-kinase (PI3K) pathway among four different non-responders and four mutations were observed among four different responders. Interestingly, *PIK3CA* mutations were found in non-responding patients and *PTEN* mutations in responding patients. Genetic alterations in or directly influencing the WNT pathway were detected in the tumor of five non-responding patients and three responding patients. The WNT pathway mutations in the three responding patients only included the commonly mutated *APC* gene. Since *APC* is commonly inactivated in an early stage and involved in colorectal cancer development, it is assumed that this mutation does not cause intrinsic resistance. This means that especially relevant mutations in the WNT pathway or directly influencing the Wnt pathway were observed in non-responding patients

in the context of intrinsic resistance. Genetic alterations in genes related to chromatin remodeling were found in six non-responding patients and in only one responding patient. Moreover, in three patients mutations were observed in the epidermal growth factor receptor (*EGFR*) or another component of this receptor family (*ERBB2* or *ERBB4*).

Since *TP53* and *APC* are common and mutated in an early stage of colorectal cancer development, we assume that these mutations might not cause intrinsic resistance. Interestingly, if not counting *TP53* and *APC* mutations, 73% of the tumors of non-responding patients were mutated in other genes than *BRAF* or *TP53* and for responding patients this was only 46%. Furthermore, two pathways were mutated in more than one non-responding patients and not in responding patients, including mutations involved in RNA splicing (n=2) and G-protein signaling (n=3).

No *KRAS* mutations were found at baseline in these 31 patients, which is not surprising since *BRAF* and *KRAS* mutations are considered mutually exclusive.(22) Additionally, no difference in outcome could be identified between microsatellite stable and unstable tumors.

To summarize, genetic alterations in the following genes seem to predict non-response; alterations in or directly influencing the WNT pathway, alterations directly influencing chromatin remodeling, alterations in *EGFR*, components of *EGFR* or other receptor tyrosine kinases or alterations in *PIK3CA*. These mutations possibly bypass the MAPK pathway in *BRAF*<sup>V600E</sup> mutant CRC. A greater part of non-responding patients had at least one genetic alteration in other genes than *TP53*, *APC* or *BRAF*. Finally, genetic alterations in genes involved in G-protein signaling, immune regulation, RNA splicing and the Hedgehog pathway were only detected in the tumors of non-responding patients, but the significance of this remains uncertain.

### Development of secondary mutations causing resistance

Since acquired resistance remains a major problem in the treatment with MAPK inhibitors, we explored the development of secondary mutations causing resistance by looking into available paired biopsies of 16 patients. From these 16 patients, ten were treated with encorafenib and cetuximab, four with encorafenib, cetuximab and binimetinib and two with the combination of encorafenib, cetuximab and alpelisib. Only mutations were included which were at least tested in molecular assessments at two time points. Several interesting trends were observed during the development of secondary resistance mutations (figure 3). One out of 16 patients did not develop a de novo mutation in a gene tested before and after treatment.

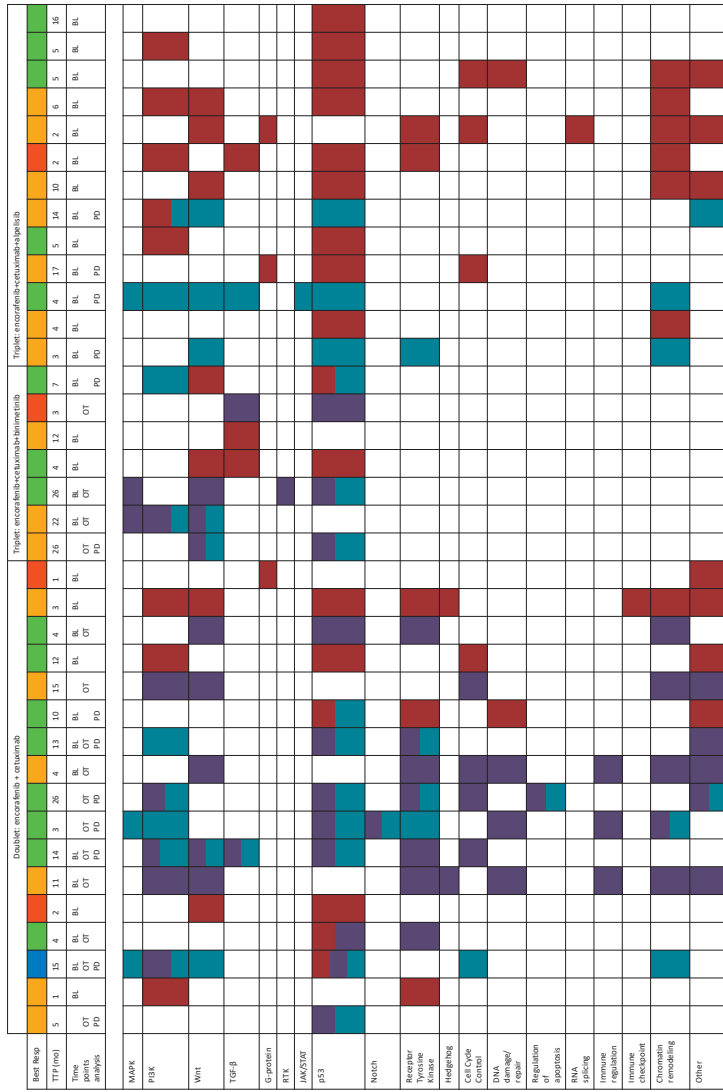


**Figure 1. Anti-tumor activity and mutational characterization per patient and per treatment arm.**  
 Genetic alterations are categorized per pathway, all included alterations are part of the pathway or directly influencing the pathway.  
 Abbreviations: TTP, time to progression; BL, baseline; OT, on treatment; PD, progressive disease.





The other 15 patients developed genetic alterations in different pathways. Four mutations were observed in receptor tyrosine kinases or their ligands (FGF, ERBB), which could lead to resistance by activation of upstream signaling. Six out of 15 patients (40%) developed mutations in the PI3K pathway, of which one patient was treated with the triple combination including alpelisib. This patient simultaneously developed genetic alterations in the MAPK and WNT pathways. We cannot exclude that the biopsy contained two clones that had acquired independent resistance mutations.

Besides interpatient variability in secondary mutations, heterogeneity was also observed within individual patients. For one patient treated with the triple combination of encorafenib, cetuximab and binimetinib, tumor tissue from three different liver metastases was available on treatment. All metastases harbored *BRAF*<sup>V600E</sup>, *APC*<sup>R1450\*</sup> and *PIK3CA*<sup>E545K</sup> mutations, but only two of the lesions harbored a *PTEN* mutation and one of these lesions a *KRAS*<sup>G12V</sup> mutation. Interestingly, the *PTEN* mutations were not identical, including a *PTEN*<sup>R173C</sup> and *PTEN*<sup>R233\*</sup> mutation, marking the heterogeneity of the disease. When correlating these genetic alterations with radiological assessment, the lesion with the *PTEN*<sup>R233\*</sup> and *KRAS*<sup>G12V</sup> mutation was progressive while the other two liver metastasis were in regression. The best response for this patient was stable disease with a TTP of 22 months. This patient demonstrates the heterogeneous character of the disease and heterogeneous response to treatment of different metastatic lesions.

In summary, the development of acquired resistance is common with intra- and interpatient heterogeneity and secondary mutations are observed on different levels in the MAPK pathway and interconnected pathways.

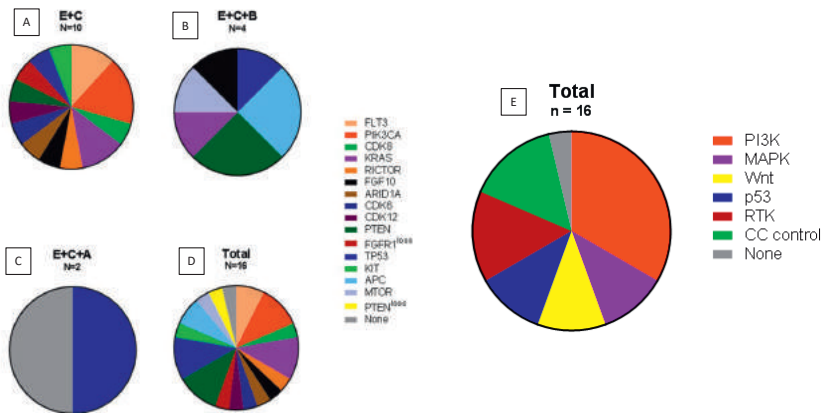


**Figure 3. Pie charts of acquired mutations during treatment with MAPK inhibitors, per treatment arm.**

Figures A to D show pie charts with the specific mutations. Figure E shows a pie chart with the involved pathways in which mutations were observed.

Abbreviations: E, encorafenib; C, cetuximab; B, binimetinib; A, alpelisib; N, number of patients.

## Discussion

In this retrospective cohort study, patterns of intrinsic and acquired resistance in patients with  $BRAF^{V600E}$  mutated metastatic CRC treated with double or triple combinations of inhibitors of the MAPK and PI3K pathways were observed. The majority of mutated pathways at baseline in our cohort study were similar to findings described in literature. A total of six prior published clinical trials report molecular results of tumor tissue and circulating free DNA (cfDNA) in patients with  $BRAF^{V600E}$  mutated metastatic CRC receiving therapies consisting of a backbone of BRAF and EGFR inhibition or BRAF inhibition monotherapy (7, 10, 13, 18, 23, 24). No difference in outcome was described between microsatellite stable and instable tumors in this cohort nor in literature (7, 12, 13). The genetic alterations identified for acquired resistance arose in genes directly or indirectly activating signaling via the MAPK pathway or cross-linked pathways. In our cohort study, genetic alterations in or directly influencing the WNT pathway, directly influencing chromatin remodeling, in the PI3K pathway, and upstream in EGFR or other receptor tyrosine kinases seem to predict for non-response as these mutations probably are considered driver mutations in  $BRAF^{V600E}$  mutant CRC. The earlier investigation of baseline biomarkers and correlation with tumor response performed by Kopetz and *et al.* included genetic alterations in the PI3K pathway which were associated with non-response, EGFR expression, micro satellite instability and rare *KRAS* or *NRAS* mutations. For none of these biomarkers a clear correlation could be observed with radiologic response. Since all patients were treated with monotherapy vemurafenib (which is considered inferior to the triplet combination), a response was not very likely to occur as upregulation of EGFR signaling during BRAF inhibitor monotherapy could be expected (7, 12). Moreover, the majority of 15 molecularly analyzed  $BRAF^{V600E}$  CRC tumor samples of patients treated with the BRAF inhibitor dabrafenib and MEK inhibitor trametinib harbored alterations in the WNT and p53 pathways without a clear correlation with treatment outcome. Five out of 15 tumors had mutations in *PIK3CA* of which 60% of patients had a PR or CR. However, no clear correlation was reported for *PTEN* loss or EGFR expression and progression free survival (13). Remarkably, in our study cohort and in cfDNA profiling by Hong *et al.* it was observed that resistance might be caused by mutations in the PI3K or genes influencing the WNT pathway or at the level of EGFR signaling, resulting in signaling through these pathways (23). Activation of the WNT pathway or upstream receptor tyrosine kinases plays a pivotal role in epithelial-to-mesenchymal transition (EMT), often associated with a CSM4 subtype, in colorectal cancers leading to an adverse prognostic phenotype causing resistance to anti-cancer therapies. Another pathway involved in the development of the EMT subtype is TGF- $\beta$ , which was probably activated in a minority of patients due to mutations in the *SMAD* gene (25). Surprisingly, Middleton *et al.* has shown that the majority of CSM4 subtype  $BRAF^{V600E}$  mutant CRC represents a BM1 signature with a better response to combined treatment with dabrafenib trametinib and panitumumab (18). Unfortunately, it was not feasible to actually determine molecular subtypes BM1 and BM2 in our patient cohort due to restrictions in sequencing data. It would nevertheless be very interesting to define those

subtypes in future research on BRAF/MEK and EGFR inhibition to confirm if screening for BM1 or BM2 at baseline could be used as predictive biomarker for sensitivity to targeted treatments in *BRAF*<sup>V600E</sup> mutant CRC.

A total of three out of 16 patients in this cohort developed *KRAS* mutations on disease progression. Focal amplification of *KRAS* was earlier reported in one post-progression biopsy of a patient treated with RAF/MEK inhibition and in cfDNA samples of patients treated with vemurafenib and panitumumab.(12, 26) In addition, *KRAS* or *NRAS* clones or subclonal *RAS* mutations were detected in respectively 48 % and 21% of patients on the time of disease progression.(24) *KRAS* mutations activate CRAF leading to sustained phosphorylation of ERK and resistance, despite combined BRAF and EGFR or MEK inhibition.(26) The simultaneous presence of *KRAS* and *BRAF* mutations also implies disease heterogeneity, since *KRAS* and *BRAF* mutations are mutually exclusive during primary tumor development.(22) Moreover, heterogeneity was demonstrated in this cohort by a patient with a different molecular pattern in three liver metastasis. Clones sensitive and resistant to treatment might be present at the same time, which must be taken into account by switching to the next line of anti-tumor therapy. Pietrantonio *et al.* cleverly responded to this heterogeneity by adding the MET/ALK inhibitor crizotinib to the BRAF inhibitor vemurafenib upon disease progression in a patient with a secondary *MET* mutation causing acquired resistance.(27) Adding an inhibitor to the current treatment regimen after development of resistance is recommendable to enhance treatment duration, if toxicity of the new drug combination is expected to be manageable. In the case of disease heterogeneity and expected severe or unpredictable toxicity of a combination, it might be better to start an alternating treatment regimen. This approach is currently investigated in resistant *BRAF*<sup>V600E</sup> mutated melanoma. In a proof of concept study, patients are treated with the histone deacetylase inhibitor vorinostat for 14 days upon resistance and thereafter BRAF and/or MEK inhibitors are reintroduced.(28)

Notably, efficacy of BRAF inhibition in *BRAF*<sup>V600E</sup> mutant CRC is depending on EGFR suppression. By single inhibition of BRAF, a rapid reactivation of ERK through EGFR-mediated activation of RAS and CRAF was observed in preclinical studies and confirmed in clinical trials.(8, 9, 13, 24) Since combination of an EGFR and BRAF inhibitor is thus necessary for anti-tumor response, this treatment might be a beneficial backbone for therapy.

By mapping genetic alterations at baseline and upon resistance, simultaneous or alternating treatments with targeted agents inhibiting the genetic alterations might improve duration of response. Monitoring of secondary mutations during treatment with MAPK inhibitors was performed by using cfDNA in prior research, which provides clonal evaluation in real time.(23, 24) It was shown in a prospective study that cfDNA analyses has a sensitivity of 92% and a specificity of 98% to detect *KRAS* or *BRAF* mutations in patients with metastatic CRC.(29) Furthermore, acquired *KRAS* mutations were detected before radiographic assessments revealed progressive disease.(30) Unfortunately, targeted therapies targeting *KRAS* mutant cancers are complicated by the notion that no effective inhibitors directly targeting *KRAS* are currently available with the exception of AMG510 targeting *KRAS*<sup>G12C</sup>.(31)

This cohort contains unique data on paired molecular analyses in tumor tissue for patients with *BRAF*<sup>V600E</sup> mutant metastatic CRC treated with encorafenib and cetuximab with or without binimetinib or alpelisib. Since this treatment combination was approved by the FDA and will likely soon be approved by the European Medicines Agency (EMA), the data are considered highly relevant for clinical practice. Despite these unique data, our study has some limitations. No statistically significant differences between non-responders and responders could be found due to the combination of the small sample size and the lack of molecular analyses on three different time points for all patients. Moreover, the sequencing methods were not similar on every time point, which restricted the number of biopsies that could be used for the paired analyses on acquired mutations. Since molecular analysis on the different time points was not always performed in tumor tissue of the same lesion, it might be that mutations detected were not necessarily newly developed. Due to tumor heterogeneity, these mutations could already have been present at start of treatment. To strengthen our data, we decided to perform the analyses on paired biopsies in 16 patients to improve robustness of the results. Despite the presence of uncertainties, the trends in our and earlier published data provide insight into the mechanisms of resistance in this specific patient group and might generate opportunities for future studies.

In conclusion, our findings show that genetic alterations causing intrinsic and acquired resistance in this patient cohort were observed before and upon treatment with BRAFV600E targeted therapies. The genetic alterations revealed for intrinsic and acquired mutations arose in genes directly or indirectly activating signaling via the MAPK pathway or cross-linked pathways. Intrinsic and acquired resistance mechanisms are heterogeneous with a high intra- and interpatient variability. Based on these results, we suggest comprehensive molecular screening of *BRAF*<sup>V600E</sup> mutant metastatic CRC before start of first line treatment in the palliative setting. Furthermore, it might be considered to closely monitor genetic alterations and accordingly switching therapy to a combined simultaneous or alternating treatment with a backbone of BRAF and EGFR inhibition combined with an inhibitor of the genetic alterations to optimize duration of treatment.

Monitoring of genetic alterations and switching therapies accordingly of course, could not be considered part of standard therapy but should be the scope of future studies. The transcriptional context, identification of responding and non-responding subtypes such as BM1 and BM2, real-time monitoring of tumor DNA and the effect of accordingly changing treatment strategies on response should be part of that.

## **Additional Information**

### **Acknowledgements**

We thank all patients for participation, the Clinical Research Unit of the NKI-AVL and the pathology department for conduct of the study.

### **Authors' contributions**

The methods and analyses were developed and performed by SH with help of MB. SH was in charge of final analyses of all the available data. All authors reviewed and approved the manuscript.

### **Ethics approval and consent to participate**

For these patients, no specific informed consent has been asked as this hospital has a general informed consent procedure in which patients give permission for the use of their residual material and data for research purposes. The principles of the Declaration of Helsinki have been followed in this retrospective cohort study.

### **Consent for publication**

All authors of this manuscript gave consent for publication.

### **Data availability**

The authors are committed to share sequencing data and patient characteristics in an anonymised manner according to applicable privacy regulations and laws. All data requests are reviewed and approved by the Institutional Review Board of the NKI-AVL on the basis of scientific relevance.

### **Conflict of interest**

All authors declare that they have no conflict of interest related to this study.

### **Funding**

No funding or other financial support was received for this manuscript.

## References

1. Rawla P, Sunkara T, Barsouk A. Epidemiology of colorectal cancer: incidence, mortality, survival, and risk factors. *Przeglad gastroenterologiczny*. 2019;14(2):89-103.
2. Van Cutsem E, Cervantes A, Nordlinger B, Arnold D. Metastatic colorectal cancer: ESMO clinical practice guidelines for diagnosis, treatment and follow-up. *Annals of oncology*. 2014;25 Suppl 3:iii1-9.
3. Van Cutsem E, Huijberts S, Grothey A, Yaeger R, Cuyle PJ, Elez E, et al. Binimetinib, encorafenib, and cetuximab triplet therapy for patients with BRAF V600E-mutant metastatic colorectal cancer: Safety lead-in results from the phase III BEACON colorectal cancer study. *Journal of clinical oncology*. 2019;Jco1802459.
4. Caputo F, Santini C, Bardasi C, Cerma K, Casadei-Gardini A, Spallanzani A, et al. BRAF-mutated colorectal cancer: clinical and molecular insights. *International journal of molecular sciences*. 2019;20(21).
5. Bahrami A, Hesari A, Khazaei M, Hassanian SM, Ferns GA, Avan A. The therapeutic potential of targeting the BRAF mutation in patients with colorectal cancer. *Journal of cellular physiology*. 2018;233(3):2162-9.
6. Davies H, Bignell GR, Cox C, Stephens P, Edkins S, Clegg S, et al. Mutations of the BRAF gene in human cancer. *Nature*. 2002;417(6892):949-54.
7. Kopetz S, Desai J, Chan E, Hecht JR, O'Dwyer PJ, Maru D, et al. Phase II pilot study of vemurafenib in patients with metastatic BRAF-mutated colorectal cancer. *Journal of clinical oncology*. 2015;33(34):4032-8.
8. Prahallad A, Sun C, Huang S, Di Nicolantonio F, Salazar R, Zecchin D, et al. Unresponsiveness of colon cancer to BRAF(V600E) inhibition through feedback activation of EGFR. *Nature*. 2012;483(7387):100-3.
9. Corcoran RB, Ebi H, Turke AB, Coffee EM, Nishino M, Cogdill AP, et al. EGFR-mediated reactivation of MAPK signaling contributes to insensitivity of BRAF mutant colorectal cancers to RAF inhibition with vemurafenib. *Cancer discovery*. 2012;2(3):227-35.
10. van Geel R, Tabernero J, Elez E, Bendell JC, Spreafico A, Schuler M, et al. A phase Ib dose-escalation study of encorafenib and cetuximab with or without alpelisib in metastatic BRAF-mutant colorectal cancer. *Cancer discovery*. 2017;7(6):610-9.
11. Kopetz S, Grothey A, Yaeger R, Van Cutsem E, Desai J, Yoshino T, et al. Encorafenib, binimetinib, and cetuximab in BRAF V600E-mutated colorectal cancer. *The New England journal of medicine*. 2019;381(17):1632-43.
12. Yaeger R, Cercek A, O'Reilly EM, Reidy DL, Kemeny N, Wolinsky T, et al. Pilot trial of combined BRAF and EGFR inhibition in BRAF-mutant metastatic colorectal cancer patients. *Clinical cancer research*. 2015;21(6):1313-20.
13. Corcoran RB, Atreya CE, Falchook GS, Kwak EL, Ryan DP, Bendell JC, et al. Combined BRAF and MEK inhibition with dabrafenib and trametinib in BRAF V600-mutant colorectal cancer. *Journal of clinical oncology*. 2015;33(34):4023-31.
14. Food and Drug Administration. FDA approves encorafenib in combination with cetuximab for metastatic colorectal cancer with a BRAF V600E mutation. 2020. <https://www.fda.gov/drugs/resources-information-approved-drugs/fda-approves-encorafenib-combination-cetuximab-metastatic-colorectal-cancer-braf-v600e-mutation>. Accessed on 20 April 2020.
15. Obaid NM, Bedard K, Huang WY. Strategies for overcoming resistance in tumours harboring BRAF mutations. *International journal of molecular sciences*. 2017;18(3).
16. Oddo D, Sennott EM, Barault L, Valtorta E, Arena S, Cassingena A, et al. Molecular landscape of acquired resistance to targeted therapy combinations in BRAF-mutant colorectal cancer. *Cancer research*. 2016;76(15):4504-15.

17. Barras D, Missiaglia E, Wirapati P, Sieber OM, Jorissen RN, Love C, et al. BRAF V600E mutant colorectal cancer subtypes based on gene expression. *Clinical cancer research*. 2017;23(1):104-15.
18. Middleton G, Yang Y, Campbell CD, Andre T, Atreya CE, Schellens JHM, et al. BRAF-mutant transcriptional subtypes predict outcome of combined BRAF, MEK, and EGFR blockade with dabrafenib, trametinib, and panitumumab in patients with colorectal cancer. *Clinical cancer research*. 2020;26(11):2466-2476.
19. National Center for Biotechnology Information. PubChem Database. Encorafenib, CID=50922675, <https://pubchem.ncbi.nlm.nih.gov/compound/Encorafenib> (accessed on Apr. 6, 2020).
20. Huijberts SC, van Geel RM, Bernards R, Beijnen JH, Steeghs N. Encorafenib, binimetinib and cetuximab combined therapy for patients with BRAFV600E mutant metastatic colorectal cancer. *Future oncology*. 2020;16(6):161-73.
21. Eisenhauer EA, Therasse P, Bogaerts J, Schwartz LH, Sargent D, Ford R, et al. New response evaluation criteria in solid tumours: revised RECIST guideline (version 1.1). *European journal of cancer*. 2009;45(2):228-47.
22. Cisowski J, Sayin VI, Liu M, Karlsson C, Bergo MO. Oncogene-induced senescence underlies the mutual exclusive nature of oncogenic KRAS and BRAF. *Oncogene*. 2016;35(10):1328-33.
23. Hong DS, Morris VK, El Osta B, Sorokin AV, Janku F, Fu S, et al. Phase IB study of vemurafenib in combination with irinotecan and cetuximab in patients with metastatic colorectal cancer with BRAFV600E mutation. *Cancer discovery*. 2016;6(12):1352-65.
24. Corcoran RB, Andre T, Atreya CE, Schellens JHM, Yoshino T, Bendell JC, et al. Combined BRAF, EGFR, and MEK inhibition in patients with BRAF(V600E)-Mmtant colorectal cancer. *Cancer discovery*. 2018;8(4):428-43.
25. Lamouille S, Xu J, Derynck R. Molecular mechanisms of epithelial-mesenchymal transition. *Nature reviews molecular cell biology*. 2014;15(3):178-96.
26. Ahronian LG, Sennott EM, Van Allen EM, Wagle N, Kwak EL, Faris JE, et al. Clinical acquired resistance to RAF inhibitor combinations in BRAF-mutant colorectal cancer through MAPK pathway alterations. *Cancer discovery*. 2015;5(4):358-67.
27. Pietrantonio F, Oddo D, Ghilini A, Valtorta E, Berenato R, Barault L, et al. MET-driven resistance to dual EGFR and BRAF blockade may be overcome by switching from EGFR to MET inhibition in BRAF-mutated colorectal cancer. *Cancer discovery*. 2016;6(9):963-71.
28. Huijberts S, Wang L, de Oliveira RL, Rosing H, Nuijen B, Beijnen J, et al. Vorinostat in patients with resistant BRAF(V600E) mutated advanced melanoma: a proof of concept study. *Future oncology*. 2020;16(11):619-629.
29. Thierry AR, Pastor B, Jiang ZQ, Katsiampoura AD, Parseghian C, Loree JM, et al. Circulating DNA demonstrates convergent evolution and common resistance mechanisms during treatment of colorectal cancer. *Clinical cancer research*. 2017;23(16):4578-91.
30. Sartore-Bianchi A, Loupakis F, Argiles G, Prager GW. Challenging chemoresistant metastatic colorectal cancer: therapeutic strategies from the clinic and from the laboratory. *Annals of oncology*. 2016;27(8):1456-66.
31. Canon J, Rex K, Saiki AY, Mohr C, Cooke K, Bagal D, et al. The clinical KRAS(G12C) inhibitor AMG 510 drives anti-tumour immunity. *Nature*. 2019;575(7781):217-223.



## Supplemental data

Supplementary table S1. Genes included in the different sequencing methods.

Sequencing panel	Tested genes
AVL panel v1.1 (Antoni van Leeuwenhoek, Amsterdam, the Netherlands)	Amino acid positions of AKT1 (p.E17), BRAF (p.G466, p.G469, p.L597, p.V600, p.K601), DDR2 (p.S768), EGFR (p.G719, p.G721, p.V774, p.R776, p.T790, p.G796, p.A840, p.V843, p.L858, p.A859, p.K860, p.L861, p.G863, p.H870, p.A871), MEK1 (p.Q56, p.K57, p.D67), PIK3CA (p.E542, p.E545, p.Q546, p.H1047), KRAS (p.A11, p.G12, p.G13, p.V14, p.Q61, p.K117, p.A146), NRAS (p.G12, p.G13, p.A59, p.Q61, p.R68, p.K117, p.A146)
AVL panel v1.2 (Antoni van Leeuwenhoek, Amsterdam, the Netherlands)	Amino acid positions of AKT1 (p.E17), BRAF (p.G466, p.G469, p.L597, p.V600, p.K601), DDR2 (p.S768), EGFR (p.G719, p.G721, p.V774, p.R776, p.T790, p.G796, p.A840, p.V843, p.L858, p.A859, p.K860, p.L861, p.G863, p.H870, p.A871), MEK1 (p.Q56, p.K57, p.D67), PIK3CA (p.E542, p.E545, p.Q546, p.Q1042, p.H1047), KRAS (p.A11, p.G12, p.G13, p.V14, p.Q61, p.A59, p.Q61, p.K117, p.A146), NRAS (p.G12, p.G13, p.A59, p.Q61, p.R68, p.K117, p.A146)
TSA CP v1.0 (MiSeq; Illumina, San Diego, CA, USA)	Hotspot mutations in ABL1, AKT1, ALK, APC, ATM, BRAF, CDH1, CDKN2A, CSF1R, CTNNB1, EGFR, ERBB2, ERBB4, FBXW7, FGFR1, FGFR2, FGFR3, FLT3, GNA11, GNAQ, GNAS, HNF1A, HRAS, IDH1, JAK2, JAK3, KDR, KIT, KRAS, MET, MLH1, MPL, NOTCH1, NPM1, NRAS, PDGFRA, PIK3CA, PTEN, PTPN11, RB1, RET, SMAD4, SMARCB1, SMO, SRC, STK11, TP53, VHL
Oncocarta panel v1.0 (Agene; San Diego, CA, USA)	Gene amplifications in EGFR, ERBB2 (HER2), MET
Foundation Medicine (Cambridge, Massachusetts, USA)	Relevant regions of genes AKT1, AKT2, BRAF, CDK, EGFR, ERBB2, FGFR1, EGR3, FLT3, HRAS, JAK2, KIT, KRAS, MET, NRAS, PDGFRA, PIK3CA, RET
	Relevant regions of genes ABL1, ACVR1B, AKT1, AKT2, AKT3, ALOX12B, ALK, AMER1, APC, AR, ARAF, ARFRP1, ARID1A, ASXL1, ATM, ATR, ATRX, AURKA, AURKB, AXIN1, AXL, BAP1, BARD1, BCL2, BCL2L1, BCL2L2, BCL6, BCOR, BCORL1, BRAF, BRCA1, BRCA2, BRD4, BRIP1, BTG1, BTG2, BTK, CALR, CARD11, CASP8, C8FB, CBL, CCND1, CCND2, CCNE1, CD22, CD274, CD70, CD79A, CD79B, CDC73, CDH1, CDK4, CDK6, CDK8, CDK12, CDKN1A, CDKN1B, CDKN2A, CDKN2B, CDKN2C, CEBPB, CHEK1, CHEK2, CIC, CREBBP, CRKL, CSF1R, CSF3R, CTCF, CTNNA1, CTNNB1, CCND3, CUL3, CUL4A, CXCR4, CYP17A1, DAXX, DDR1, DDR2, DIS3, DNMT3A, DOT1L, EED, EGF, EP300, EPHA3, EPHB1, EPHB4, ERBB2, ERBB3, ERBB4, ERCC4, ERG, ERFF1, ESR1, EZH2, FAM46C, FANCA, FANCC, FANCG, FANCL, FAS, FBXW7, FGF3, FGF4, FGF6, FGF10, FGF12, FGF14, FGF19, FGF23, FGFRI, FGFR2, FGFR3, FGFR4, FH, FLCN, FLT1, FLT3, FOXL2, FUBP1, GABRA6, GATA3, GATA4, GATA6, GID4, GNA11, GNA13, GNAQ, GNAS, GRM3, GSK3B, H3F3A, HDAC1, HGF, HNF1A, HRAS, HSD3B1, ID3, IDH1, IDH2, IGF1R, IKBKE, IKZF1, INPP4B, IRF2, IRF4, IRS2, JAK1, JAK2, JAK3, JUN, KDM5A, KDM5C, KDM6A, KDR, KEAP1, KEL, KIT, KLHL6, KMT2A, KMT2D, KRAS, LTK, LYN, MAF, MAP2K1, MAP2K2, MAP2K4, MAP3K1, MAP3K13, MAPK1, MCL1, MDM2, MDM4, MED12, MEF2B, MEN1, MERTK, MET, MIF, MKNK1, MLH1, MLL, MLL2, MPL, MRE11A, MSH2, MSH3, MSH6, MST1R, MTAP, MTOR, MUTYH, MYC, MYCL, MYCN, MYD88, NBN, NF1, NF2, NFE2L2, NFKBIA, NKK2-1, NOTCH1, NOTCH2, NOTCH3, NPM1, NRAS, NT5C2, NTRK2, NTRK3, P2RY8, PALB2, PARK2, PARP1, PARP2, PARP3, PAX5, PBRM1, PDCD1, PDCD1LG2, PDGFRA, PDGFRB, PDK1, PIK3C2B, PIK3CG, PIK3CA, PIK3CB, PIK3RI, PIM1, PMS2, POLD1, POLE, PPARG, PPP2R1A, PPP2R2A, PRDM1, PRKARIA, PRKCI, PTCH1, PTEN, PTPN11, PTPRO, QKI, RAC1, RAC2, RAC3, RAC4, RAC5, RAC6, RAC7, RAC8, RAC9, RAC10, RAC11, RAC12, RAC13, RAC14, RAC15, RAC16, RAC17, RAC18, RAC19, RAC20, RAC21, RAC22, RAC23, RAC24, RAC25, RAC26, RAC27, RAC28, RAC29, RAC30, RAC31, RAC32, RAC33, RAC34, RAC35, RAC36, RAC37, RAC38, RAC39, RAC40, RAC41, RAC42, RAC43, RAC44, RAC45, RAC46, RAC47, RAC48, RAC49, RAC50, RAC51, RAC52, RAC53, RAC54, RAC55, RAC56, RAC57, RAC58, RAC59, RAC60, RAC61, RAC62, RAC63, RAC64, RAC65, RAC66, RAC67, RAC68, RAC69, RAC70, RAC71, RAC72, RAC73, RAC74, RAC75, RAC76, RAC77, RAC78, RAC79, RAC80, RAC81, RAC82, RAC83, RAC84, RAC85, RAC86, RAC87, RAC88, RAC89, RAC90, RAC91, RAC92, RAC93, RAC94, RAC95, RAC96, RAC97, RAC98, RAC99, RAC100, RAC101, RAC102, RAC103, RAC104, RAC105, RAC106, RAC107, RAC108, RAC109, RAC110, RAC111, RAC112, RAC113, RAC114, RAC115, RAC116, RAC117, RAC118, RAC119, RAC120, RAC121, RAC122, RAC123, RAC124, RAC125, RAC126, RAC127, RAC128, RAC129, RAC130, RAC131, RAC132, RAC133, RAC134, RAC135, RAC136, RAC137, RAC138, RAC139, RAC140, RAC141, RAC142, RAC143, RAC144, RAC145, RAC146, RAC147, RAC148, RAC149, RAC150, RAC151, RAC152, RAC153, RAC154, RAC155, RAC156, RAC157, RAC158, RAC159, RAC160, RAC161, RAC162, RAC163, RAC164, RAC165, RAC166, RAC167, RAC168, RAC169, RAC170, RAC171, RAC172, RAC173, RAC174, RAC175, RAC176, RAC177, RAC178, RAC179, RAC180, RAC181, RAC182, RAC183, RAC184, RAC185, RAC186, RAC187, RAC188, RAC189, RAC190, RAC191, RAC192, RAC193, RAC194, RAC195, RAC196, RAC197, RAC198, RAC199, RAC200, RAC201, RAC202, RAC203, RAC204, RAC205, RAC206, RAC207, RAC208, RAC209, RAC210, RAC211, RAC212, RAC213, RAC214, RAC215, RAC216, RAC217, RAC218, RAC219, RAC220, RAC221, RAC222, RAC223, RAC224, RAC225, RAC226, RAC227, RAC228, RAC229, RAC230, RAC231, RAC232, RAC233, RAC234, RAC235, RAC236, RAC237, RAC238, RAC239, RAC240, RAC241, RAC242, RAC243, RAC244, RAC245, RAC246, RAC247, RAC248, RAC249, RAC250, RAC251, RAC252, RAC253, RAC254, RAC255, RAC256, RAC257, RAC258, RAC259, RAC260, RAC261, RAC262, RAC263, RAC264, RAC265, RAC266, RAC267, RAC268, RAC269, RAC270, RAC271, RAC272, RAC273, RAC274, RAC275, RAC276, RAC277, RAC278, RAC279, RAC280, RAC281, RAC282, RAC283, RAC284, RAC285, RAC286, RAC287, RAC288, RAC289, RAC290, RAC291, RAC292, RAC293, RAC294, RAC295, RAC296, RAC297, RAC298, RAC299, RAC300, RAC301, RAC302, RAC303, RAC304, RAC305, RAC306, RAC307, RAC308, RAC309, RAC310, RAC311, RAC312, RAC313, RAC314, RAC315, RAC316, RAC317, RAC318, RAC319, RAC320, RAC321, RAC322, RAC323, RAC324, RAC325, RAC326, RAC327, RAC328, RAC329, RAC330, RAC331, RAC332, RAC333, RAC334, RAC335, RAC336, RAC337, RAC338, RAC339, RAC340, RAC341, RAC342, RAC343, RAC344, RAC345, RAC346, RAC347, RAC348, RAC349, RAC350, RAC351, RAC352, RAC353, RAC354, RAC355, RAC356, RAC357, RAC358, RAC359, RAC360, RAC361, RAC362, RAC363, RAC364, RAC365, RAC366, RAC367, RAC368, RAC369, RAC370, RAC371, RAC372, RAC373, RAC374, RAC375, RAC376, RAC377, RAC378, RAC379, RAC380, RAC381, RAC382, RAC383, RAC384, RAC385, RAC386, RAC387, RAC388, RAC389, RAC390, RAC391, RAC392, RAC393, RAC394, RAC395, RAC396, RAC397, RAC398, RAC399, RAC400, RAC401, RAC402, RAC403, RAC404, RAC405, RAC406, RAC407, RAC408, RAC409, RAC410, RAC411, RAC412, RAC413, RAC414, RAC415, RAC416, RAC417, RAC418, RAC419, RAC420, RAC421, RAC422, RAC423, RAC424, RAC425, RAC426, RAC427, RAC428, RAC429, RAC430, RAC431, RAC432, RAC433, RAC434, RAC435, RAC436, RAC437, RAC438, RAC439, RAC440, RAC441, RAC442, RAC443, RAC444, RAC445, RAC446, RAC447, RAC448, RAC449, RAC450, RAC451, RAC452, RAC453, RAC454, RAC455, RAC456, RAC457, RAC458, RAC459, RAC460, RAC461, RAC462, RAC463, RAC464, RAC465, RAC466, RAC467, RAC468, RAC469, RAC470, RAC471, RAC472, RAC473, RAC474, RAC475, RAC476, RAC477, RAC478, RAC479, RAC480, RAC481, RAC482, RAC483, RAC484, RAC485, RAC486, RAC487, RAC488, RAC489, RAC490, RAC491, RAC492, RAC493, RAC494, RAC495, RAC496, RAC497, RAC498, RAC499, RAC500, RAC501, RAC502, RAC503, RAC504, RAC505, RAC506, RAC507, RAC508, RAC509, RAC510, RAC511, RAC512, RAC513, RAC514, RAC515, RAC516, RAC517, RAC518, RAC519, RAC520, RAC521, RAC522, RAC523, RAC524, RAC525, RAC526, RAC527, RAC528, RAC529, RAC530, RAC531, RAC532, RAC533, RAC534, RAC535, RAC536, RAC537, RAC538, RAC539, RAC540, RAC541, RAC542, RAC543, RAC544, RAC545, RAC546, RAC547, RAC548, RAC549, RAC550, RAC551, RAC552, RAC553, RAC554, RAC555, RAC556, RAC557, RAC558, RAC559, RAC560, RAC561, RAC562, RAC563, RAC564, RAC565, RAC566, RAC567, RAC568, RAC569, RAC570, RAC571, RAC572, RAC573, RAC574, RAC575, RAC576, RAC577, RAC578, RAC579, RAC580, RAC581, RAC582, RAC583, RAC584, RAC585, RAC586, RAC587, RAC588, RAC589, RAC590, RAC591, RAC592, RAC593, RAC594, RAC595, RAC596, RAC597, RAC598, RAC599, RAC600, RAC601, RAC602, RAC603, RAC604, RAC605, RAC606, RAC607, RAC608, RAC609, RAC610, RAC611, RAC612, RAC613, RAC614, RAC615, RAC616, RAC617, RAC618, RAC619, RAC620, RAC621, RAC622, RAC623, RAC624, RAC625, RAC626, RAC627, RAC628, RAC629, RAC630, RAC631, RAC632, RAC633, RAC634, RAC635, RAC636, RAC637, RAC638, RAC639, RAC640, RAC641, RAC642, RAC643, RAC644, RAC645, RAC646, RAC647, RAC648, RAC649, RAC650, RAC651, RAC652, RAC653, RAC654, RAC655, RAC656, RAC657, RAC658, RAC659, RAC660, RAC661, RAC662, RAC663, RAC664, RAC665, RAC666, RAC667, RAC668, RAC669, RAC670, RAC671, RAC672, RAC673, RAC674, RAC675, RAC676, RAC677, RAC678, RAC679, RAC680, RAC681, RAC682, RAC683, RAC684, RAC685, RAC686, RAC687, RAC688, RAC689, RAC690, RAC691, RAC692, RAC693, RAC694, RAC695, RAC696, RAC697, RAC698, RAC699, RAC700, RAC701, RAC702, RAC703, RAC704, RAC705, RAC706, RAC707, RAC708, RAC709, RAC710, RAC711, RAC712, RAC713, RAC714, RAC715, RAC716, RAC717, RAC718, RAC719, RAC720, RAC721, RAC722, RAC723, RAC724, RAC725, RAC726, RAC727, RAC728, RAC729, RAC730, RAC731, RAC732, RAC733, RAC734, RAC735, RAC736, RAC737, RAC738, RAC739, RAC740, RAC741, RAC742, RAC743, RAC744, RAC745, RAC746, RAC747, RAC748, RAC749, RAC750, RAC751, RAC752, RAC753, RAC754, RAC755, RAC756, RAC757, RAC758, RAC759, RAC760, RAC761, RAC762, RAC763, RAC764, RAC765, RAC766, RAC767, RAC768, RAC769, RAC770, RAC771, RAC772, RAC773, RAC774, RAC775, RAC776, RAC777, RAC778, RAC779, RAC780, RAC781, RAC782, RAC783, RAC784, RAC785, RAC786, RAC787, RAC788, RAC789, RAC790, RAC791, RAC792, RAC793, RAC794, RAC795, RAC796, RAC797, RAC798, RAC799, RAC800, RAC801, RAC802, RAC803, RAC804, RAC805, RAC806, RAC807, RAC808, RAC809, RAC810, RAC811, RAC812, RAC813, RAC814, RAC815, RAC816, RAC817, RAC818, RAC819, RAC820, RAC821, RAC822, RAC823, RAC824, RAC825, RAC826, RAC827, RAC828, RAC829, RAC830, RAC831, RAC832, RAC833, RAC834, RAC835, RAC836, RAC837, RAC838, RAC839, RAC840, RAC841, RAC842, RAC843, RAC844, RAC845, RAC846, RAC847, RAC848, RAC849, RAC850, RAC851, RAC852, RAC853, RAC854, RAC855, RAC856, RAC857, RAC858, RAC859, RAC860, RAC861, RAC862, RAC863, RAC864, RAC865, RAC866, RAC867, RAC868, RAC869, RAC870, RAC871, RAC872, RAC873, RAC874, RAC875, RAC876, RAC877, RAC878, RAC879, RAC880, RAC881, RAC882, RAC883, RAC884, RAC885, RAC886, RAC887, RAC888, RAC889, RAC890, RAC891, RAC892, RAC893, RAC894, RAC895, RAC896, RAC897, RAC898, RAC899, RAC900, RAC901, RAC902, RAC903, RAC904, RAC905, RAC906, RAC907, RAC908, RAC909, RAC910, RAC911, RAC912, RAC913, RAC914, RAC915, RAC916, RAC917, RAC918, RAC919, RAC920, RAC921, RAC922, RAC923, RAC924, RAC925, RAC926, RAC927, RAC928, RAC929, RAC930, RAC931, RAC932, RAC933, RAC934, RAC935, RAC936, RAC937, RAC938, RAC939, RAC940, RAC941, RAC942, RAC943, RAC944, RAC945, RAC946, RAC947, RAC948, RAC949, RAC950, RAC951, RAC952, RAC953, RAC954, RAC955, RAC956, RAC957, RAC958, RAC959, RAC960, RAC961, RAC962, RAC963, RAC964, RAC965, RAC966, RAC967, RAC968, RAC969, RAC970, RAC971, RAC972, RAC973, RAC974, RAC975, RAC976, RAC977, RAC978, RAC979, RAC980, RAC981, RAC982, RAC983, RAC984, RAC985, RAC986, RAC987, RAC988, RAC989, RAC990, RAC991, RAC992, RAC993, RAC994, RAC995, RAC996, RAC997, RAC998, RAC999, RAC1000, RAC1001, RAC1002, RAC1003, RAC1004, RAC1005, RAC1006, RAC1007, RAC1008, RAC1009, RAC1010, RAC1011, RAC1012, RAC1013, RAC1014, RAC1015, RAC1016, RAC1017, RAC1018, RAC1019, RAC1020, RAC1021, RAC1022, RAC1023, RAC1024, RAC1025, RAC1026, RAC1027, RAC1028, RAC1029, RAC1030, RAC1031, RAC1032, RAC1033, RAC1034, RAC1035, RAC1036, RAC1037, RAC1038, RAC1039, RAC1040, RAC1041, RAC1042, RAC1043, RAC1044, RAC1045, RAC1046, RAC1047, RAC1048, RAC1049, RAC1050, RAC1051, RAC1052, RAC1053, RAC1054, RAC1055, RAC1056, RAC1057, RAC1058, RAC1059, RAC1060, RAC1061, RAC1062, RAC1063, RAC1064, RAC1065, RAC1066, RAC1067, RAC1068, RAC1069, RAC1070, RAC1071, RAC1072, RAC1073, RAC1074, RAC1075, RAC1076, RAC1077, RAC1078, RAC1079, RAC1080, RAC1081, RAC1082, RAC1083, RAC1084, RAC1085, RAC1086, RAC1087, RAC1088, RAC1089, RAC1090, RAC1091, RAC1092, RAC1093, RAC1094, RAC1095, RAC1096, RAC1097, RAC1098, RAC1099, RAC1100, RAC1101, RAC1102, RAC1103, RAC1104, RAC1105, RAC1106, RAC1107, RAC1108, RAC1109, RAC1110, RAC1111, RAC1112, RAC1113, RAC1114, RAC1115, RAC1116, RAC1117, RAC1118, RAC1119, RAC1120, RAC1121, RAC1122, RAC1123, RAC1124, RAC1125, RAC1126, RAC1127, RAC1128, RAC1129, RAC1130, RAC1131, RAC1132, RAC1133, RAC1134, RAC1135, RAC1136, RAC1137, RAC1138, RAC1139, RAC1140, RAC1141, RAC1142, RAC1143, RAC1144, RAC1145, RAC1146, RAC1147, RAC1148, RAC1149, RAC1150, RAC1151, RAC1152, RAC1153, RAC1154, RAC1155, RAC1156, RAC1157, RAC1158, RAC1159, RAC1160, RAC1161, RAC1162, RAC1163, RAC1164, RAC1165, RAC1166, RAC1167, RAC1168, RAC1169, RAC1170, RAC1171, RAC1172, RAC1173, RAC1174, RAC1175, RAC1176, RAC1177, RAC1178, RAC1179, RAC1180, RAC1181, RAC1182, RAC1183, RAC1184, RAC1185, RAC1186, RAC1187, RAC1188, RAC1189, RAC1190, RAC1191, RAC1192, RAC1193, RAC1194, RAC1195, RAC1196, RAC1197, RAC1198, RAC1199, RAC1200, RAC1201, RAC1202, RAC1203, RAC1204, RAC1205, RAC1206, RAC1207, RAC1208, RAC1209, RAC1210, RAC1211, RAC1212, RAC1213, RAC1214, RAC1215, RAC1216, RAC1217, RAC1218, RAC1219, RAC1220, RAC1221, RAC1222, RAC1223, RAC1224, RAC1225, RAC1226, RAC1227, RAC1228, RAC1229, RAC1230, RAC1231, RAC1232, RAC1233, RAC1234, RAC1235, RAC1236, RAC1237, RAC1238, RAC1239, RAC1240, RAC1241, RAC1242, RAC1243, RAC1244, RAC1245, RAC1246, RAC1247, RAC1248, RAC1249, RAC1250, RAC1251, RAC1252, RAC1253, RAC1254, RAC1255, RAC1256, RAC1257, RAC1258, RAC1259, RAC1260, RAC1261, RAC1262, RAC1263, RAC1264, RAC1265, RAC1266, RAC1267, RAC1268, RAC1269, RAC1270, RAC1271, RAC1272, RAC1273, RAC1274, RAC1275, RAC1276, RAC1277, RAC1278, RAC1279, RAC1280, RAC1281, RAC1282, RAC1283, RAC1284, RAC1285, RAC1286, RAC1287, RAC1288, RAC1289, RAC1290, RAC1291, RAC1292, RAC1293, RAC1294, RAC1295, RAC1296, RAC1297, RAC1298, RAC1299, RAC1300, RAC1301, RAC1302, RAC1303, RAC1304, RAC1305, RAC1306, RAC1307, RAC1308, RAC1309, RAC1310, RAC1311, RAC1312, RAC1313, RAC1314, RAC1315, RAC1316, RAC1317, RAC1318, RAC1319, RAC1320, RAC1321, RAC1322, RAC1323, RAC1324, RAC1325, RAC1326, RAC1327, RAC1328, RAC1329, RAC1330, RAC1331, RAC1332, RAC1333, RAC1334, RAC1335, RAC1336, RAC1337, RAC1338, RAC1339, RAC1340, RAC1341, RAC1342, RAC1343, RAC1344, RAC1345, RAC1346, RAC1347, RAC1348, RAC1349, RAC1350, RAC1351, RAC1352, RAC1353, RAC1354, RAC1355, RAC1356, RAC1357, RAC1358, RAC1359, RAC1360, RAC1361, RAC1362, RAC1363, RAC1364, RAC1365, RAC1366, RAC1367, RAC1368, RAC1369, RAC1370, RAC1371, RAC1372, RAC1373, RAC1374, RAC1375, RAC1376, RAC1377, RAC1378, RAC1379, RAC1380, RAC1381, RAC1382, RAC1383, RAC1384, RAC1385, RAC1386, RAC1387, RAC1388, RAC1389, RAC1390, RAC1391, RAC1392, RAC1393, RAC1394, RAC1395, RAC1396, RAC1397, RAC1398, RAC1399, RAC1400, RAC1401, RAC1402, RAC1403, RAC1404, RAC1405, RAC1406, RAC1407, RAC1408, RAC1409, RAC1410, RAC1411, RAC1412, RAC1413, RAC1414, RAC1415, RAC1416, RAC1417, RAC1418, RAC1419, RAC1420, RAC1421, RAC1422, RAC1423, RAC1424, RAC1425, RAC1426, RAC1427, RAC1428, RAC1429, RAC1430, RAC1431, RAC1432, RAC1433, RAC1434, RAC1435, RAC1436, RAC1437, RAC1438, RAC1439, RAC1440, RAC1441, RAC1442, RAC1443, RAC1444, RAC1445, RAC1446, RAC1447, RAC1448, RAC1449, RAC1450, RAC1451, RAC1452, RAC1453, RAC1454, RAC1455, RAC1456, RAC1457, RAC1458, RAC1459, RAC1460, RAC1461, RAC1462, RAC1463, RAC1464, RAC1465, RAC1466, RAC1467, RAC1468, RAC1469, RAC1470, RAC1471, RAC1472, RAC1473, RAC1474, RAC1475, RAC1476, RAC1477, RAC1478, RAC1479, RAC1480, RAC1481, RAC1482, RAC1483, RAC1484, RAC1485, RAC1486, RAC1487, RAC1488, RAC1489, RAC1490, RAC1491, RAC1492, RAC1493, RAC1494, RAC1495, RAC1496, RAC1497, RAC1498, RAC1499, RAC1500, RAC1501, RAC1502, RAC1503, RAC1504, RAC1505, RAC1506, RAC1507, RAC1508, RAC1509, RAC1510, RAC1511, RAC1512, RAC1513, RAC1514, RAC1515, RAC1516, RAC1517, RAC1518, RAC1519, RAC1520, RAC1521, RAC1522, RAC1523, RAC1524, RAC1525, RAC1526, RAC1527, RAC1528, RAC1529, RAC1530, RAC1531, RAC1532, RAC1533, RAC1534, RAC1535, RAC1536, RAC1537, RAC1538, RAC1539, RAC1540, RAC1541, RAC1542, RAC1543, RAC1544, RAC1545, RAC1546, RAC1547, RAC1548, RAC1549, RAC1550, RAC1551, RAC1552, RAC1553, RAC1554, RAC1555, RAC1556, RAC1557, RAC1558, RAC1559, RAC1560, RAC1561, RAC1562, RAC1563, RAC1564, RAC1565, RAC1566, RAC1567, RAC1568, RAC1569, RAC1570, RAC1571, RAC1572, RAC1573, RAC1574, RAC1575, RAC1576, RAC1577, RAC1578, RAC1579, RAC1580, RAC1581, RAC1582, RAC1583, RAC1584, RAC1585, RAC1586, RAC1587, RAC1588, RAC1589, RAC1590, RAC1591, RAC1592, RAC1593, RAC1594, RAC1595, RAC1596, RAC1597, RAC1598, RAC1599, RAC1600, RAC1601, RAC1602, RAC1603, RAC1604, RAC1605, RAC1606, RAC1607, RAC1

	<p>SMAD2, SMAD4, SMARCA4, SMARCB1, SMO, SNCAIP, SOCS1, SOX2, SOX9, SPEN, SPOP, SRC, STAG2, STAT3, STK11, SUFU, SYK, TEK, TBX3, TET2, TGFBR2, TIPARP, TNFAIP3, TNFRSF14, TP53, TSC1, TSC2, TYRO3, U2AF1, VEGFA, VHL, WHSC1, WHSC1L1, WT1, XRCC2, XPO1, ZNF217, ZNF703</p> <p>Hotspot mutations in AKT exon 3, BRAF exon 15, EGFR exon 12,18,19,20,21, HER2 (ERBB2) exon 17-21, 24, 26, FOXL2-gen exon 1, GNA11 exon 5, GNAQ exon 5, KIT exon 8-11, 13, 14, 17, 18, KRAS exon 2-4, MET exon 16, 18, 20 NRAS exon 1-4, PDGFRA exon 12, 14, 18, PIK3CA 9 en 20, RET exon 16, TP53 exon 1-11</p> <p>Relevant regions of genes B1.1, AKT1, ALK, APC, ATM, BRAF, CDH1, CDKN2A, CSF1R, CTNNB1, EGFR, ERBB2, ERBB4, EZH2, FBXW7, FGFR1, FGFR2, FGFR3, FLT3, GNA11, GNAQ, GNAS, HNF1A, HRAS, IDH1, IDH2, JAK2, JAK3, KDR, KIT, KRAS, MET, MLH1, MPL, NOTCH1, NPM1, NPM1, NRAS, PDGFRA, PIK3CA, POLE, PTEN, PTPN11, RBB1, RET, ROS1, SMAD4, SMARCB1, SMO, SRC, STK11, TP53, VHL</p>
<p>Trisuit tumor 15 kit (illumina, San Diego, CA, USA)</p> <p>Ampliseq Cancer hotspot panel v2 - SOC v1 (illumina, San Diego, CA, USA) (Standard of Care USA) (Standard of Care genes added by Antoni van Leeuwenhoek, Amsterdam, the Netherlands)</p> <p>Ampliseq Cancer hotspot panel v3 (Thermo Fisher, Watham, MA, USA)</p> <p>NGS Path v2D (Radboud UMC, Nijmegen, the Netherlands)</p>	<p>ARAF exon 7, 10, CTNNB1 exon 1, 2, 4, 7, 8, 12, 15, KRAS exon 2-4, HRAS exon 2, 3, NRAS exon 2-4, BRAF exon 11, 15, EGFR exon 2, 7, 15, 18-21, GNAQ exon 5, GNAS exon 8, 9, H3F3A exon 2, H3F3B exon 2, IDH1 exon 4, IDH2 exon 4, KIT exon 2, 9-18, YD88 exon 3b, 5, MUTYH exon 7,13, PDGFRA exon 12, 14, 15, 18, 23, PIK3CA exon 2, 5, 6-10, 14, 18 21, POLE exon 9, 11, 13, 14, RET exon 10-12, 15, 16, TP53 exon 1-11</p> <p>Hotspot mutations in ABL1, AKT1, ALK, APC, ATM, CARD11, CD79A, CD79B, CDH1, CDKN2A, CSF1R, CTNBB1, ERBB2, ERBB4, EZH2, FBXW7, FGFR1, FGFR2, FGFR3, FLT3, GNA11, HNF1A, JAK2, JAK3, KDR, MET, MLH1, MPL, NOTCH1, NPM1, PTEN, PTPN11, RBB1, SMAD4, SMARCB1, SMO, SRC, STK11, VHL</p> <p>Relevant regions of genes AKT1, AKT2, AKT3, ALK, ARAF, BRAF, DDR2, EGFR, ERBB2, GNAS, GNAQ, GNA11, HRAS, IDH1, IDH2, JAK2, KIT, KRAS, MAP2K1, MET, MTOR, NRAS, PDGFRA, PIK3CA, POLE, PTEN, RAF1, ROS1, TP53</p>

**Supplementary table S2. Case-series of BRAFV600E mutant colorectal cancer patients treated with double or triple targeted therapy inhibiting the MAPK pathway and genetic alterations at baseline, newly developed genetic alterations during treatment and at time of progression.**

Patient	Age (yrs)	Sex	Prior treatment lines	MSI status	Best response	Time on treatment (months)	Genetic alterations at baseline	Genetic alterations on treatment	Genetic alterations at progressive disease	Analytical method
9	68	F	2	MSS	SD	5	-	TP53 <sup>G293fs</sup>	TP53 <sup>G293fs</sup>	BL: AVL panel v1.0, TSACP v1.0 OT and PD: Ampliseq Cancer

Double combination: encorafenib+cetuximab

13	51	F	51	3		MSS	PR	1	AKT1 <sup>splice</sup> ERBB2 <sup>A689L</sup> ERBB2 <sup>655V</sup> KIT <sup>M541L</sup> TP53 <sup>H179R</sup>	NA	NA	hotspot panel v2- SOC v1 BL: TruSight tumor 15 kit OT and PD: NA
16	59	F	59	2		MSS	CR	15	TP53 <sup>H179R</sup> PIK3CA <sup>E542K</sup>	TP53 <sup>H179R</sup> PIK3CA <sup>E542K</sup> RNF43 <sup>sup</sup> KRAS <sup>G601pl</sup> EZH2 <sup>del</sup> CHECK2 <sup>loss</sup>	BL: TSACP v1.0 OT: Ampliseq Cancer hotspot panel v2- SOC v1 PD: Whole genome sequencing	
17	55	F	55	2		MSS	PR	4	TP53 <sup>splice</sup> KIT <sup>R634W</sup>	TP53 <sup>splice</sup> KIT <sup>R634W</sup>	BL: at least hotspot mutations in TP53, KRAS and BRAF OT: Ampliseq Cancer hotspot panel v2- SOC v1 PD: NA	
18	66	F	66	2		MSS	PD	2	APC <sup>S141L/A65*4</sup> TP53 <sup>T234A</sup>	NA	BL: AVL panel v1.1 and TSACP v1.0 OT and PD: NA	
20	66	F	66	3		MSI	SD	11	- EP300 <sup>P925T</sup> KDM5A <sup>R1157H</sup> PIK3CA <sup>R108H</sup> SF3B1 <sup>R831Q</sup> APC <sup>Q231S*</sup> CREBBP <sup>splice</sup> BRCA2 <sup>T2560fs*5</sup> CTNNA1 <sup>splice</sup> CTNNA1 <sup>fs43*</sup> SMARCA4 <sup>R8397*</sup> SMARCA4 <sup>G1478*</sup> FLT3 <sup>fs986fs*9+</sup> GATA3 <sup>fs437fs*9+</sup> MLH1 <sup>Y157fs*3</sup> PTCH1 <sup>fs1208fs6852</sup> TSC2 <sup>P1042fs+11</sup>	NA	BL: Oncocarta panel v1.0 OT: Foundation Medicine PD: NA	
21	65	F	65	2		NA	PR	14	-	PTEN <sup>loss</sup> RNF43 <sup>fs48T</sup>	BL: Oncocarta panel v1.0 OT and PD: Foundation	

22	61	M	1	MSS	PR	3	NA	<p><b>TP53<sup>E366fs*9</sup></b>  <b>SMAD4<sup>dupl</sup></b>  FGF14<sup>amp</sup>  IRS2<sup>amp</sup>  CDK8<sup>amp</sup>  FLT3<sup>amp</sup>  <b>TP53<sup>R273H</sup></b>  <b>Notch4<sup>Y1359fs*10+</sup></b>  MYC<sup>amp</sup>  PAX5<sup>v266</sup>  PRKDC<sup>fusion</sup></p>	<p><b>TP53<sup>E366fs*9</sup></b>  <b>SMAD4<sup>dupl</sup></b>  <b>TP53<sup>R273H</sup></b>  <b>Notch4<sup>C1360fs*102</sup></b>  MYC<sup>amp</sup>  RICTOR<sup>amp</sup>  FGF10<sup>amp</sup>  ARID1A<sup>trunc</sup>  KRAS<sup>G12R</sup>  FBXW7<sup>R465C</sup>  TP53<sup>M169fs*5</sup>  MCL1<sup>amp</sup>  RICTOR<sup>amp</sup>  FGF10<sup>amp</sup></p>	<p>Medicine  BL: NA  OT and PD: Foundation  Medicine</p>
23	63	M	2	NA	PR	26	NA	<p><b>FBXW7<sup>R465C</sup></b>  <b>TP53<sup>M169fs*5</sup></b>  MCL1<sup>amp</sup>  RICTOR<sup>amp</sup>  FGF10<sup>amp</sup>  PIK3CA<sup>H1047R</sup>  HGF<sup>amp</sup>  CDK6<sup>amp</sup></p>	<p>BL: NA  OT and PD: Foundation  Medicine</p>	
24	63	F	2	NA	SD	4	-	<p>FGF3  CREBBP<sup>Q1152*</sup>  NF1<sup>A2617V</sup>  BCORL1<sup>Y814*</sup>  BCORL1<sup>Q888fs*29</sup>  MLL2<sup>splice</sup>  MLL2<sup>N2977fs*13</sup>  RAD50<sup>R1200*</sup>  WT1<sup>Y2618</sup>  <b>CDK12<sup>G1461fs*31+</sup></b>  CIC<sup>P1116fs*45</sup>  MEN1<sup>R521fs*43</sup>  PBRM1<sup>F993fs*15</sup>  BCOR<sup>S336fs*45</sup>  BCORFL1<sup>Y814*</sup></p>	<p>NA  BL: Oncocarta panel v1.0  OT: Foundation Medicine PD:  NA</p>	

25	64	M	2	NA	PR	13	-	BCORFL1 <sup>Q888fs*29</sup> BRIP1 <sup>N1087fs*4</sup> FBXW7 <sup>R473fs*4</sup> EGFR <sup>V292L</sup> TP53 <sup>R213*</sup> PTEN <sup>loss</sup>	EGFR <sup>V292L</sup> TP53 <sup>R213*</sup> PTEN <sup>loss</sup> TP53 <sup>R175H</sup>	BL: at least KRAS and BRAF OT: Foundation Medicine PD: TSACP v1.0 BL: Foundation Medicine OT: NA PD: TSACP v1.0, NRAS codon 117 and 146 BL and PD: NA OT: Foundation Medicine
26	73	M	1	MSS	PR	10	TP53 <sup>R175H</sup> MUTYH <sup>G382D</sup> VEGFA <sup>amp1</sup> FGFR1 <sup>amp1</sup>	NA	NA	BL: Foundation Medicine OT: NA PD: TSACP v1.0, NRAS codon 117 and 146 BL and PD: NA OT: Foundation Medicine
29	62	M	3	NA	SD	15	NA	APC <sup>T1556fs*3</sup> APC <sup>L620fs*13</sup> FBXW7 <sup>R367*</sup> PIK3R1 <sup>K459del</sup> ASXL1 <sup>G645fs*58</sup> KDM5C <sup>G1504fs*40</sup> RB1 <sup>M484fs*8</sup>	NA	BL: Foundation Medicine OT: NA PD: TSACP v1.0, NRAS codon 117 and 146 BL and PD: NA OT: Foundation Medicine
33	64	F	1	NA	PR	12	TP53 <sup>R213*</sup> IRS <sup>amp1</sup> CDK8 <sup>amp1</sup> SPEN <sup>T448fs*25</sup> SPEN <sup>G1860fs*9</sup>	NA	NA	BL: Foundation Medicine OT and PD: NA
36	57	M	1	NA	PR	4	-	APC <sup>E1554*</sup> APC <sup>G661fs*12</sup> EPHA5 <sup>G287R</sup> TP53 <sup>G245S</sup> BCORL1 <sup>T63fs*53</sup>	NA	BL: Oncocarta panel v1.0 OT: Foundation Medicine PD: NA
43	60	F	1	NA	SD	3	CD79A <sup>R131fs*61</sup> CTCF <sup>A175T</sup> EGFR <sup>R776C</sup> EPHB4 <sup>A800T</sup> MLL3 <sup>K2797fs*26</sup> PIK3CA <sup>T104L</sup> PTCH1 <sup>G43E</sup> TP53 <sup>R273C</sup> TP53 <sup>splice</sup>	NA	NA	BL: Foundation Medicine OT and PD: NA

46	73	F	2	NA	SD	6	-	ARID1A <sup>G2765*87</sup> BAP1 <sup>V6*</sup> FAM123B <sup>E112*</sup> MLL2 <sup>R2235f*29</sup> SPEN <sup>T448f*25</sup> SPEN <sup>G1860f*9</sup> TSC2 <sup>splice</sup>	NA	NA	NA	BL: AVL panel v1.1 OT and PD: NA BL: Foundation Medicine OT and PD: NA BL: NRAS exon 2-4, BRAF exon 11, 15, KRAS exon 2-4 OT and PD: NA BL: NRAS exon 2-4, BRAF exon 11, 15, KRAS exon 2-4 OT and PD: NA BL: NRAS exon 2-4, BRAF exon 11, 15, KRAS exon 2-4 OT and PD: NA
50	52	F	1	NA	PD	1	GNAS <sup>G201H</sup> CDH1 <sup>R598*</sup>		NA	NA	NA	
51	54	F	3	MSS	SD	8	-		NA	NA	NA	
52	68	F	3	NA	PR	17	-		NA	NA	NA	
53	57	F	3	MSS	PD	3	-		NA	NA	NA	
Triple combination: encorafenib+cetuximab+binimetinib												
1	69	M	3	MSS	SD	26	NA	TP53 <sup>S1465f5</sup> APC <sup>G245D</sup>	TP53 <sup>S1465f5</sup> APC <sup>G245D</sup>	TP53 <sup>S1465f5</sup> APC <sup>G245D</sup>	TP53 <sup>S1465f5</sup> APC <sup>G245D</sup>	BL: NA OT: TSACP v1.0 PD: TSACP v1.0 BL: NRAS exon 4, codon 117 and 146, TSACP v1.0 OT: AVL panel v1.2, TSACP v1.0 PD: NA
2	47	F	3	MSS	SD	22	APC <sup>R1450*</sup> PIK3CA <sup>E545K</sup>	APC <sup>R1450*</sup> PIK3CA <sup>E545K</sup> PTEN <sup>R173C</sup> KRAS <sup>G12V</sup> PTEN <sup>R233*</sup>	APC <sup>R1450*</sup> PIK3CA <sup>E545K</sup> PTEN <sup>R173C</sup> KRAS <sup>G12V</sup> PTEN <sup>R233*</sup>	APC <sup>R1450*</sup> PIK3CA <sup>E545K</sup> PTEN <sup>R173C</sup> KRAS <sup>G12V</sup> PTEN <sup>R233*</sup>	APC <sup>R1450*</sup> PIK3CA <sup>E545K</sup> PTEN <sup>R173C</sup> KRAS <sup>G12V</sup> PTEN <sup>R233*</sup>	BL: TP53 exon 2-10, TSACP v1.0 OT: TSACP v1.0, NRAS exon 4, codon 117 and 146 PD: NA BL: TSACP v1.0, NRAS exon 4, codon 117 and 146 OT and PD: NA
3	45	M	2	MMS	PR	26	TP53 <sup>R175H</sup>	TP53 <sup>R175H</sup> APC <sup>C1502*</sup> KRAS <sup>G12A</sup> MET <sup>TempI</sup>	TP53 <sup>R175H</sup> APC <sup>C1502*</sup> KRAS <sup>G12A</sup> MET <sup>TempI</sup>	TP53 <sup>R175H</sup> APC <sup>C1502*</sup> KRAS <sup>G12A</sup> MET <sup>TempI</sup>	TP53 <sup>R175H</sup> APC <sup>C1502*</sup> KRAS <sup>G12A</sup> MET <sup>TempI</sup>	
4	46	F	2	MSS	PR	4	TP53 <sup>P151S</sup> APC <sup>I556f5</sup> SMAD4 <sup>G365D</sup>	TP53 <sup>P151S</sup> APC <sup>I556f5</sup> SMAD4 <sup>G365D</sup>	TP53 <sup>P151S</sup> APC <sup>I556f5</sup> SMAD4 <sup>G365D</sup>	TP53 <sup>P151S</sup> APC <sup>I556f5</sup> SMAD4 <sup>G365D</sup>	TP53 <sup>P151S</sup> APC <sup>I556f5</sup> SMAD4 <sup>G365D</sup>	

5	68	F	3		MSS	PR	8	-	NA	NA	NA	BL: AVL panel v1.2, TSACP v.0, NRAS exon 4, codon 117 and 146 OT and PD: NA BL: AVL panel v1.2 OT and PD: NA BL: AVL panel v1.2 OT and PD: NA BL: KRAS exon 2-4, BRAF exon 11, 15, NRAS exon 2-4 OT and PD: NA BL: Ampliseq Cancer hotspot panel v3- SOC v1 OT and PD: NA BL: KRAS exon 2-4, BRAF exon 11, 15, NRAS exon 2-4 BL and OT: Ampliseq Cancer hotspot panel v2- SOC v1 PD: NA BL and OT: AVL panel v1.2 PD: NA BL: TSACP v1.0 OT: NA PD: NGS Path v2D
6	56	F	3		MSS	SD	7	-	NA	NA	NA	BL: AVL panel v1.2 OT and PD: NA
7	60	M	2		MSS	SD	9	-	NA	NA	NA	BL: AVL panel v1.2 OT and PD: NA
8	65	F	2		NA	SD	10	-	NA	NA	NA	BL: KRAS exon 2-4, BRAF exon 11, 15, NRAS exon 2-4 OT and PD: NA
10	38	M	2		MSS	SD	12	SMAD4 <sup>A36H</sup>	NA	NA	NA	BL: Ampliseq Cancer hotspot panel v3- SOC v1 OT and PD: NA
11	67	F	2		MSS	PR	7	-	NA	NA	NA	BL: KRAS exon 2-4, BRAF exon 11, 15, NRAS exon 2-4
12	43	F	2		MSS	PD	3	-	TP53 <sup>D259Y</sup> SMAD4 <sup>D355V</sup>	NA	NA	BL and OT: Ampliseq Cancer hotspot panel v2- SOC v1 PD: NA
14	62	F	3		MSS	SD	8	-	-	NA	NA	BL and OT: AVL panel v1.2 PD: NA
15	74	M	2		MSS	PR	7	TP53 <sup>R282W</sup> APC <sup>R1450*</sup>	NA	TP53 <sup>R282W</sup> MTOR <sup>I1973F</sup>	TP53 <sup>R282W</sup> MTOR <sup>I1973F</sup>	BL: TSACP v1.0 OT: NA PD: NGS Path v2D
Triple combination: encorafenib + cetuximab + alpelisib												
19	60	F	1		MSS	SD	3	-	NA	NA	TP53 <sup>G245S</sup> APC <sup>E1554*</sup> APC <sup>C661fs*12</sup> EPhA5 <sup>G287R</sup> BCORL1 <sup>T631fs*53</sup>	BL: Colon AVL panel OT: NA PD: Foundation Medicine
27	75	M	2		NA	SD	31	-	-	-	-	BL, OT and PD: Colon AVL panel
28	70	F	2		NA	PR	5	-	NA	NA	NA	BL: Oncocarta panel v1.1 OT and PD: NA
30	64	M	2		NA	SD	4	TP53 <sup>R306*</sup> MYC <sup>ampI</sup> MYST3 <sup>ampI</sup>	NA	NA	NA	BL: Foundation Medicine OT and PD: NA

31	46	M	1	NA	PR	4	-	NA	APC <sup>T1556fs*3</sup> KRAS <sup>G12V</sup> STAT4 <sup>R320Q</sup> TP53 <sup>R213*</sup> PBRM1 <sup>S295fs*5</sup> PTEN <sup>loss</sup> SMAD2 <sup>loss</sup> NA	BL: Colon AVL panel OT: NA PD: Foundation Medicine
32	59	F	3	NA	SD	3	-	NA	NA	BL: Oncocarta panel v1.0 and TSACP v1.0 OT and PD: NA
34	69	F	2	MSS	SD	17	TP53 <sup>K132N</sup> GNAS <sup>F201H</sup> CCND3 <sup>ampl</sup>	NA	-	BL: Foundation Medicine OT: NA
35	63	F	2	NA	PR	5	TP53 <sup>R282W</sup> PTEN <sup>R130*</sup>	NA	NA	PD: AVL panel v1.2 BL: Foundation Medicine OT and PD: NA
37	65	F	1	MSS	SD	14	PIK3CA <sup>E542K</sup>	NA	PIK3CA <sup>E542K</sup> TP53 <sup>R282W</sup> SOX9 <sup>G375*</sup> APC <sup>H1791fs*7</sup> APC <sup>S1505fs*1</sup> NA	BL: AVL panel OT: NA PD: Foundation medicine
38	63	M	2	MSI	SD	3	-	NA	NA	BL: Colon AVL panel OT and PD: NA
39	69	F	2	MSI	SD	5	-	NA	NA	BL: KRAS exon 1, BRAF exon 15, EGFR exon 19, 21, PIK3CA exon 9, 20 OT and PD: NA
40	66	F	1	MSS	SD	10	-	NA	NA	BL: Oncocarta panel v1.0 OT and PD: NA
41	47	M	1	MSS	PR	10	APC <sup>C978*</sup> PBRM1 <sup>R298*</sup> TP53 <sup>L257R</sup> FBXW7 <sup>E327*</sup>	NA	NA	BL: Foundation Medicine OT and PD: NA
42	68	F	1	NA	PD	2	TP53 <sup>R306*</sup> PIK3CA <sup>Q546P</sup> ERBB2 <sup>ampl</sup> TOP2A <sup>ampl</sup> SMAD4 <sup>loss</sup>	NA	NA	BL: Foundation Medicine OT and PD: NA



44	59	M	1	NA	SD	2	BLM <sup>M515fs*16</sup> CCNE1 <sup>A410V</sup> CDH1 <sup>P126fs*89</sup> ERBB4 <sup>D861V</sup> GNAS <sup>R203C</sup> HNF1A <sup>P291fs*51</sup> MLL3 <sup>K2797fs*26</sup> ARID1A <sup>P225fs*175</sup> CREBBP <sup>P1946fs*30</sup> FLCN <sup>splice</sup> LRP1B <sup>K3773fs*26</sup> MLL2 <sup>A1390fs*27</sup> QKI <sup>K134fs*14</sup> RNF43 <sup>G659fs*41</sup> SLIT2 <sup>T415fs*21</sup>	NA	NA	NA	BL: Foundation Medicine OT and PD: NA
45	38	F	2	MSS	SD	6	PIK3CA <sup>E542K</sup> TP53 <sup>C176F</sup> MYC <sup>amp1</sup> RNF43 <sup>D96fs*62</sup>	NA	NA	BL: Foundation Medicine OT and PD: NA	
47	54	F	1	MSS	PR	5	CDH2 <sup>V491I</sup> FANCA <sup>A586T</sup> FLCN <sup>A324V</sup> TP53 <sup>splice</sup> TP53 <sup>D228fs*1</sup> MYST3 <sup>amp1</sup> CDKN2A <sup>oss</sup> CDKN2B <sup>loss</sup>	NA	NA	BL: Foundation Medicine, AVL panel v1.1 OT and PD: NA	
48	60	F	1	MSS	PR	5	PIK3CA <sup>H1047R</sup> APC <sup>E1353*</sup> APC <sup>E1554*</sup> PTEN <sup>Y188*</sup> TP53 <sup>I195T</sup>	NA	NA	BL: TSACP v1.0 OT and PD: NA	
49	67	F	1	MSS	PR	16	TP53 <sup>R175H</sup>	NA	NA	BL: TSACP v1.0 OT and PD: NA	

Abbreviations: yrs, years; MSI microsatellite instable; MSS, microsatellite stable; M, male; F, Female; SD, stable disease; BL, baseline; OT, on treatment; PD, progressive disease; †, no other genetic alterations than BRAFV600E; NA, no data available. Mutations in bold were analyzed at more than one time point.

¶These mutations were found in another lesion, which was progressive at time of biopsy, than the other reported mutations.



# CHAPTER 4

Combining pan-HER and  
MEK inhibitors for  
*KRAS* mutant solid tumors



# CHAPTER 4.1

Phase I study of the pan-HER inhibitor dacomitinib plus the MEK1/2 inhibitor PD-0325901 in patients with KRAS-mutation positive colorectal, non-small cell lung and pancreatic cancer

Sanne CFA Huijberts, Robin MJM van Geel, Emilie MJ van Brummelen, Ferry ALM Eskens, Filip YFL de Vos, Martijn PJK Lolkema, Lot A Devriese, Frans L Opdam, Serena Marchetti, Neeltje Steeghs, Kim Monkhorst, Bas Thijssen, Hilde Rosing, Alwin, DR Huitema, Jos H Beijnen, Rene Bernardts, Jan HM Schellens

## **Abstract**

### **Background**

Mutations in *KRAS* result in a constitutively activated MAPK pathway. In *KRAS* mutant tumors existing treatment options, e.g. MEK inhibition, have limited efficacy due to resistance through feedback activation of epidermal growth factor receptors (HER).

### **Methods**

In this phase I study, the pan-HER inhibitor dacomitinib, was combined with the MEK1/2 inhibitor PD-0325901 in patients with *KRAS* mutant colorectal, pancreatic and non-small cell lung cancer (NSCLC). Patients received escalating oral doses of once daily dacomitinib and twice daily PD-0325901 to determine the recommended phase II dose (RP2D).

(Clinicaltrials.gov: NCT02039336)

### **Results**

Eight out of 41 evaluable patients (27 colorectal cancer, 11 NSCLC, 3 pancreatic cancer) among 8 dose-levels experienced dose-limiting toxicities. The RP2D with continuous dacomitinib dosing was 15 mg dacomitinib plus 6 mg PD-0325901 (21 days on/7 days off), but major toxicity including rash (85%), diarrhea (88%) and nausea (63%) precluded long-term treatment.

Therefore, other intermittent schedules were explored, which only slightly improved toxicity. Tumor regression was seen in 8 patients with longest treatment duration (median 102 days) in NSCLC.

### **Conclusions**

Although preliminary signs of anti-tumor activity in NSCLC were seen, we do not recommend further exploration of this combination in *KRAS* mutant patients due to its negative safety profile.

## Introduction

The RAS-RAF-MEK-ERK (MAPK) pathway plays a pivotal role in the regulation of cell proliferation, survival and differentiation. Persistent activation of this pathway is frequently observed in human cancers and is associated with high rates of cancer cell proliferation. Commonly, pathway activation occurs as a consequence of oncogenic gain-of-function mutations in Kirsten rat sarcoma viral oncogene homolog (*KRAS*). The *KRAS* protein stimulates multiple downstream effector pathways, which are activated in a growth factor-independent way in cancer cells expressing oncogenic *KRAS*.(1-3) The high frequency of *KRAS* mutations in human cancers (~20%) makes these proteins a potential target for anti-tumor therapy. The frequency of *KRAS* mutations is particularly high in pancreatic cancer (90%), colorectal cancer (CRC) (45%) and non-small cell lung cancer (NSCLC) (35%).(1)

To date, with the exception of selective *KRAS*G12C inhibitors such as AMG510(4), therapeutic approaches targeting and blocking *KRAS* directly have been unsuccessful. Small molecule inhibitors against the downstream effectors of *KRAS*, such as MEK, demonstrated only limited anti-tumor activity in *KRAS* mutated (*KRAS*m) cancers as well.(2, 3, 5, 6)

Preclinical work from Sun and colleagues revealed that in *KRAS*m cancer cells, inhibition of MEK leads to feedback activation of upstream tyrosine kinase receptors, human epidermal growth factor receptor 2 (HER2) and 3 (HER3) in particular, causing intrinsic resistance through reactivation of the MAPK and phosphoinositide 3-kinase (PI3K) pathways.(7) Concurrent treatment with a MEK inhibitor and an inhibitor of multiple HER receptor subtypes (pan-HER inhibitor) completely suppressed this feedback activation and resulted in synergistic anti-tumor activity in *KRAS*m cells *in vitro* and in xenograft models.(7) As proof of concept was obtained in both *KRAS*m CRC and NSCLC models, we hypothesized that the anti-tumor activity of this approach would be independent of tumor histology. The unmet medical need for patients with *KRAS*m tumors and the high frequency of these mutations provided rationale to investigate the combination of a MEK and pan-HER inhibitor in humans.

In this phase I dose-finding study, we investigated the combination of dacomitinib, a potent irreversible ATP-competitive inhibitor of the HER kinase family (*in vitro* IC<sub>50</sub> values of 6.0 nM, 45.7 nM and 74 nM against the human catalytic domains of HER1, HER2 and HER4), with PD-0325901, a highly specific non-ATP-competitive inhibitor of MEK1 and MEK2, in patients with *KRAS*m CRC, NSCLC or pancreatic cancer. The primary study objective was to determine the recommended phase II dose (RP2D) and schedule. Secondary objectives included characterizing safety and tolerability, exploring anti-tumor activity, and assessing the pharmacokinetic profiles of dacomitinib and PD-0325901 when given concomitantly.

## Patients and Methods

### Patient population

This investigator-initiated, multi-center, open-label, phase I dose-escalation study enrolled patients at three sites in The Netherlands. Adult patients with histologically- or cytologically-confirmed advanced CRC, NSCLC or pancreatic cancer were enrolled on the basis of

documented *KRAS* mutations in exon 2, 3 or 4, and *PIK3CA* wildtype status. Methods for analyzing *KRAS* and *PIK3CA* status were analytically validated and assessments were performed by a trained pathologist. *PIK3CA* wildtype was required to avoid treatment resistance via activation of signaling proteins downstream of PIK3CA. Eligibility criteria included: Eastern Cooperative Oncology Group (ECOG) performance status of < 2, life expectancy of  $\geq 3$  months, measurable disease according to Response Evaluation Criteria In Solid Tumors (RECIST) version 1.1, adequate bone marrow (absolute neutrophil count  $\geq 1.5 \times 10^9/L$ , platelets  $\geq 100 \times 10^9/L$ , hemoglobin  $\geq 6.0$  mmol/L), hepatic (total bilirubin  $\leq 1.5 \times$  upper limit of normal [ULN], aspartate aminotransferase (AST) and alanine aminotransferase (ALT)  $\leq 2.5 \times$  ULN), and renal (serum creatinine  $\leq 1.5 \times$  ULN) functions. Radiotherapy, immunotherapy, chemotherapy or any treatment with investigational medication within four weeks prior to study treatment were not allowed, and patients with a history of other primary malignancies were excluded with the exception of patients who had been disease-free for  $\geq 3$  years or with completely resected non-melanoma skin cancer. Additional exclusion criteria included symptomatic or untreated leptomeningeal disease, symptomatic brain metastasis, history of interstitial lung disease or pneumonitis, history of retinal vein occlusion, and prior therapy containing targeted drug combinations known to interfere with EGFR, HER2, HER3, HER4 or MAPK- and PI3K-pathway components, including PI3K, AKT, mTOR, BRAF, MEK and ERK. The study was conducted in accordance with guidelines for Good Clinical Practice as defined by the International Conference on Harmonization. Regulatory authorities and the institutional review boards approved the study protocol and all amendments. All patients gave written informed consent, per Declaration of Helsinki recommendations.

The study was registered at ClinicalTrials.gov (NCT02039336). Pfizer Inc. funded this study and provided the investigational drugs dacomitinib and PD-0325901.

### **Study design and procedures**

Patients were treated at varying dose-levels of orally administered dacomitinib and PD-0325901 in cycles of 28 days. The starting doses were based on previous data from single agent phase I studies with both compounds, taking into account the potential for synergistic toxicity. Dose-level one consisted of 30 mg dacomitinib once daily (QD) continuously, which is 67% of the maximum tolerated dose and the recommended starting dose for EGFR-positive NSCLC as a single agent, and 2 mg PD-0325901 twice daily (BID) administered on the first 21 days of each 28-day cycle, which is 25% of its single agent recommended dose. Subsequently, PD-0325901 was escalated according to a classical 3 + 3 design with fixed maximum escalation increments. Dose-escalation decisions were based on safety evaluation of all evaluable patients, performed after completion of the first treatment cycle. Patients were considered evaluable for the dose-determining part of this study if at least one cycle of study treatment was completed, with the minimum safety evaluation conducted and at least one administration of both drugs received or if dose-limiting toxicity (DLT) had occurred during the first cycle. If one out of three patients experienced a DLT, the number



of patients treated at that dose-level was expanded to a maximum of six. Dose-escalation continued until a dose-level was reached at which no more than one out of six patients experienced DLT during the first 28 days of treatment, provided that the single agent recommended doses of both compounds were not exceeded. Patients were continuing study treatment until disease progression, unacceptable toxicity, or investigator/patient decision to discontinue.

Safety was monitored throughout the treatment by physical examination, laboratory assessments, electrocardiography, ophthalmic evaluation, and collection of adverse events. Adverse events were recorded according to Common Terminology Criteria for Adverse Events version 4.0. All adverse events that were possible, probable or definite related to study drug were considered as study treatment related. DLT was defined as an adverse event or laboratory abnormality occurring within the first treatment cycle meeting at least one of the criteria described in supplementary table S1.

Radiologic tumor measurements were performed using computed tomography (CT) scans at baseline and every 6 weeks throughout the study. After a protocol amendment, the frequency was changed to every 8 weeks. Tumor response was evaluated according to RECIST 1.1.(8) Patients were evaluable for anti-tumor activity if at least one follow-up radiologic evaluation was performed after the start of study treatment.

#### **Pharmacokinetic and pharmacodynamic analyses**

For pharmacokinetic analyses, serial blood samples were obtained from all patients prior to treatment administration on day one, and 1, 2, 3, 4, 6, 8, 12, 24, 72, and 144 hours after the first dose. On day one of cycle 2, blood samples were drawn before and 1, 2, 3, 4, 6, 8, 12 and 24 hours after administration. Plasma samples were assayed using a validated high-performance liquid chromatography tandem mass spectrometry method (HPLC-MS/MS). Briefly, dacomitinib and PD-0325901 were extracted from plasma by protein precipitation with a mixture of acetonitrile/methanol (1:1 v/v). Compounds were chromatographically separated using a Waters Xbridge BEH Phenyl column (50 x 2.1 mm ID, 5 µm particle size) and detection was performed using an API4000 tandem mass spectrometer equipped with a turbo ion spray interface, operating in the positive ion mode. Transitions from m/z 480 to 329 and m/z 489 to 255 were monitored for the detection of dacomitinib and PD-0325901, respectively. Stable isotope labelled internal standards were used for the quantification. The lower and upper limits of quantification were respectively 0.5 and 50 ng/ml for dacomitinib, and 5 and 500 ng/ml for PD-0325901. Pharmacokinetic parameters were calculated in R using an in-house developed validated script for non-compartmental pharmacokinetic analyses (version 3.6.0).(9)

During the study, the protocol was amended to allow incorporation of tumor biopsies for pharmacodynamic analyses. Biopsies were taken before treatment, in the second week of treatment and upon treatment discontinuation. Phosphorylated (p) ERK and ribosomal pS6 (pS6-r) levels were assessed by validated immunohistochemistry (IHC) staining methods and semi-quantitative H-scores (percentage of positive cells (0–100) multiplied by staining

intensity (0–3)) were assessed by an independent pathologist who was blinded for sample identification. Tumour biopsy samples were fixed in formalin for 16–24 hours and embedded in paraffin subsequently. Immunohistochemistry of formalin-fixed paraffin-embedded tumour samples was performed on a BenchMark Ultra autostainer (Ventana Medical Systems). Briefly, paraffin sections were cut at 3 µm, heated at 75°C for 28 minutes and deparaffinised in the instrument with EZ prep solution (Ventana Medical Systems). Heat-induced antigen retrieval was carried out using Cell Conditioning 1 (CC1, Ventana Medical Systems) at 95°C for 32 and 64 minutes, for pS6-r and pERK1/2, respectively. pS6-r was detected using clone D68F8 (1:1000 dilution, 32 minutes at room temperature, Cell Signalling) and phospho-p44/42 MAPK (pERK1/2) (Thr202/Tyr204) using clone D13.14.4E (1:400 dilution, 1 hour at room temperature, Cell Signalling). pERK was detected using the UltraView Universal DAB Detection Kit (Ventana Medical Systems), while detection of pS6-r was performed using the OptiView DAB Detection Kit (Ventana Medical Systems). Slides were counterstained with hematoxylin.

### **Statistical analysis**

Pharmacokinetics, pharmacodynamics, safety and tumor response data were reported descriptively.

## **Results**

### **Patient disposition and characteristics**

Between April 2014 and April 2018, 41 patients (27 (66%) with CRC, 11 (27%) with NSCLC and three (7%) with pancreatic cancer) were enrolled onto this study. The majority of patients had *KRAS* exon 2 mutations and were pretreated with at least two lines of antineoplastic therapy for advanced disease (table 1). One patient with CRC did not wish to receive any antineoplastic therapy before enrollment, which was allowed per protocol. Thirty-eight patients were evaluable for dose-determination (figure 1); three patients were considered not evaluable due to clinical deterioration, patient refusal and mistakenly administration of the wrong dose. At end of study all (n=41) patients had discontinued treatment due to progressive disease (n=30), adverse events (n=7), clinical deterioration/lack of benefit (n=3), or patient refusal (n=1).

**Table 1. Patient and disease characteristics at baseline.**

	Patients (n = 41)	
Sex, n (%)		
Female	22	(54%)
Male	19	(46%)
Age, median (range), years	62	(43–81)
Tumour types, n (%)		
Colorectal	27	(66%)
Non-small cell lung	11	(27%)
Pancreatic	3	(7%)
ECOG PS, n (%)		
0	16	(39%)
1	25	(61%)
Number of prior lines of therapy, n (%)		
0	1	(2%)
1	7	(17%)
2	13	(32%)
≥ 3	20	(49%)
KRAS mutation, n (%)		
Exon 2	36	(88%)
Exon 3	3	(7%)
Exon 4	2	(5%)

Abbreviations: ECOG PS, Eastern Cooperative Oncology Group performance status; KRAS, Kirsten rat sarcoma viral oncogene homolog.

### Dose finding

At the first dose-level consisting of 30 mg QD dacomitinib plus 2 mg BID PD-0325901 (21 days on/7 days off), three out of six patients experienced DLTs, being grade 3 increased AST/ALT, grade 3 fatigue, and inability to receive at least 75% of the planned dose due to grade 2 fatigue and diarrhea (figure 1). Therefore, we decided to continue with a reduced dacomitinib dose of 15 mg in a continuous dosing schedule to allow for escalation of PD-0325901. In the subsequent dose-levels with continuous administration of dacomitinib, DLTs were reported in two out of 21 patients; grade 3 AST/ALT increase (dose-level 2) and grade 3 skin rash (dose-level 5), respectively (figure 1). Although the formal RP2D was not reached, the escalation of PD-0325901 was halted in view of the increasing number of multiple grade 2 adverse events (e.g. diarrhea, nausea, fatigue) beyond the DLT window of 28 days, together with the emergence of ocular toxicity at dose-level 5 (including retinopathy grade 1, retinal detachment grade 1 and grade 2 and dry eyes grade 1). The latter with knowing the potential of more severe ocular toxicity at higher PD-0325901 doses.(10-12) Consequently, the established maximum dose-level with continuous dacomitinib dosing consisted of 15 mg dacomitinib QD plus 6 mg PD-0325901 BID. Subsequently, other intermittent regimens were initiated with the aim of optimizing drug exposure and tolerability. A slight increase in exposure to dacomitinib was intended with dose-level 6 consisting of 30 mg dacomitinib QD 4 days on/3 days off for 28 days, and PD-0325901 6 mg BID for 21 days. No DLTs were observed at this dose-level, which allowed further escalation of dacomitinib to 30 mg QD 5 days on /2 days off. In view of patient

convenience, it was decided to use a 5 days on /2 days off regimen for both agents which should increase the exposure of dacomitinib with the same dose. Out of three patients, two experienced DLTs consisting of grade 2 neuropathy leading to treatment delay of >7 days and inability to receive 75% of the planned doses in one patient, and dyspnea grade 3 in the other patient.

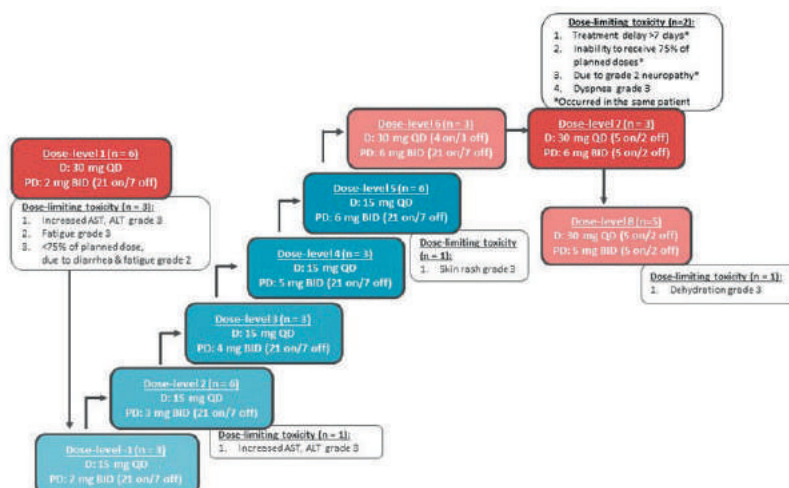


**Figure 1. Dose-escalation cohorts and dose-limiting toxicities.**

Abbreviations: D, dacomitinib; PD, PD-0325901; QD, once daily; BID, twice daily; AST, aspartate transaminase; ALT, alanine transaminase; n, number of patients.

This warranted dose de-escalation. Because a 5 days on /2 days off regimen was considered preferential, this regimen was maintained and PD-0325901 was de-escalated to 5 mg PD-0325901 BID combined with 30 mg dacomitinib QD in dose-level 8. One DLT (dehydration grade 3) was observed and apart from this event the dose-level was otherwise also not tolerable due to several grade 1 and 2 toxicities, most likely related to MEK inhibition with PD-0325901. The combination of dacomitinib and PD-0325901 was considered as too toxic and therefore not feasible in this relatively frail patient population.

### Safety

Study treatment-related adverse events were reported in all patients, with the most common being maculopapular and papulopustular rash (85%), diarrhea (88%), nausea (63%), vomiting (41%) and fatigue (34%) (table 2). Supportive care, including minocycline and cetomacrogol cream or class I corticosteroid cream were sufficient to manage skin rash, with the exception of one patient in dose-level 5 who had to discontinue treatment due to dose-limiting skin rash. The most frequent grade 3 events were diarrhea (20%), nausea (12%), and fatigue (10%). Treatment interruption was caused by diarrhea in five patients, by

nausea in three patients, by rash in three patients and by fatigue in two patients. In all other cases, supportive care was sufficient to decrease the severity to grade 1 or less.

Eye toxicities included grade 1 retinopathy, dry eyes grade 1, watering eyes grade 1, retinopathy grade 1 and retinal detachment grade 1 and 2 which occurred in four patients in dose-levels 1, 5 and 6. All patients could continue study treatment without further progression of ocular toxicity. Cases of retinal vein occlusion were not observed in this study.

### Pharmacokinetic analysis

Pharmacokinetic parameters after the first dose and at steady-state are summarized in the supplementary data (table S2). PD-0325901 and dacomitinib exposure increased approximately dose-proportionally with moderate and high inter-patient variability, respectively (figure 2). The half-life of dacomitinib could not be accurately calculated by non-compartmental analysis, due to its long terminal half-life. The long half-life and the high variability was known from previous studies and was also reflected in our results.<sup>(12)</sup> The mean dacomitinib peak plasma concentration ( $C_{max}$ ) and area under the plasma concentration-time curve from time 0 to 24 hours ( $AUC_{0-24h}$ ) increased approximately 3- to 5-fold after multiple dosing indicating extensive accumulation. A slight increase in AUC and  $C_{max}$  was also observed for PD-0325901 after multiple doses indicating minimal accumulation, which is in agreement with the relative short half-life (mean 7.7 hours, range 5.0 – 9.9). Figure 2 shows the plasma-concentration time curves per dose-level.

### Anti-tumor activity

Thirty-six patients were evaluable for anti-tumor activity (figure 3); five patients did not reach the first radiological evaluation due to clinical deterioration (n=1), adverse events (n=2), patient refusal (n=1) or insufficient treatment (n=1). Out of the evaluable patients, 20 achieved stable disease (including one patient with CRC and no prior treatment lines) and 16 had progressive disease on their first evaluation scan (n=36). Tumor regression was seen in eight patients (18%) treated at various dose-levels 1, 3, 5, 6 and 8 (figure 3A). Out of the eight evaluable patients with NSCLC, six achieved tumor regression within the limits of stable disease according to RECIST v1.1 criteria and one had no change in target lesion volume as best response.

**Table 2. Treatment-related adverse events, occurring in > 10% of patients.**

Adverse Event, n (%)	Dose-level -1 (n = 4)		Dose-level 1 (n = 6)		Dose-level 2 (n = 6)		Dose-level 3 (n = 3)		Dose-level 4 (n = 3)		Dose-level 5 (n = 8)		Dose-level 6 (n = 3)		Dose-level 7 (n = 3)		Dose-level 8 (n = 5)		Total (n = 41) All dose-levels	
	Gr 1/2	Gr 3	Gr 1/2	Gr 3	Gr 1/2	Gr 3	Gr 1/2	Gr 3	Gr 1/2	Gr 3	Gr 1/2	Gr 3	Gr 1/2	Gr 3	Gr 1/2	Gr 3	Gr 1/2	Gr 3		
Dacomitinib QD PP-0925904/BID																				
Any skin toxicity*	3 (7%)		5 (12%)	1 (2%)	6 (15%)		3 (7%)		3 (7%)		5 (12%)	1 (2%)	3 (7%)		3 (7%)		4 (10%)		37 (90%)	
Rash	3 (7%)		5 (12%)	1 (2%)	6 (15%)		3 (7%)		3 (7%)		4 (10%)	1 (2%)	3 (7%)		2 (5%)		4 (10%)		35 (85%)	
Dry skin			3 (7%)		1 (2%)						2 (5%)		1 (2%)		1 (2%)		1 (2%)		9 (22%)	
Skin fissures			2 (5%)				2 (5%)												4 (10%)	
PPE	1 (2%)				1 (2%)		1 (2%)		1 (2%)		2 (5%)								6 (15%)	
Diarrhea	4 (10%)		6 (15%)	2 (5%)	4 (10%)		1 (2%)	1 (2%)	1 (2%)		4 (10%)	3 (7%)	1 (2%)	1 (2%)	3 (7%)		3 (7%)	1 (2%)	36 (88%)	
Nausea	4 (10%)		2 (5%)	1 (2%)	1 (2%)	1 (2%)	2 (5%)		2 (5%)	1 (2%)	5 (12%)	1 (2%)	2 (5%)		3 (7%)		3 (7%)	1 (2%)	26 (63%)	
Vomiting	3 (7%)		2 (5%)		2 (5%)		2 (5%)		2 (5%)		5 (12%)	1 (2%)					1 (2%)		17 (41%)	
Fatigue	1 (2%)		3 (7%)	1 (2%)	1 (2%)	1 (2%)	1 (2%)		1 (2%)		3 (7%)			1 (2%)	1 (2%)				14 (34%)	
Anorexia	1 (2%)		3 (7%)		1 (2%)		1 (2%)		1 (2%)		3 (7%)				2 (5%)				12 (29%)	
CPK increased			1 (2%)		2 (5%)		1 (2%)		1 (2%)		2 (5%)	2 (5%)	2 (5%)						10 (24%)	
ALT/AST increased			3 (7%)	1 (2%)	1 (2%)	1 (2%)			1 (2%)		1 (2%)	1 (2%)	1 (2%)						9 (22%)	
Mucositis	2 (5%)		1 (2%)		1 (2%)		1 (2%)		1 (2%)		2 (5%)	2 (5%)	2 (5%)		2 (5%)				11 (27%)	
Eye toxicity*			3 (7%)						1 (2%)		2 (5%)	2 (5%)	2 (5%)						8 (20%)	
Alopecia			3 (7%)				1 (2%)		1 (2%)		5 (12%)	1 (2%)							5 (12%)	
Dry mouth			2 (5%)				1 (2%)		1 (2%)		1 (2%)				1 (2%)				5 (12%)	

All adverse events that are possible, probable or definite related to study drug were considered as study treatment related. \*Some patients experienced one or more skin toxicities, only one was counted for the combined group of any toxicity \* includes neurosensory detachment, blurred vision, retinopathy, cataract and dry eyes. Abbreviations: QD, once daily; BID, twice daily; ALT/AST, alanine/aspartate transaminase; 4/3, 4 days on / 3 days off; 5/2, 5 days on/2 days off; CPK, creatine phosphokinase; PPE, palmar plantar dyesthesia syndrome.

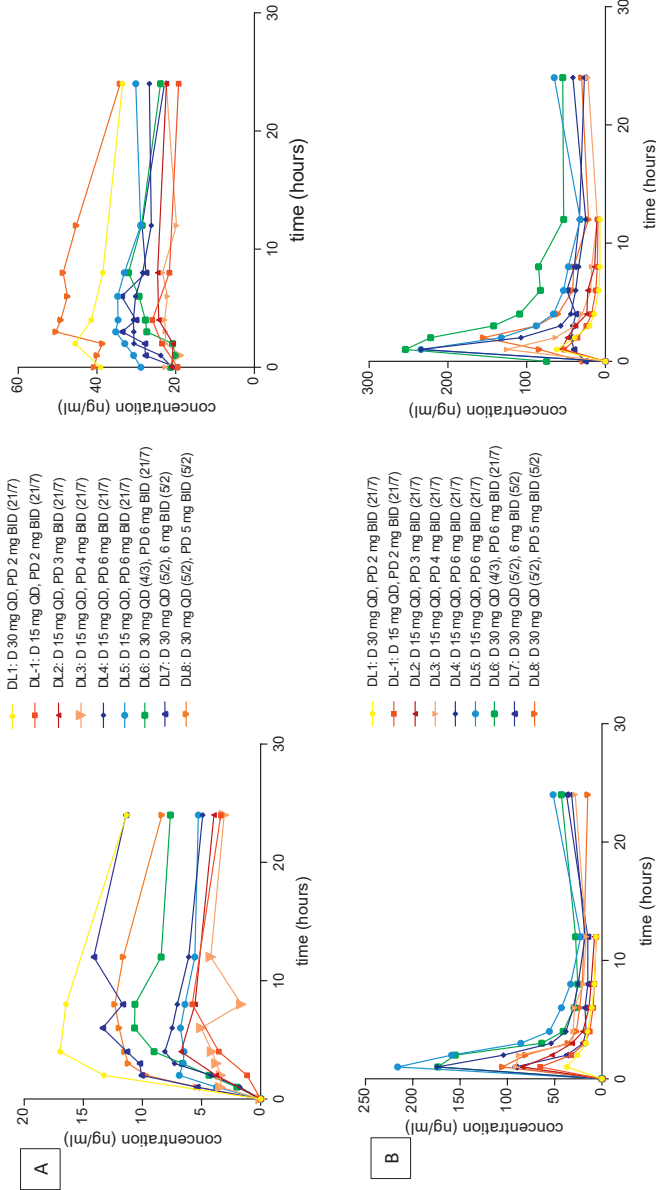


**Figure 2. Pharmacokinetic profiles of dacomitinib and PD-0325901.**

All figures: Plasma concentration time curves of mean plasma levels per dose-level

Abbreviations: DL dose-level; 21/7 21 days on, 7 days off; 4/3 4 days on, 3 days off; 5/2 5 days on/2 days off.

A. Dacomitinib per dose-level: cycle 1 day 1 (left) and cycle 2 day 1 or the last day of concomitant use of both drugs for intermittent dosing (right).

B. PD-0324901 per dose-level: cycle 1 day 1 (left) and cycle 2 day 1 or the last day of concomitant use of both drugs for intermittent dosing (right).

The overall median treatment duration was 90 days (range 3–469). Patients with NSCLC achieved the longest median treatment duration, 102 days (range 14–239), versus 87 days (range 3–469) for patients with CRC and 73 days (42–96) for patients with pancreatic cancer. Median treatment duration was the longest in the dose-levels that contained 30 mg dacomitinib. In dose-level 1 with 30 mg dacomitinib and 2 mg PD-0325901, treatment duration was the longest (239 days, range 42–469), followed by dose-level 6 (dacomitinib 30 mg 4 days on/3 days off and PD-0325901 6 mg [79 days, range 49–96]) and 8 (dacomitinib 30 mg and PD-0325901 5 mg, both 5 days on /2 days off [77 days, range 43–134]) (figure 3B; n=36).

### Pharmacodynamic analyses

Tumor biopsies were taken from seven patients at baseline and from four patients also on-treatment (figure S1). In two patients from whom a paired biopsy was available, pERK was decreased whereas from two other patients pERK was increased during treatment. Reduction would be expected based on the mechanism of action of the drug combination. Only one of these two patients was evaluable for response and showed progressive disease. For one of the two patients with an increase in pERK, the biopsy was taken after four days of study treatment interruption, which may explain the lack of pERK modulation. In the other patient, the formalin-fixation of the baseline biopsy was delayed whereas direct fixation was desired. This delay might have caused degradation of phosphorylated proteins. These deviations will be discussed further in the next section.

Besides pERK staining, pS6 staining was also performed on tumor biopsies. However, pS6 staining results have to be interpreted with caution, because the quality of this staining could not be assured due to the lack of reliable controls. For this reason, pS6 staining results were not taken into account during the pharmacodynamic analyses of this clinical trial.

### Discussion

In this phase I study we investigated the combination of the MEK inhibitor PD-0325901 with the pan-HER inhibitor dacomitinib in patients with *KRAS*<sup>mut</sup> NSCLC, CRC and pancreatic cancer. Based on preliminary efficacy results of the current trial and two comparable trials exploring the same treatment strategy, it was decided to limit recruitment to patients with *KRAS*<sup>mut</sup> NSCLC in December 2016. At that moment recruitment was ongoing in the dose expansion cohort of dose-level 7.

Dose escalation was discontinued due to major toxicities in both continuous and intermittent dosing schedules. A rapid decline in performance status and poor overall tolerability played a major role in this. Furthermore, lack of efficacy was the second reason for the decision to discontinue enrollment.



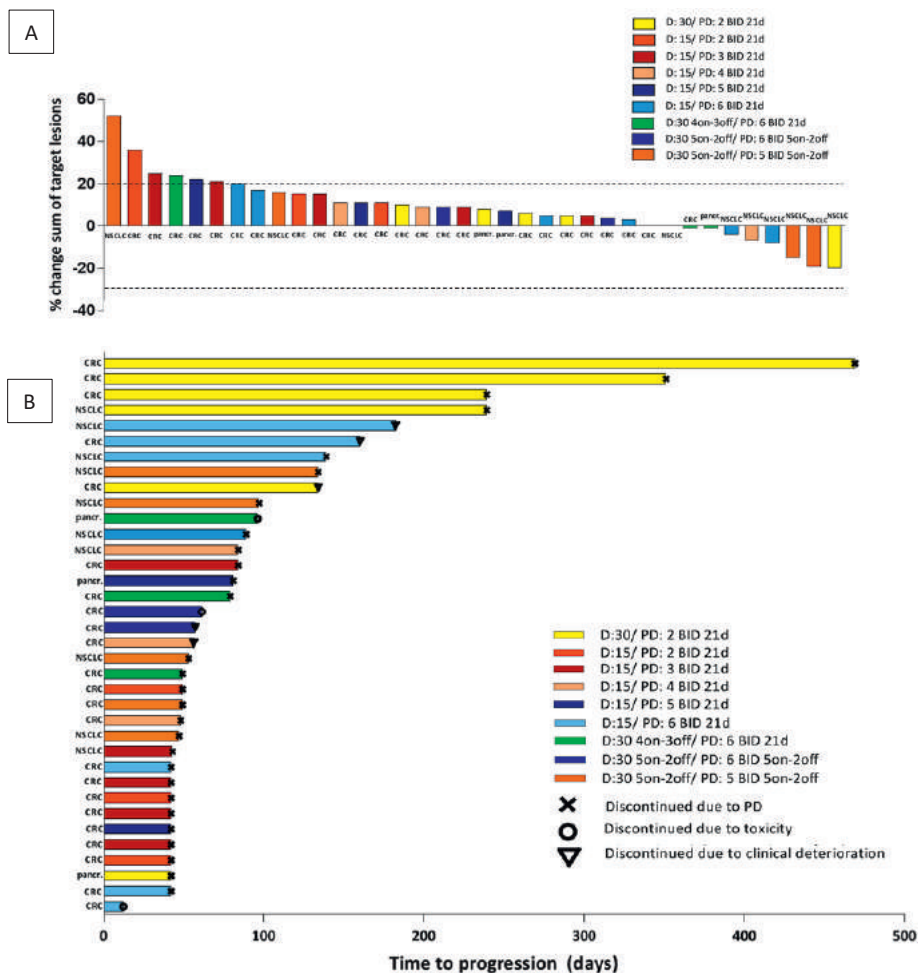


**Figure 3. Anti-tumor activity of dacomitinib and PD-0325901 in KRASm CRC, NSCLC and pancreatic cancer.**

A. Maximum percentage change in sum of target lesion size from baseline, including responses assessed by RECIST, by dose-level.

B. Swimmer plot of treatment duration, by dose-level. Symbols at the end of each bar represent the reason for end of treatment for each individual patient.

Abbreviations: D, dacomitinib; PD, PD-0325901; BID, twice daily; CRC, colorectal cancer; NSCLC, non-small cell lung cancer; pancr., pancreatic cancer; 21d, 21 days on, 7 days off; 4on-3off, 4 days on, 3 days off; 5on-2off, 5 days on/2 days off; PD progressive disease.

Our study data showed that combining dacomitinib with PD-0325901 in a continuous or intermittent dosing schedule was not tolerated for the majority of patients. In a previous phase I dose-escalation study, PD-0325901 doses up to 20 mg BID in a continuous dosing schedule, 30 mg BID in a 21 days on / 7 days off schedule, and 10 mg in a 5 days on / 2 days off schedule have been investigated. Although formal RP2Ds were established at 15 mg BID

and 10 mg BID in continuous and 5 days on / 2 days off schedules, respectively, the occurrence of ocular toxicity, retinal vein occlusion in particular, decided us to reconsider the RP2D.(10) As dacomitinib shows potential overlapping toxicity with PD-0325901, starting doses for both agents were 25-70% of their monotherapy doses, being 2 mg PD-0325901 BID in a 21 days on / 7 days off schedule and 30 mg dacomitinib QD. Although relatively low, these doses demonstrated target engagement and clinical activity in their respective single agent studies.(10-12) Nevertheless, the initial dose-level was already not tolerated as indicated by DLTs in three out of six patients. Given the relatively low dose of PD-0325901 in relation to its single agent maximum-tolerated dose, toxicity was likely to be associated with dacomitinib in particular. Therefore, the dacomitinib dose was reduced to enable dose-escalation of PD-0325901, as we hypothesized that robust MEK inhibition was necessary to block the KRAS-activated MAPK pathway before tumor cells activate their escape mechanism through upstream tyrosine kinase receptors.(7) Because ocular toxicity, i.e. asymptomatic central serous retinopathy, emerged at the 5 mg and 6 mg dose-levels, we halted dose escalation at 6 mg and established the RP2D with continuous dacomitinib dosing at 15 mg dacomitinib QD plus 6 mg PD-0325901 BID 21 days on / 7 days off. At doses of 5 and 6 mg, the plasma concentration of PD-0325901 exceeded the target level (16.5 ng/ml), consistent with target inhibition based on xenograft mouse models,(13) during the entire dose interval (figure 2B). However, at 15 mg dacomitinib doses, the plasma concentration did not exceed the preclinical target of 22 ng/ml, which is the IC<sub>50</sub> for HER2/HER3 inhibition (unpublished data), for a substantial number of patients. Therefore, after determination of the RP2D with continuous dacomitinib dosing, intermittent dosing schedules were initiated in an effort to optimize exposure and preserve tolerability. Dacomitinib 30 mg QD 4 days on / 3 days off combined with PD-0325901 6 mg BID 21 days on / 7 days off was better tolerated, but in view of therapy compliance it was decided to further explore a 5 days on / 2 days off regimen. Due to one DLT (dehydration grade 3) and multiple grade 1 and 2 toxicities in two additional patients, this dose-level was considered intolerable. The combination of dacomitinib and PD-0325901 in a dose exceeding target levels was considered not manageable in these frail lung cancer patients. Pharmacokinetic parameters of both agents were in line with previously reported single agent data. Our data show no signs of pharmacokinetic interactions between the two agents.(10, 12)

Unfortunately, pERK modulation in relation to tumor response data could only be assessed in one patient. Despite pERK reduction, this patient showed progressive disease. This could mean that target engagement was insufficient for anti-tumor response, in terms of duration or magnitude.

Patients with metastatic *KRAS*<sup>m</sup> tumors represent a population with a high unmet medical need. Multiple strategies to target KRAS have been explored, including farnesyltransferase inhibitors, small molecules interfering with the prenyl-binding protein PDE $\delta$ -KRAS interaction, and small molecules targeting downstream effectors of KRAS, e.g. RAF, MEK, or PI3K. However, none of these approaches has been successful.(2, 14, 15) Since all these

strategies rely on targeting a single protein or pathway, rapid onset of resistance due to tumor escape mechanisms exploiting alternative pathways is to be expected.(16) Therefore, combination strategies may have a more sustained anti-tumor effect. Previously, van Geel *et al.* demonstrated clinical proof of concept for combining BRAF and EGFR inhibition in patients with *BRAF* mutant CRC,(17) based on a synthetic lethality drug screen.(18) The BEACON CRC phase III trial investigating the combination of BRAF and EGFR inhibition with or without a MEK inhibitor also showed favorable results.(19) Similarly, in *KRASm* cells, inhibition of MEK was found to synergize with HER2 and HER3 inhibition in an identical screen to identify synthetic lethal interactions.(7) However, in contrast to these preclinical observations, the preliminary clinical activity with dacomitinib plus PD-0325901 in *KRASm* tumors was relatively disappointing. Toxicity restricted combining full single agent doses, leading to a lower exposure, which potentially limits clinical anti-tumor activity.

Another explanation for the limited anti-tumor activity of this combination may lie in the extensive inter-pathway connections of the *KRAS* protein. Although we excluded patients with concurrent *KRAS* and *PIK3CA* mutations, activation of the PI3K pathway may as well be triggered by mutated *KRAS* directly, particularly in the presence of downstream MEK inhibition.(20) Additionally, reactivation of the MAPK pathway may occur as well, analogous to the observation with *BRAF* inhibition in *BRAF* mutant CRC cells,(21) especially when upstream receptors are not adequately inhibited. Indeed, although this concerns a small cohort, patients treated with doses of 30 mg dacomitinib had disease stabilization for a longer period of time compared to patients on dose-levels containing 15 mg dacomitinib (figure 3B).

Interestingly, six out of eight patients (75%) with NSCLC achieved tumor regression, compared to one out of 24 patients (4%) with CRC (figure 3A). In addition, the median treatment duration in patients with NSCLC (102 days) was longer than that of CRC patients (87 days), suggesting a difference in sensitivity to study treatment between these malignancies (figure 3B). This finding was also reflected in the results of two separate studies. Höchster *et al.* showed that adding a MEK inhibitor to second line irinotecan therapy in patients with *KRASm* CRC did not result in clinical benefit.(22) However, patients with *KRASm* NSCLC had an improved response rate by the addition of the MEK inhibitor selumetinib to second line treatment with docetaxel as reported by Jänne *et al.*, although no significant effect on progression-free survival and overall survival was observed.(5)

To explain differences in sensitivity between tumor types, several biomarkers will be explored in a translational study on paired tumor biopsies from patients with *KRASm* tumors treated with three different combinations of pan-HER inhibitors and MEK inhibitors in this phase I trial and 2 other clinical trials. In the translational study, analyses will include at least the following biomarkers; HER3, heregulin, BCL-XL, *KRAS* mutant to *KRAS* wildtype allele frequency ratio, *KRAS* copy number, *KRAS* expression levels and the nature of the *KRAS* mutation.

In conclusion, dacomitinib could only be combined safely with PD-0325901 in a continuous or intermittent dosing schedule at doses much lower than the recommended single agent

doses. Toxicity prevented continuous dosing of dacomitinib and PD-0325901. Although preliminary signs of anti-tumor activity in NSCLC were seen, defining a dose and regimen with manageable (long-term) toxicity was not feasible. Therefore, it is not recommended to further explore the combination of dacomitinib and PD-0325901 in *KRAS*<sup>M</sup> NSCLC patients.

## **Additional information**

### **Ethics approval and consent to participate**

The study was approved by the accredited Medical Ethics Committee of the NKI-AVL. All substantial protocol amendments were also approved by the same Medical Ethics Committee. The principles of the Declaration of Helsinki and the Medical Research Involving Human Subject Act (WMO) have been followed in this protocol and it is compliant to ICH-GCP. Patients were registered by the trial office of the NKI-AVL after informed consent is given. The study was registered at ClinicalTrials.gov (NCT02039336).

### **Consent for publication**

Neither the whole nor any part of the results of the study carried out under this protocol will be published or passed on to any third party without written consent of the sponsor of this study. All authors of this manuscript and involved pharmaceutical companies gave consent for publication.

### **Data availability**

The clinical datasets analysed during this clinical trial are available from the corresponding author on reasonable request and only if anonymization of patient data can be fully ensured.

### **Conflict of interest**

JB and JS (partly) hold a patent on oral taxane formulations, are shareholders and part-time employees of Modra Pharmaceuticals, a spin out company developing oral taxanes. Not related to the manuscript. All other authors declare that they have no conflict of interest related to this study.

### **Funding**

Pfizer Inc. funded this study and provided the investigational drugs dacomitinib and PD-0325901.

### **Author's contributions**

The preclinical work was done by RB. RG and JS have written the clinical study protocol in collaboration with RB and JB. EB, RG, SH coordinated the clinical study. ML, FV, SH, LD, FE, FO, SM, JS and NS were principal or sub-investigators in the participating centers. Pharmacodynamic analysis was performed by KM and pharmacokinetic analyses by BT, HR and AH. EB, RG and SH were in charge of final analyses of all the available data. The

manuscript was written by EB, RG and SH and all authors reviewed and approved the manuscript.

### **Acknowledgements**

We thank all patients for participation, the clinical research units of Erasmus Medical Center Rotterdam, University Medical Center Utrecht and the Antoni van Leeuwenhoek hospital – Netherlands Cancer Institute Amsterdam for conduct of the trial and Pfizer Inc. for providing study drugs and an unrestricted grant.

## References

1. Downward J. Targeting RAS signalling pathways in cancer therapy. *Nature reviews cancer*. 2003;3(1):11-22.
2. Adjei AA, Cohen RB, Franklin W, Morris C, Wilson D, Molina JR, et al. Phase I pharmacokinetic and pharmacodynamic study of the oral, small-molecule mitogen-activated protein kinase kinase 1/2 inhibitor AZD6244 (ARRY-142886) in patients with advanced cancers. *Journal of clinical oncology*. 2008;26(13):2139-46.
3. Migliardi G, Sassi F, Torti D, Galimi F, Zanella ER, Buscarino M, et al. Inhibition of MEK and PI3K/mTOR suppresses tumor growth but does not cause tumor regression in patient-derived xenografts of RAS-mutant colorectal carcinomas. *Clinical cancer research*. 2012;18(9):2515-25.
4. Canon J, Rex K, Saiki AY, Mohr C, Cooke K, Bagal D, et al. The clinical KRAS(G12C) inhibitor AMG 510 drives anti-tumour immunity. *Nature*. 2019;575(7781):217-23.
5. Janne PA, van den Heuvel MM, Barlesi F, Cobo M, Mazieres J, Crino L, et al. Selumetinib plus docetaxel compared with docetaxel alone and progression-free survival in patients with KRAS-mutant advanced non-small cell lung cancer: The SELECT-1 randomized clinical trial. *Jama*. 2017;317(18):1844-53.
6. Janne PA, Shaw AT, Pereira JR, Jeannin G, Vansteenkiste J, Barrios C, et al. Selumetinib plus docetaxel for KRAS-mutant advanced non-small-cell lung cancer: a randomised, multicentre, placebo-controlled, phase 2 study. *The Lancet oncology*. 2013;14(1):38-47.
7. Sun C, Hobor S, Bertotti A, Zecchin D, Huang S, Galimi F, et al. Intrinsic resistance to MEK inhibition in KRAS mutant lung and colon cancer through transcriptional induction of ERBB3. *Cell reports*. 2014;7(1):86-93.
8. Eisenhauer EA, Therasse P, Bogaerts J, Schwartz LH, Sargent D, Ford R, et al. New response evaluation criteria in solid tumours: revised RECIST guideline (version 1.1). *European journal of cancer*. 2009;45(2):228-47.
9. R Core Team. R: A language and environment for statistical computing. R Foundation for Statistical Computing. Vienna, Austria. 2014. <http://www.r-project.org/>.
10. LoRusso PM, Krishnamurthi SS, Rinehart JJ, Nabell LM, Malburg L, Chapman PB, et al. Phase I pharmacokinetic and pharmacodynamic study of the oral MAPK/ERK kinase inhibitor PD-0325901 in patients with advanced cancers. *Clinical cancer research*. 2010;16(6):1924-37.
11. Haura EB, Ricart AD, Larson TG, Stella PJ, Bazhenova L, Miller VA, et al. A phase II study of PD-0325901, an oral MEK inhibitor, in previously treated patients with advanced non-small cell lung cancer. *Clinical cancer research*. 2010;16(8):2450-7.
12. Janne PA, Boss DS, Camidge DR, Britten CD, Engelman JA, Garon EB, et al. Phase I dose-escalation study of the pan-HER inhibitor, PF299804, in patients with advanced malignant solid tumors. *Clinical cancer research*. 2011;17(5):1131-9.
13. Mansour SJ, Matten WT, Hermann AS, Candia JM, Rong S, Fukasawa K, et al. Transformation of mammalian cells by constitutively active MAP kinase kinase. *Science*. 1994;265(5174):966-70.
14. Samatar AA, Poulidakos PI. Targeting RAS-ERK signalling in cancer: promises and challenges. *Nature reviews drug discovery*. 2014;13(12):928-42.
15. Baines AT, Xu D, Der CJ. Inhibition of Ras for cancer treatment: the search continues. *Future medicinal chemistry*. 2011;3(14):1787-808.
16. Bernards R. A missing link in genotype-directed cancer therapy. *Cell*. 2012;151(3):465-8.
17. van Geel R, Tabernero J, Elez E, Bendell JC, Spreafico A, Schuler M, et al. A Phase Ib dose-escalation study of encorafenib and cetuximab with or without alpelisib in metastatic BRAF-mutant colorectal cancer. *Cancer discovery*. 2017;7(6):610-9.
18. Prahallad A, Sun C, Huang S, Di Nicolantonio F, Salazar R, Zecchin D, et al. Unresponsiveness of colon cancer to BRAF(V600E) inhibition through feedback activation of EGFR. *Nature*. 2012;483(7387):100-3.

19. Kopetz S, Grothey A, Yaeger R, Van Cutsem E, Desai J, Yoshino T, et al. Encorafenib, binimetinib, and cetuximab in BRAF V600E-mutated colorectal cancer. *The New England journal of medicine*. 2019.
20. Engelman JA, Chen L, Tan X, Crosby K, Guimaraes AR, Upadhyay R, et al. Effective use of PI3K and MEK inhibitors to treat mutant Kras G12D and PIK3CA H1047R murine lung cancers. *Nature medicine*. 2008;14(12):1351-6.
21. Corcoran RB, Ebi H, Turke AB, Coffee EM, Nishino M, Cogdill AP, et al. EGFR-mediated re-activation of MAPK signaling contributes to insensitivity of BRAF mutant colorectal cancers to RAF inhibition with vemurafenib. *Cancer discovery*. 2012;2(3):227-35.
22. Hochster HS, Uboha N, Messersmith W, Gold PJ, BH ON, Cohen D, et al. Phase II study of selumetinib (AZD6244, ARRY-142886) plus irinotecan as second-line therapy in patients with K-RAS mutated colorectal cancer. *Cancer chemotherapy and pharmacology*. 2015;75(1):17-23.

## Supplemental data

**Table S1. Criteria for defining dose-limiting toxicities in 4 categories, including hematologic, non-hematologic, cardiac and other toxicities.**

Toxicity	DLT definition
Hematologic	<ul style="list-style-type: none"> <li>Grade 4 neutropenia for <math>\geq 5</math> days</li> <li>Grade <math>\geq 3</math> febrile neutropenia</li> <li>Grade 4 anemia</li> <li>Grade 4 thrombocytopenia</li> </ul>
Non-hematologic	<ul style="list-style-type: none"> <li>AST <math>&gt; 5X</math> ULN OR, ALT <math>&gt; 3X</math> ULN AND bilirubin <math>&gt; 2X</math> ULN (after exclusion of disease progression and/or bile duct obstruction)</li> <li>Grade <math>\geq 4</math> rash, hand-foot syndrome or photosensitivity</li> <li>Grade 3 rash, hand-foot syndrome or photosensitivity for <math>&gt; 7</math> days despite adequate supportive treatment.</li> <li>Grade <math>\geq 3</math> nausea, vomiting or diarrhea in the presence of maximal supportive care</li> <li>Grade <math>\geq 2</math> peripheral sensory or motor neuropathy</li> <li>Grade <math>\geq 3</math> clinically significant non-hematologic toxicity other than those listed above, with the following exceptions:               <ul style="list-style-type: none"> <li>Electrolyte disturbances that respond to correction within 24 hours</li> <li>Grade 3 hypertension that is adequately controlled by the addition of up to 2 additional antihypertensive medications</li> <li>Grade 3 pyrexia that does not result in study discontinuation</li> </ul> </li> </ul>
Cardiac	<ul style="list-style-type: none"> <li>Ejection fraction <math>&lt;</math> lower limit of normal (LLN) with an absolute decrease of <math>&gt;10\%</math> from baseline with confirmation within 14 days</li> </ul>
Other	<ul style="list-style-type: none"> <li>Inability to receive <math>\geq 75\%</math> of scheduled doses in treatment period due to toxicity related to study treatment</li> <li>Treatment delay of <math>&gt; 7</math> days due to study treatment-related toxicity</li> <li>Grade <math>\geq 2</math> toxicity that occurs beyond 28 days which in the judgment of the investigator is a DLT</li> </ul>

Abbreviations: AST, aspartate aminotransferase; ALT, alanine aminotransferase; ULN, upper limit of normal; LLN, lower limit of normal; DLT, dose limiting toxicity

**Figure S1. Pharmacodynamic effects of dacomitinib and PD-0325901.**

The pERK intensity scores (H-scores) of tumor biopsies at baseline and on-treatment (day 15) are presented as determined by immunohistochemistry staining.

Abbreviations: D, dacomitinib; PD, PD-0325901; BID, twice daily; CRC, colorectal cancer; NSCLC, non-small cell lung cancer; 5/2 5 days on/2 days off.

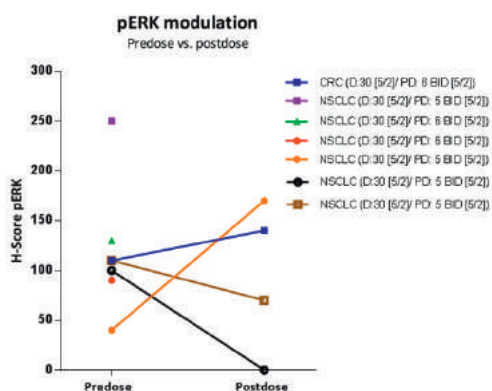




Table S2. Pharmacokinetic parameters of dacomitinib and PD-0325901, at baseline and steady-state, per dose-level.

Dose-level	1	2	3	4	5	6	7	8	All 15 mg doses	All 30 mg doses
Dacomitinib QD	30 mg	15 mg	15 mg	15 mg	15 mg	30 mg (4/3)	30 mg (5/2)	30 mg (5/2)		
PD-0325901 BID	2 mg	3 mg	4 mg	5 mg	6 mg	6 mg	6 mg (5/2)	5 mg (5/2)		
Dacomitinib	Cycle 1 Day 1									
Mean (CV%)	n = 6	n = 4	n = 2	n = 3	n = 8	n = 3	n = 3	n = 5	All 15 mg doses	
C <sub>max</sub> (ng/ml)	19.2 (52)	7.9 (43)	2.5 (48)	8.5 (11)	11.4 (74)	11.1 (23)	19.1 (38)	14.2 (19)	n = 23	n = 17
t <sub>max</sub> (h)	7.5	5.6	12	4.7	7.9	7.3	13.3	6.6	8.6 (69)	16.0 (44)
AUC <sub>0-24h</sub> (ng* h/ml)	318 (50)	126 (40)	45 (37)	137 (17)	136 (60)	159 (36)	290 (47)	200 (46)	7.6	8.3
Dacomitinib	Cycle 2 Day 1*									
Mean (CV%)	n = 6	n = 3	n = 2	n = 3	n = 5	n = 1	n = 2	n = 2	All 6 mg doses	
C <sub>max</sub> (ng/ml)	47.4 (71)	26.3 (76)	25.7 (18)	33.5 (47)	37.3 (33)	32.0	37.5 (44)	55.9 (9)	n = 18	n = 11
t <sub>max</sub> (h)	7.6	11	2	5	4.4	8.0	4.5	4.5	31.2 (49)	51.7 (45)
AUC <sub>0-24h</sub> (ng* h/ml)	888 (70)	513 (75)	262 (11)	654 (40)	747 (43)	647	658 (38)	789 (44)	7.2	4.8
PD-0325901	Cycle 1 Day 1									
Mean (CV%)	n = 6	n = 4	n = 2	n = 3	n = 8	n = 3	n = 3	n = 4	All 6 mg doses	
C <sub>max</sub> (ng/ml)	68.7 (32)	43.7 (59)	106.5 (5)	179 (83)	262 (30)	192 (32)	192 (32)	134 (80)	n = 14	n = 14
t <sub>max</sub> (h)	1.2	1.3	2	1.4	1.4	1.3	1.3	1.5	227 (43)	1.5
AUC <sub>0-12h</sub> (ng* h/ml)	188 (20)	160 (20)	452 (46)	552 (55)	822 (32)	635 (17)	635 (17)	463 (63)	706 (41)	
PD-0325901	Cycle 2 Day 1*									
Mean (CV%)	n = 6	n = 3	n = 2	n = 4	n = 5	n = 1	n = 2	n = 2	All 6 mg doses	
C <sub>max</sub> (ng/ml)	58.3 (28)	47.7 (38)	125 (61)	229 (68)	242 (27)	254	56 (17)	155 (23)	n = 6	n = 6
t <sub>max</sub> (h)	1.5	1.1	1	1	1.2	1	4.5	2	217 (25)	2.2
AUC <sub>0-12h</sub> (ng* h/ml)	210 (10)	145 (92)	376 (33)	638 (65)	855 (35)	1341	406 (24)	667 (33)	954 (36)	

\* Samples taken on cycle 2 day 1 or for intermittent dosing on the last day of concomitant use of both drugs.

Abbreviations: C<sub>max</sub>, peak plasma concentration; t<sub>max</sub>, time of maximum plasma concentration observed; AUC<sub>0-24h</sub>, area under the plasma concentration-time curve from time zero to 24 hours; T<sub>1/2</sub>, elimination half-life; N/C, could not be calculated; 4/3, 4 days on / 3 days off; 5/2, 5 days on / 2 days off.



# CHAPTER 4.2

Phase I study of lapatinib plus trametinib in patients with *KRAS* mutant colorectal, non-small cell lung and pancreatic cancer

Sanne CFA Huijberts, Robin MJM van Geel, Emilie MJ van Brummelen, Frans L Opdam, Serena Marchetti, Neeltje Steeghs, Saskia Pulleman, Bas Thijssen, Hilde Rosing, Kim Monkhorst, Alwin DR Huitema, Jos H Beijnen, Rene Bernards, Jan HM Schellens

## **Abstract**

### **Purpose**

*KRAS* oncogene mutations cause sustained signaling through the MAPK pathway. Concurrent inhibition of MEK, EGFR and HER2 resulted in complete inhibition of tumor growth in *KRAS* mutant (*KRAS*<sup>m</sup>) and *PIK3CA* wildtype tumors, *in vitro* and *in vivo*. In this phase I study, patients with advanced *KRAS*<sup>m</sup> and *PIK3CA* wildtype colorectal cancer (CRC), non-small cell lung cancer (NSCLC) and pancreatic cancer, were treated with combined lapatinib and trametinib to assess the recommended phase 2 regimen (RP2R).

### **Methods**

Patients received escalating doses of continuous or intermittent once daily (QD) orally administered lapatinib and trametinib, starting at 750 mg and 1 mg continuously, respectively.

### **Results**

Thirty-four patients (16 CRC, 15 NSCLC, 3 pancreatic cancer) were enrolled across six dose-levels and eight patients experienced dose-limiting toxicities, including grade 3 diarrhea (n=2), rash (n=2), nausea (n=1), multiple grade 2 toxicities (n=1), and aspartate aminotransferase elevation (n=1) resulting in the inability to receive 75% of planned doses (n=2) or treatment delay (n=2). The RP2R with continuous dosing was 750 mg lapatinib QD plus 1 mg trametinib QD and with intermittent dosing 750 mg lapatinib QD and trametinib 1.5 mg QD 5 days on/2 days off. Regression of target lesions was seen in six of the twenty-four patients evaluable for response, with one confirmed partial response in NSCLC. Pharmacokinetic results were as expected.

### **Conclusion**

Lapatinib and trametinib could be combined in an intermittent dosing schedule in patients with manageable toxicity. Preliminary signs of anti-tumor activity in NSCLC have been observed and pharmacodynamic target engagement was demonstrated.

## Introduction

Approximately 20% of all human cancers carry mutations in the *KRAS* oncogene, including 90% of pancreatic cancers, 45% of colorectal cancers (CRC), and 35% of non-small cell lung cancers (NSCLC).(1) *KRAS* gain-of-function mutations cause continuous activation of the mitogen-activated protein kinase (MAPK) pathway, resulting in the development and progression of malignant cells. The high frequency of *KRAS* mutations in three of the most lethal tumor types makes targeting of these mutated proteins with small molecule tyrosine kinase inhibitors an attractive treatment strategy. However, despite extensive efforts over the past decades, with the exception of *KRAS*<sup>G12C</sup> selective inhibitors (NCT03600883), effective *KRAS* inhibitors have not yet reached the clinic.(2, 3) An alternative approach to target *KRAS*-driven tumors comprises inhibition of downstream effectors of *KRAS*, such as MEK or ERK. Although MEK inhibitors were found to be among the most active agents against *KRAS* mutant (*KRAS*m) cell lines, their effect was mostly cytostatic rather than cytotoxic, and the anti-tumor activity in xenograft models and patients has been limited.(4-6)

The underlying mechanism of intrinsic resistance to MEK inhibitors was elucidated by Sun *et al.* who demonstrated that upon MEK inhibition, MYC-dependent transcriptional upregulation of the human epidermal growth factor receptor (HER) 3 takes place. Subsequently, reactivation of downstream signaling pathways results in sustained activation of multiple tumorigenic mechanisms. As HER3 requires formation of heterodimers with the epidermal growth factor receptor (EGFR) or HER2 in order to activate downstream signaling, inhibition of EGFR and HER2 in addition to MEK was sufficient to obtain synergistic anti-tumor activity *in vitro* and in xenograft models.(7) These findings provided a rationale for clinical evaluation of such a combination of targeted agents.

Therefore, a phase I dose-finding study was initiated, in which the dual EGFR/HER inhibitor lapatinib and the MEK inhibitor trametinib were combined in patients with advanced *KRAS*m colorectal cancer, non-small cell lung cancer or pancreatic cancer with the aim of defining the recommended phase II regimen (RP2R) and the most tolerable regimen. Patients with *PIK3CA* mutations were excluded to avoid treatment resistance via the PI3K-pathway. Lapatinib is an ATP-competitive dual tyrosine kinase inhibitor targeting EGFR and HER2, approved as standard of care for inhibiting HER2 activity in HER2-positive breast cancer.(8-10) Trametinib is a reversible, highly selective, allosteric MEK1 and MEK2 inhibitor, approved for the treatment of patients with unresectable or metastatic *BRAFV600* mutant melanoma in combination with a BRAF inhibitor.(11, 12) Furthermore, trametinib is approved in combination with the BRAF inhibitor dabrafenib for the treatment of *BRAFV600E* mutant non-small cell lung cancer.(13)

Here we present the results of the phase 1 clinical study with orally administered lapatinib and trametinib in *KRAS*m CRC, NSCLC and pancreatic cancer.

## Materials and methods

### Patient population

In this investigator-initiated, single-center, open label phase I study, patients with histologically- or cytologically-confirmed advanced CRC, NSCLC or pancreatic cancer and a documented *KRAS* exon 2, 3 or 4 mutation and *PIK3CA* wild type were included. Eligible patients were 18 years or older, had an Eastern Cooperative Oncology performance status of 0 or 1, had a life expectancy  $\geq 3$  months, had measurable disease per Response Evaluation Criteria in Solid Tumors (RECIST) v1.1, and had adequate bone marrow (absolute neutrophil count  $\geq 1.5 \times 10^9/L$ , platelets  $\geq 100 \times 10^9/L$ , hemoglobin  $\geq 6.0$  mmol/L) and organ function (total bilirubin  $\leq 1.5 \times$  upper limit of normal [ULN], aspartate aminotransferase and alanine aminotransferase  $\leq 2.5 \times$  ULN, serum creatinine  $\leq 1.5 \times$  ULN). Any treatment within four weeks prior to the first dose of study treatment was not allowed. Patients with symptomatic or untreated leptomeningeal disease were excluded, as well as patients with symptomatic brain metastasis, history of interstitial lung disease, pneumonitis or retinal vein occlusion, and patients previously treated with combinations of targeted agents known to interfere with EGFR, HER2, HER3, HER4 or MAPK- and PI3K-pathway components, including BRAF, MEK, ERK, PI3K, AKT and mTOR. The study protocol and all amendments were approved by regulatory authorities and the medical ethics committee of the Netherlands Cancer Institute. All patients gave written informed consent per Declaration of Helsinki recommendations. In December 2016, the study protocol was amended to restrict inclusion to NSCLC patients only, based on emerging preclinical and clinical evidence on preferential activity in this tumor type.

The study was registered at ClinicalTrials.gov (NCT02230553). GlaxoSmithKline Inc. and Novartis Pharma Inc. funded this study and provided study medication.

### Study design and procedures

The primary objective of this trial was to determine the recommended phase 2 regimen (RP2R) of combined lapatinib plus trametinib. Secondary objectives included characterizing safety and tolerability, assessing preliminary anti-tumor activity and pharmacodynamic effects, and evaluating the pharmacokinetic parameters of lapatinib and trametinib when given concomitantly. For this aim, patients were assigned to dose-levels with varying lapatinib and trametinib doses starting at approximately 50% of their monotherapy doses, which is 750 mg lapatinib once daily (QD) and 1 mg trametinib QD, accounting for potentially synergistic toxicities. Since the bioavailability of lapatinib and trametinib is food dependent, patients were instructed to take lapatinib and trametinib with a large glass of water in the morning at least 1 hour before or 2 hours after a meal at approximately the same time each day. Food intake within 1 hour after study drug administration was prohibited.

Dose-escalation followed an alternate escalation schedule with fixed increments according to a classical 3 + 3 design. Intra-patient dose-escalation was not allowed. Dose escalation decisions were based on the occurrence of dose-limiting toxicity (DLT) during the first 28

days (cycle one). Patients were considered evaluable for DLT if at least 75% of the assigned lapatinib and trametinib doses were administered in cycle one, or if a DLT had occurred. The RP2R was defined as the dose at which no more than one out of six patients experienced a DLT during treatment cycle one. After assessing the RP2R of lapatinib plus trametinib at continuous dosing schedules, the protocol was amended to initiate intermittent dosing schedules in order to optimize the exposure and tolerability. Previous publications substantiate that intermittent dosing of lapatinib or trametinib monotherapy might reduce toxicity without a substantial decrease in exposure and efficacy.(14-17)

Study treatment was continued until disease progression, unacceptable treatment-related toxicity despite supportive measures and dose modifications, or investigator/patient decision to withdraw study consent.

Safety evaluations were performed at baseline and throughout the study and included physical examination, vital signs, routine laboratory assessments, electrocardiography, ophthalmic examination, and multi-gated acquisition (MUGA) scans to assess the left ventricular ejection fraction (LVEF). Adverse events were recorded according to Common Terminology Criteria for Adverse Events version 4.0. DLTs were defined as adverse events or laboratory abnormalities occurring within the first 28 days of study treatment that meet at least one of the criteria described in supplementary table S1. Tumor response was assessed radiographically according to RECIST version 1.1. For the first twenty-two patients this was done every six weeks. After a protocol amendment, tumor response was assessed every eight weeks. Patients were evaluable for efficacy if at least one follow-up radiographic evaluation was performed.

#### **Pharmacokinetic and pharmacodynamic analysis**

For pharmacokinetic analyses, extensive blood sampling was performed in all patients. Serial blood samples were taken on the first day of cycle one and cycle two predose and 0.5, 1, 2, 4, 6, 8, and 24 hours after dosing. Plasma was isolated and stored at -80°C until analysis. Analysis was performed using a validated high-performance liquid chromatography tandem mass spectrometry (HPLC-MS/MS) method. Briefly, lapatinib and trametinib were extracted from plasma by protein precipitation with a mixture of acetonitrile/methanol (1:1 v/v). Compounds were chromatographically separated using a Waters Xbridge BEH Phenyl column (50 x 2.1 mm ID, 5 µm particle size) and detection was performed using an API4000 tandem mass spectrometer equipped with a turbo ion spray interface, operating in the positive ion mode. Transitions from m/z 581 to 365 and m/z 616 to 491 were monitored for the detection of lapatinib and trametinib, respectively. Stable isotopically labelled internal standards were used for the quantification. The lower and upper limits of quantification were respectively 0.5 and 50 ng/mL for trametinib, and 50 and 5000 ng/mL for lapatinib. Pharmacokinetic parameters were calculated in R using an in-house developed validated script for non-compartmental pharmacokinetic analyses (version 3.6.0).(18) Data points below the lower limit of quantification (LLOQ) were imputed as LLOQ/2, which means for trametinib 0.25 ng/ml and for lapatinib 25 ng/ml.

For pharmacodynamic analyses, tumor biopsies were taken before treatment, in the second week of treatment and if feasible upon treatment discontinuation. Phosphorylated (p) ERK and ribosomal pS6 (pS6-r) levels were measured by validated immunohistochemistry (IHC) staining methods and semi-quantitative H-scores (percentage of positive cells (0–100) multiplied by staining intensity (0–3)) were assessed by an independent pathologist who was blinded for sample identification. Tumor biopsy samples were fixed in formalin for 16–24 hours and embedded in paraffin subsequently. Immunohistochemistry of formalin-fixed paraffin-embedded tumor samples was performed on a BenchMark Ultra autostainer (Ventana Medical Systems). Briefly, paraffin sections were cut at 3 µm, heated at 75°C for 28 minutes and deparaffinised in the instrument with EZ prep solution (Ventana Medical Systems). Heat-induced antigen retrieval was carried out using Cell Conditioning 1 (CC1, Ventana Medical Systems) at 95°C for 32 and 64 minutes, for pS6-r and pERK1/2, respectively. pS6-r was detected using clone D68F8 (1:1000 dilution, 32 minutes at room temperature, Cell Signalling) and p-p44/42 MAPK (pERK1/2) (Thr202/Tyr204) using clone D13.14.4E (1:400 dilution, one hour at room temperature, Cell Signalling). pERK was detected using the UltraView Universal DAB Detection Kit (Ventana Medical Systems), while detection for pS6-r was performed using the OptiView DAB Detection Kit (Ventana Medical Systems). Slides were counterstained with hematoxylin.

### **Statistical analysis**

Patient characteristics, efficacy and safety data were summarized using descriptive statistics. A paired t-test was used to determine the statistical significance of the pharmacodynamic modulation (i.e. pERK and pS6-r) in tumor tissue taken before study start and while on treatment. A linear regression analysis was performed to explore the correlation between exposure of lapatinib and trametinib in terms of AUC on cycle one day one and pERK modulation.

## **Results**

### **Patient disposition and characteristics**

In total, 34 patients were enrolled in the study across six different dose-levels; 16 patients with CRC, 15 patients with NSCLC and three patients with pancreatic cancer. The majority of these patients (n=32) had a mutation in *KRAS* exon 2 (codon 12 or 13), and two patients had an exon 4 (codon 146) *KRAS* mutation. The specific mutated codons per different exon are described in table 1. Among the tumor types, G12D mutations occurred most frequently in NSCLC and CRC, while all three pancreatic cancer patients had different mutations (G12D, G12V and G12R). The majority of patients had been pretreated with at least two prior lines of therapy for metastatic disease (table 1). All patients had discontinued study treatment, 23 patients due to progressive disease, six due to adverse events, four due to patient refusal and one patient due to symptomatic deterioration.



**Table 1. Patient and disease characteristics at baseline.**

	Patients (n = 34)
Sex, n (%)	
Female	14 (41%)
Male	20 (59%)
Age, mean (range), years	60 (43–76)
Tumor types, n (%)	
Colorectal	16 (47%)
Non-small cell lung	15 (44%)
Pancreatic	3 (9%)
ECOG PS, n (%)	
0	19 (56%)
1	15 (44%)
Number of prior treatment lines, n (%)	
1	5 (15%)
2	18 (53%)
≥ 3	11 (32%)
KRAS mutation, n (%)	
Exon 2	32 (94%)
p.G12D	9 (26%)
p.G12V	6 (18%)
p.G12A	6 (18%)
p.G12C	5 (14%)
p.G13D	2 (6%)
p.G12R	2 (6%)
p.G12S	1 (3%)
p.G13C	1 (3%)
Exon 3	0
Exon 4	2 (6%)
p.A146V	2 (6%)

Abbreviations: ECOG PS, Eastern Cooperative Oncology performance status; KRAS, Kirsten rat sarcoma viral oncogene homolog

### Dose finding

Out of the 34 patients, 28 were evaluable for DLT. The five non-evaluable patients discontinued early (n=3) due to patient refusal, received less than 75% of the administrations planned in cycle 1 (n=2) due to adverse events not related to treatment or had toxicities from which the relationship to study medication could not be properly assessed (n=1). Dose-limiting toxicities were not observed in the first cohort of three patients on dose-level 1 (750 mg lapatinib QD, 1 mg trametinib QD), allowing escalation of trametinib. However, in the subsequent dose-level 2 comprising 750 mg lapatinib QD plus 1.5 mg trametinib QD dose-limiting toxicities were reported in two out of six patients. Thereafter dose-level 3 was initiated with a lowered lapatinib dose of 500 mg QD and trametinib 1.5 mg QD. In this dose-level two out of three patients experienced a DLT. Therefore, we enrolled an additional three patients on the initial dose-level 1. Finally, one DLT was observed amongst six patients which resulted in 750 mg lapatinib QD plus 1 mg trametinib QD continuously being the RP2R. Dose-limiting adverse events were grade 3 diarrhea in dose-level 1, grade 3 rash and grade 3 aspartate aminotransferase elevation in dose-level 2, and in dose-level 3 were grade 3 diarrhea and inability to receive at least 75% of the planned dose due to a grade 4 creatine phosphokinase (CPK) elevation (figure 1).

Although the RP2R for continuous dosing was formally determined, severe gastro-intestinal and skin toxicity were a major problem reported by the patients and their treating oncologist, also after the DLT period was completed. Therefore, intermittent dosing regimens were initiated, which in theory might optimize the toxicity profile without significant loss of anti-tumor activity. A 5 days on/2 days off regimen was chosen to achieve a more gradual increase in plasma levels with short recovery periods. Dose-level 4 consisted of 750 mg QD in a 5 days on/2 days off regimen and trametinib 1.5 mg QD continuously. No DLTs were observed at this dose-level. Dose-level 5 with 750 mg lapatinib QD and 2 mg trametinib QD, both in a 5 days on/2 days off regimen, resulted in DLT in two out of four patients. DLTs consisted of nausea grade 3 resulting in a treatment delay >7 days in one patient and rash grade 3 resulting in treatment delay of >7 days and intake of <75% of the planned doses in another patient. Formally, the previous dose-level should have been expanded. However, because the investigators preferred a 5 days on/2 days off regimen for both agents in view of patient convenience, the study protocol was amended and a new dose-level 6 was opened consisting of 750 mg lapatinib and 1.5 mg trametinib both in a 5 days on/2 days off regimen. Out of the three initially treated patients in this dose-level, one patient experienced several grade 2 toxicities during cycle 1 related to the study medication and not manageable with optimal supportive care, which was a DLT as judged by the principal investigator. Dose-level 6 was expanded with three patients and no DLTs were observed. As a result, the combination of lapatinib 750 mg and trametinib 1.5 mg QD 5 days on/2 days off is considered as the RP2R for intermittent dosing.

### **Safety**

As shown in table 2, the most frequent adverse events at least possibly related to treatment were skin toxicity (97%), diarrhea (82%), and fatigue (59%). These toxicities occurred mainly within the first weeks of treatment. Skin toxicity presented as acneiform, maculo-papular or papulo-pustular rash (97%), mainly on the face, chest and back, hand-foot syndrome (18%), and as dry skin (24%). One grade 3 event of abscess-forming folliculitis was observed at dose-level 5. All patients received prophylactic cetomacrogol cream and were instructed to use cream with sun protection. At the time of emerge of symptoms doxycycline 100 mg QD was administered.

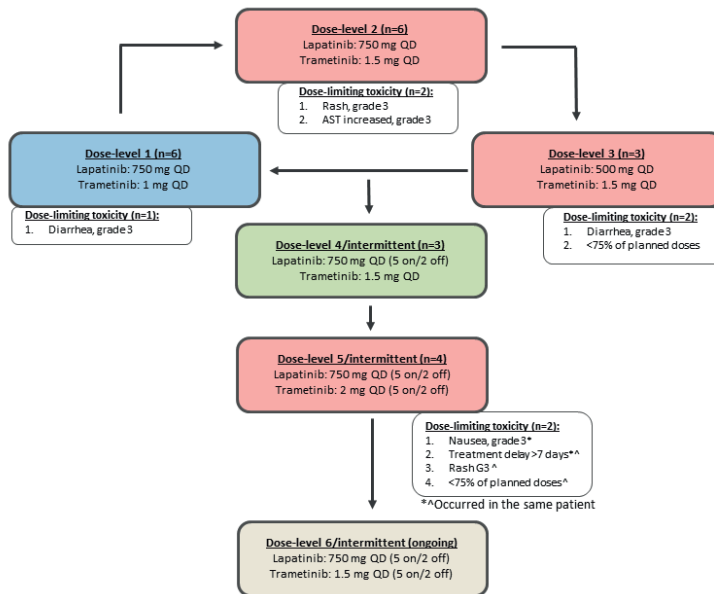


**Figure 1. Dose-escalation cohorts and dose-limiting toxicities.**

Abbreviations: QD, once daily; AST, aspartate transaminase

Maculo-papular rash grade 3 was experienced by three patients and led in all patients to a dose interruption until recovery to grade 1. For 2 of these patients a dose reduction was necessary.

Diarrhea was predominantly grade 1-2 and was mostly manageable with standard supportive care. Diarrhea was the major cause of treatment interruption (n=4) or discontinuation (n=3). Treatment-related ocular toxicity, mostly dry eyes, was observed in nine patients and did cause discontinuation of study treatment in one patient with ocular vein occlusion. Five patients experienced a decrease in left ventricular ejection fraction with a median of 15% [range: 12-46%], including two patients with grade 3 events. One patient discontinued study treatment permanently due to a decreased LVEF from 70% at baseline to 24% after nine cycles that did not improve to more than 50% within four weeks of treatment interruption. The other patient with a 21% LVEF decrease had several treatment interruptions and one dose-reduction of lapatinib which allowed recovery to grade 2. All other LVEF events did not require treatment interruption, were asymptomatic and recovered over time.

### Pharmacokinetic analysis

For lapatinib and trametinib, day one and steady state  $AUC_{0-24}$ ,  $T_{max}$ , and  $C_{max}$  at each dose-level are summarized in table 3. Day one and steady-state (day 29 or day 26 in the 5/2 dose-levels) plasma concentration time profiles at each dose-level are given in figure 2.

**Table 2. Adverse events of all treatment cycles, at least possibly related occurring in ≥ 10% of patients, highest grade per patient.**

Adverse Event, n %	Dose-level 1 (n = 7) 750 mg 1 mg		Dose-level 2 (n = 7) 750 mg 1.5 mg		Dose-level 3 (n = 4) 500 mg 1.5 mg		Dose-level 4 (n = 4) 750 mg (5/2) 1.5 mg		Dose-level 5 (n = 5) 750 mg (5/2) 2 mg (5/2)		Dose-level 6 (n=7) 750 mg (5/2) 1.5 mg (5/2)		Total (n=34)
	Grade 1/2	Grade 3	Grade 1/2	Grade 3	Grade 1/2	Grade 3	Grade 1/2	Grade 3	Grade 1/2	Grade 3	Grade 1/2	Grade 3	Grade 1-3
Lapatinib QD													
Trametinib QD													
Any skin toxicity	7 100%	3	5 71%	3 43%	4 100%	4 100%	4 100%	4 100%	4 80%	1 20%	6 86%	33 97%	
Rash	5 71%		5 71%	2 29%	4 100%		4 100%	1 20%	1 20%	4 57%	4 57%	33 97%	
Hand-foot syndrome	2 29%		2 29%					1 20%	1 20%	1 14%	1 14%	6 18%	
Dry skin	2 29%							2 40%	2 40%	4 57%	4 57%	8 24%	
Folliculitis				1 14%								1 3%	
Diarrhea	4 57%	2 29%	5 71%	1 14%	1 25%	1 25%	3 75%	3 75%	4 80%	1 20%	2 29%	1 14%	28 82%
Fatigue	6 86%		4 57%	1 14%	2 50%		1 25%	1 25%	1 20%	4 57%	4 57%	4 12%	20 59%
Vomiting	1 14%		4 57%		1 25%		2 50%	2 50%	5 100%	1 20%	3 43%	1 14%	18 53%
Nausea	3 43%		2 29%		2 50%		2 50%	2 50%	4 80%	2 29%	2 29%	1 14%	16 47%
CPK increased	2 29%		2 29%				1 25%	1 25%	2 40%		4 57%	4 12%	11 32%
ALT/AST increased	1 14%		4 57%		2 50%				2 40%		1 14%	1 14%	10 29%
Ocular toxicity	4 57%	1 14%	1 14%						1 20%		1 14%	1 14%	8 24%
Dry eyes	1 14%		1 14%						1 20%		1 14%	1 14%	4 12%
Serous retinopathy	2 29%	1 14%	1 14%						1 20%		1 14%	1 14%	3 9%
Uveitis	1 14%										1 14%	1 14%	1 3%
Ocular vein occlusion													1 3%
Anorexia/dysgeusia	1 14%		1 14%						1 20%		1 14%	1 14%	2 6%
Mucositis			4 57%						2 40%	1 20%	2 29%	1 14%	8 24%
LVEF decreased	1 14%	2 29%	2 29%		1 25%				1 20%		1 14%	1 14%	7 21%
Edema	1 14%		1 14%						1 20%		1 14%	1 14%	5 15%
Weight loss	2 29%		1 14%						1 20%		1 14%	1 14%	5 15%
Hypertension	1 14%		1 14%				1 25%		1 20%		1 14%	1 14%	5 15%
													4 12%

Abbreviations: CPK, creatine phosphokinase; ALT/AST, alanine aminotransferase / aspartate aminotransferase; LVEF, left ventricular ejection fraction; 5/2, 5 days on / 2 days off

Table 3. Pharmacokinetic parameters of lapatinib and trametinib at cycle 1 and steady state.

Dose-level	1	2	3	4	5	6	Lapatinib All 750 mg doses	Trametinib All 1.5 mg doses
Lapatinib QD	750 mg 1 mg	750 mg 1.5 mg	500 mg 1.5 mg	750 mg (5/2) 1.5 mg	750 mg (5/2) 2 mg (5/2)	750 mg (5/2) 1.5 mg (5/2)		
Trametinib QD								
Lapatinib	Cycle 1 Day 1							
Mean (%CV)	n = 7	n = 6	n = 3	n = 4	n = 5	n = 6	n = 28	-
C <sub>max</sub> ( $\cdot 10^3$ ng/mL)	1.1 (46)	1.4 (71)	0.99 (36)	0.67 (44)	1.6 (18)	0.95 (46)	1.1 (32)	
T <sub>max</sub> (h)	3.5	3.6	4.7	3.1	2.8	4.0	3.4	
AUC <sub>0-24h</sub> ( $\cdot 10^3$ ng*h/mL)	13 (48)	17 (63)	13 (25)	10 (28)	20 (25)	12 (48)	14 (28)	
Lapatinib	Cycle 2 Day 1							
Mean (%CV)	n = 4	n = 3	n = 1	n = 2*	n = 2*	n = 6*	n = 16	-
C <sub>max</sub> (ng/mL)	2.1 (60)	1.7 (64)	0.80	0.81 (8)	2.1 (36)	1.4 (48)	1.6 (33)	
T <sub>max</sub> (h)	3.9	3.3	4.0	3.0	4.0	5.3	3.9	
AUC <sub>0-24h</sub> ( $\cdot 10^3$ ng*h/mL)	33 (56)	23 (64)	12	11 (18)	30 (19)	24 (57)	24 (35)	
Trametinib	Cycle 1 Day 1							
Mean (%CV)	n = 7	n = 6	n = 3	n = 4	n = 5	n = 6	-	n = 19
C <sub>max</sub> (ng/mL)	2.7 (52)	4.0 (36)	3.9 (32)	2.9 (27)	5.7 (59)	3.0 (66)		3.5 (17)
T <sub>max</sub> (h)	0.9	2.3	2.0	1.9	1.0	1.8		2.0
AUC <sub>0-24h</sub> ( $\cdot 10^1$ ng*h/mL)	2.1 (43)	3.4 (39)	3.7 (19)	3.7 (19)	3.9 (32)	2.5 (38)		3.3 (17)
Trametinib	Steady state							
Mean (%CV)	n = 4	n = 3	n = 1	n = 2*	n = 2*	n = 6*	-	n = 12
C <sub>max</sub> (ng/mL)	13 (27)	15.9 (50)	9.1	17.3 (41)	16.5 (2)	15.7 (30)		14.5 (25)
T <sub>max</sub> (h)	1.14	2.5	8	2.0	3.0	3.2		3.9
AUC <sub>0-24h</sub> ( $\cdot 10^1$ ng*h/mL)	23 (26)	27 (46)	19	28 (9)	36 (0.3)	31 (35)		26 (20)

\*Pharmacokinetic samples were taken at the last day of cycle 1 on which lapatinib and trametinib were given concurrently, i.e. cycle 1 day 26. Data are listed as geometric mean. AUC<sub>0-24</sub> and C<sub>max</sub> data are given as mean (CV%). 5/2; 5 days on, 2 days off.

Pharmacokinetic parameters are in line with previously reported data for lapatinib and trametinib administered as single agents.(17, 19) Trametinib and lapatinib were absorbed with a time to maximum plasma concentration ( $T_{max}$ ) of approximately 4 hours for lapatinib (750 mg and 500 mg), and 1 to 3 hours for trametinib (1 mg and 1.5 mg). Repeated lapatinib dosing resulted in an approximate 1.7-fold increase in exposure at steady-state relative to day one, with a mean area under the plasma concentration time curve from time zero to 24 hours ( $AUC_{0-24}$ ) of  $14 \cdot 10^3$  ng\*h/mL (between subject coefficient of variation [CV%], 57%) at day one and  $24 \cdot 10^3$  ng\*h/mL (CV 65%) at steady-state. Compared to 750 mg continuously, intermittent dosing of lapatinib and de-escalation to 500 mg resulted in lower exposure in cycle 2, as expected. The unique exposure profile of trametinib, including a small peak-to-trough-ratio, long effective half-life and low interpatient variability were recognized in our data as well. Trametinib exposure at day 1 was increased by escalations of trametinib from 1 mg, to 1.5 mg and 2 mg. Trametinib accumulated by 8-fold after multiple administrations. See figure 2 for the plasma concentration time curves at cycle 1 day 1 and steady state for both drugs.

### Antitumor activity

Twenty-four patients were evaluable for efficacy; ten patients did not reach the first radiographic evaluation, which was a criterion to be evaluable for efficacy according to the protocol, due to withdrawal of consent (n=4), adverse events (n=3), clinical progressive disease (n=2) or a lack of evaluable target lesions (n=1). The patient with the lack of evaluable target

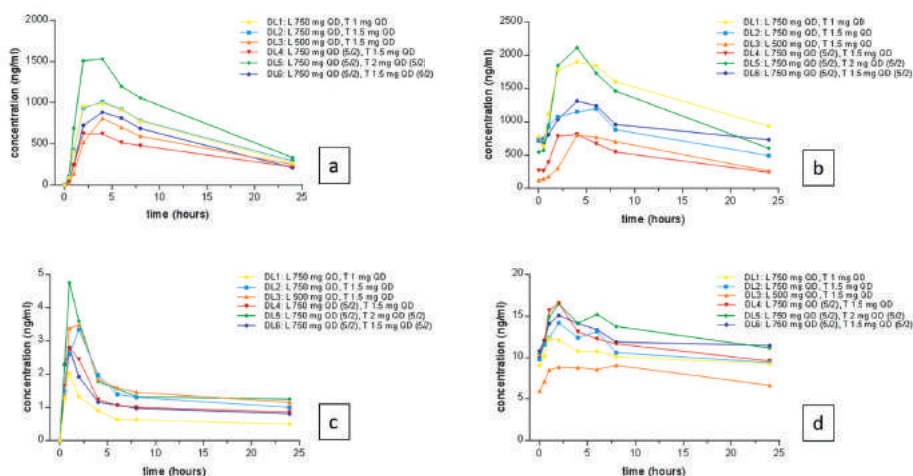


**Figure 2. Pharmacokinetic profiles of lapatinib and trametinib.** Mean plasma concentration curves for lapatinib (a, b) and trametinib (c, d), per dose-level at day 1 (a, c) and at cycle 2 day 1 or the last day of concomitant use of both drugs in cycle 1 after at least 3 weeks of administration (b, d). The dotted line indicates target levels of 10.4 ng/ml for trametinib (20) and 9.43 ng/ml for lapatinib.(21)

lesions should not have been enrolled, since the inclusion criteria including measurable disease according to RECIST 1.1. were not met. Out of the evaluable patients, one patient (4%) achieved a confirmed partial response, 13 (54%) had stable disease as best response, and ten (42%) had progressive disease at the first response evaluation. Although only one partial response (>30% decrease of tumor volume according to RECIST 1.1.) was observed, tumor regression was achieved in six patients at dose-levels 1, 2 and 5. Ten out of 11 patients with NSCLC had stable disease, including three patients with tumor regression of more than 20% and one confirmed partial response (tumor regression >30%) (figure 3a). The median time on treatment was 69 days (range 25–350). Separated by tumor type, median time on treatment was 105 days (range 25–350) for patients with NSCLC, 59 days (range 38-133) for CRC patients, and 85 days for the evaluable patient with pancreatic cancer (figure 3b).

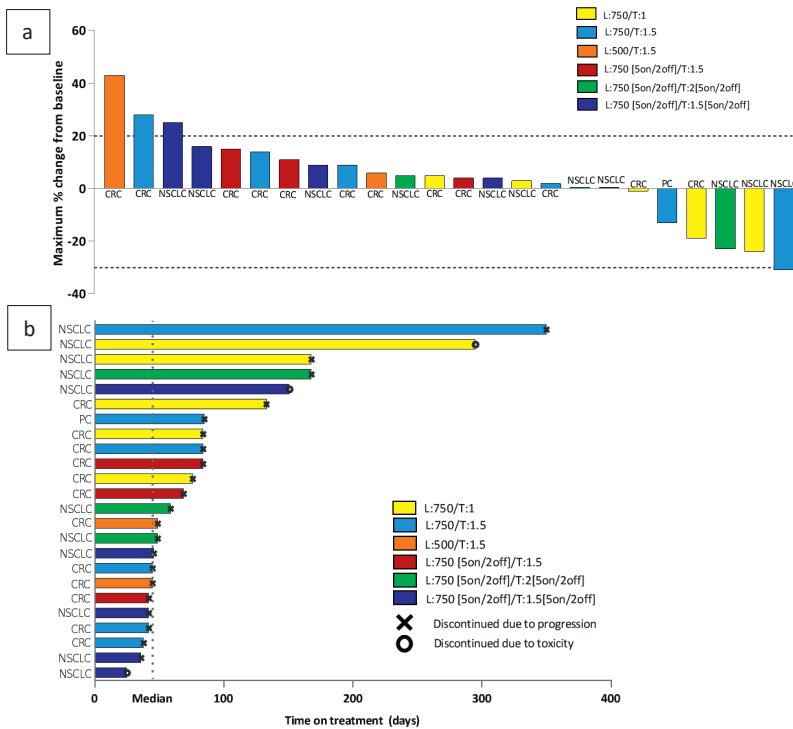


**Figure 3. Anti-tumor activity of lapatinib and trametinib in KRASm CRC, NSCLC and pancreatic cancer.**

a. Maximum percentage change in sum of target lesion size from baseline by dose-level, including response evaluation by RECIST

b. Swimmer plot of treatment duration, by dose level. Bars represent duration on treatment by dose-level, with the reason for end of treatment displayed at the end of each bar. Abbreviations: L, lapatinib; T, trametinib; CRC, colorectal cancer; NSCLC, non-small cell lung cancer; PC, pancreatic cancer; QD, once daily.

### Pharmacodynamic analysis

Paired tumor biopsies were obtained at baseline and on treatment from 19 patients. In total, 15 paired tumor biopsies contained sufficient numbers of tumor cells (at least 100 tumor cells) and were considered evaluable for pharmacodynamic analysis. The mean pERK H-score modulation was -43%, with ten out of 15 patients showing reduction in pERK H-score (figure S2a). In 15 patients, the biopsied lesion could also be evaluated on CT which allowed exploring the correlation between pERK H-score and response of the corresponding lesion after six weeks of treatment. Unfortunately, pERK changes were not significant correlated with RECIST response (figure S2b).

The pS6 staining results are not included in the pharmacodynamic analysis, because the quality of this staining could not be assured due to lack of reliable controls.

Figure S1 illustrates how pERK and pS6 modulation was visualized.

### Discussion

Our findings show that trametinib and lapatinib can be combined without unacceptable toxicity, at approximately 50% of their single agent doses. Although the RP2R was determined for continuous and intermittent dosing, the intermittent dosing regimen is preferable for future purposes due to better manageable toxicity. In a continuous dosing regimen, 750 mg lapatinib plus 1 mg trametinib was declared the RP2R. The RP2R in an intermittent administration regimen was 750 mg lapatinib and 1.5 mg trametinib QD 5 days on/2 days off. On this intermittent dose-level, three grade 3 toxicities were observed compared to eight among patients who received 750 mg lapatinib combined with 1.5 mg trametinib continuously. In previous studies, lapatinib was well tolerated at doses up to 1,600 mg QD, and the RP2R of trametinib was established at 2 mg QD.(17, 19, 22) Although the AUC and other pharmacokinetic parameters of intermittent dosing were comparable to continuous dosing, the rate of adverse events and DLTs was reduced in intermittent dosing. Therefore, intermittent dosing appears to be a favorable alternative to maintain efficacy and reduce toxicity. This is in line with previously reported studies with lapatinib or trametinib exploring continuous and intermittent dosing regimens.(14-17)

In combination, full single-agent doses could not be administered due to the occurrence of dose-limiting events including rash, diarrhea and liver enzyme elevation. However, previous studies showed that even at 50% of the monotherapy doses, target engagement and clinical responses can be achieved in patients with *BRAF*m melanoma and EGFR-expressing and/or HER2-overexpressing breast cancer, respectively.(17, 19, 22) This was confirmed by the target engagement observed in tumor biopsies. Relevant suppression of the MAPK-pathway was achieved, as indicated by a reduction of pERK in the majority of patients and in all histological tumor types. Although the pharmacodynamic effects were promising, a correlation with clinical activity (e.g. response rate, time on treatment) could not be confirmed. One possible explanation for this is that pERK suppression may be transient or insufficient and tumor cells find escape mechanisms to reactivate ERK phosphorylation or



another preferred survival pathway quickly after the on-treatment biopsy. This hypothesis is supported by the finding that pERK modulation, measured in the second week of treatment, did not clearly correlate with radiologic regression of the corresponding lesion, evaluated after six weeks of treatment, in the majority of patients (figure S2b). Secondly, inter-metastasis heterogeneity and sensitivity within patients may play a role. Indeed, the biopsied lesions in two patients showed radiological changes of -11% and -44%, whereas the sum of target lesion diameters had increased. In these lesions, pERK scores decreased upon treatment with -56% and -100% respectively.

Another explanation for limited clinical efficacy lies in the pharmacokinetics. In general, pharmacokinetic data obtained in this study were in line with single agent data from previous studies,(17, 19) indicating the absence of an obvious pharmacokinetic drug-drug interaction between lapatinib and trametinib. The unique pharmacokinetic profile of trametinib, with a long effective half-life and small peak-to-trough ratio allows constant target inhibition with relatively low  $C_{max}$ .(11) However, at 1 and 1.5 mg, the preclinical plasma concentration target of 10.4 ng/mL (i.e. the estimated mean inhibitory concentration at which 50% growth occurs in *BRAF*m melanoma cell lines),(22) was reached for only 50% of the patients and only 15 hours of the 24-hour dosing interval at steady state. In a previous phase I study with single agent trametinib, Infante *et al.* showed that the preclinical target concentration was exceeded during the entire dosing interval only at doses of 2 mg and higher.(17) As robust MEK and MAPK pathway inhibition is crucial for optimal anti-tumor activity and because higher trametinib doses yielded stronger pERK suppression and improved clinical outcome in previous studies with trametinib as single agent or in combination (22) in patients with *BRAF* or *NRAS* mutated melanoma,(17, 19, 22) dose-escalation was considered desirable. To reach increased exposure to lapatinib and trametinib with preserved tolerability, intermittent dosing regimens were initiated starting with continuous trametinib in combination with intermittent lapatinib, followed by another dose-level with intermittent administration of both drugs. This strategy was supported by *in vitro* data from our institute, demonstrating that sequential administration of concurrent MEK and EGFR-HER2 inhibition resulted in similar fractions of apoptotic cells in *KRAS*m cell lines as with concurrent administration (Bernards, unpublished data).

As expected, given the overlapping toxicity profiles of lapatinib and trametinib, gastrointestinal and skin-related toxicity were the most common treatment-related adverse events. In the majority of patients, early recognition and instant treatment was sufficient to make these effects manageable. During our study, five occurrences of LVEF reduction were reported. One patient experienced a LVEF reduction from 70% at baseline to 45% after five cycles of study treatment. As the LVEF recovered to >50% within two weeks upon treatment interruption, the patient continued on the same dose-level. However, after nine cycles LVEF had decreased to 24%. Because treatment interruption did not result in improvement of LVEF to  $\leq$  grade 1 within four weeks, the patient discontinued study treatment permanently. Three months after study discontinuation, LVEF had recovered to >50%. LVEF decrease is common for MEK inhibitors and has been reported with lapatinib as well. For this reason, it

can reasonably be expected that the incidence of LVEF reduction is slightly higher in this combination than reported for the single agents. Moreover, decrease in LVEF was only observed in continuous dosing schedules. Beside skin and gastro-intestinal toxicity, intermittent dosing appears to reduce cardiotoxicity as well.

Unfortunately, at tolerable doses, the anti-tumor activity obtained with trametinib plus lapatinib in patients with *KRAS* malignancies was limited, with only one confirmed partial response so far. Previously, van Geel *et al.* and Kopetz *et al.* demonstrated promising clinical activity with a combination strategy for patients with *BRAF* CRC.(23-25) This combination therapy was based on a preclinical synthetic lethality drug screen showing synergistic activity between *BRAF* inhibition and an anti-EGFR directed antibody with or without MEK inhibition.(26) The exact same screening method identified dual EGFR-HER2 inhibitors to synergize with MEK inhibitors in *KRAS* cells.(7) However, whereas in the *BRAF* setting clinical responses were achieved already at low *BRAF* inhibitor doses, this was not the case in this study in *KRAS* tumors.

Remarkably, ten out of 11 patients with NSCLC achieved stable disease, including three patients with tumor regression of more than 20% and one confirmed partial response. Since only one single pancreatic cancer patient was included in this trial, no conclusion about efficacy of the study treatment in pancreatic cancer can be drawn. Based on these findings, we hypothesized that there may be a difference in sensitivity between NSCLC and CRC. This hypothesis was supported by the time-on-treatment data, showing a median disease stabilization time of four months in the NSCLC patients compared to two months in patients with CRC. Previous studies suggested a difference in sensitivity to MEK inhibition between NSCLC and CRC as well. Hochster *et al.* demonstrated marginal additional benefit for adding a MEK inhibitor to second-line irinotecan in patients with *KRAS* CRC,(27) whereas Jänne *et al.* showed that the overall response rate in patients with *KRAS* NSCLC could be improved by adding the MEK inhibitor selumetinib to second-line treatment with docetaxel, although no significant effect on the progression-free survival and overall survival was observed.(6, 28) Additional work planned in a sizeable translational study therefore includes tumor and blood samples from this and other phase I trials with combination treatments for *KRAS* tumors, trying to elucidate the underlying biological mechanism of this difference in sensitivity. Evaluation of additional potential biomarkers, including the nature of the *KRAS* mutation, heregulin, HER2 and HER3 protein expression levels, may be relevant for that matter. Recent literature implicated that *KRAS*<sup>G12C</sup> mutations, which are mostly found in NSCLC, are more dependent on upstream signaling than other *KRAS* mutations.(29, 30) This may also answer the question why NSCLC patients respond better on the study treatment than CRC or pancreatic cancers. Furthermore, RNA and DNA sequencing will be performed on baseline and on-treatment tumor material to gain insight in changes in protein expression and mutation profiles upon treatment. Lastly, given the primarily cytostatic effect of MEK inhibitors in *KRAS* tumors,(31) it may be interesting to investigate markers for apoptosis (e.g. Bcl-XL, caspase 3), and to explore the potential of adding anti-apoptotic protein inhibitors such as navitoclax.(32)

Taken together, our study established the RP2R for the combination of lapatinib and trametinib when given concurrently in a continuous or intermittent dosing schedule. In a continuous dosing regimen, 750 mg lapatinib QD plus 1 mg trametinib QD was declared the RP2R, although significant non-serious and serious adverse events were common. The intermittent schedule was better tolerable in the RP2R of 750 mg lapatinib QD and 1.5 mg trametinib QD 5 days on/2 days off. We provided evidence of pharmacodynamic effects in terms of target engagement in *KRAS* tumor tissue and we demonstrated moderate preliminary clinical anti-tumor activity in patients with *KRAS* NSCLC. Mechanisms of resistance and response must be clarified before a phase II trial might be considered. If a predictive biomarker profile can be established, a phase II trial with optimized patient selection based on this profile may be considered.

### **Acknowledgements**

We thank all patients for participation, the clinical research unit of the Antoni van Leeuwenhoek hospital – Netherlands Cancer Institute Amsterdam for conduct of the trial and Novartis for providing study drugs and an unrestricted grant.

### **Conflicts of interest**

JB and JS (partly) hold a patent on oral taxane formulations, are shareholders and part-time employees of Modra Pharmaceuticals, a spin out company developing oral taxanes. Not related to the manuscript. RB holds a patent on the use of MEK and HER inhibitors in *KRAS* mutant cancers. The other authors declare that they do not have a conflict of interest related to this manuscript.

## References

1. Downward J. Targeting RAS signalling pathways in cancer therapy. *Nature reviews cancer*. 2003;3(1):11-22.
2. Cox AD, Fesik SW, Kimmelman AC, Luo J, Der CJ. Drugging the undruggable RAS: Mission possible? *Nature reviews drug discovery*. 2014;13(11):828-51.
3. Canon J, Rex K, Saiki AY, Mohr C, Cooke K, Bagal D, et al. The clinical KRAS(G12C) inhibitor AMG 510 drives anti-tumour immunity. *Nature*. 2019;575(7781):217-223.
4. Migliardi G, Sassi F, Torti D, Galimi F, Zanella ER, Buscarino M, et al. Inhibition of MEK and PI3K/mTOR suppresses tumor growth but does not cause tumor regression in patient-derived xenografts of RAS-mutant colorectal carcinomas. *Clinical cancer research*. 2012;18(9):2515-25.
5. Adjei AA, Cohen RB, Franklin W, Morris C, Wilson D, Molina JR, et al. Phase I pharmacokinetic and pharmacodynamic study of the oral, small-molecule mitogen-activated protein kinase kinase 1/2 inhibitor AZD6244 (ARRY-142886) in patients with advanced cancers. *Journal of clinical oncology*. 2008;26(13):2139-46.
6. Janne PA, Shaw AT, Pereira JR, Jeannin G, Vansteenkiste J, Barrios C, et al. Selumetinib plus docetaxel for KRAS-mutant advanced non-small-cell lung cancer: a randomised, multicentre, placebo-controlled, phase 2 study. *The Lancet oncology*. 2013;14(1):38-47.
7. Sun C, Hobor S, Bertotti A, Zecchin D, Huang S, Galimi F, et al. Intrinsic resistance to MEK inhibition in KRAS mutant lung and colon cancer through transcriptional induction of ERBB3. *Cell reports*. 2014;7(1):86-93.
8. Xia W, Mullin RJ, Keith BR, Liu LH, Ma H, Rusnak DW, et al. Anti-tumor activity of GW572016: a dual tyrosine kinase inhibitor blocks EGF activation of EGFR/erbB2 and downstream Erk1/2 and AKT pathways. *Oncogene*. 2002;21(41):6255-63.
9. Guan Z, Xu B, DeSilvio ML, Shen Z, Arpornwirat W, Tong Z, et al. Randomized trial of lapatinib versus placebo added to paclitaxel in the treatment of human epidermal growth factor receptor 2-overexpressing metastatic breast cancer. *Journal of clinical oncology*. 2013;31(16):1947-53.
10. Untch M, Loibl S, Bischoff J, Eidtmann H, Kaufmann M, Blohmer JU, et al. Lapatinib versus trastuzumab in combination with neoadjuvant anthracycline-taxane-based chemotherapy (GeparQuinto, GBG 44): a randomised phase 3 trial. *The Lancet oncology*. 2012;13(2):135-44.
11. Gilmartin AG, Bleam MR, Groy A, Moss KG, Minthorn EA, Kulkarni SG, et al. GSK1120212 (JTP-74057) is an inhibitor of MEK activity and activation with favorable pharmacokinetic properties for sustained in vivo pathway inhibition. *Clinical cancer research*. 2011;17(5):989-1000.
12. Long GV, Stroyakovskiy D, Gogas H, Levchenko E, de Braud F, Larkin J, et al. Dabrafenib and trametinib versus dabrafenib and placebo for Val600 BRAF-mutant melanoma: a multicentre, double-blind, phase 3 randomised controlled trial. *Lancet*. 2015;386(9992):444-51.
13. Planchard D, Besse B, Groen HJM, Souquet PJ, Quoix E, Baik CS, et al. Dabrafenib plus trametinib in patients with previously treated BRAF(V600E)-mutant metastatic non-small cell lung cancer: an open-label, multicentre phase 2 trial. *The Lancet oncology*. 2016;17(7):984-93.
14. Tolcher AW, Patnaik A, Papadopoulos KP, Rasco DW, Becerra CR, Allred AJ, et al. Phase I study of the MEK inhibitor trametinib in combination with the AKT inhibitor afuresertib in patients with solid tumors and multiple myeloma. *Cancer chemotherapy and pharmacology*. 2015;75(1):183-9.
15. Chew HK, Somlo G, Mack PC, Gitlitz B, Gandour-Edwards R, Christensen S, et al. Phase I study of continuous and intermittent schedules of lapatinib in combination with vinorelbine in solid tumors. *Annals of oncology*. 2012;23(4):1023-9.

16. Chien AJ, Munster PN, Melisko ME, Rugo HS, Park JW, Goga A, et al. Phase I dose-escalation study of 5-day intermittent oral lapatinib therapy in patients with human epidermal growth factor receptor 2-overexpressing breast cancer. *Journal of clinical oncology*. 2014;32(14):1472-9.
17. Infante JR, Fecher LA, Falchook GS, Nallapareddy S, Gordon MS, Becerra C, et al. Safety, pharmacokinetic, pharmacodynamic, and efficacy data for the oral MEK inhibitor trametinib: a phase 1 dose-escalation trial. *The Lancet oncology*. 2012;13(8):773-81.
18. Vogelstein B, Kinzler KW. The path to cancer --Three strikes and you're out. *The New England journal of medicine*. 2015;373(20):1895-8.
19. Burris HA, 3rd, Hurwitz HI, Dees EC, Dowlati A, Blackwell KL, O'Neil B, et al. Phase I safety, pharmacokinetics, and clinical activity study of lapatinib (GW572016), a reversible dual inhibitor of epidermal growth factor receptor tyrosine kinases, in heavily pretreated patients with metastatic carcinomas. *Journal of clinical oncology*. 2005;23(23):5305-13.
20. Falchook G, Kurzrock R, Gouw L, Hong D, McGregor KA, Zhou X, et al. Investigational Aurora A kinase inhibitor alisertib (MLN8237) as an enteric-coated tablet formulation in non-hematologic malignancies: phase 1 dose-escalation study. *Investigational new drugs*. 2014;32(6):1181-7.
21. Rusnak DW, Lackey K, Affleck K, Wood ER, Alligood KJ, Rhodes N, et al. The effects of the novel, reversible epidermal growth factor receptor/ErbB-2 tyrosine kinase inhibitor, GW2016, on the growth of human normal and tumor-derived cell lines in vitro and in vivo. *Molecular cancer therapeutics*. 2001;1(2):85-94.
22. Falchook GS, Lewis KD, Infante JR, Gordon MS, Vogelzang NJ, DeMarini DJ, et al. Activity of the oral MEK inhibitor trametinib in patients with advanced melanoma: a phase 1 dose-escalation trial. *The Lancet oncology*. 2012;13(8):782-9.
23. van Geel R, Tabernero J, Elez E, Bendell JC, Spreafico A, Schuler M, et al. A Phase Ib dose-escalation study of encorafenib and cetuximab with or without alpelisib in metastatic BRAF-mutant colorectal cancer. *Cancer discovery*. 2017;7(6):610-9.
24. Van Cutsem E, Huijberts S, Grothey A, Yaeger R, Cuyle PJ, Elez E, et al. Binimetinib, encorafenib, and cetuximab triplet therapy for patients with BRAF V600E-mutant metastatic colorectal cancer: Safety lead-in results from the phase III BEACON colorectal cancer study. *Journal of clinical oncology*. 2019;37(17):1460-1469.
25. Kopetz S, Grothey A, Yaeger R, Van Cutsem E, Desai J, Yoshino T, et al. Encorafenib, binimetinib, and cetuximab in BRAF V600E-mutated colorectal cancer. *The New England journal of medicine*. 2019;381(17):1632-1643.
26. Prahallad A, Sun C, Huang S, Di Nicolantonio F, Salazar R, Zecchin D, et al. Unresponsiveness of colon cancer to BRAF(V600E) inhibition through feedback activation of EGFR. *Nature*. 2012;483(7387):100-3.
27. Hochster HS, Uboha N, Messersmith W, Gold PJ, BH ON, Cohen D, et al. Phase II study of selumetinib (AZD6244, ARRY-142886) plus irinotecan as second-line therapy in patients with K-RAS mutated colorectal cancer. *Cancer chemotherapy and pharmacology*. 2015;75(1):17-23.
28. Janne PA, van den Heuvel MM, Barlesi F, Cobo M, Mazieres J, Crino L, et al. Selumetinib Plus docetaxel compared with docetaxel alone and progression-free survival in patients with KRAS-mutant advanced non-small cell lung cancer: The SELECT-1 randomized clinical trial. *Jama*. 2017;317(18):1844-53.
29. Mainardi S, Mulero-Sanchez A, Prahallad A, Germano G, Bosma A, Krimpenfort P, et al. SHP2 is required for growth of KRAS-mutant non-small-cell lung cancer in vivo. *Nature medicine*. 2018;24(7):961-7.
30. Nichols RJ, Haderk F, Stahlhut C, Schulze CJ, Hemmati G, Wildes D, et al. RAS nucleotide cycling underlies the SHP2 phosphatase dependence of mutant BRAF-, NF1- and RAS-driven cancers. *Nature cell biology*. 2018;20(9):1064-73.

31. Verissimo CS, Overmeer RM, Ponsioen B, Drost J, Mertens S, Verlaan-Klink I, et al. Targeting mutant RAS in patient-derived colorectal cancer organoids by combinatorial drug screening. *eLife*. 2016;5.
32. Corcoran RB, Cheng KA, Hata AN, Faber AC, Ebi H, Coffee EM, et al. Synthetic lethal interaction of combined BCL-XL and MEK inhibition promotes tumor regressions in KRAS mutant cancer models. *Cancer cell*. 2013;23(1):121-8.

## Supplemental data

**Table S1. Criteria for defining dose-limiting toxicities.**

Toxicity	DLT definition
Hematologic	<ul style="list-style-type: none"> <li>• Grade 4 neutropenia for <math>\geq 5</math> days</li> <li>• Grade <math>\geq 3</math> febrile neutropenia</li> <li>• Grade 4 anemia</li> <li>• Grade 4 thrombocytopenia</li> </ul>
Non-hematologic	<ul style="list-style-type: none"> <li>• AST <math>&gt; 5X</math> ULN OR, ALT <math>&gt; 3X</math> ULN AND bilirubin <math>&gt; 2X</math> ULN (after exclusion of disease progression and/or bile duct obstruction)</li> <li>• Grade <math>\geq 3</math> nausea, vomiting or diarrhea in the presence of maximal supportive care</li> <li>• Grade <math>\geq 2</math> peripheral sensory or motor neuropathy</li> <li>• Grade 3 or greater clinically significant non-hematologic toxicity per CTCAEv4.0, other than those listed above, with the following exceptions:               <ul style="list-style-type: none"> <li>○ Electrolyte disturbances that respond to correction within 24 hours</li> <li>○ Grade 3 hypertension that is adequately controlled by the addition of up to 2 additional antihypertensive medications</li> <li>○ Grade 3 pyrexia that does not result in study discontinuation</li> </ul> </li> </ul>
Cardiac	<ul style="list-style-type: none"> <li>• Ejection fraction <math>&lt; LLN</math> with an absolute decrease of <math>&gt;10\%</math> from baseline with confirmation within 14 days</li> </ul>
Other	<ul style="list-style-type: none"> <li>• Inability to receive <math>\geq 75\%</math> of scheduled doses in treatment period due to toxicity</li> <li>• Treatment delay of <math>&gt; 7</math> days due to study treatment-related toxicity</li> <li>• Grade 2 or higher toxicity that occurs beyond 28 days which in the judgment of the investigator is considered to be a DLT</li> </ul>

Abbreviations: AST, aspartate aminotransferase; ALT alanine aminotransferase; ULN, upper limit of normal; CTCAE, Common Terminology Criteria for Adverse Events; LLN, lower limit of normal; DLT, dose limiting toxicity

**Figure S1. Representative immunohistochemistry sections of pERK (A) and pS6 (B) stainings in tumor biopsies (zoom 40x).**

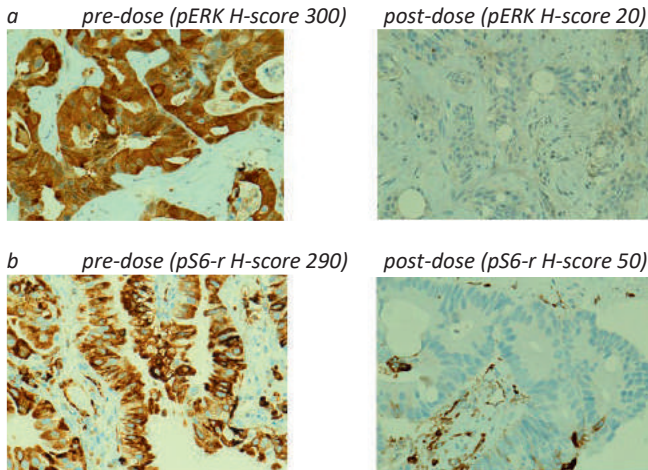
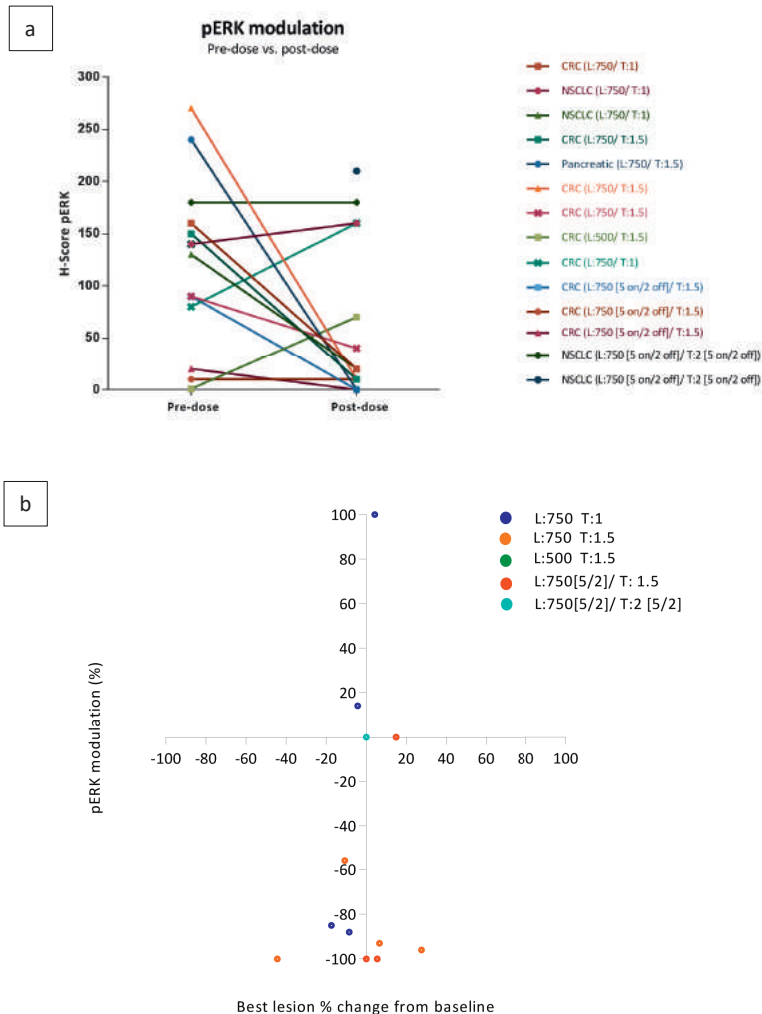


**Figure S2. Pharmacodynamic modulation in paired tumor biopsies.**

Tumor biopsies were obtained pre-dose (up to 1 week prior to treatment initiation) and post-dose (15–18 days after treatment start). Biopsy samples were analyzed for pERK<sup>Thr202/Tyr204</sup> by immunohistochemistry. Pre- and post-dose H-scores of pERK (A) are shown per individual. The correlation between pERK modulation and volume change of the biopsied lesion (B) are plotted for individual patients per dose-level. Abbreviations: CRC, colorectal cancer; NSCLC, non-small cell lung cancer; L, lapatinib; T, trametinib; 5 on/2 off, 5 days on/2 days off regimen.









# CHAPTER 4.3

Phase I study of afatinib and selumetinib in patients with *KRAS* mutated colorectal, non-small cell lung and pancreatic cancer

Sanne CFA Huijberts, Emilie MJ van Brummelen, Carla ML van Herpen, Ingrid ME Desar, Frans L Opdam, Robin MJM van Geel, Serena Marchetti, Neeltje Steeghs, Kim Monkhorst, Bas Thijssen, Hilde Rosing, Alwin DR Huitema, Jos H Beijnen, Rene Bernards, Jan HM Schellens

*Submitted for publication*

## **Abstract**

### **Introduction**

Anti-tumor effects of MEK inhibitors are limited in *KRAS* mutated tumors due to feedback activation of upstream epidermal growth factor receptors (HER) which reactivates the MAPK and the phosphoinositide 3-kinase (PI3K)-AKT pathway. Based on these data, this phase I trial was initiated with the pan-HER inhibitor afatinib plus the MEK inhibitor selumetinib to determine the recommended dose (RP2D) of this combination in patients with *KRAS* mutant, *PIK3CA* wild type tumors.

### **Materials and methods**

Patients received escalating doses of afatinib and selumetinib according to a 3+3 design in continuous and intermittent schedules. Blood and tumor samples were taken for pharmacokinetic and pharmacodynamic analyses. The study is registered at ClinicalTrials.gov (NCT2450656).

### **Results**

In total, 26 patients were enrolled with colorectal cancer (n=19), non-small cell lung cancer (NSCLC) (n=6) and pancreatic cancer (n=1). Dose-limiting toxicities occurred in six patients, including grade 3 diarrhea, dehydration, decreased appetite, nausea, vomiting and mucositis. The RP2D was 20 mg afatinib QD and 25 mg selumetinib BID (21 days on/7 days off) for continuous afatinib dosing and also for intermittent dosing with both drugs 5 days on/2 days off. Clinical efficacy was limited with disease stabilisation for 221 days in a patient with NSCLC as best response.

### **Conclusion**

Afatinib and selumetinib can be combined in continuous and intermittent schedules in patients with *KRAS* mutant tumors. However, although target engagement was observed, we do not recommend to further develop this combination until better biomarkers for response and resistance are defined.

**Implications for practice**

Currently, no effective therapies that directly target *KRAS* or inhibit downstream effectors in *KRAS* mutated cancers are available on the market. Preclinical studies show that combined inhibition of MEK, EGFR and HER2 results in complete inhibition of tumor growth. In this phase 1 trial, we show that the pan-HER inhibitor afatinib and the MEK inhibitor selumetinib could be combined safely in a continuous or intermittent treatment schedule in patients with *KRAS* mutated colorectal, non-small cell lung and pancreatic cancer. Target engagement was observed, but improved understanding of mechanisms of response and resistance is necessary before further development of this combination.

## Introduction

The RAS proteins play pivotal roles in the regulation of cell proliferation, survival and differentiation. Whereas RAS is normally activated by growth factors that bind to the extracellular domains of Receptor Tyrosine kinases (RTKs), activating *KRAS* mutations can cause a constant and RTK independent stimulation of cell proliferation.(1, 2)

Mutations in the *KRAS* gene occur as frequently as 45% in colorectal cancer (CRC), 35% in non-small cell lung cancer (NSCLC) and 90% in pancreatic cancer.(1) In these tumor types, *KRAS* mutations have been associated with poor responses to standard-of-care treatment. Approaches to inhibit *KRAS* signaling include targeting *KRAS* directly or targeting proteins activated by *KRAS*, such as RAF, MEK or ERK. The outcomes of these strategies have been disappointing in the preclinical and clinical setting.(2-5) Therefore, no targeted treatment options are currently available for this group of patients indicating a high medical need for new therapeutic strategies. There are encouraging early results of selective *KRAS*<sup>G12C</sup> inhibitors, providing some hope for future targeted therapies for patients having tumor with this mutation.(6)

Pre-clinical data show that intrinsic resistance upon MEK inhibition is due to feedback activation of upstream epidermal growth factor receptors (HER) in *KRAS* mutant CRC and NSCLC. This overexpression reactivates the MAPK pathway and phosphoinositide 3-kinase (PI3K)-AKT pathway.(7) *In vitro*, cell growth of *KRAS* mutant cell lines could be completely suppressed by inhibiting the proteins MEK and HER. Among various combinations, the combination of the MEK inhibitor selumetinib (AZD6244, ARRY-142886) and the potent irreversible inhibitor of multiple HER family kinases afatinib (*in vitro* IC<sub>50</sub> values of 0.5 nM, 14 nM and 1 nM against the human catalytic domains of HER1, HER2 and HER4) showed the strongest anti-tumor effects. The activity of the combination was subsequently confirmed in mice with *KRAS* mutated NSCLC.(2)

The unmet medical need and the promising pre-clinical results provided a strong rationale to evaluate the combination of afatinib and selumetinib in patients with *KRAS* mutant CRC, NSCLC and pancreatic cancer. In these patients, absence of *PIK3CA* mutations was required to avoid treatment resistance via activation of signaling proteins downstream of PI3K.(7) In this phase I trial, we investigated the safety, tolerability and preliminary anti-tumor activity of afatinib and selumetinib in order to determine the optimal dose (recommended phase II dose) and regimen (RP2D).

## Materials and methods

### Patient population

This investigator-initiated, open-label, phase I dose-escalation study enrolled patients at two sites in the Netherlands. Adult patients with histologically- or cytologically-confirmed advanced CRC, NSCLC or pancreatic cancer were enrolled on the basis of a documented *KRAS* mutation in exon 2, 3 or 4, and *PIK3CA* wild type status. Eligibility criteria included: Eastern Cooperative Oncology Group (ECOG) performance status of  $\leq 2$ , life expectancy of  $\geq 3$  months, measurable disease according to Response Evaluation Criteria In Solid Tumors (RECIST)

version 1.1, adequate bone marrow (absolute neutrophil count  $\geq 1.5 \times 10^9/L$ , platelets  $\geq 100 \times 10^9/L$ , hemoglobin  $\geq 6.0$  mmol/L), hepatic (total bilirubin  $\leq 1.5 \times$  upper limit of normal (ULN), aspartate aminotransferase (AST) and alanine aminotransferase (ALT)  $\leq 2.5 \times$  ULN), and renal (serum creatinine  $\leq 1.5 \times$  ULN) functions. Radiotherapy, immunotherapy, chemotherapy or any treatment with investigational medication within four weeks prior to study treatment were not allowed, and patients with a history of other primary malignancies were excluded. Additional exclusion criteria included symptomatic or untreated leptomeningeal disease, symptomatic brain metastasis, history of interstitial lung disease or pneumonitis, history of retinal vein occlusion, and prior therapy containing targeted drug combinations known to interfere with EGFR, HER2, HER3, HER4 or MAPK- and PI3K-pathway components, including PI3K, AKT, mTOR, BRAF, MEK and ERK. The study (ClinicalTrials.gov identifier: NCT2450656) was conducted in accordance with guidelines for Good Clinical Practice as defined by the International Conference on Harmonization. Regulatory authorities and the institutional review boards approved the study protocol and all amendments, and all patients gave written informed consent, per Declaration of Helsinki recommendations.

### Study design and procedures

Patients were treated at different dose-levels of orally administered afatinib and selumetinib in cycles of 28 days. The starting doses were chosen based on previous data from single agent phase I studies with both compounds, also taking into account a potential synergy in toxicities. Dose-level 1 consisted of 20 mg afatinib once daily (QD) continuously, which is 50% of its recommended dose as single agent, and 25 mg selumetinib twice daily (BID) administered on the first 21 days of each 28-day cycle, which is 33% of its recommended dose as single agent. First, selumetinib was escalated according to a classical 3 + 3 design with fixed maximum escalation increments. Dose-escalation decisions were based on safety evaluation of all evaluable patients, performed after completion of the first treatment cycle. Patients were considered evaluable for toxicity if at least one cycle of study treatment was completed, with the minimum safety evaluation and drug exposure ( $\geq 75\%$  of the planned doses of selumetinib and afatinib) or if dose-limiting toxicity (DLT) had occurred during the first cycle. If one out of three patients experienced DLT, the number of patients treated at that dose-level was expanded to a maximum of six. Dose-escalation continued until a dose-level was reached at which no more than one out of six patients experienced DLT during the first 28 days of treatment. Subsequently, afatinib was escalated with fixed increments of 10 mg following the same dose-escalation rules. Upon assessment of the optimal dose of the two-drug combination in this regimen, an intermittent 5 days on/2 days off dosing regimen was investigated for both drugs with the aim of optimizing drug exposure and improving tolerability. Patients continued study treatment until disease progression, unacceptable toxicity despite supportive measures and dose modifications, or investigator's or patient's decision to discontinue.

Safety was monitored by physical examination, laboratory assessments, electrocardiography, ophthalmic evaluation, left ventricular ejection fraction monitoring by multigated acquisition

scan (MUGA) and recording adverse events graded according to Common Terminology Criteria for Adverse Events version 4.03. DLT was defined as an adverse event or laboratory abnormality occurring within the first treatment cycle meeting at least one of the criteria described in supplementary table S1.

Radiologic tumor measurements were performed using computed tomography (CT) scans at baseline and every six weeks throughout the study. After a protocol amendment, CT scans were performed every eight weeks. Tumor response was evaluated according to RECIST version 1.1.(8) Patients were evaluable for anti-tumor activity if at least one on-treatment radiologic evaluation was performed. If relevant, serum tumor markers were collected every four weeks.

#### Pharmacokinetic and pharmacodynamic analyses

For pharmacokinetic analyses, serial blood samples for plasma concentration analysis were obtained from all patients in cycle 1 before and 1, 1.5, 2, 3, 4, 5, 8, 12, 24, 96, and 192, 360 and 528 hours after the first dose. On day 1 of cycle 2, blood samples were drawn before and 1, 1.5, 2, 3, 4, 5, 8, 12 and 24 hours after administration. Plasma was isolated and stored at -80°C until analysis. Plasma samples were analyzed using a validated high-performance liquid chromatography tandem mass spectrometry (HPLC-MS/MS) method. Briefly, selumetinib and afatinib were extracted from plasma by protein precipitation with a mixture of acetonitrile/methanol (1:1 v/v). Compounds were chromatographically separated using a Waters Xbridge BEH Phenyl column (50 x 2.1 mm ID, 5 µm particle size) and detection was performed using an API4000 tandem mass spectrometer equipped with a turbo ion spray interface, operating in the positive ion mode. Transitions from m/z 486 to 371 and m/z 459 to 397 were monitored for the detection of afatinib and selumetinib, respectively. Stable labelled internal standards were used for the quantification. The lower and upper limits of quantification were respectively 0.5 and 50 ng/mL for afatinib, and 5 and 500 ng/mL for selumetinib. Pharmacokinetic parameters were calculated in R using an in-house developed validated script for non-compartmental pharmacokinetic analyses (version 3.6.0).(9)

For pharmacodynamic analyses, tumor biopsies were taken before treatment, in the second week of treatment and upon treatment discontinuation. Phosphorylated (p) ERK and ribosomal pS6 (pS6-r) levels were measured by validated immunohistochemistry (IHC) staining methods and semi-quantitative H-scores (percentage of positive cells (0–100) multiplied by staining intensity (0–3)) were assessed by an independent pathologist who was blinded for sample identification. Tumor biopsy samples were fixed in formalin for 16–24 hours and embedded in paraffin subsequently. Thereafter, IHC was performed on a BenchMark Ultra autostainer (Ventana Medical Systems). Briefly, paraffin sections were cut at 3 µm, heated at 75°C for 28 minutes and deparaffinised with EZ prep solution (Ventana Medical Systems). Heat-induced antigen retrieval was carried out using Cell Conditioning 1 (CC1, Ventana Medical Systems) at 95°C for 32 and 64 minutes, for pS6-r and pERK1/2, respectively. pS6-r was detected using clone D68F8 (1:1000 dilution, 32 minutes at room temperature, Cell Signalling) and p-p44/42 MAPK (pERK1/2) (Thr202/Tyr204) using clone D13.14.4E (1:400 dilution, one hour at room temperature, Cell Signalling). pERK was detected



using the UltraView Universal DAB Detection Kit (Ventana Medical Systems), while detection of pS6-r was performed using the OptiView DAB Detection Kit (Ventana Medical Systems). Slides were counterstained with hematoxylin.

### Statistical analysis

Baseline characteristics, pharmacokinetics, pharmacodynamics, safety and tumor response data were reported descriptively.

## Results

### Patient characteristics

Between July 2015 and February 2020, 26 patients were enrolled onto this study, 19 patients (73%) with CRC, six with NSCLC (23%) and one (4%) with pancreatic cancer. The majority of patients had *KRAS* exon 2 mutations. Most patients were pretreated with at least two prior lines of antineoplastic therapy for advanced disease (table 1). Twenty-two patients were evaluable for toxicity; four patients were considered not evaluable due to early clinical deterioration or patient refusal. All patients discontinued treatment due to progressive disease (n=20), adverse events (n=3), clinical deterioration (n=2) or patient refusal (n=1).

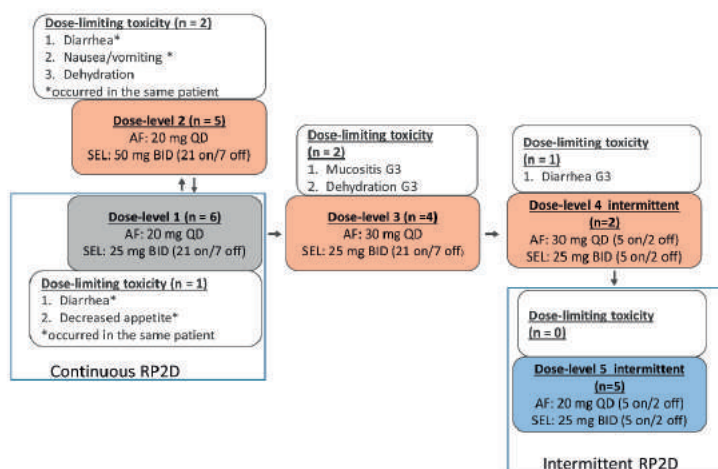


**Figure 1. Overview of dose-levels and dose-limiting toxicities.**

Abbreviations: n, number of patients; AF, afatinib; SEL, selumetinib; QD, once daily; BID, twice daily; G, grade; RP2D, recommended phase 2 dose.

### Dose finding

A total of 22 patients was evaluable for DLT assessment. At the initial dose-level, no DLTs occurred in the three included patients. Therefore, doses of selumetinib were escalated to 50 mg BID with the same dose of afatinib 20 mg QD. At this dose-level, two out of five patients experienced DLTs, being grade 3 diarrhea and nausea/vomiting in one patient, and diarrhea and dehydration in the other patient. The previous dose-level was expanded to six patients. One patient experienced a DLT being grade 3 diarrhea and decreased appetite, which

indicated that the highest dose for selumetinib was 25 mg BID in this combination. Subsequently, afatinib was escalated to 30 mg QD which caused DLTs in two out of four patients consisting of grade 3 mucositis and dehydration, which rendered this dose-level intolerable (figure 1). Consequently, the established maximum tolerated dose-level with continuous afatinib dosing consisted of 20 mg afatinib QD plus 25 mg selumetinib BID. To explore if further dose-escalation was possible when the drugs were both administered intermittently, a 5 days on/2 days off regimen was initiated starting with a slightly higher dose of afatinib than the RP2D for continuous dosing.

**Table 1. Patient and disease characteristics at baseline.**

	Patients (n = 26)
Sex, n (%)	
Female	13 (50%)
Male	13 (50%)
Age, median (range), years	63 (47-77)
Tumor types, n (%)	
Colorectal	19 (73%)
Non-small cell lung	6 (23%)
Pancreatic	1 (4%)
ECOG PS, n (%)	
0	20 (77%)
1	6 (23%)
Number of prior treatment lines, n (%)	
1	3 (12%)
2	7 (27%)
≥ 3	16 (62%)
KRAS mutation, n (%)	
Exon 2	23 (88%)
p.G12D	10 (38%)
p.G12C	5 (19%)
p.G12A	1 (4%)
p.G12V	4 (15%)
p.G13A	1 (4%)
p.G13D	2 (8%)
Exon 3	2 (8%)
p.Q61R	2 (8%)
Exon 4	1 (4%)
p.A146V	1 (4%)

Abbreviations: ECOG PS, Eastern Cooperative Oncology performance status; KRAS, Kirsten rat sarcoma viral oncogene homolog

Table 2. Adverse events possibly, probably and definitely related to study medication, occurring in ≥ 10% of patients.

Adverse Event, n (%)	DL 1 (n = 6) 20 mg 25 mg (21/7)		DL 2 (n = 5) 20 mg 50 mg (21/7)		DL 3 (n = 4) 30 mg 25 mg (21/7)		DL 4 (n = 2) 30 mg (5/2) 25 mg (5/2)		DL 5 (n = 5) 20 mg (5/2) 25 mg (5/2)		Total (n = 22)	
	Gr 1/2	Gr 3	Gr 1/2	Gr 3	Gr 1/2	Gr 3	Gr 1/2	Gr 3	Gr 1/2	Gr 3	Gr 1/2	Gr 3
Afatinib QD												
Selumetinib BID												
Any skin toxicity*	6 27%	5 23%	4 18%	1 5%	2 9%	2 9%	5 23%	2 9%	2 9%	2 9%	22 100%	1 5%
Rash acneiform	4 18%	6 27%	4 18%	1 5%	2 9%	2 9%	4 18%	4 18%	4 18%	2 9%	20 91%	1 5%
Dry skin	2 9%	1 5%	4 18%				1 5%				10 25%	
Erosive skin	1 5%	1 5%					1 5%				2 9%	
Eczema		2 9%					1 5%				1 5%	
Skin infection		3 14%					2 9%				3 14%	
Diarrhea	5 23%	1 5%	5 23%	4 18%	5 23%	3 14%	2 9%	2 9%	3 14%	18 82%	8 36%	
Edema	2 9%	2 9%	3 14%	1 5%	3 14%	1 5%	1 5%	1 5%	1 5%	8 36%	1 5%	
Dyspepsia/reflux	1 5%	2 9%	3 14%		3 14%		2 9%	2 9%	2 9%	7 32%		
Vomiting		2 9%					1 5%	2 9%	2 9%	6 27%	1 5%	
Nausea		2 9%					1 5%	1 5%	3 14%	6 27%	1 5%	
Fatigue		1 5%	1 5%	1 5%	1 5%	1 5%	2 9%	1 5%	1 5%	5 23%	2 9%	
Mucositis		2 9%	2 9%	1 5%	2 9%	1 5%	1 5%	1 5%	2 9%	5 23%	1 5%	
Pain	1 5%	1 5%	1 5%		1 5%		1 5%		2 9%	5 23%		
Eye toxicity	2 9%	2 9%			1 5%					5 23%		
Blurred vision	2 9%	1 5%			1 5%					3 14%		
Neurosens detachm		1 5%			1 5%					1 5%		
Retinopathy		1 5%			1 5%					1 5%		
Photosensitivity	1 5%									1 5%		
Dry eyes		1 5%	1 5%		1 5%					1 5%		
Anorexia/dysgeusia	1 5%	1 5%	3 14%	1 5%	3 14%	1 5%				4 18%	1 5%	
Dehydration		2 9%	2 9%	2 9%	1 5%	1 5%				4 18%		
Hypophosphatemia	1 5%	1 5%								2 9%	2 9%	
CPK elevation	1 5%	1 5%					1 5%			4 18%		
Fever	1 5%	1 5%			1 5%					2 9%	1 5%	
Epistaxis	1 5%	1 5%	1 5%		1 5%					2 9%	1 5%	
Hypertension		1 5%			1 5%					2 9%	1 5%	
Neuropathy		1 5%			1 5%					2 9%	1 5%	
Dry mouth		1 5%	1 5%		1 5%					4 18%		

Abbreviations: DL, dose-level; Gr, grade; Neurosens detachm; neurosensory detachment, CPK, creatine phosphokinase; 21/7, 21 days on, 7 days off; 5/2, 5 days on/2 days off; QD, once daily; BID, twice daily. \* Some patients had multiple skin toxicities and were only counted once for the category of any skin toxicity.

**Table 3. Pharmacokinetic parameters of afatinib and selumetinib at cycle 1, day 1 and cycle 2, day 1, per dose-level.**

Dose-level	1		2		3		4		5		Afatinib	Afatinib	Selumetinib	Selumetinib	
	20 mg	20 mg	20 mg	30 mg	30 mg	20 mg	20 mg	20 mg	20 mg	20 mg	All 20 mg doses	All 30 mg doses	All 25 mg doses	All 50 mg doses	
Afatinib QD															
Selumetinib BID	25 mg (21/7)	50 mg (21/7)	25 mg (21/7)	25 mg (5/2)	25 mg (5/2)	25 mg (5/2)	25 mg (5/2)	25 mg (5/2)	25 mg (5/2)	25 mg (5/2)					
<b>Afatinib</b>															
<i>Cycle 1 Day 1</i>															
Mean	n = 7	n = 7	n = 5	n = 2	n = 5	n = 5	n = 5	n = 5	n = 5	n = 19	n = 7	n = 7	-	-	-
C <sub>max</sub> (ng/mL)	15.4	13.1	46.1	21.8	12.3	13.6	(range 16.5-33.5)	3.7	3.2	3.7	34.0	(range 11-63.3)	-	-	-
T <sub>max</sub> (h)	3.7	3.4	1.9	4.5	4.0	3.9	157	147	157	(range 61-339)	379	(range 162-534)	-	-	-
AUC <sub>0-24h</sub> (ng* <sup>h</sup> /mL)	162	159	429	252	147	326	(range 109-649)	272	326	(range 259-1312)	584	(range 219-1190)	-	-	-
<i>Cycle 2 Day 1</i>															
Mean	n = 4	n = 4	n = 3	n = 2	n = 5	n = 13	n = 5	n = 5	n = 5	n = 13	n = 5	n = 5	-	-	-
C <sub>max</sub> (ng/mL)	25.7	16.0	60.5	36.3	20.1	20.6	(range 8.6-34.3)	3.4	3.9	2.0	48.4	(range 16.6-99.4)	-	-	-
T <sub>max</sub> (h)	4.8	3.5	2.3	1.7	3.4	3.9	1691	1647	1691	(range 835-3321)	584	(range 2920-5744)	-	-	-
AUC <sub>0-24h</sub> (ng* <sup>h</sup> /mL)	468	250	800	260	272	326	(range 109-649)	272	326	(range 259-1312)	584	(range 219-1190)	-	-	-
<b>Selumetinib</b>															
<i>Cycle 1 Day 1</i>															
Mean	n = 7	n = 7	n = 5	n = 2	n = 5	n = 5	n = 5	n = 5	n = 5	n = 19	n = 7	n = 7	-	-	-
C <sub>max</sub> (ng/mL)	472.1	842.6	618.0	302.0	516.0	477.0	(range 201-1190)	1.3	1.3	1.3	842.6	(range 238-1280)	-	-	-
T <sub>max</sub> (h)	1.3	1.8	1.3	1.5	1.2	1.8	1691	1647	1691	(range 835-3321)	4081	(range 2920-5744)	-	-	-
AUC <sub>0-12h</sub> (ng* <sup>h</sup> /mL)	1837	4081	2033	1245	1647	1691	(range 835-3321)	1647	1691	(range 835-3321)	4081	(range 2920-5744)	-	-	-
<i>Cycle 2 Day 1</i>															
Mean	n = 4	n = 4	n = 3	n = 2	n = 5	n = 14	n = 4	n = 4	n = 4	n = 14	n = 4	n = 4	-	-	-
C <sub>max</sub> (ng/mL)	413.8	1059.5	759.0	402.0	601.2	544.0	(range 219-916)	1.2	1.2	1.2	1059.5	(range 782-1250)	-	-	-
T <sub>max</sub> (h)	1.3	1.5	1.0	1.3	1.2	1.2	2037	1928	2037	(range 1057-2988)	3670	(range 2877-4420)	-	-	-
AUC <sub>0-12h</sub> (ng* <sup>h</sup> /mL)	1560	3670	3201	1459	1928	2037	(range 1057-2988)	1928	2037	(range 1057-2988)	3670	(range 2877-4420)	-	-	-

Data are listed as geometric mean. Abbreviations: 21/7, 21 days on/ 7 days off; 5/2, 5 days on/2 days off.

Afatinib was administered in a dose of 30 mg QD combined with 25 mg BID selumetinib in the first intermittent dosing schedule for both drugs. After the treatment of two patients, this dose-level was considered too toxic due to a DLT in one patient, being diarrhea grade 3, and several unmanageable grade 2 toxicities in the other patient (figure 1). The dose of afatinib was therefore de-escalated in dose-level 5 to 20 mg QD 5 days on/2 days off simultaneously with an unchanged dose of 25 mg BID selumetinib 5 days on/2 days off. Since none of the five patients in this dose-level experienced a DLT, this dose-level was determined as the RP2D for intermittent dosing.

### Safety

Study treatment-related adverse events were reported in all patients, with the most common being skin toxicity (100%), diarrhea (91%) and edema (36%). Skin toxicity and gastrointestinal toxicity developed mostly within the first weeks of treatment (table 2). Diarrhea was the major cause for DLT and dose interruptions. Supportive care included loperamide and diarrhea resolved to grade 1 or less in all patients upon interruption of study drugs. Skin toxicity mainly included acneiform rash and dry skin and was limited to grade 1-2 in the majority of patients. Prophylactic

cetomacrogol cream starting at the first day of study drug administration and the addition of minocycline or corticosteroid cream in case of symptoms was sufficient to manage skin toxicity in most patients. One grade 3 rash occurred in dose-level 3 which resulted in treatment discontinuation. In total, seven patients (32%) required a dose-interruption because of grade 3 events including diarrhea (n=5), dehydration (n=2), rash, mucositis and nausea (each n=1). Finally, five patients (21%) discontinued due to grade 3 diarrhea (n=2), grade 2 diarrhea (n=1), grade 3 dehydration (n=1) or hemoptoe not related to study medication (n=1). All toxicities resolved to grade 1 or less upon interruption or discontinuation of study treatment. Retinopathy and ocular neurosensory detachment were observed in two patients at dose-level 2, in which the highest doses of selumetinib were given, but were limited to grade 1-2 without treatment interruptions. Retinopathy was completely reversible, whereas the neurosensory detachment was grade 1 at the last follow-up. Creatine kinase elevation grade 1-2 was observed in four patients at dose-levels 1, 2, 4 and 5 and was also reversible without treatment interruptions.

### Pharmacokinetic analysis

Pharmacokinetic parameters after the first dose and at steady-state are summarized for each dose-level in table 3 and figure 2. Selumetinib exposure increased dose-proportionally with moderate inter-patient variability. For afatinib, plasma levels from patients treated with 30 mg showed a two to three-fold increase in exposure compared to the 20 mg cohorts. Taking into account the high inter-individual variability, no conclusions on dose-proportionality can be drawn. In line with its long half-life of 37 hours (10), the mean afatinib area under the plasma concentration-time curve from time 0 to 24 hours ( $AUC_{0-24h}$ ) increased approximately two-fold from cycle 1 day 1 to steady state for the continuous dose-levels. The plasma-

concentration time curves per dose-level showed that the target level of 30 ng/ml for afatinib, based on preclinical proliferation experiments (unpublished data Boehringer Ingelheim) and clinically active plasma concentrations (11) of 352 ng/ml for selumetinib (12) have not been reached in all patients. For afatinib, the target level was only achieved in dose-level 3 with continuous afatinib 30 mg QD. For selumetinib the target level was reached in all dose-levels except for dose-level 4 with 25 mg selumetinib BID 5 days on/2 days off, but the plasma concentrations in dose-level 4 were only based on two patients which may have led to variable results.

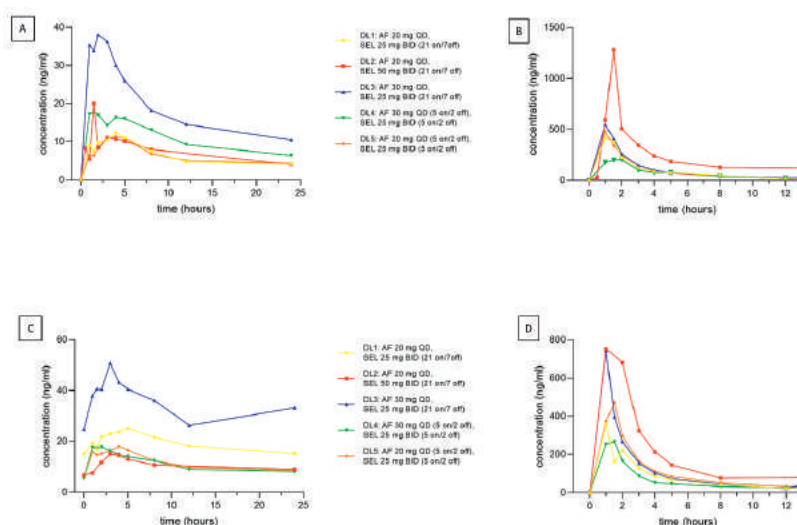


**Figure 2. Pharmacokinetic profiles of afatinib and selumetinib.**

All figures: mean plasma-concentration-time curves per dose-level.

A. Afatinib per dose-level: Cycle 1 day 1. B. Selumetinib per dose-level: Cycle 1 day 1.

C. Afatinib per dose-level: Cycle 2 day 1. D. Selumetinib per dose-level: Cycle 2 day 1.

Abbreviations: DL, dose-level; AF, afatinib; QD, once daily; SEL, selumetinib; BID, twice daily; 21 on/7 off, 21 days on/7 days off; 5 on/2 off, 5 days on, 2 days off.

### Anti-tumor activity

A total of 19 patients was evaluable for anti-tumor activity; seven patients did not reach the first radiological evaluation after eight weeks of study treatment due to clinical deterioration (n=5) or toxicity (n=2). Out of the evaluable patients, no complete or partial responses were observed. Ten patients achieved stable disease and nine patients had progressive disease on their first radiologic evaluation scan. The largest tumor regression of -16% was seen in a NSCLC patient treated in dose-level 3. All other patients had changes of -7% to +46% in tumor volume (figure 3A). The overall median treatment duration was 64 days (range 11–221), with five CRC patients having disease stabilization  $\geq 105$  days (15 weeks).

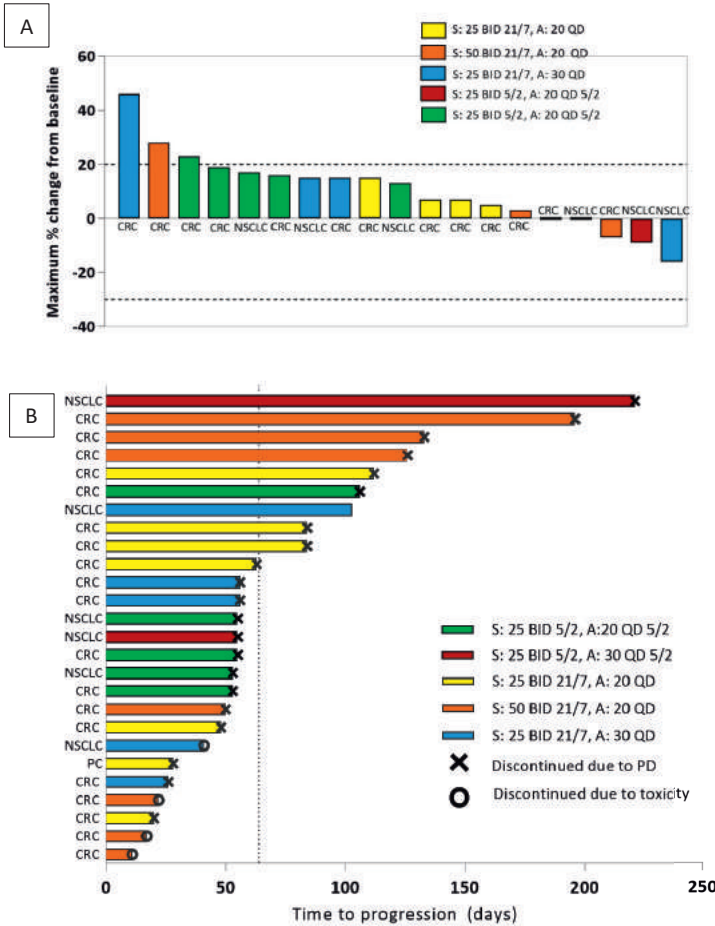


**Figure 3. Anti-tumor activity of afatinib and selumetinib in KRAS mutant colorectal, non-small cell lung and pancreatic cancer.**

A. Maximum percentage change in sum of target lesion size from baseline, by dose-level.

Abbreviations: A, afatinib; S, selumetinib; QD, once daily; BID, twice daily; 21/7, 21 days on/7days off; 5/2, 5 days on/2 days off; CRC, colorectal cancer; NSCLC, non-small cell lung cancer. Doses of both drugs are in milligrams.

B. Swimmer plot of treatment duration, by dose-level.

Abbreviations: A, afatinib; S, selumetinib; QD, once daily; BID, twice daily; 21/7, 21 days on/ 7 days off; 5/2, 5 days on/2 days off; CRC, colorectal cancer; NSCLC, non-small cell lung cancer; PC, pancreatic cancer. Doses of both drugs are in milligrams. Symbols at the end of each bar represent the reason for end of treatment for each individual patient. The dotted line represents the median time-on-treatment of 64 days.

## Pharmacodynamic analyses

IHC staining was evaluable for 20 patients, of whom six had evaluable pre- and on-treatment biopsies which allowed assessment of treatment effects. The other biopsies could not be obtained, were not evaluable because of low percentages of tumor cells or were not reliable due to cytoplasmic background staining instead of clear nuclear staining. The median decrease of pERK was -52% ( $p=0.02$ ) and for pS6-r -39% ( $p=0.2$ ), indicating inhibition of MEK and HER signaling by the combination treatment (figure 4). Modulation of pERK was achieved in all patients at all doses and matched with modulation of pS6-r in five out of six patients. The degree of pERK modulation significantly correlated with the plasma AUC of selumetinib as assessed on cycle 1 day 1 ( $R^2 = 0.85$ ,  $p < 0.01$ ).

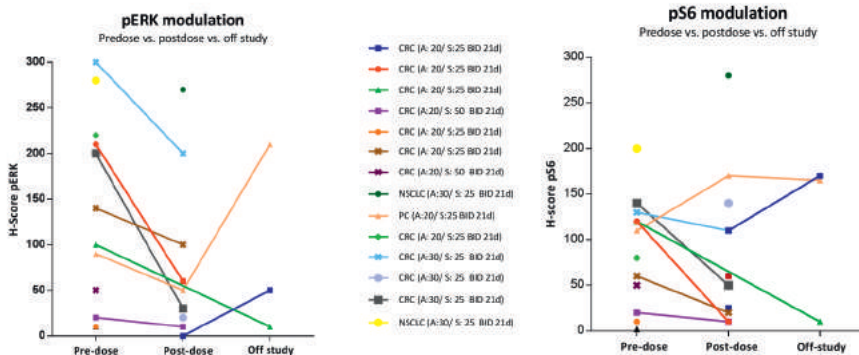


**Figure 4. Pharmacodynamic effects of afatinib and selumetinib.**

Individual pERK and pS6r intensity scores (H-scores) of tumor biopsies at baseline, on-treatment (day 15) and upon study discontinuation are presented as determined by immunohistochemistry staining. Mean H-score decreases were -52% for pERK and -39% for pS6-r. CRC, colorectal cancer; PC, pancreatic cancer; NSCLC, non-small cell lung cancer; A, afatinib; S, selumetinib; BID, twice daily; d, days.

## Discussion

In this clinical study we demonstrate that the MEK inhibitor selumetinib can be combined with the multiple-HER inhibitor afatinib without unacceptable toxicity, although not at full single agent doses because of dose-limiting toxicities. The RP2D was 20 mg afatinib QD and 25 mg selumetinib BID (21 days on/7 days off) for continuous afatinib dosing and also for intermittent dosing with both drugs in a 5 days on/2 days off regimen. The observed toxicities are in line with the monotherapy toxicity profiles of both agents. Yet, the use of high doses was not feasible as a result of overlapping toxicities such as gastro-intestinal toxicities and dehydration.

In parallel with this trial, two other studies with combined MEK and pan-HER inhibition were conducted in patients with *KRAS* mutant tumors.(13, 14) Emerging data from these trials showed a trend towards preferential activity in NSCLC compared to CRC and pancreatic cancer. These clinical observations are also supported by previous clinical studies that show that MEK inhibition added to second line docetaxel in patients with NSCLC can lead to



improved responses, whereas in CRC the addition of a MEK inhibitor to second line irinotecan did not result in clinical benefit.(15, 16)

Stable disease was the best overall response among all dose-levels. Although a patient with NSCLC had a tumor regression of -16% in dose-level 3, treatment was discontinued due to intolerable toxicity. This illustrates what has been observed throughout the study; the combination of afatinib and selumetinib is potentially effective at higher doses, yet reaching these doses seems clinically not feasible in this combination. The intermittent regimens that were explored, were expected to allow improvement of the efficacy to toxicity ratio. Unfortunately, patients still experienced unmanageable toxicities in the intermittent dose-levels, which also restricted dose increases for intermittent dosing. Moreover, the RP2D for intermittent dosing was determined at exactly the same dose for both drugs in the continuous regimen.

Both for selumetinib and afatinib, pharmacokinetic parameters are largely in line with previous studies.(10, 12) Our data show no signs of pharmacokinetic interactions between afatinib and selumetinib although the study design does not enable us to completely rule out a drug-drug interaction. The RP2D with continuous afatinib administration was found to be 25 mg BID selumetinib (21 days on/7 days off) and 20 mg afatinib continuously which is 33% and 50% of their monotherapy doses. At these doses, plasma concentration-time curves show that relatively low plasma levels are reached. For selumetinib, a concentration of 352 ng/ml is needed for 50% of pERK inhibition in peripheral blood mononuclear cells, as reported in a previous phase I trial. In this study, this concentration was reached for only 17% of each 12-hour dosing interval in the 21 days on/7 days off regimen. For afatinib, the concentration needed for 50% inhibition of cell proliferation in preclinical setting was determined as approximately 30 ng/ml, which is also supported by clinical efficacy in patients in whom these plasma concentrations were reached.(11) This target-concentration was consistently reached only in patients treated with continuous afatinib 30 mg, which was not tolerable in combination with selumetinib in the applied schedule. Although the relevance of target levels in this combination setting is unsure because these target levels are based on single-agent use, we assumed that the probability of response increases when the target levels of both drugs are more consistently reached. Based on this, it was decided to explore other regimens with the aim of increasing the plasma levels and exposure, starting with a 5 days on/2 days off regimen with doses of 30 mg afatinib QD and 25 mg selumetinib BID. Unfortunately, de-escalation of the afatinib dose from 30 mg to 20 mg QD (5 days on/2 days off) was necessary to manage toxicity, which resulted in not reaching afatinib concentrations needed for sufficient target engagement. No DLTs were observed in dose-level 5 and therefore the RP2D for intermittent dosing was established at 20 mg afatinib QD plus 25 mg selumetinib BID 5 days on/2 days off.

Despite relatively low plasma levels, we did observe pharmacodynamic effects in on-treatment biopsies that were taken in the second week of treatment. The intra-tumoral levels of pERK and pS6 decreased by on average 52% and 39%, respectively. This indicates that relevant MEK and pan-HER inhibition is reached during the treatment. Moreover, pERK

modulation correlated with exposure to selumetinib. However, this did not translate into objective clinical responses. The best responses were observed in patients with NSCLC, including tumor regression of 16% and disease stabilization for 8 months. It is unknown if these patients had relevant modulation of pERK and pS6 because no paired biopsies were available. Additionally, no reliable pERK or pS6 stainings were available from the patients treated in dose-level 5, which makes it unclear if relevant pharmacodynamic effects were established at RP2D for intermittent dosing.

The poor correlation between pathway modulation and clinical response could be due to a variety of mechanisms. First, inter-metastasis heterogeneity may play an important role because the pharmacodynamic analyses were based on a single lesion only. Insight into the relevance of this mechanism may be obtained by correlating the radiological response of the biopsied lesion to the pERK/pS6 modulation. For this study, data were not sufficient to perform these analyses.

Secondly, the observed pathway modulation may be transient or insufficient, meaning that resistance mechanisms occur shortly after the on-treatment biopsy which was performed in the second week. Several resistance mechanisms could play a role. Corcoran *et al.* reported that upon MEK inhibition, resistance occurs via expression of anti-apoptotic proteins BCL-XL.(17) Therefore, addition of a third agent such as the BCL-XL inhibitor navitoclax could be of interest, if clinically feasible. Furthermore, Burgess *et al.* showed that *KRAS* copy numbers, *KRAS* expression levels and the ratio *KRAS* mutant to wildtype can explain resistance to MEK inhibition (18) and Sun *et al.* showed that high tumor-expression of HER2/HER3 at baseline increased the probability of response on MEK and pan-HER inhibition.(2) Conversely, upregulation of HER2/HER3 during treatment could theoretically cause treatment resistance via pathway reactivation. Another important biomarker might be the nature of the *KRAS* mutation. Recent studies demonstrated that *KRAS*<sup>G12C</sup> mutations are more dependent on upstream signaling than other *KRAS* mutations. *In vitro* and *in vivo*, these *KRAS*<sup>G12C</sup> mutations are more sensitive to combined pan-HER and MEK inhibition.(19, 20) An ongoing phase I study with the specific *KRAS*<sup>G12C</sup> inhibitor AMG510 shows a partial response in three out of 225 patients and stable disease in 13 patients with *KRAS*<sup>G12C</sup> mutant solid tumors.(21)

For patients treated in our trial and in the other two trials investigating the combination of pan-HER and MEK inhibition, tumor material is being analyzed for a broad spectrum of biomarkers in a translational study on paired biopsies. DNA and RNA sequencing, multiplex IHC stainings and reverse phase protein arrays (RPPA) are being used with the aim of exploring the true mechanisms of response and resistance. The final results of these analyses are expected soon and may give us new insights into rational use of MEK and pan-HER inhibitors in the clinic. These results may also reveal differences in sensitivity of NSCLC versus the other tumor types, and the impact of the different *KRAS* mutations on response and resistance.

To improve treatment options for patients with a *KRAS* mutation, triple combinations could be effective to overcome resistance mechanisms. Potentially, synergistic effects may allow the use of relatively low doses of all agents, which is supported by preliminary data of MEK and pan-HER inhibition in *KRAS* mutant CRC organoids (unpublished). The same unpublished data

show that the dual combination, probably in combination with a chemotherapeutic agent, might provide an effective treatment option for patients with *KRAS* wild type tumors.

### **Conclusion**

Afatinib and selumetinib can be combined in continuous or intermittent dosing schedules in patients with *KRAS* mutant tumors, although single agent full doses cannot be applied due to overlapping toxicities. Although target engagement was demonstrated, no complete or partial responses were observed. We do therefore not recommend to further explore this combination until relevant biomarkers for response and resistance are defined to optimize patient inclusion.

### **Acknowledgements**

We thank all patients for participation, the clinical research units of the Radboud University Medical Center Nijmegen and the Antoni van Leeuwenhoek hospital – Netherlands Cancer Institute Amsterdam for conduct of the trial and Boehringer Ingelheim and AstraZeneca for providing study drugs and an unrestricted grant.

### **Disclosure of potential conflicts of interest**

JB and JS (partly) hold a patent on oral taxane formulations, are shareholders and part-time employees of Modra Pharmaceuticals, a company developing oral taxanes. JS is also CMO and board member of Byondis. Not related to the manuscript.

All other authors declare that they have no conflict of interest related to this study.

## References

1. Downward J. Targeting RAS signalling pathways in cancer therapy. *Nature reviews cancer*. 2003;3(1):11-22.
2. Sun C, Hobor S, Bertotti A, Zecchin D, Huang S, Galimi F, et al. Intrinsic resistance to MEK inhibition in KRAS mutant lung and colon cancer through transcriptional induction of ERBB3. *Cell reports*. 2014;7(1):86-93.
3. Migliardi G, Sassi F, Torti D, Galimi F, Zanella ER, Buscarino M, et al. Inhibition of MEK and PI3K/mTOR suppresses tumor growth but does not cause tumor regression in patient-derived xenografts of RAS-mutant colorectal carcinomas. *Clinical cancer research*. 2012;18(9):2515-25.
4. Adjei AA, Cohen RB, Franklin W, Morris C, Wilson D, Molina JR, et al. Phase I pharmacokinetic and pharmacodynamic study of the oral, small-molecule mitogen-activated protein kinase kinase 1/2 inhibitor AZD6244 (ARRY-142886) in patients with advanced cancers. *Journal of clinical oncology*. 2008;26(13):2139-46.
5. Janne PA, Shaw AT, Pereira JR, Jeannin G, Vansteenkiste J, Barrios C, et al. Selumetinib plus docetaxel for KRAS-mutant advanced non-small-cell lung cancer: a randomised, multicentre, placebo-controlled, phase 2 study. *The Lancet oncology*. 2013;14(1):38-47.
6. Canon J, Rex K, Saiki AY, Mohr C, Cooke K, Bagal D, et al. The clinical KRAS(G12C) inhibitor AMG 510 drives anti-tumour immunity. *Nature*. 2019;575(7781):217-23.
7. Huang L, Fu L. Mechanisms of resistance to EGFR tyrosine kinase inhibitors. *Acta pharmaceutica Sinica B*. 2015;5(5):390-401.
8. Eisenhauer EA, Therasse P, Bogaerts J, Schwartz LH, Sargent D, Ford R, et al. New response evaluation criteria in solid tumours: revised RECIST guideline (version 1.1). *European journal of cancer*. 2009;45(2):228-47.
9. R core development team. A language and environment for statistical computing. R foundation for statistical computing. Vienna, Austria. 2016. Available at <http://www.R-project.Org/>. Accessed April 12, 2020.
10. Wind S, Schmid M, Erhardt J, Goeldner RG, Stopfer P. Pharmacokinetics of afatinib, a selective irreversible ErbB family blocker, in patients with advanced solid tumours. *Clinical pharmacokinetics*. 2013;52(12):1101-9.
11. Yang JC, Sequist LV, Zhou C, Schuler M, Geater SL, Mok T, et al. Effect of dose adjustment on the safety and efficacy of afatinib for EGFR mutation-positive lung adenocarcinoma: post hoc analyses of the randomized LUX-Lung 3 and 6 trials. *Annals of oncology*. 2016;27(11):2103-10.
12. Banerji U, Camidge DR, Verheul HM, Agarwal R, Sarker D, Kaye SB, et al. The first-in-human study of the hydrogen sulfate (Hyd-sulfate) capsule of the MEK1/2 inhibitor AZD6244 (ARRY-142886): a phase I open-label multicenter trial in patients with advanced cancer. *Clinical cancer research*. 2010;16(5):1613-23.
13. Huijberts S, van Geel R, van Brummelen EMJ, Opdam FL, Marchetti S, Steeghs N, et al. Phase I study of lapatinib plus trametinib in patients with KRAS-mutant colorectal, non-small cell lung, and pancreatic cancer. *Cancer chemotherapy and pharmacology*. 2020;85:917-930.
14. van Geel R, van Brummelen EMJ, Eskens F, Huijberts S, de Vos F, Lolkema M, et al. Phase 1 study of the pan-HER inhibitor dacomitinib plus the MEK1/2 inhibitor PD-0325901 in patients with KRAS-mutation-positive colorectal, non-small-cell lung and pancreatic cancer. *British journal of cancer*. 2020;122:1166-1174.
15. Hochster HS, Uboha N, Messersmith W, Gold PJ, BH ON, Cohen D, et al. Phase II study of selumetinib (AZD6244, ARRY-142886) plus irinotecan as second-line therapy in patients with K-RAS mutated colorectal cancer. *Cancer chemotherapy and pharmacology*. 2015;75(1):17-23.
16. Janne PA, van den Heuvel MM, Barlesi F, Cobo M, Mazieres J, Crino L, et al. Selumetinib plus docetaxel compared with docetaxel alone and progression-free survival in patients with KRAS-mutant advanced non-small cell lung cancer: The SELECT-1 randomized clinical trial. *Jama*. 2017;317(18):1844-53.

17. Corcoran RB, Cheng KA, Hata AN, Faber AC, Ebi H, Coffee EM, et al. Synthetic lethal interaction of combined BCL-XL and MEK inhibition promotes tumor regressions in KRAS mutant cancer models. *Cancer cell*. 2013;23(1):121-8.
18. Burgess MR, Hwang E, Mroue R, Bielski CM, Wandler AM, Huang BJ, et al. KRAS allelic imbalance enhances fitness and modulates MAP kinase dependence in cancer. *Cell*. 2017;168(5):817-29.e15.
19. Nichols RJ, Haderk F, Stahlhut C, Schulze CJ, Hemmati G, Wildes D, et al. RAS nucleotide cycling underlies the SHP2 phosphatase dependence of mutant BRAF-, NF1- and RAS-driven cancers. *Nature cell biology*. 2018;20(9):1064-73.
20. Mainardi S, Mulero-Sanchez A, Prahallad A, Germano G, Bosma A, Krimpenfort P, et al. SHP2 is required for growth of KRAS-mutant non-small-cell lung cancer in vivo. *Nature medicine*. 2018;24(7):961-7.
21. Hong D, Kuo J, Sachter A et al. Codebreak100: Phase I study of AMG 510, a novel KRASG12C inhibitor, in patients (pts) with advanced solid tumors other than non-small cell lung cancer (NSCLC) and colorectal cancer (CRC). *Journal of clinical oncology*. 2020;38;15\_suppl 3511-3511.

## Supplemental data

**Table S1. Criteria for defining dose-limiting toxicities.**

Toxicity	DLT definition
Hematologic	<ul style="list-style-type: none"> <li>• Grade 4 neutropenia for <math>\geq 5</math> days</li> <li>• Grade <math>\geq 3</math> febrile neutropenia</li> <li>• Grade 4 anemia</li> <li>• Grade 4 thrombocytopenia</li> </ul>
Non-hematologic	<ul style="list-style-type: none"> <li>• AST <math>&gt; 5X</math> ULN OR ALT <math>&gt; 3X</math> ULN AND bilirubin <math>&gt; 2X</math> ULN (after exclusion of disease progression and/or bile duct obstruction)</li> <li>• Grade <math>\geq 4</math> rash, hand-foot syndrome or photosensitivity</li> <li>• Grade 3 rash, hand-foot syndrome or photosensitivity for more than 7 days despite adequate supportive treatment.</li> <li>• Grade <math>\geq 3</math> nausea, vomiting or diarrhea in the presence of maximal supportive care</li> <li>• Grade <math>\geq 2</math> peripheral sensory or motor neuropathy</li> <li>• Grade <math>\geq 3</math> clinically significant toxicity related to study treatment, other than those listed above, with the following exceptions:               <ul style="list-style-type: none"> <li>○ Electrolyte disturbances that respond to correction within 24 hours</li> <li>○ Grade 3 hypertension that is adequately controlled by the addition of up to 2 additional antihypertensive medications</li> <li>○ Grade 3 pyrexia that does not result in study discontinuation</li> </ul> </li> </ul>
Cardiac	<ul style="list-style-type: none"> <li>• Ejection fraction <math>&lt; 55\%</math> with an absolute decrease of <math>&gt;10\%</math> from baseline with confirmation within 14 days</li> </ul>
Other	<ul style="list-style-type: none"> <li>• Inability to receive <math>\geq 75\%</math> of scheduled doses in treatment period due to toxicity related to study treatment</li> <li>• Grade 2 or higher toxicity that occurs beyond 28 days which in the judgment of the investigator is a DLT</li> </ul>

Abbreviations: AST, aspartate aminotransferase; ALT alanine aminotransferase; ULN, upper limit of normal; DLT, dose limiting toxicity







# CHAPTER 5

Conclusions and  
perspectives

The past decades, the scope of anticancer therapy has been shifted from treatment with cytotoxic agents in unselected patient populations to personalized therapies with targeted agents in biomarker-selected populations. The main focus of this thesis is to optimize personalized therapies by the rational combination of inhibitors of the EGFR-RAS-RAF-MEK-ERK (MAPK) pathway. Activating mutations, for example in the genes *BRAF* or *KRAS*, lead to sustained proliferative signaling. By inhibiting proteins of the MAPK pathway, e.g. the BRAF protein, with targeted agents proliferation can be encountered leading to anti-tumor response.(1, 2) Despite many preclinical and clinical studies devoted to the inhibition of the MAPK pathway, the effectiveness of targeted agents remains disappointing with modest response and survival rates. Here, the major challenge is to improve efficacy by overcoming intrinsic and acquired resistance.(3, 4) Combining targeted agents might improve efficacy and overcome this resistance.

As already touched upon in the Introduction, the principles of synthetic lethality and collateral vulnerability to overcome resistance formed the bases for the treatment combinations in this thesis. Although all drugs were rationally combined, not all were successful due to a number of conditions that were not met. Firstly, the timing of treatment and selection of patients needs further optimization. Therefore, refinement of the understanding of molecular characteristics of tumors and mapping of drivers for intrinsic or acquired resistance is pivotal. Furthermore, the efficacy-toxicity balance should be acceptable on individual and group level. These conditions are necessary for the development of successful personalized targeted therapies.

All above-mentioned conditions were met for the most part for the effective combination of encorafenib and cetuximab in *BRAF*<sup>V600E</sup> mutant colorectal cancer as described in **chapter 3**, but could still be optimized further to improve treatment outcome.

Following the disappointing response rate of only 5% with the BRAF inhibitor vemurafenib in patients with *BRAF*<sup>V600E</sup> mutant colorectal cancer (5, 6), detailed preclinical information was necessary to investigate the difference in molecular biology of colorectal cancer and melanoma. In contrast to *BRAF*<sup>V600E</sup> mutant melanoma, BRAF inhibition in *BRAF* mutant colorectal cancer cell lines resulted in upregulation of EGFR causing activation of RAS and CRAF. This signaling cascade sustained MAPK pathway activation and ongoing tumor cell proliferation. Nevertheless, by blocking EGFR and BRAF simultaneously, a significant anti-tumor effect was acquired.(7) Several double and triple combinations of EGFR and BRAF inhibitors with or without a MEK inhibitor confirmed this preclinical results in the clinic and one of these combinations is described in **chapter 3**. In this phase III trial, the combination of the EGFR inhibitor cetuximab, the BRAF inhibitor encorafenib with or without the MEK inhibitor binimetinib is compared to standard of care in patients with *BRAF*<sup>V600E</sup> mutant colorectal cancer. Although the response rate and progression free survival were better in the triplet than the doublet combination in the Safety Lead-In part of this study (**chapter 3.1**), no significant difference in efficacy was observed in the full population of the trial (objective response rate triplet 26% and doublet 20%; overall survival triplet 9.0 months and doublet 8.4 months).(8) Nevertheless, both regimens improved efficacy compared to

standard of care (objective response rate 2 % and overall survival 5.4 months). Furthermore, the toxicity of the triplet combination was worse than the doublet combination with a significantly higher incidence of skin and gastro-intestinal toxicity. As a result of the better efficacy-toxicity profile of the doublet, this regimen is recently approved by the Food and Drug Administration (FDA) for the treatment of *BRAF*<sup>V600E</sup> mutant colorectal cancer patients.(9) Additionally, approval of this combination by the European Medicines Agency is expected in the near future.

The next step is to optimize treatment timing by investigating if overall survival could be prolonged by administration of the doublet or the triplet in the first line palliative setting for metastatic disease. This is being studied in the ANCHOR-CRC study (clinicaltrials.gov identifier: NCT03693170).

Although the abovementioned intrinsic resistance mechanism could be overcome by combining EGFR and BRAF inhibitors, an anti-tumor effect was not observed in all patients of the cohort study in **chapter 3.3** and acquired resistance still limits the duration of response. Intrinsic and acquired resistance seems to rely on secondary mutations in the MAPK pathway, upstream signaling and cross-linked pathways. Moreover, *BRAF* and *KRAS* mutations seem not mutually exclusive upon treatment. In this retrospective cohort study was searched for single mutations driving resistance, but the question is if it might be better to take a comprehensive view on tumor biology by looking at a signature or profile of gene expression levels. By mapping expression levels into a heat map, Tian *et al.* and In 't Veld *et al.* described a BRAF-like signature for colorectal cancer. The *BRAF* gene is not mutated in these tumors, but the tumors behave similar to 'real' *BRAF* mutated colorectal cancers as a result of the expression profile of other genes and have the same poor prognosis.(10, 11) Future research should focus on finding an effective personalized treatment for these BRAF-like tumors. Furthermore, not all 'real' *BRAF* mutated tumors are similar and two gene expression subtypes were earlier identified. *BRAF*<sup>V600E</sup> mutant subtype 1 harbored activation of KRAS/mTOR/AKT/4EBP1 and EMT with high infiltration of immune cells and epithelial to mesenchymal transition, while *BRAF*<sup>V600E</sup> mutant subtype 2 was mainly dysregulated in cell cycle checkpoints. Subtype 1 revealed a higher sensitivity for EGFR, BRAF and MEK inhibition than subtype 2. These results show the complex molecular landscape of *BRAF* mutations and imply that patient selection should be further refined to improve treatment outcomes.(12, 13)

In short, the doublet of encorafenib and cetuximab was recently approved by the FDA for the treatment of *BRAF*<sup>V600E</sup> mutant colorectal cancer. However, the treatment should be further optimized on patient selection and timing.

Not only in *BRAF*<sup>V600E</sup> mutant colorectal cancer the refinement of patient selection and treatment timing is of pivotal importance, but also in *BRAF*<sup>V600E</sup> mutant melanoma that developed resistance to BRAF and/or MEK inhibitors (**chapter 2**). Here, the crucial mechanism of resistance is the development of secondary mutations of the MAPK pathway leading to a short-term hyperactivation of the pathway that can be exploited by the HDAC inhibitor vorinostat. Vorinostat leads to a prolonged hyperactivation and upregulation of

reactive oxygen species (ROS) levels resulting in cell death (**chapter 2.1**). Although the preclinical results were compelling, the first patients treated with vorinostat continuously showed 'mixed responses'. Paired biopsies of these patients were analyzed and showed that secondary mutations, such as *NRAS* or *KRAS* mutations, caused resistance and were eliminated within 14 days of short-term treatment with vorinostat. Therefore, the treatment schedule was changed according to these emerging findings. Patients are currently treated with vorinostat for 14 days and thereafter BRAF and/or MEK inhibition is re-introduced. This proof of concept study is ongoing, but the results of the first 11 patients are promising with one partial response and three patients with a clinically relevant stable disease of > 5 months.

At baseline and every two weeks, blood samples are being taken for the analyses of circulating tumor DNA (ctDNA). ctDNA will only be used for exploratory endpoints in this study, but hopefully treatment might be changed based on ctDNA findings in the future. Ideally, the treatment will be switched back and forth between vorinostat and BRAF inhibition upon the development and elimination of resistant clones with secondary mutations. Furthermore, since a major part of the patients that developed resistance to BRAF and/or MEK inhibitors are rapidly progressive, resistance should ideally be detected in an early stage. Only relatively fit patients might have the time to benefit from treatment switch, before their physical condition decreases due to rapid disease progression. ctDNA can detect resistance in an earlier stage than the conventional radiological assessments.(14, 15) This so-called 'track and treat' concept is currently investigated in *EGFR* mutant non-small cell lung cancer patients in our institute. The MET inhibitor crizotinib will be added to *EGFR* inhibition upon detection of *MET* amplification (clinicaltrials.gov identifier: NCT04148066). Additionally, the analysis of ctDNA at baseline might provide biomarkers such as *NRAS* or *KRAS* mutations to restrict enrollment to patients that might benefit from vorinostat treatment based on the molecular profile of the tumor. In this way, liquid biopsies will help to optimize treatment timing and patient selection as well.

The efficacy and toxicity balance was a major concern in the three phase I trials in **chapter 4** investigating the combination of a pan-HER inhibitor and MEK inhibitor in patients with *KRAS* mutant tumors. The efficacy was low with only one partial responder in the study with lapatinib and trametinib and no complete responders among the three trials. One of the reasons for this low efficacy lies in the impossibility to dose the drugs on full single agent doses due to modest tolerability of the combinations. The tolerability of the lapatinib and trametinib combination was the best of the three combinations tested, whereby the recommended phase two regimen consisted of approximately 50% of the single agent dose of both drugs. The combination of afatinib and selumetinib resulted in a maximum tolerable dose of 50% and 25% of single agent doses respectively. For the combination of dacomitinib and PD-0325901, no recommended phase two dose could be established due to major toxicity that precluded long-term treatment. Although intermittent treatment schedules were investigated to optimize the efficacy-toxicity balance, no significant improvement was made.

Currently, a large translational retrospective study investigating the lack of efficacy is being performed in paired tumor biopsies of patients treated in the three trials. In this project, a broad spectrum of biomarkers is being analyzed by different analytical methods, including DNA and RNA sequencing, multiplex immunohistochemistry staining and reverse phase protein arrays (RPPA). By DNA and RNA sequencing, the nature of the *KRAS* mutation and the allelic imbalance between *KRAS* mutant and *KRAS* wildtype will be investigated. New insights into the biology of *KRAS* mutated tumors have shown that *KRAS*<sup>G12C</sup> mutations are more dependent on upstream signaling than other variants (16, 17), which might make these specific mutations more sensitive for the combination of pan-HER and MEK inhibition. Furthermore, Burgess *et al.* reported that the ratio between *KRAS* mutant and *KRAS* wildtype modulates the cells dependency on MAPK signaling.(18) Immunohistochemistry staining will include, but is not limited to markers of apoptosis, phosphorylation levels of proteins of the MAPK and cross-linked pathways and immune cells. Finally, signaling markers, proliferation markers, survival markers and immune markers will be analyzed by RPPA. The results are expected soon and may provide information to refine patient selection for the combination of pan-HER and MEK inhibitors. We recommend to await these results and if a clear pattern for resistance or response is established, this might form the basis of further development of an effective treatment regimen for patients with *KRAS* mutant solid tumors.

In conclusion, the research described in this thesis provides evidence of combination strategies with targeted agents inhibiting the MAPK pathway to overcome and to interfere with resistance. Although the treatment rationales among the different clinical trials are all based on the principles of synthetic lethality and collateral vulnerability, treatment outcomes differ among tumor types and patients. Here, intra- and inter-patient tumor heterogeneity is a remaining challenge. This emphasizes that more detailed knowledge of predictive biomarkers and resistance mechanisms is pivotal to construct an effective therapy. The majority of inclusion criteria for clinical trials use one driver mutation detected in a single tumor biopsy to select patients. This way of selection has some limitations, since more than one mutation might drive tumor development and signaling pathways interconnect. Additionally, a single tumor biopsy may only present one clone of the tumor. To overcome these limitations, valuable novel technologies such as liquid biopsies are under development to optimize patient selection. By investigating the comprehensive molecular landscape of tumors, more detailed, useful information on biology and behavior might be provided. Moreover, liquid biopsies analyzing circulating tumor DNA or RNA may further optimize personalized medicine. Interestingly, real-time monitoring becomes available by using liquid biopsies to detect resistance in an early stage. This might ideally lead to sequentially or simultaneously administered combinations according to the underlying intrinsic and acquired resistance mechanisms. These combinations should not be restricted to targeted agents, but also include other treatment modalities such as radiotherapy, chemotherapy, hormonal therapy or immunotherapy.

## References

1. Zia Y, Chen L, Daud A. Future of combination therapy with dabrafenib and trametinib in metastatic melanoma. *Expert opinion on pharmacotherapy*. 2015;16(14):2257-63.
2. Wang L, Bernards R. Taking advantage of drug resistance, a new approach in the war on cancer. *Frontiers of medicine*. 2018;12(4):490-5.
3. Obaid NM, Bedard K, Huang WY. Strategies for overcoming resistance in tumours harboring BRAF mutations. *International journal of molecular sciences*. 2017;18(3):585.
4. Michielin O, Hoeller C. Gaining momentum: New options and opportunities for the treatment of advanced melanoma. *Cancer treatment reviews*. 2015;41(8):660-70.
5. Kopetz S, Desai J, Chan E, Hecht JR, O'Dwyer PJ, Maru D, et al. Phase II pilot study of vemurafenib in patients with metastatic BRAF-mutated colorectal cancer. *Journal of clinical oncology*. 2015;33(34):4032-8.
6. Prahallad A, Sun C, Huang S, Di Nicolantonio F, Salazar R, Zecchin D, et al. Unresponsiveness of colon cancer to BRAF(V600E) inhibition through feedback activation of EGFR. *Nature*. 2012;483(7387):100-3.
7. Corcoran RB, Ebi H, Turke AB, Coffee EM, Nishino M, Cogdill AP, et al. EGFR-mediated reactivation of MAPK signaling contributes to insensitivity of BRAF mutant colorectal cancers to RAF inhibition with vemurafenib. *Cancer discovery*. 2012;2(3):227-35.
8. Kopetz S, Grothey A, Yaeger R, Van Cutsem E, Desai J, Yoshino T, et al. Encorafenib, Binimetinib, and Cetuximab in BRAF V600E-mutated colorectal cancer. *The New England journal of medicine*. 2019;381(17):1632-43.
9. Food and Drug Administration. FDA approves encorafenib in combination with cetuximab for metastatic colorectal cancer with a BRAF V600E mutation. 2020. Available from: <https://www.fda.gov/drugs/resources-information-approved-drugs/fda-approves-encorafenib-combination-cetuximab-metastatic-colorectal-cancer-braf-v600e-mutation>. Accessed on 20 April 2020.
10. In 't Veld S, Duong KN, Snel M, Witteveen A, Beumer IJ, Delahaye L, et al. A computational workflow translates a 58-gene signature to a formalin-fixed, paraffin-embedded sample-based companion diagnostic for personalized treatment of the BRAF-mutation-like subtype of colorectal cancers. *High-throughput*. 2017;6(4):6-16.
11. Tian S, Simon I, Moreno V, Roepman P, Tabernero J, Snel M, et al. A combined oncogenic pathway signature of BRAF, KRAS and PI3KCA mutation improves colorectal cancer classification and cetuximab treatment prediction. *Gut*. 2013;62(4):540-9.
12. Barras D, Missiaglia E, Wirapati P, Sieber OM, Jorissen RN, Love C, et al. BRAF V600E mutant colorectal cancer subtypes based on gene expression. *Clinical cancer research*. 2017;23(1):104-15.
13. Middleton G, Yang Y, Campbell CD, Andre T, Atreya CE, Schellens JHM, et al. BRAF-mutant transcriptional subtypes predict outcome of combined BRAF, MEK, and EGFR blockade with dabrafenib, trametinib, and panitumumab in patients with colorectal cancer. *Clinical cancer research* 2020. E-pub ahead of print.
14. Calapre L, Warburton L, Millward M, Ziman M, Gray ES. Circulating tumour DNA (ctDNA) as a liquid biopsy for melanoma. *Cancer letters*. 2017;404:62-9.
15. Gray ES, Rizos H, Reid AL, Boyd SC, Pereira MR, Lo J, et al. Circulating tumor DNA to monitor treatment response and detect acquired resistance in patients with metastatic melanoma. *Oncotarget*. 2015;6(39):42008-18.
16. Mainardi S, Mulero-Sanchez A, Prahallad A, Germano G, Bosma A, Krimpenfort P, et al. SHP2 is required for growth of KRAS-mutant non-small-cell lung cancer in vivo. *Nature medicine*. 2018;24(7):961-7.
17. Nichols RJ, Haderk F, Stahlhut C, Schulze CJ, Hemmati G, Wildes D, et al. RAS nucleotide cycling underlies the SHP2 phosphatase dependence of mutant BRAF-, NF1- and RAS-driven cancers. *Nature cell biology*. 2018;20(9):1064-73.

18. Burgess MR, Hwang E, Mroue R, Bielski CM, Wandler AM, Huang BJ, et al. KRAS allelic imbalance enhances fitness and modulates MAP kinase dependence in cancer. *Cell*. 2017;168(5):817-29.e15.





# APPENDICES

Summary

Nederlandse samenvatting

List of Publications

Affiliations

Dankwoord

Curriculum Vitae

## Summary

Activating mutations of the EGFR-RAS-RAF-MEK-ERK (MAPK) pathway, mostly in the *BRAF* or *KRAS* gene, lead to sustained proliferation of cancer cells. The inhibition of proteins of the MAPK pathway with targeted agents such as BRAF inhibitors encounters this proliferation resulting in an anti-tumor response. Although a large number of novel anticancer agents targeting the MAPK pathway have been developed and investigated in the past decade, response rates and overall survival remain disappointing. A major problem here is intrinsic and acquired resistance. Therefore, the focus of this thesis was to optimize combinations of targeted inhibitors of the MAPK pathway to overcome resistance.

The Introduction (**chapter 1**) focuses on two strategies, synthetic lethality and collateral vulnerability, to overcome resistance. The rational combinations of targeted agents in this thesis are based on these strategies. Synthetic lethality is defined as combining two or more mutations or drugs causing lethality to cancer cells, but do not have a lethal effect by single appearance. Collateral vulnerability is highlighted by the development of new vulnerabilities of cancer cells after acquired resistance to an anticancer agent. After the development of acquired resistance, the cancer cells become sensitive to a drug that was not effective before administration of the first drug.

**Chapter 2** describes the treatment with the histone deacetylase inhibitor vorinostat in *BRAF<sup>V600E</sup>* mutant metastatic melanoma resistant to BRAF inhibition, starting with the preclinical development in **chapter 2.1**. The resistance is mostly caused by reactivation of the MAPK pathway. This resistance mechanism is associated with increased levels of reactive oxygen species (ROS) in which the cysteine-glutamate antiporter SLC7A11 plays a pivotal role. By suppression of SLC7A11 with vorinostat, the already high levels of ROS in resistant melanoma cells were increased to a lethal level. The result was a selective apoptotic death of the drug resistant tumor cells. Additionally, a dramatic tumor regression could be established in mice with BRAF inhibitor resistant melanoma treated with vorinostat. Based on the preclinical results a clinical proof of concept study was initiated with oral treatment of vorinostat 360 mg daily in patients with *BRAF<sup>V600E</sup>* mutant melanoma resistant to BRAF inhibitors. The first six patients treated with continuously vorinostat showed a 'mixed response', meaning progression of BRAF inhibitor sensitive cell clones and regression of BRAF inhibitor resistant cell clones. Acquired mutations in the MAPK pathway, e.g. *NRAS<sup>Q61H</sup>* and *KRAS<sup>G12C</sup>*, were found in the baseline tumor biopsies of the patients. This secondary mutations causing resistance were eliminated after 14 days of vorinostat treatment. These results were the basis for a protocol amendment in which the continuous treatment was switched to sequential treatment with 14 days of vorinostat and thereafter reintroduction of BRAF inhibitors/MEK inhibitors. The protocol of this proof of concept study is described in **chapter 2.2**. The study was designed with a Simon Two-stage design recruiting a total of 26 patients. The primary aim was to demonstrate a response rate of progressive target lesion of  $\geq 30\%$ . Secondary aims were to determinate the safety of vorinostat and to demonstrate that acquired mutations in the MAPK pathway can be detected by circulating tumor DNA (ctDNA) and eliminated by short treatment with

vorinostat. Furthermore, pharmacokinetic, pharmacodynamic and pharmacogenetic analyses in tumor and blood samples will be performed to explore mechanisms of resistance and response. The first results of this proof of concept study are presented in the interim analysis in **chapter 2.3**. A total of 11 patients with resistant *BRAF*<sup>V600E</sup> mutant melanoma were treated with vorinostat for 14 days and thereafter BRAF inhibitors/MEK inhibitors were reintroduced. An overall response rate of 25% was observed in the 11 evaluable patients. In these patients, the median time to progression was 50 days. In three patients was the time on treatment more than five months, which is considered as a significant clinical benefit. The toxicity profile of this alternating regimen was good without serious adverse events related to vorinostat. The ctDNA analysis showed acquired mutations in the *NRAS* gene at baseline in three patients, but this secondary mutation causing resistance was not eliminated upon vorinostat treatment in all three patients. Currently, seven more patients need to be recruited to draw conclusions for part 1 of the Simon Two-stage design. In case of three or more favorable responders, eight additional patients will be recruited in part 2 of the study.

The *BRAF*<sup>V600E</sup> mutation is also found in 10-15% of the patients with colorectal cancer and results in a poor prognosis and treatment failure after first line treatment in the palliative setting. **Chapter 3** highlights several aspects of a novel treatment combination for patients with *BRAF*<sup>V600E</sup> mutant metastatic colorectal cancer. This treatment is a combination of the BRAF inhibitor encorafenib and the EGFR inhibitor cetuximab with or without the MEK inhibitor binimetinib. Promising results were achieved in a phase I and phase II trial with the doublet therapy of encorafenib and cetuximab and therefore the randomized BEACON CRC phase III trial was initiated to investigate if this triplet or doublet therapy was more effective than standard care. Since the triplet combination was never administered in patients before, this phase III trial started with a safety lead-in part to determine safety and preliminary efficacy of the triplet combination of encorafenib, cetuximab and binimetinib (**chapter 3.1**). A total of 30 patients were treated in this safety lead-in part with encorafenib 300 mg daily, binimetinib 45 mg twice daily and cetuximab, initial infusion 400 mg/m<sup>2</sup> followed by 250 mg/m<sup>2</sup> weekly. Dose-limiting toxicities were observed in five patients, including cetuximab-related infusion reactions (n=2), serous retinopathy (n=2) and reversible decreased left ventricular ejection fraction (n=1). Fatigue (13%), urinary tract infections (10%), anemia (10%), increased aspartate aminotransferase (10%) and increased creatine phosphokinase (10%) were most common grade 3 or 4 adverse events. The confirmed overall response rate was 48% with a median progression free survival of 8.0 months and median overall survival of 15.2 months. These results show that the triplet combination can be safely administered and that the preliminary efficacy was promising. Although the results of the safety lead-in part were very promising, the efficacy of the triplet was slightly disappointing in the full population of the phase III trial. Here, resistance limits the clinical benefit of the treatment and therefore we performed the retrospective cohort study described in **chapter 3.3**. Tumor biopsies of 37 patients were included to search for

genetic alterations causing intrinsic or acquired resistance. Mutations were mostly found in the PI3K pathway and upstream receptor tyrosine kinases for both types of resistance. A better understanding of these genetic alterations might improve response duration of simultaneously or alternatingly administered combinations of targeted inhibitors. **Chapter 3.2** discusses a review of the clinical pharmacology, including pharmacokinetics, pharmacodynamics, safety and efficacy, of the combination of encorafenib and cetuximab with or without binimetinib. To place the novel doublet or triplet regimen in a broader perspective, the current treatment field for patients with BRAFV600E mutant metastatic colorectal cancer is also summarized in this review.

**Chapter 4** describes the results of three phase I trials investigating different combinations of MEK and pan-HER inhibition in patients with *KRAS* mutant metastatic colorectal cancer, non-small cell lung cancer (NSCLC) or pancreatic cancer. Currently, no direct inhibitors of the *KRAS* protein are available with the exception of AMG510 targeting *KRAS*<sup>G12C</sup>. Preclinical results showed that relevant responses can be achieved by combined MEK and pan-HER inhibition in *KRAS* mutated colorectal cancer cell lines and mouse-models. This approach was translated into three treatment combinations for patient with *KRAS* mutant solid tumors. **Chapter 4.1** discusses the combination of the MEK inhibitor PD-0325901 and pan-HER inhibitor dacomitinib. **Chapter 4.2** highlights the results for the combination of trametinib and lapatinib investigated in 34 patients. Furthermore, 26 patients were treated with the combination of selumetinib and afatinib as described in **chapter 4.3**. The primary aim of the three clinical trials was to determine the recommended phase two regimen of the combination. Secondary aims were to investigate the safety and anti-tumor effect. Unfortunately, dose escalation was limited due to toxicity and single agent doses were not tolerable in the combinations. In our effort to optimize the efficacy-toxicity balance, we investigated continuous and intermittent treatment schedules. However, tolerability remained a limitation for dose-escalation. For the combination of dacomitinib and PD-0325901 was the recommended phase 2 dose established on 15 mg dacomitinib and 6 mg PD-0325901 (21 days on/ 7 days off), but long-term treatment was impossible due to the toxicity profile. Most common toxicities in the 41 treated patients were rash (85%), diarrhea (88%) and nausea (63%). The longest treatment duration was seen in a patient with NSCLC and no responses were observed. Therefore, we do not recommend to further explore this combination in patients due to its toxicity profile. A total of eight patients treated with the combination of trametinib and lapatinib among different dose-levels experienced dose-limiting toxicities, including grade 3 rash, diarrhea, aspartate aminotransferase elevation and multiple grade 2 toxicities leading to treatment delay or inability to receive 75% of planned doses. Trametinib and lapatinib was tolerable in an intermittent dosing schedule with sufficient target engagement. Moreover, preliminary signs of anti-tumor activity were observed in NSCLC patients.

For the last combination of selumetinib and afatinib, the recommended phase 2 regimen for continues afatinib dosing was established at a dose of afatinib 20 mg daily and selumetinib 25 mg twice daily 21 days on/7 days off. The recommended phase 2 dose for intermittent

dosing was 20 mg afatinib QD and 25 mg selumetinib BID, both 5 days on/2 days off. The best response was stable disease for 221 days and was observed in a patient with NSCLC. Overall, we do not recommend further investigation of one of the three combinations with MEK plus pan-HER inhibitors, before a better biomarker for patient selection has been defined that might improve response.

## Nederlandse samenvatting

Activerende mutaties in de EGFR-RAS-RAF-MEK-ERK (MAPK) signaaltransductie route worden vooral gevonden in het *BRAF* of *KRAS* gen en leiden tot aanhoudende proliferatie in kankercellen. De remming van deze eiwitten van de MAPK signaaltransductie route met doelgerichte geneesmiddelen zoals BRAF remmers gaat deze proliferatie tegen resulterend in een anti-tumor respons. Ondanks dat een groot aantal nieuwe anti-kanker geneesmiddelen gericht tegen de MAPK signaaltransductie route zijn ontwikkeld en onderzocht in het afgelopen decennium, blijven het responspercentage en de overleving tegenvallen. Een groot probleem hierbij is intrinsieke en verworven resistentie.

De Introductie (**hoofdstuk 1**) van dit proefschrift richt zich op twee strategieën, synthetische letaliteit en collaterale kwetsbaarheid, om resistentie tegen te gaan. De rationale combinatie van doelgerichte geneesmiddelen in de verschillende hoofdstukken is gebaseerd op deze strategieën. Synthetische letaliteit wordt gekenmerkt door de combinatie van twee of meer mutaties of geneesmiddelen die letaal zijn voor kankercellen, maar apart van elkaar dit effect niet hebben. Collaterale kwetsbaarheid is de ontwikkeling van nieuwe kwetsbaarheden van kankercellen, nadat er verworven resistentie tegen een antikanker medicijn is opgetreden. Na de ontwikkeling van deze resistentie zijn kankercellen gevoelig geworden voor een tweede medicijn dat eerder niet effectief was.

**Hoofdstuk 2** beschrijft de behandeling met de histon deacetylase remmer, vorinostat, in *BRAF<sup>V600E</sup>* gemuteerde, gemetastaseerde melanomen die resistent zijn geworden voor BRAF-remmers. Dit hoofdstuk start met de preklinische ontwikkeling van deze behandeling in **hoofdstuk 2.1**. De resistentie tegen BRAF-remmers wordt meestal veroorzaakt door reactivatie van de MAPK signaaltransductie route. Dit resistentie mechanisme is geassocieerd met verhoogde waarden van vrije zuurstofradicalen, waarbij de cysteine-glutamaat antiporter SLC7A11 een belangrijke rol speelt. Door suppressie van SLC7A11 met vorinostat worden de al hoge waarden van vrij zuurstofradicalen in resistente melanoomcellen verder verhoogd tot een letaal niveau. Het resultaat hiervan is een selectieve geprogrammeerde celdood (apoptose) van resistente tumorcellen. Ook in muizen met resistente *BRAF<sup>V600E</sup>* gemuteerde melanomen werd een dramatische tumor afname gezien met vorinostat. Gebaseerd op deze preklinische resultaten werd een klinische *proof of concept* studie gestart met orale behandeling met vorinostat 360 mg per dag in patiënten met *BRAF<sup>V600E</sup>* gemuteerde melanomen, die resistentie hadden ontwikkeld op BRAF-remming. De eerste 6 behandelde patiënten met dagelijks vorinostat hadden een gemengde respons op de behandeling, waarbij progressie van BRAF-remmer gevoelige cellen en regressie van BRAF-remmer resistente cellen optrad. Verworven mutaties in de MAPK signaaltransductie route, bijvoorbeeld *NRAS<sup>Q61H</sup>* en *KRAS<sup>G12C</sup>*, werden gevonden in de baseline tumorbipten van deze patiënten. Deze secundaire mutaties die resistentie veroorzaken werden geëlimineerd na een 14-daagse behandeling met vorinostat. Deze resultaten vormden de basis voor een protocol aanpassing waarbij de continue behandeling werd omgezet naar een sequentiële behandeling met 14 dagen vorinostat en daarna herstart van BRAF-remmers/MEK-remmers. Het studieprotocol is terug te vinden in **hoofdstuk 2.2**. De studie is opgezet met een Simon

Two-stage design met een totale studiepopulatie van 26 patiënten. Het primaire doel was het aantonen van een responspercentage van progressieve target laesies van minimaal 30%. Secundaire doelen bestaan uit het vaststellen van de veiligheid van vorinostat, het onderzoeken of verworven mutaties in de MAPK signaaltransductie route gedetecteerd konden worden in circulerend tumor DNA (ctDNA) en of deze mutaties geëlimineerd kunnen worden door kortdurende behandeling met vorinostat. Verder zullen er farmacokinetische, farmacodynamische en farmacogenetische analyses plaatsvinden in tumor materiaal en bloed om te kijken naar mechanismen die resistentie of respons kunnen veroorzaken. De eerste resultaten van deze *proof of concept* studie worden gepresenteerd in de interim analyse in **hoofdstuk 2.3**. In totaal zijn 11 patiënten met resistente *BRAF*<sup>V600E</sup> gemuteerde melanomen behandeld. Het responspercentage was 25% in deze patiënten en de tijd tot progressie was gemiddeld 50 dagen. Drie patiënten waren langer dan vijf maanden onder behandeling en dat wordt gezien als een significant klinische voordeel. Het toxiciteitsprofiel van deze alternerende behandeling was goed zonder dat er ernstige toxiciteit gerelateerd aan vorinostat is opgetreden. De ctDNA analyse toonde verworven mutaties in het *NRAS* gen aan in drie patiënten, maar deze resistentie veroorzakende mutatie kon niet in alle patiënten worden geëlimineerd met kortdurende vorinostat behandeling. Op dit moment zijn er nog zeven patiënten nodig om een conclusie te kunnen trekken uit het eerste deel van het Simon Two-stage design. Als er dan drie of meer goed responderende patiënten zijn, zullen er nog acht aanvullende patiënten worden behandeld in het tweede deel van de studie.

De *BRAF*<sup>V600E</sup> mutatie wordt ook gevonden in 10-15% van de patiënten met een colorectaal carcinoom en zorgt voor een slechte prognose met falen van therapie na de eerstelijns behandeling in de palliatieve setting. **Hoofdstuk 3** belicht verschillende aspecten van een nieuwe behandelcombinatie voor patiënten met gemetastaseerd, *BRAF*<sup>V600E</sup> gemuteerd colorectaal carcinoom. Deze behandeling bestaat uit een combinatie van de *BRAF*-remmer encorafenib, de *EGFR*-remmer cetuximab met of zonder de *MEK*-remmer binimetinib. Veelbelovende resultaten werden geboekt in fase I en II studies met de duale combinatie van encorafenib en cetuximab en daarom is de gerandomiseerde BEACON CRC fase III studie opgezet om te onderzoeken of de duale of *triplet* combinatie effectiever is dan standaardbehandeling. Omdat de *triplet* niet eerder was getest in patiënten, werd deze fase III studie gestart met een *safety lead-in* deel om de veiligheid en preliminaire effectiviteit vast te stellen (**hoofdstuk 3.1**). In totaal werden 30 patiënten behandeld in deze *safety lead-in* met encorafenib 300 mg per dag, binimetinib 45 mg, twee keer per dag en cetuximab met een startdosering van 400 mg/m<sup>2</sup> en daarna wekelijks 250 mg/m<sup>2</sup>. Ernstige dosis-limiterende bijwerkingen (DLTs) werden gezien in vijf patiënten, inclusief cetuximab-gerelateerde infusie reacties (n=2), sereuze retinopathie (n=2) en reversibele daling van de linker ventrikel ejectiefractie (n=1). Vermoeidheid (13%), urineweginfecties (10%), anemie (10%), verhoogd aspartaat aminotransferase (0%) en verhoogd creatine-fosfokinase (10%) waren de meest voorkomende graad 3 en 4 bijwerkingen. Het bevestigde responspercentage was 48% met een mediane progressievrije overleving van 8.0 maanden en een mediane overleving van 15.2 maanden. Deze resultaten laten zien dat de *triplet* combinatie veilig kan worden

toegediend aan patiënten en dat de preliminaire effectiviteit veelbelovend is. Ondanks deze goede resultaten in de *safety lead-in*, viel de effectiviteit in de volledige populatie van de fase III studie lichtelijk tegen. Resistentie limiteert hier waarschijnlijk de effectiviteit van de behandeling en om dat beter te onderzoeken hebben we de retrospectieve cohortstudie in **hoofdstuk 3.3** uitgevoerd. Tumor bipten van 37 patiënten werden geïncludeerd om te onderzoeken welke genetische afwijkingen intrinsieke of verworven resistentie kunnen veroorzaken. Mutaties werden met name aangetoond in de PI3K signaaltransductie route en in receptor tyrosine kinases voor beide vormen van resistentie. Een beter begrip van deze genetische afwijkingen kan de respons duur van gelijktijdig of alternerend toegediende, doelgerichte behandelcombinaties verbeteren.

**Hoofdstuk 3.2** bespreekt een review van de klinische farmacologie, inclusief farmacokinetiek, farmacodynamiek, veiligheid en effectiviteit, van de gecombineerde toediening van encorafenib en cetuximab met of zonder binimetinib. Om deze duale en triplet behandeling in een breder perspectief te plaatsen, wordt in dit review ook het huidige veld besproken voor de behandeling van patiënten met *BRAF*<sup>V600E</sup> gemuteerd, gemetastaseerd colorectaal kanker.

Op dit moment zijn er geen directe doelgerichte remmers van het KRAS eiwit beschikbaar met uitzondering van de selectieve *KRAS*<sup>G12C</sup> remmer, AMG510. Preklinische resultaten toonden aan dat relevante respons kon worden verkregen door de combinatie van MEK-remmers en pan-HER-remmers in *KRAS* gemuteerde colorectaal kankercellijnen en muismodellen. Deze strategie werd vertaald naar 3 behandelcombinaties voor patiënten met *KRAS* gemuteerd colorectaal carcinoom, niet kleincellig longcarcinoom of pancreascarcinoom zoals beschreven in **hoofdstuk 4**. **Hoofdstuk 4.1** behandelt de combinatie van de MEK-remmer PD-0325901 en de pan-HER-remmer dacomitinib. **Hoofdstuk 4.2** focust op de resultaten van de combinatie van trametinib en lapatinib in 34 patiënten. Verder werden 26 patiënten behandeld met de combinatie van selumetinib en afatinib in de studie beschreven in **hoofdstuk 4.3**. Het hoofddoel van de drie klinische studies was om het juiste doseerschema te bepalen voor verdere klinische ontwikkeling van de combinaties (aanbevolen fase II doseerschema (RP2D)). Secundaire doelen bestonden uit het onderzoeken van de veiligheid en het anti-tumor effect. Helaas werd escalatie van de dosering belemmert door toxiciteit en daarom was het niet mogelijk om de monotherapie doseringen te behalen. We hebben getracht om de balans tussen de toxiciteit en effectiviteit te verbeteren door een intermitterend doseerschema toe te passen, maar helaas bleef de toxiciteit van de middelen hierbij beperkend voor het ophogen van de dosering. Voor de combinatie van dacomitinib en PD-0325901 werd het RP2R vastgesteld op een dosering van 15 mg dacomitinib en 6 mg PD-0325901. Langdurige behandeling bleef echter onmogelijk vanwege het bijwerkingenprofiel van de combinatie. Meest voorkomende bijwerkingen in de 41 behandelde patiënten waren huiduitslag (85%), diarree (88%) en misselijkheid (63%). Een patiënt met niet kleincellig longcarcinoom was het langst onder behandeling en er werden geen responderende patiënten gezien. Daarom bevelen wij het niet aan om deze combinatie verder te ontwikkelen, met name vanwege het toxiciteitsprofiel.



In totaal werden in acht patiënten, behandeld met de combinatie van trametinib en lapatinib, DLTs gezien. Deze DLTs bestonden uit graad 3 huiduitslag, diarree, verhoogd aspartaat aminotransferase en verschillende graad 2 bijwerkingen met als gevolg uitgestelde dosering of een onmogelijkheid om 75% van de geplande dosering toe te dienen. Trametinib en lapatinib waren goed te tolereren voor patiënten in een intermitterend doseringsschema met voldoende farmacodynamisch effect. Bovendien werden er preliminaire tekenen van anti-tumor activiteit gezien in patiënten met niet kleincellig longcarcinoom. Voor de combinatie van selumetinib en afatinib werd het RP2D vastgesteld op een dosering van dagelijks 20 mg afatinib en twee keer per dag 25 mg selumetinib (21 dagen op/7 dagen af). Voor het intermitterende schema is de RP2D 20 mg afatinib QD en 25 mg selumetinib BID, beiden 5 dagen op/2 dagen af. De beste respons was ziekte stabilisatie voor 221 dagen in een patiënt met niet kleincellig longcarcinoom.

Over het algemeen bevelen wij het op dit moment niet aan om deze drie combinaties met MEK-remmers en pan-HER-remmers verder te ontwikkelen, totdat er een betere biomarker voor patiënt selectie is gevonden die de effectiviteit zou kunnen verbeteren.

## List of Publications

### ARTICLES

**Huijberts S**, Buurman BM, de Rooij SE. End-of-life care during and after an acute hospitalization in older patients with cancer, end-stage organ failure, or frailty: A sub-analysis of a prospective cohort study. *Palliative medicine*. 2016;30(1):75-82.

Wang L, Leite de Oliveira R, **Huijberts S**, Bosdriesz E, Pencheva N, Brunen D, et al. An acquired Vulnerability of Drug-Resistant Melanoma with Therapeutic Potential. *Cell*. 2018;173(6):1413-25.e14.

Tibben MM, **Huijberts S**, Li W, Schinkel AH, Gebretensae A, Rosing H, et al. Liquid chromatography-tandem mass spectrometric assay for the quantification of galunisertib in human plasma and the application in a pre-clinical study. *Journal of pharmaceutical and biomedical analysis*. 2019;173:169-75.

Van Cutsem E, **Huijberts S**, Grothey A, Yaeger R, Cuyle PJ, Elez E, et al. Binimetinib, Encorafenib, and Cetuximab Triplet Therapy for Patients With BRAF V600E-Mutant Metastatic Colorectal Cancer: Safety Lead-In Results From the Phase III BEACON Colorectal Cancer Study. *Journal of clinical oncology*. 2019;37(17):1460-9.

Van Geel R, van Brummelen EMJ, Eskens F, **Huijberts S**, de Vos F, Lolkema M, et al. Phase 1 study of the pan-HER inhibitor dacomitinib plus the MEK 1/2 inhibitor PD-0325901 in patients with KRAS-mutation-positive colorectal, non-small cell lung and pancreatic cancer. *British journal of cancer*. 2020;122(8):1166-74.

**Huijberts SC**, van Geel RM, Bernards R, Beijnen JH, Steeghs N. Encorafenib, binimetinib and cetuximab combined therapy for patients with BRAFV600E mutant metastatic colorectal cancer. *Future oncology*. 2020;16(6):161-73.

**Huijberts S**, van Geel R, van Brummelen EMJ, Opdam FL, Marchetti S, Steeghs N, et al. Phase I study of lapatinib and trametinib in patients with KRAS-mutant colorectal, non-small cell lung, and pancreatic cancer. *Cancer chemotherapy and pharmacology*. 2020;85(5):917-920

**Huijberts S**, Wang L, de Oliveira RL, Rosing H, Nuijen B, Beijnen J, et al. Vorinostat in patients with resistant BRAF(V600E) mutated advanced melanoma: a proof of concept study. *Future oncology*. 2020;16(11):619-29.

### ABSTRACTS AND PRESENTATIONS

**Huijberts S**, Schellens JHM, Elez E, Cuyle P-J, Cutsem E, Yaeger R, et al. BEACON CRC: safety lead-in (SLI) for the combination of binimetinib (BINI), encorafenib (ENCO), and cetuximab (CTX) in patients (pts) with BRAF-V600E metastatic colorectal cancer (mCRC). *Annals of oncology*. 2017 28 suppl\_5: v158-v208.

**Huijberts S**, Schellens JHM, Fakih M, Peeters M, Kopetz S, Grothey A, et al. BEACON CRC (binimetinib [BINI], encorafenib [ENCO], and cetuximab [CTX] combined to treat BRAF-

mutant metastatic colorectal cancer [mCRC]): A multicenter, randomized, open-label, three-arm phase III study of ENCO plus CTX plus or minus BINI vs irinotecan (IRI)/CTX or infusional 5-fluorouracil/folinic acid/IRI (FOLFIRI)/CTX with a safety lead-in of ENCO + BINI + CTX in patients (Pts) with BRAF<sup>V600E</sup> mCRC. *Journal of clinical oncology*. 2017 35:15\_suppl, TPS3622-TPS3622.

Cutsem E, Cuyle PJ, **Huijberts S**, Schellens J, Elez E, Yaeger R, et al. O-027BEACON CRC study safety lead-in: Assessment of the BRAF inhibitor encorafenib + MEK inhibitor binimetinib + anti-epidermal growth factor receptor antibody cetuximab for BRAFV600E metastatic colorectal cancer. *Annals of oncology*. 2018;29-29.

Van Cutsem E, Cuyle PJ, **Huijberts S**, Yaeger R, Schellens JHM, Elez E, et al. BEACON CRC study safety lead-in (SLI) in patients with BRAFV600E metastatic colorectal cancer (mCRC): Efficacy and tumor markers. *Journal of clinical oncology*. 2018 36:4\_suppl, 627-627.

**Huijberts SCFA**, Wang L, Rosing H, Nuijen B, Beijnen JH, Leite de Oliveira R, et al. Proof of concept study with vorinostat in patients with resistant BRAF<sup>V600E</sup> mutated advanced melanoma. FIGON Dutch Medicine Days 2018.

Kopetz S, Grothey A, Yaeger R, Cuyle PJ, **Huijberts S**, Schellens JHM, et al. Updated results of the BEACON CRC safety lead-in: Encorafenib (ENCO) + binimetinib (BINI) + cetuximab (CETUX) for BRAFV600E-mutant metastatic colorectal cancer (mCRC). *Journal of clinical oncology*. 2019 37:4\_suppl, 688-688.

**Huijberts SCFA**, Wang L, Rosing H, Nuijen B, Beijnen JH, Leite de Oliveira R, et al. Proof of concept study with the histone deacetylase inhibitor (HDACi) vorinostat in patients with resistant BRAF<sup>V600E</sup> mutated advanced melanoma. Scientific meeting dutch society for clinical pharmacology and biopharmacy 2019.

**Huijberts SCFA**, van Brummelen E, van Geel R, Opdam FL, Marchetti S, Steeghs N, et al. Phase I study of lapatinib and trametinib in patients with KRAS mutant colorectal, non-small cell lung and pancreatic cancer. *Annals of oncology*. 2019 30:suppl\_5, v159-v193.

**Huijberts S**, Wang L, Wilgenhof S, Rosing H, Nuijen B, Beijnen JH, et al. Proof of concept study with the histone deacetylase inhibitor vorinostat in patient with resistant BRAFV600 mutated advanced melanoma. *Annals of oncology*. 2019 30:suppl\_5, v533-v563.

**Huijberts S**, van Brummelen E, van Herpen CML, Desar IME, Opdam FL, van Geel RMJM, et al. Phase 1 study of afatinib and selumetinib in patients with KRAS mutation positive colorectal, non-small cell lung and pancreatic cancer. *Journal of clinical oncology*. 2020 38:15\_suppl; 3613-3613

## Affiliations

J.H. Beijnen	The Netherlands Cancer Institute, Department of Pharmacy & Pharmacology, Amsterdam, the Netherlands Utrecht Institute for Pharmaceutical Sciences, Utrecht University, Utrecht, the Netherlands
R. Bernards	The Netherlands Cancer Institute, Department of Molecular Carcinogenesis and Oncode Institute, Amsterdam, the Netherlands Faculty of Science, Utrecht University, Utrecht, the Netherlands
M.C. Boelens	The Netherlands Cancer Institute, Department of Pathology, Amsterdam, the Netherlands
E. Bosdriesz	The Netherlands Cancer Institute, Department of Molecular Carcinogenesis, Amsterdam, the Netherlands
A. Bosma	The Netherlands Cancer Institute, Department of Molecular Carcinogenesis, Amsterdam, the Netherlands
E.M.J. van Brummelen	The Netherlands Cancer Institute, Department of pharmacology, Amsterdam, the Netherlands Center for Human Drug Research, Leiden, the Netherlands
D. Brunen	The Netherlands Cancer Institute, Department of Molecular Carcinogenesis, Amsterdam, the Netherlands
J. Christy-Bittel	Array Biopharma Inc, Boulder, USA
F. Ciardiello	University of Campania "Luigi Vanvitelli", Naples, Italy
E. van Cutsem	University Hospitals Gasthuisberg and KU, Leuven, Belgium
P.J. Cuyle	University Hospitals Gasthuisberg and KU, Imelda General Hospital, Leuven, Belgium
J. Desai	Peter MacCallum Cancer Centre, Melbourne, Australia
I.M.E. Desar	Radboud University Medical Center, Department of Medical Oncology, Nijmegen, the Netherlands

L. A. Devriese	UMC Utrecht Cancer Center, Department of Medical Oncology, Utrecht, the Netherlands
E. Elez	Vall d'Hebron Institute of Oncology, Universitat Autònoma de Barcelona, Barcelona, Spain
F.A.L.M. Eskens	Erasmus Medical Center Cancer Institute, Department of Medical Oncology, Rotterdam, the Netherlands
M. Fakih	City of Hope Comprehensive Cancer Center, Duarte, USA
R.M.J.M. van Geel	The Netherlands Cancer Institute, Department of Pharmacology, Amsterdam, the Netherlands Maastricht University Medical Center +, Department of Clinical Pharmacology and Toxicology, Maastricht, the Netherlands Cardiovascular Research Institute Maastricht (CARIM), Maastricht University, Maastricht, the Netherlands
A. Gollerkeri	Array Biopharma Inc, Boulder, USA
A. Grothey	West Cancer Center, Germantown, USA
C.M.L. van Herpen	Radboud University Medical Center, Department of Medical Oncology, Nijmegen, the Netherlands
H. Horlings	The Netherlands Cancer Institute, Department of Molecular Carcinogenesis and Department of Molecular Genetics, Amsterdam, the Netherlands
A.D.R. Huitema	University Medical Center Utrecht, Department of Clinical Pharmacy, Utrecht, the Netherlands The Netherlands Cancer Institute, Department of Pharmacy & Pharmacology, Amsterdam, the Netherlands
S. Kopetz	The University of Texas MD Anderson Cancer Center, Houston, USA
R. Leite de Oliveira	The Netherlands Cancer Institute, Department of Molecular Carcinogenesis and Onco Institute, Amsterdam, the Netherlands

M.P.J.K. Lolkema	Erasmus Medical Center Cancer Institute, Department of Medical Oncology, Rotterdam, the Netherlands
T. Los-de Vries	The Netherlands Cancer Institute, Department of Molecular Carcinogenesis, Amsterdam, the Netherlands
K. Maharry	Array Biopharma Inc, Boulder, USA
S. Marchetti	The Netherlands Cancer Institute, Department of Medical Oncology, Amsterdam, the Netherlands
K. Monkhorst	The Netherlands Cancer Institute, Department of Pathology, Amsterdam, the Netherlands
C. Montagut	Hospital del Mar-Institut Hospital del Mar d'Investigacions Mèdiques, Universitat Pompeu Fabra, Barcelona, Spain
B. Nuijen	The Netherlands Cancer Institute, Department of Pharmacy & Pharmacology, Amsterdam, the Netherlands
F.L. Opdam	The Netherlands Cancer Institute, Department of Medical Oncology, Amsterdam, the Netherlands
M. Peeters	Antwerp University Hospital, Edegem, Belgium
N. Pencheva	The Netherlands Cancer Institute, Department of Molecular Carcinogenesis, Amsterdam, the Netherlands
S. Pulleman	The Netherlands Cancer Institute, Department of Medical Oncology, Amsterdam, the Netherlands
H. Rosing	The Netherlands Cancer Institute, Department of Pharmacy & Pharmacology, Amsterdam, the Netherlands
V. Sandor	Array Biopharma Inc, Boulder, USA
J.H.M. Schellens	Utrecht University, Utrecht, the Netherlands
J. Song	The Netherlands Cancer Institute, Department of Molecular Genetics, Amsterdam, the Netherlands

N. Steeghs	The Netherlands Cancer Institute, Department of Medical Oncology, Amsterdam, the Netherlands
J. Tabernero	Vall d'Hebron Insitute of Oncology, Universitat Autònoma de Barcelona, Barcelona, Spain
B. Thijssen	The Netherlands Cancer Institute, Department of Pharmacy & Pharmacology, Amsterdam, the Netherlands
L. Wang	The Netherlands Cancer Institute, Department of Molecular carcinogenesis and Oncode Institute, Amsterdam, the Netherlands
H. Wasan	Hammersmith Hospital, Imperial College London, Londen, United Kingdom
S. Wilgenhof	The Netherlands Cancer Institute, Department of Medical Oncology, Amsterdam, the Netherlands
F.Y.F.L. de Vos	UMC Utrecht Cancer Center, Department of Medical Oncology, Utrecht, the Netherlands
R. Yaeger	Memorial Sloan Kettering Cancer Center, New York, USA
T. Yoshino	National Cancer Center Hospital East, Edegem, Belgium
J. Zevenhoven	The Netherlands Cancer Institute, Department of Molecular Genetics, Amsterdam, The Netherlands

## Dankwoord

Eindelijk, het is af! Het enige boek dat ik ooit in mijn leven zal schrijven, nu eindelijk compleet. Een hele gekke tijd om een proefschrift af te ronden vanwege de COVID-19 pandemie. Iedereen bedankt die me op virtuele wijze heeft bijgestaan, want hierdoor heb ik ook werkend vanuit huis nooit het gevoel gehad om er alleen voor te staan.

Het meest dankbaar ben ik alle patiënten en hun families die wilden deelnemen aan de studies in dit proefschrift. Geen gemakkelijke keus om als patiënt in een intensief traject met onzekere uitkomsten te stappen, waarvoor mijn grote waardering!

Er zijn ontzettend veel mensen die geholpen hebben met de onderzoeken in dit proefschrift. De basis hiervoor is gemaakt door **Jan**, waarop ik later verder kon bouwen. Veel dank voor het delen van je wetenschappelijke inzichten en de introductie in de onderzoekswereld. Ik heb in de eerste jaren van mijn promotie ontzettend veel van je geleerd!

**Jos en Rene**, mede door jullie hulp heb ik de basis kunnen uitbreiden naar een volwaardig proefschrift. **Jos**, heel erg bedankt voor de rots in de branding die je was in toch wel onrustige tijden. Het voelde voor jou misschien vanzelfsprekend om mijn collega's en mij op te vangen, maar dat was het zeker niet. Door jouw hulp ben ik nooit het doel uit het oog verloren en je gaf me het vertrouwen dat het goed zou komen. Heel fijn om te weten dat je altijd op iemand met zoveel ervaring terug kan vallen!

**Rene**, ik weet nog dat ik zenuwachtig bij jou zat, omdat ik je wilde vragen om mijn tweede promotor te worden. Wat was ik blij dat je daar enthousiast op reageerde! Je hebt me veel geleerd over translationeel onderzoek en achterliggende mechanismen voor respons en resistentie. Bedankt, voor je wetenschappelijke inzichten en je aanstekelijke enthousiasme!

Ook wil ik **Neeltje** bedanken voor het bij staan van de klinische kant van mijn onderzoeken. Je hebt er zorg voor gedragen dat al mijn projecten doorgang konden vinden, helaas is daarvan niet alles in mijn proefschrift terecht gekomen. Ondanks dat heb ik er nuttige kennis voor de toekomst aan over gehouden. **Frans**, op papier sloot je je als laatste aan bij mijn promotieteam. Maar je hulp kwam zeker niet op de laatste plaats. Ik vond het altijd prettig met je samenwerken en je uitleg over de klinische farmacologische aspecten van de geneesmiddelen heeft me bruikbare inzichten gegeven. Dank, dat je mij ook als copromotor bij wilde staan!

**Alwin**, dank voor de goede begeleiding als mentor tijdens mijn klinische farmacologie opleiding. Ik weet zeker dat ik in de toekomst een betere dokter voor mijn patiënten word met de kennis die ik hier heb opgedaan.

Lieve **collega OIO's**, door jullie aanwezigheid ben ik altijd met plezier naar mijn werk gegaan. En ook als dat een dagje niet zo was, dan zorgden jullie er in ieder geval voor dat ik er weer plezier in kreeg. Veel dank voor de kinetiekers, zo fijn dat jullie altijd voor me klaar stonden om dingen over te nemen als ik weer eens op vakantie wilde. Het meest zal ik de Vermaat koffietjes missen, heerlijk om even vrij uit te kunnen zeuren in deze pauze momentjes en om het met jullie dan ook even niet over werk te hebben. En wat heb ik me goed vermaakt



tijdens de OIO-weekenden en congressen. Met Barcelona als hoogtepunt, waar naast de wetenschappelijke info ook de cava rijkelijk vloeide.

Dear **Liqn and Rodrigo**, thank you for the great preclinical and clinical collaboration in the vorinostat study. Our meetings were not only very interesting, but also very much fun! **Sofie**, bedankt dat je PI wilde worden van de vorinostat studie en je collega's uit de melanoomgroep scherp hield om hun patiënten voor de studie naar ons door te verwijzen. Ook wil ik alle **co-auteurs** bedanken voor hun kritische blik op mijn onderzoeken. Jullie feedback heeft mijn manuscripten naar een hoger niveau getild!

Alle collega's van de **CRU, de apotheek, het trialbureau, pathologie en het triallab**, dank voor jullie ondersteuning. Jullie doen goed werk en waarborgen de hoge kwaliteit van de studies in het AVL. Hier wil ik graag ook **Carla** apart noemen, want wat moest ik nou zonder jou! Als CRA heb je me op weg geholpen in de wereld van GCP en datamanagement. Voor ons beiden was het nieuw om internationale studies op te zetten en uit te voeren. Ik wil je graag bedanken voor je betrokkenheid, hulp en luisterend oor.

Lieve paranimfen, **Jill en Marit**, jullie waren mijn grootste steun en toeverlaat in het AVL. Ik kon altijd bij jullie terecht voor vragen, een kwartiertje zeuren of gewoon voor de gezelligheid. Heel veel dank voor jullie steun! Nu ik weet dat jullie me tijdens mijn verdediging bij zullen staan, heb ik er de volle vertrouwen in dat het helemaal goed gaat komen!

Naast alle bovengenoemde collega's heb ik gelukkig ook veel steun gehad van vrienden buiten het AVL. Jullie afleiding was en is altijd heel belangrijk voor me. Met avondjes eten of wijn drinken, weekendjes weg, carnavallen, wielrennen en vooral jullie dierbare vriendschappen hebben jullie me erdoorheen gesleept. Ik hoop dat we nog eeuwig alle leuke en soms ook minder leuke dingen van het leven blijven delen.

Lieve **pap, mam, Mariel en Inge**, ik had me geen fijner gezin kunnen wensen. Bedankt pap en mam dat jullie me altijd lieten geloven dat je met hard werken veel kan bereiken, maar ook dat presteren niet het allerbelangrijkste is. Doordat jullie altijd achter me staan, voel ik me altijd gesteund en weet ik dat alles goed komt. Mariel en Inge, ik weet dat jullie regelmatig denken dat ik een zelfverzonnen taal uitkraam, maar hopelijk kan ik jullie met dit boek bewijzen dat dat gebrabbel toch wel echt ergens op slaat.

**Allerliefste TiTi**, wat een feest om jou in mijn leven te hebben. Ook al begreep je niet altijd waar mijn onderzoeken over gingen, aan jou heb ik zeker de meeste steun gehad. Als ik soms verdrietig thuiskwam, wist je me altijd weer vrolijk te krijgen. Ook leerde je me dat je niet altijd alles zelf in de hand moet willen houden en dingen dan ook wel loslopen. Hierdoor was mijn stress vaak snel een stuk minder. Ik weet zeker dat de toekomst voor ons samen nog heel veel mooie dingen in petto heeft!



## Curriculum Vitae

Sanne Huijberts was born on November 1<sup>st</sup>, 1988 in Sint Michielsgestel, The Netherlands. In 2006 she graduated from Gymnasium Beekvliet in Sint Michielsgestel, after which she moved to Utrecht to study Biomedical Sciences at Utrecht University. After 1 year of Biomedical Sciences she was admitted to the study Medicine at the University of Amsterdam. During this study, she performed a 5-month prospective cohort study at the department of Geriatric Medicine at the Amsterdam UMC, location AMC, in Amsterdam, focusing on end-of-life care during and after acute hospitalization in older patients. In 2014 she received her Master of Science in Medicine and started working as a resident not in training at the Antoni van Leeuwenhoek hospital. In 2015 she went to work as a resident not in training at the Spaarne Gasthuis in Hoofddorp, the Netherlands, after that she started her PhD research at the department of Clinical Pharmacology at the Netherlands Cancer Institute – Antoni van Leeuwenhoek hospital under supervision of prof. dr. Jan Schellens and later under supervision of prof. dr. Jos Beijnen, prof. dr. Rene Bernards and dr. Neeltje Steeghs. Her PhD research was focusing on clinical trials with genotype-directed targeted anticancer agents in colorectal cancer, non-small cell lung cancer and melanoma. The results of this PhD research are presented in this thesis. In addition to her PhD project, Sanne also followed the clinical pharmacology training of the Dutch Society for Clinical Pharmacology and Biopharmacy.







